

**MULTIDISCIPLINARY APPROACH TO UNDERSTAND THE  
LOCALIZATION OF GEOTHERMAL ANOMALIES IN THE UPPER RHINE  
GRABEN FROM REGIONAL TO LOCAL SCALE**

Thesis presented at the Faculty of Sciences of the University of Neuchâtel to satisfy the requirements  
of the degree of Doctor of Philosophy in Science

by

Paul Baillieux

---

**Thesis defense date:** December 18<sup>th</sup>, 2012

**PhD thesis evaluation committee:**

Prof. Eva Schill	University of Neuchâtel (CH)	Thesis director
Dr. Chrystel Dezayes	BRGM Orléans (FR)	Jury member
Dr. Albert Genter	GEIE EMC Sultz (FR)	Jury member
Prof. Philippe Renard	University of Neuchâtel (CH)	Jury member



## IMPRIMATUR POUR THESE DE DOCTORAT

---

La Faculté des sciences de l'Université de Neuchâtel  
autorise l'impression de la présente thèse soutenue par

**Monsieur Paul BAILLIEUX**

**Titre: Multidisciplinary approach to understand the localization of  
geothermal anomalies in the Upper Rhine Graben from regional to  
local scale**

**sur le rapport des membres du jury:**

- Prof. Eva Schill, Université de Neuchâtel, directrice de thèse
- Prof. Philippe Renard, Université de Neuchâtel
- Dr Albert Genter, GEIE Sultz, Kutzenhausen, France
- Dr Chrystel Dezayes, BRGM, Orléans, France

Neuchâtel, le 26 février 2013

Le Doyen, Prof. P. Kropf



## General abstract

This thesis is devoted to understanding the localization of geothermal anomalies in extensional tectonic settings away from active volcanic areas. In this context, the European Cenozoic Rift System (ECRIS) hosts some of the major geothermal anomalies in Europe. Its central segment, the Upper Rhine Graben (URG), stretching over 300km between Basel (Switzerland) and Frankfurt (Germany), reveals several surface heat flow anomalies in the order of up to  $> 150 \text{ mW m}^{-2}$  (compared to an average of  $60 \text{ mW m}^{-2}$  in Europe) and temperatures up to  $120^\circ\text{C}$  at 1km depth, when usually a mean temperature gradient of  $30^\circ\text{C km}^{-1}$  is observed.

In the Upper Rhine Graben, geothermal activity has mainly been attributed to free hydrothermal convection at graben scale, as well as free convection along the major faults in the area of Landau and at the European Enhanced Geothermal System (EGS) test-site Soultz.

These local phenomena emphasize that temperature is not homogeneously distributed in the URG and neither are geothermal anomalies. Different geological facts were solicited to explain the localization of geothermal anomalies in the URG. The geothermal anomaly at Soultz has been on the one hand attributed to recent compressive shear strain occurring parallel to the central segment of the graben, allowing hydrothermal circulation to occur along favorably oriented fracture zones in the basement and in the high porosity sandstone aquifer above it. On the other hand it has been correlated to the lithological nature of the basement and its inherited orientations.

In this thesis, 3D geological modeling, boreholes temperatures distribution, gravity, magnetics, slip and dilation tendencies analysis, neotectonic activity and geodynamic modeling have been used to investigate geological patterns associated with the localization of geothermal anomalies at graben-wide scale (the URG) and pluri-kilometric scale (in the area of the EGS Soultz).

The comparison of geophysical data with the temperature distribution at graben scale has shown that zones of temperature highs can be related to the occurrence of low density basement that can be attributed to crystalline ridges offering an optimal radiogenic heat production and heat conductivity but also to porosity changes associated with faulting and hydrothermal circulation. In particular, zones of magnetic highs and gravity lows are related to additional temperatures in the order  $10\text{-}20^\circ\text{C}$  at 2000m true-vertical depth (TVD) at a graben wide scale (temperature  $100\text{-}110^\circ\text{C}$  compared to a mean  $90^\circ\text{C}$  with minimum value of  $75^\circ\text{C}$ ).

Additionally, the occurrence of compression shear and uplift regime, with low Quaternary sedimentation, in the central segment of the URG appears to be linked to the major geothermal anomalies ( $120$  to  $> 140^\circ\text{C}$  at 2000 m TVD) in the area of Soultz, Landau and Speyer. This may be explained by a change in tectonic regime from the Early Miocene to up to Present, and is in favor of the interpretation of the central segment of the URG being a restraining band separating two-pull apart basin in a sinistral strike-slip regime. Surprisingly, a relative low seismicity is observed in this area, which to an uncertain extent, maybe linked to the occurrence of naturally circulating fluids.

More locally in Soultz area, a new 3D geological model has been elaborated on the basis of a high density set of 2D seismic profiles and deep boreholes to understand the links between structural and

lithological patterns and the temperature distribution. A mean temperature anomaly of 40 °C at top basement has been linked to a light and magnetic granodioritic pluton offering a rather high radiogenic heat production. Moreover, hydrothermal circulation has been found to occur along N-S directed major faults with a West dipping signature in the western side of horst structures, and is held responsible for temperature anomalies above 60 °C, and this correlates with magnetotelluric observations and fracture orientations in Soultz boreholes. The majority of faults are favorably oriented in the current stress field to be reactivated and undergo dilation at depth and thus allow hydrothermal convection, but no clear relationship between these phenomena has been observed in the slip and dilation tendency analyses, and this can possibly be explained by asymmetric deformation patterns in the area, or by the sealing of the other faults due to intense mineralization. Another possible explanation is the fluid circulation characterized by an upward flow of hot water with a meteoric signature as a result of fluid inclusions analyses, and this deep circulation is interpreted to be coming from the Vosges mountain basement to the West, and this correlates with gravity residuals analyses.

Finally, the geodynamic modeling of the graben opening showed that simple models can explain the patterns of deformation observed along the deep seismic profiles perpendicular to the graben. In particular, the observed graben asymmetric geometry is reproduced and asymmetric localized faulting is observed on the side opposite to the master fault accommodating the majority of vertical deformation.

## **Keywords**

Upper Rhine Graben; Geothermics; Geothermal Energy; Enhanced Geothermal Systems; EGS; Hydraulic Permeability; Hydraulic Conductivity; Geophysics; Gravity; Gravimetry; Magnetics; Geodynamics; Seismicity; Tectonic Processes; Temperature; Neotectonic Activity; Radiogenic Heat Production; Hydrothermal Circulation; Fault; Stress; Strain; Crustal Extension; Extensional Tectonics; Soultz; Magnetotellurics; Porosity; Slip and Dilation Tendency Analysis; Uplift; Compression; Extension; Subsidence; Basement Rocks; Granite; 3D Geological Modeling; Geology; Hydrogeology; Thermal Anomalies; Crystalline Basement; Graben System; Magnetism; Neotectonics

## **Organisation of this thesis**

The present thesis is organized as a succession of 5 chapters, three of which were prepared for submission to scientific journals. The topics of the individual chapters and the contributions of the various authors are outlined below.

### **Chapter 1: Introduction**

This chapter presents the foundations studies and main objectives of the present thesis, the geological framework and methodology thereby applied.

### **Chapter 2: Localization of temperature anomalies in the Upper Rhine Graben: insights from geophysics and neotectonic activity**

By

Paul Baillieux, Eva Schill, Jean-Bernard Edel and Guillaume Mauri

This chapter proposes to compare the observed temperature distribution at depth in the Upper Rhine Graben with the different map associated to explanations for its localization. It illustrates how geophysical data and neotectonic patterns can be linked to the temperature distribution. The contribution of these different sources is qualified semi-quantitatively.

The first author looked through the literature to find the solicited explanation for the localization of the temperature anomalies and drew the different maps, and eventually wrote a first draft of the paper. The second author offered scientific questions and suggestions and helped shaping ideas and text. The third author contributed in the paper by sharing the geophysical database and its geophysical and geological experience on the studied area. The fourth author helped in reviewing the manuscript.

### **Chapter 3: Insights on the localization of temperature anomalies in Soultz area from gravity, magnetics and slip and dilation tendency analysis**

By

Paul Baillieux, Eva Schill, Yassine Abdelfettah and Chrystel Dezayes

This chapter proposes a higher resolution and more local approach to link the temperature distribution with observed structural patterns, with the surface geophysical data around the area, and the observed local stress patterns, around the area of the European EGS test-site Soultz, in the recently developed 3D geological model (Appendix A and B). The contribution of these different sources is qualified semi-quantitatively.

Firstly, the first author constructed the 3D geological model with the help of all other authors (Appendix A). Secondly, the first author used this 3D geological model as a basis for studying the temperature distribution and constructed the different maps to quantify the contribution of the different possible sources to explain the distribution of temperature, and eventually wrote a first draft of the manuscript. The second author offered scientific questions and suggestions and helped shaping ideas and text. The third author was involved in the different steps of the geophysical processing. The fourth author helped in reviewing the manuscript with its long experience in the field.

## **Chapter 4: Investigation of natural permeability in extensional tectonic settings: insights from a 2D geodynamic modeling of the Upper Rhine Graben opening**

By

Paul Baillieux, Eva Schill and Louis Moresi

This chapter offers a new approach to understand the creation and development of natural faulting and hydraulic conductivities in a graben system through geological time using geodynamics modeling, with emphasis on geothermal application. A recently developed geodynamics code which allows the modeling of complex long-term geological processes and enables the user to visualize the geological creation of complex geometries such as brittle faulting, mantle upwelling in continental extension for example, has been used. For benchmarking these models, seismic sections through the Upper Rhine valley were selected.

The first author carried out analyses to set up geodynamic models in order to approach reasonable scientific and practical questions raised by the topic. He wrote a first draft of the manuscript, which was improved by the second author. The third author, as a specialist in geodynamic modeling, helped both in creating the geodynamic model and reviewing the manuscript.

## **Chapter 5: Summary, discussion and conclusions**

This chapter summarizes the results described in previous chapter, and discusses the impact of the different chapters to the understanding of the localization of geothermal anomalies in the Upper Rhine Graben.

## **Appendix A: 3D structural regional model of the EGS Soultz site (northern Upper Rhine Graben, France): Insights and perspectives**

By

Paul Baillieux, Eva Schill and Chrystel Dezayes

Presented in: Thirty-Sixth Workshop on Geothermal Reservoir Engineering at Stanford University, 2011



This conference paper presents the insights and perspectives from the new 3D geological model of the EGS Soutz area, with emphasis on geophysical and structural patterns such as the orientations and density of regional faults and their link to reservoir fractures, as well as a first interpretation of the temperature distribution at depth.

## **Appendix B: 3-D visualization of a fractured geothermal field: The example of the EGS Soutz site (northern Upper Rhine Graben, France)**

By

Chrystel Dezayes, Laurent Beccaletto, Gwennole Oliviero, Paul Baillieux, Laure Capar and Eva Schill

Presented in: Thirty-Sixth Workshop on Geothermal Reservoir Engineering at Stanford University, 2011

This conference paper presents the geological data and procedure used to build the new 3D geological model including the fault network of the EGS Soutz area.



# Table of Content

General abstract .....	v
Organisation this thesis .....	vii
Chapter I: Introduction .....	21
1.1 Main objectives of the PhD thesis .....	21
1.2 Geological framework .....	26
1.3 Methodology .....	29
1.4 References .....	30
Chapter II: Localization of temperature anomalies in the Upper Rhine Graben: insights from geophysics and neotectonic activity .....	33
Abstract .....	33
2.1 Introduction .....	33
2.2 Geological settings .....	35
2.2.1 Pre-Permian Basement in the URG .....	35
2.2.2 Structural development of the Upper Rhine Graben .....	37
2.2.3 Recent stress and strain distribution .....	38
2.3 Data processing .....	40
2.3.1 Temperature interpolation .....	40
2.3.2 Compilation of geophysical data .....	42
2.4 Results and discussion .....	43
2.4.1 Temperature distribution in the URG .....	43
2.4.2 Links between geophysical grids and temperature .....	46
2.4.3 Links between recent stress and strain rate-hydrothermal convection .....	50
2.5 Conclusions .....	51
2.6 Acknowledgements .....	52
2.7 References .....	52

Chapter III: Insights on the localization of temperature anomalies in Soultz area from gravity, magnetics and slip and dilation tendency analysis .....	57
Abstract .....	57
3.1 Introduction.....	57
3.2 Geological settings .....	59
3.2.1 Pre-Permian Basement inferred from Geophysics.....	59
3.2.2 Structural development of the Upper Rhine Graben .....	60
3.2.3 3D structural model of the Soultz area .....	61
3.3 Data processing .....	63
3.3.1 Temperature data.....	63
3.3.2 Geophysical data .....	64
3.3.3 Slip and dilation tendencies analysis.....	65
3.4 Results and Discussion .....	67
3.4.1 Temperature distribution at top basement .....	67
3.4.2 Geophysics.....	70
3.4.3 Slip and dilation tendencies analyses.....	76
3.5 Conclusions.....	79
3.6 Acknowledgements .....	80
3.7 References .....	80

Chapter IV - Investigation of natural permeability in extensional tectonic settings: insights from a 2D geodynamic modeling of the Upper Rhine Graben opening .....	85
Abstract .....	85
4.1 Introduction.....	85
4.1.1 Review of geodynamic modeling of continental extension .....	87
4.2 2D crustal extension of the Upper Rhine Graben .....	88
4.2.1 Methods .....	88
4.2.2 Sensivity study .....	89
4.2.3 Variation in viscosity.....	89
4.2.4 Comparison with independent geophysical data.....	94
4.3 Discussion and implication for geothermal exploration .....	95
4.4 Conclusions.....	95
4.5 Acknowledgements .....	95
4.6 References .....	95

Chapter V: Discussion and conclusions .....	99
Outlook.....	102
References.....	102
All references.....	105
Acknowledgements .....	113
Appendix A: 3D structural regional model of the EGS Soultz site (northern Upper Rhine Graben, France): Insights and perspectives .....	115
Appendix B: 3-D visualization of a fractured geothermal field: The example of the EGS Soultz site (northern Upper Rhine Graben, France) .....	124
Curriculum Vitae of Paul BAILLIEUX .....	131



## Table of figures

Figure 1-1 : Map of temperature in Europe extrapolated to 5km depth - modified after Genter (2004) and Hurtig <i>et al.</i> (1992). URG: Upper Rhine Graben; U: Urach - molasse basin area; LG: Limagne graben-French Massif Central; C: Catalonia; Ca: Campidano graben; Cm: Camborne granite; GB: German basin; T: Tuscany; PB: Pannonian Basin. ....	22
Figure 1-2 : Temperature contour map of the Rhine Graben at a depth of 800 m modified after Pribnow and Schellschmidt (2000). Profile AA' approximately corresponds to cross-sections in Figure 1-4 and Figure 1-5. ....	23
Figure 1-3 : top) Outline of a typical Enhanced geothermal system (EGS) for heat and electricity production in a fractured crystalline rock (after CREGE, 2010, Neuchâtel, Switzerland, <a href="http://www.crege.ch">www.crege.ch</a> ) bottom) Photograph of the surface EGS power plant of Soultz (Soultz GEIE EMC, France, <a href="http://www.geothermie-soultz.fr">www.http://www.geothermie-soultz.fr</a> ). ....	24
Figure 1-4 : Generalized cross-section through the Rhinegraben South of Karlsruhe showing hydrothermal convection in shear controlled fissures of the basement, but heat conduction in the sedimentary fill (Illies <i>et al.</i> , 1981). ....	25
Figure 1-5 : 2D computed temperature field across Soultz and Baden-Baden geothermal areas, modified after Sausse (1998) and Le Carlier de Veslud <i>et al.</i> (1994). Interpretation of fluid flow field (blue arrows) after Pribnow and Schellschmidt (2000).....	25
Figure 1-6 : Emplacement of Graben Systems on the Digital Elevation Model of the European Cenozoic Rift System (ECRIS) area with superimposed ECRIS fault systems (thin lines), based on GTOPO30 with horizontal grid spacing of 30 arc sec, USGS, modified after Ziegler and Dèzes (2007). LRG: Lower Rhine Graben; HG: Hessian Graben; EG: Eger Graben; URG: Upper Rhine Graben; LG: Limagne Graben; BG: Bresse Graben. ....	26
Figure 1-7 : Geological overview map of the Upper Rhine Graben area, modified after Lahner and Wellmer (2004) and Christian Röhr, 2006 ( <a href="http://www.oberrheingraben.de">http://www.oberrheingraben.de</a> ) . OMh: Odenwald Mountains high; PWh: Pfälzerwald high; KGd: Kreichgau depression; PBd: Pflazburger depression; VMh: Vosges Mountains high; BFMh: Black Forest Mountains high. Location of the geothermal anomalies of the European EGS test-site Soultz, Landau and Speyer (red stars). Dashed blue lines approximately indicate location of traces of the cross-sections of Figure 1-8. ....	27

Figure 1-8 : Interpreted cross-sections of the Rhine Graben from the ECORS-DEKORP seismic investigation of the crustal structure of the Upper Rhine Graben. a) northern profile. b) southern profile. Red lines denote the interpreted master fault accommodating the maximum offset. Modified after Brun *et al.* (1992) and Valley (2007). Locations of cross-sections on Figure 3..... 28

Figure 1-9: Block diagrams of the general Rhine Graben structure. Various hatching corresponds to the thickness of the Cenozoic sedimentary fill. Modified after Illies (1972) and Valley (2007). Location of the European EGS test-site Soultz (red point). ..... 29

Figure 2-1 : Compilation of Edel (2004) and Edel and Schulmann (2009) interpretative maps showing the major units and tectonic features beneath the pre-Late Carboniferous - Permian basin. Id :low density; md: medium density; hd: high density; RHZ:Rhenohercynian Zone; STZ: Saxo-Thuringian Zone; MZ: Moldanubian Zone; VM: Vosges mountains; BFM: Blackforest mountains; OM: Odenwald mountains; KV: Kaiserstuhl Volcanic massif. Lambert II coordinates. .... 36

Figure 2-2 : Map showing the interpretation of neotectonic activity of the Upper Rhine Graben including the main direction of stress, adapted from Illies & Greiner (1979), the thickness of quaternary sediments, after Schumacher (2002), and the present day seismic activity, after Ahorner (1975; Schumacher, 2002), Bonjer (1997), Plenefisch & Bonjer (1997), Edel *et al.* (2006). VM: Vosges mountains; BFM: Blackforest mountains; OM: Odenwald mountains; KV: Kaiserstuhl Volcanic massif. Lambert II coordinates. .... 39

Figure 2-3 : Distribution and quality of borehole temperature measurements in the URG area. Categories of quality among the measurements come from the study by Agemar *et al.* (2012). ..... 41

Figure 2-4 : Temperature distribution at 2000 m TVD in the Upper Rhine Graben (URG) derived from a 3D interpolation of 6531 temperature data from 1600 boreholes from the URG and adjacent areas using the dataset of Pribnow & Schellschmidt (2000) and Agemar *et al.* (2012). The location of the two main petroleum and geothermal areas at Pechelbronn/Soultz-sous-Forêts and Landau are indicated. The boreholes with a depth > 2000 m TVD are indicated by triangles. VM: Vosges mountains; BFM: Black Forest mountains; OM: Odenwald mountains; KV: Kaiserstuhl Volcanic massif. Lambert II coordinates. .... 44

Figure 2-5 : Temperature distribution with depth in the boreholes of the URG and surroundings (after Pribnow & Schellschmidt (2000) and Agemar *et al.* (2012), with emphasis on the Soultz boreholes (red) and expected temperature regime in Soultz area (e.g. Kohl *et al.*, 2000). ..... 45



Figure 2-6 : (left) Superposition isolines of temperature at 2000 m TVD after Pribnow and Schellschmidt (2000) and Agemar *et al.* (2012), and magnetic anomaly reduced to pole map after Edel *et al.* (1982) and Papillon (1995); VM: Vosges mountains; BFM: Black Forest mountains; OM: Odenwald mountains; KV: Kaiserstuhl Volcanic massif. Lambert II coordinates. (right) Graph representing the mean value and standard deviation of temperature values at 2000 m TVD corresponding to the magnetic anomaly (10 nT interval). Label number indicates the number of information that has been used to calculate the mean value and standard deviation. .... 47

Figure 2-7 : (left) Superposition isolines of temperature at 2000 m TVD after Pribnow and Schellschmidt (2000) and Agemar *et al.* (2012), and Bouguer Anomaly map after Rotstein *et al.* (2006); VM: Vosges mountains; BFM: Black Forest mountains; OM: Odenwald mountains; KV: Kaiserstuhl Volcanic massif. Lambert II coordinates. (right) Graph representing the average and standard deviation of temperature values at 2000 m TVD corresponding to the Bouguer Anomaly (2.5 mgals interval). Label number indicates the number of information that has been used to calculate the mean value and standard deviation. .... 48

Figure 2-8 : (left) Superposition isolines of temperature at 2000 m TVD after Pribnow and Schellschmidt (2000) and Agemar *et al.* (2012), and Gravity vertical gradient map after Edel *et al.* (2007); VM: Vosges mountains; BFM: Black Forest mountains; OM: Odenwald mountains; KV: Kaiserstuhl Volcanic massif. Lambert II coordinates. (right) Graph representing the average and standard deviation of temperature values at 2000 m TVD corresponding to the Gravity vertical gradient (0.5 mgal/km interval). Label number indicates the number of information that has been used to calculate the mean value and standard deviation. .... 49

Figure 2-9 : Map representing the superposition temperature at 2000 m TVD after Pribnow and Schellschmidt (2000) and Agemar *et al.* (2012), and interpretation of neotectonic activity of the Upper Rhine Graben adapted from Illies & Greiner (1979), and the present day seismic activity, after Ahorner (1975), Bonjer (1997), Plenefisch & Bonjer (1997), Edel *et al.* (2006). VM: Vosges mountains; BFM: Blackforest mountains; OM: Odenwald mountains; KV: Kaiserstuhl Volcanic massif. Lambert II coordinates..... 50

Figure 3-1 : Compilation of Edel (2004) and Edel and Schulmann (2009) interpretative maps showing the major units and tectonic features beneath the pre-Late Carboniferous - Permian basin. Id :low density; md: medium density; hd: high density; mag: high magnetic susceptibility; RHZ:Rhenohercynian Zone; STZ: Saxo-Thuringian Zone; MZ: Moldanubian Zone; VM: Vosges mountains; BFM: Blackforest mountains; OM: Odenwald mountains; KV: Kaiserstuhl Volcanic massif. Lambert II coordinates. .... 60

Figure 3-2 : Interpretation of neotectonic activity in the upper Rhine Graben after Illies and Greiner (1979). Superposition of fault traces (Illies and Greiner, 1979), thickness of Quaternary sediments - after Bartz (1974) and Schumacher (2002). The mean direction of stress is adapted from Illies and Greiner (1979; 2002). VM: Vosges mountains; BFM: Blackforest mountains; OM: Odenwald mountains; KV: Kaiserstuhl Volcanic massif. Lambert II coordinates. ....	62
Figure 3-3 : visualization of the geological model of the Soultz area (31x18.5x6 km). The upper tertiary sedimentary filling was intentionally left transparent for best visualization. Location of the model area on Figure 3-1 and Figure 3-2. ....	63
Figure 3-4 : Top basement elevation, fault traces and dip directions (black lines) at top basement in the area of the 3D geological model. Red star indicates the location of the European EGS test-site Soultz. ....	64
Figure 3-5 : Temperature distribution in the 112 boreholes of Soultz area. Database from Pribnow and Schellschmidt (2000) and Agemar <i>et al.</i> (2012). ....	68
Figure 3-6 : Visualization of the temperature distribution at -1000, -2000 and -3000 m above sea-level, temperature measurements distribution along boreholes (red crosses) and 3D basement elevation (grey) within the limited area of the 3D geological model. Temperature database from Pribnow and Schellschmidt (2000) and Agemar <i>et al.</i> (2012). ....	68
Figure 3-7 : Temperature anomaly at top basement, distribution of temperature measurements and their distance to top basement, and fault traces and dip directions (black lines) at top basement in the area of the 3D geological model. A temperature gradient of 39.2°C per km, corresponding to the lowest observed temperature gradient in the area, is subtracted from the temperature field at top basement to obtain this temperature anomaly map at top basement. Temperature database from Pribnow and Schellschmidt (2000) and Agemar <i>et al.</i> (2012). ....	69
Figure 3-8 : Distribution and quality of borehole temperature measurements in the area of the 3D geological model. Categories of quality among the measurements come from the study by Agemar <i>et al.</i> (2012). ....	69
Figure 3-9 : (top) Magnetic anomaly reduced to pole, surface features from the 3D model (fault system, horizons) (bottom) Magnetic anomaly reduced to pole, surface features from the 3D model (fault system, horizons) and contours of temperature anomaly at top basement .....	72
Figure 3-10 : (top) Bouguer anomaly with reference density 2670 kg m <sup>-3</sup> , surface features from the 3D model (fault system, horizons). (bottom) Gravity forward response of the model with reference density 2670 kg m <sup>-3</sup> , and surface features from the 3D model (fault system, horizons). ....	73

Figure 3-11 : (top) Gravity residuals after 20 km Butterworth filter, and surface features from the 3D model (fault system, horizons). Red circles refer to zones of low gravity residuals described in the text. (bottom) Gravity residuals after 80 km Butterworth filter, and surface features from the 3D model (fault system, horizons). Red circles refer to zones of low gravity residuals described in the text. ....	74
Figure 3-12 : (top) Gravity residuals after 20 km Butterworth filter, surface features from the 3D model (fault system, horizons) and contours of temperature anomaly at top basement. (bottom) Gravity residuals after 80 km Butterworth filter, surface features from the 3D model (fault system, horizons) and contours of temperature anomaly at top basement. ....	75
Figure 3-13 : Bouguer anomaly with reference density $2670 \text{ kg m}^{-3}$ , surface features from the 3D model (fault system, horizons) and contours of temperature anomaly at top basement .....	76
Figure 3-14 : Slip tendency on the fault system of the 3D geological model.....	77
Figure 3-15 : (top) Slip tendency on the fault system at top basement and temperature anomaly at top basement in the area of the 3D geological model. Direction of maximum horizontal stress at depth is taken from boreholes analysis at Soultz (Valley and Evans, 2007). (bottom) Dilation tendency on the fault system at top basement and temperature anomaly at top basement in the area of the 3D geological model. Direction of maximum horizontal stress at depth is taken from boreholes analysis at Soultz (Valley and Evans, 2007).....	78
Figure 4-1 : Structural interpretation of the Upper Rhine Graben. Red lines denote the spatial distribution of the graben master faults. Blue dashed lines show the location of the ECORS-DEKORP seismic lines. Red stars show the main geothermal anomalies of the upper Rhine Graben. Modified after Derer <i>et al.</i> (2005).....	86
Figure 4-2 : Interpreted cross-sections of the Rhine Graben from the ECORS-DEKORP seismic investigation of the crustal structure of the Upper Rhine Graben. a) northern profile. b) southern profile. Red lines denote the interpreted master fault accommodating the maximum offset. Modified after Valley (2007) and Brun <i>et al.</i> (1992).....	87
Figure 4-3 : Model setup with plastic upper crust (Drucker-Prager frictional plastic pressure dependent law) and with viscous lower crust and an initial singularity .....	89
Figure 4-4 : Model setup. Grey dots represent the distribution (5%) of initially damaged material....	90

Figure 4-5 : Final Lagrangian particle swarm distribution (in km) (upper picture) and cumulative strain rate distribution ( $s^{-1}$ ) (lower picture) after 10 km of extension using a lower crust viscosity of A)  $10^{21}$  Pa s, B)  $5 \cdot 10^{21}$  Pa s, C)  $10^{22}$  Pa s..... 92

Figure 4-6 : Final Lagrangian particle swarm distribution (in km) (upper picture) and cumulative strain rate distribution ( $s^{-1}$ ) (lower picture) after 15 km of extension using a lower crust viscosity of A)  $10^{21}$  Pa s, B)  $5 \cdot 10^{21}$  Pa s, C)  $10^{22}$  Pa s..... 94

# Chapter I: Introduction

## 1.1 Main objectives of the PhD thesis

Electric power has been produced from geothermal energy since more than 100 years in Tuscany, where high temperatures of  $> 230^{\circ}\text{C}$  are observed at shallow depth ( $< 1000 - 2000 \text{ m}$ ) in an extensional core complex area. A similar tectonic setting at larger scale occurs in North-West USA, where the majority of the today total capacity of about 10 GW world-wide is installed. Another important contribution to the world-wide electricity production is obtained from volcanic areas (Bertani, 2012). With a world-wide capacity factor of 70% this renewable energy is able to provide base load electricity. These high-enthalpy resources are, however, limited to the described particular tectonic situations. Due to the small number of installation, a mean capacity factor for unconventional deep geothermal resources, i.e. mainly Enhanced Geothermal Systems (EGS), cannot be calculated. However, values up to  $> 80 \%$  have been reached. With this in mind, current research focuses on the development of unconventional deep geothermal systems, which may enlarge the tectonic portfolio for significant electricity production with respect to the high-enthalpy areas and thus, increase independence from particular tectonic settings such as volcanic areas and extensional core-complexes. While natural two-phase transmissivity influences the productivity of self-flowing high-enthalpy geothermal wells, in EGS the hydraulic transmissivity and flow rate control the amount of producible energy to a significant part.

Different challenges are related to hydraulic transmissivity:

- 1) Prospection of naturally enhanced hydraulic transmissivity zones e.g. using geophysical methods
- 2) Exploration of naturally enhanced hydraulic transmissivity zones by drilling
- 3) Technical improvement of zones of economically insufficient hydraulic conditions using stimulation techniques
- 4) Fracking tight reservoirs

With the exception of the Pannonian Basin in Hungaria and its surrounding countries and the Tuscany region in Italy, which both are characterized by recent large extensional environments and recent magmatism, major temperature anomalies in Europe appear in graben systems and sedimentary basins (Figure 1-1). In this context, the research in the present study aims to investigate the formation and localization of natural transmissivities in a representative naturally fractured granitic basement of a typical graben system. The European Cenozoic Rifts System (ECRIS) hosts some of the major geothermal anomalies in Europe away from active volcanic areas. Its central segment, the Upper Rhine Graben (URG), stretching over 300 km between Basel (Switzerland) and Frankfurt (Germany), reveals several heat flow anomalies in the order of up to  $> 150 \text{ mW m}^{-2}$  and temperatures up to  $120^{\circ}\text{C}$  at 1km depth, including the anomalies of Soultz and Landau (Figure 1-2) which are currently under exploitation for electricity generation (1.5MW and 3MW electrical power size, respectively).

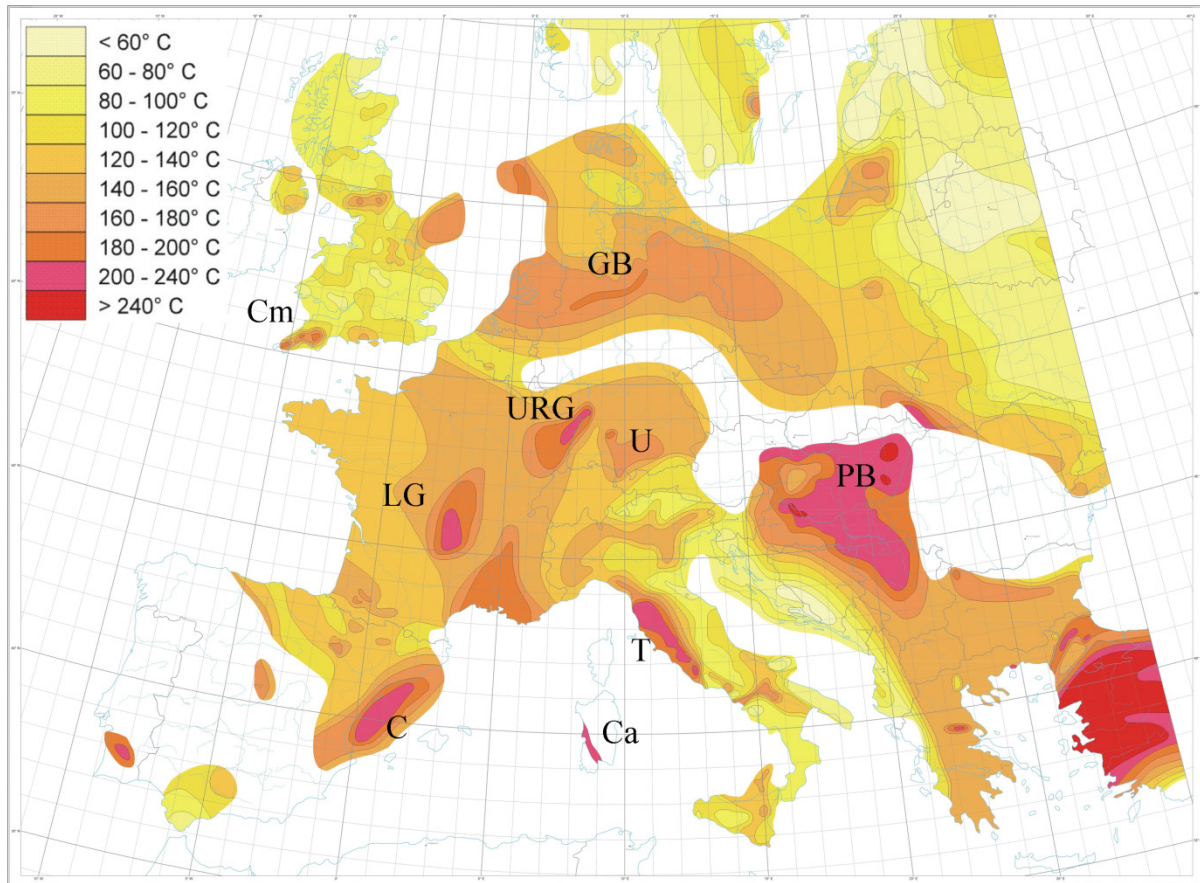


**Figure 1-1 : Map of temperature in Europe extrapolated to 5km depth - modified after Genter (2004) and Hurtig *et al.* (1992). URG: Upper Rhine Graben; U: Urach - molasse basin area; LG: Limagne graben-French Massif Central; C: Catalonia; Ca: Campidano graben; Cm: Camborne granite; GB: German basin; T: Tuscany; PB: Pannonian Basin.**

Before achieving electric power production, different proto-type projects have been realized in this tectonic setting. One of those at Soultz-sous-Forêts has been selected to develop the Hot Dry Rock (HDR) technology in 1987. The intention of HDR is the development of artificial permeability at depth of significant temperature  $> 200^{\circ}\text{C}$  to develop an artificial heat exchanger in the deep subsurface. Thus, HDR involves fracking technology in tight basement rock. Given the occurrence of natural fractures and hydrothermal fluid in the subsurface, the project has been developed as Enhanced Geothermal System (EGS) and represents today the only EGS project under exploitation world-wide (Figure 1-3 bottom). It should be mentioned here that the economic viability has to be questioned due to the current rather low net production of 250 kW from two 5000 m deep wells. In terms of technology the Landau project, which involves also zones of free convection, is situated in between hydrothermal aquifer utilization and EGS, since the production well reveals economic flow rates due to natural fracture permeability and the injection well has been hydraulically stimulated (Schindler *et al.*, 2010).

Since long the enhanced surface heat flux in the Upper Rhine valley has been related to the circulation of thermal water along fault zones (Illies, 1965). Illies & Greiner (1979) suggest that convective heat transport occurs along N-S striking fractures zones in the basement and in the high porosity sandstone (Buntsandstein) aquifer above it (Figure 1-4), because these fracture zones are favorably oriented with respect to the present day stress orientation and thus, may be reactivated, host slip movements and undergo dilatancy at depth under the hydraulic load.

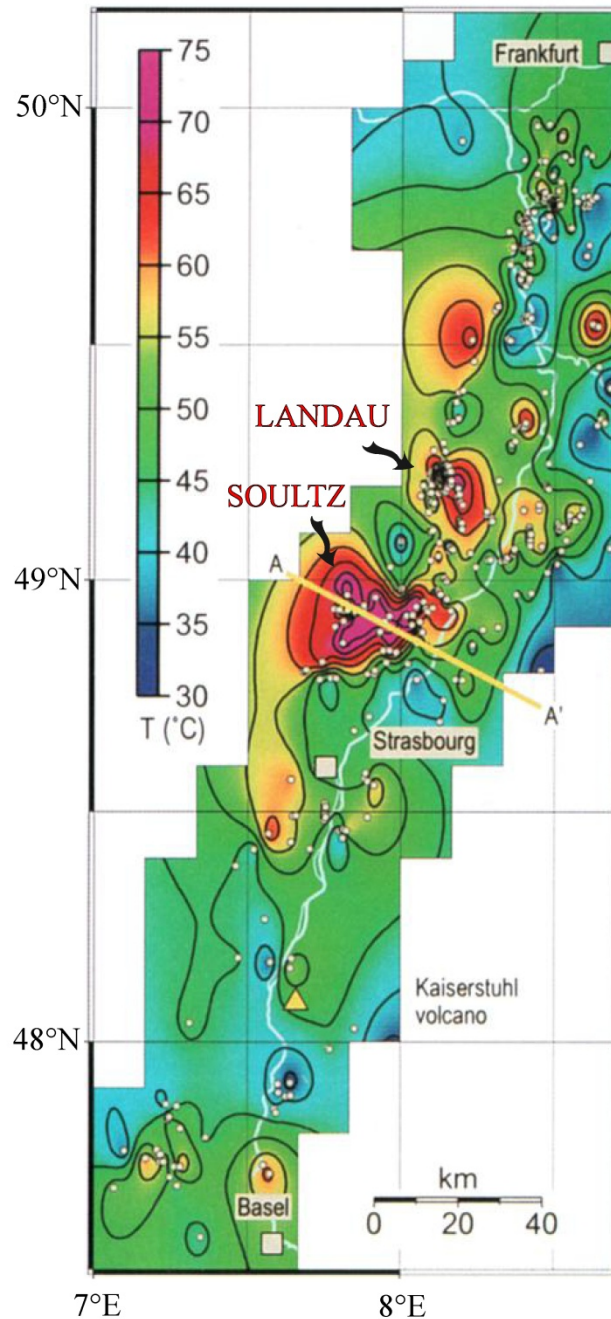


**Figure 1-2 : Temperature contour map of the Rhine Graben at a depth of 800 m modified after Pribnow and Schellschmidt (2000). Profile AA' approximately corresponds to cross-sections in Figure 1-4 and Figure 1-5.**

On a graben-wide scale, conceptual models have been developed involving E-W directed and vertical fluid transport. The models are based on the temperature distribution in the URG assuming advective or convective heat transport processes and geochemical observations showing a mixing of low salinity surface water from the West with higher salinity deep formational water from the East (Aquilina *et al.*, 1997 and references therein). Confirmed by numerical modeling of coupled thermo-hydraulic processes the temperature distribution has been attributed to a regional E-W directed flow in combination with local convection cells across several N-S trending fault systems (Figure 1-5) (e.g. Le Carlier de Veslud *et al.*, 1994; Pribnow and Schellschmidt, 2000).

### Enhanced geothermal system for heat and electricity production

1. Production and injection wells in stimulated reservoir
2. Heat exchangers
3. Power plant: ORC turbine and generator
4. Cooling tower
5. District heating

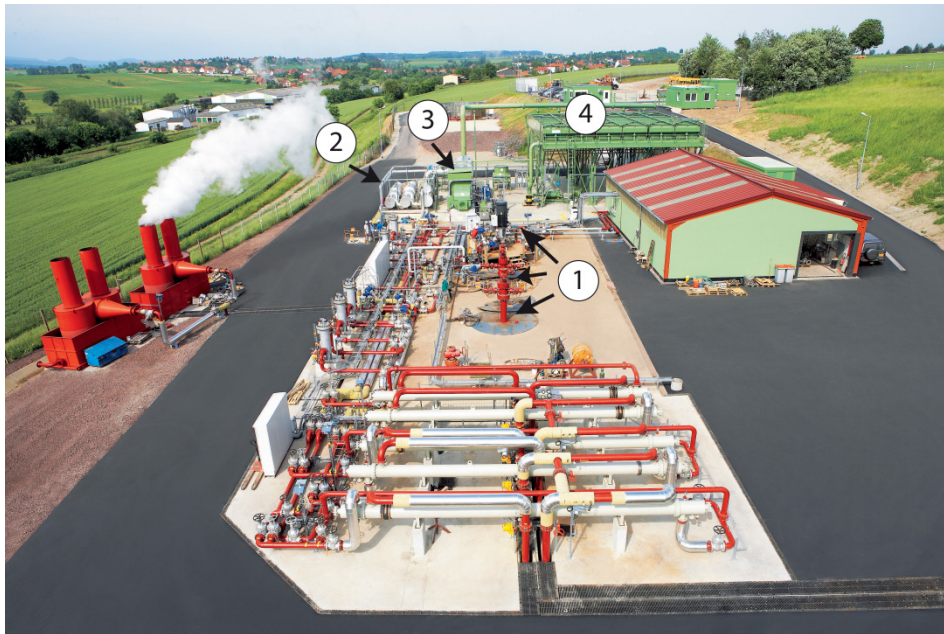
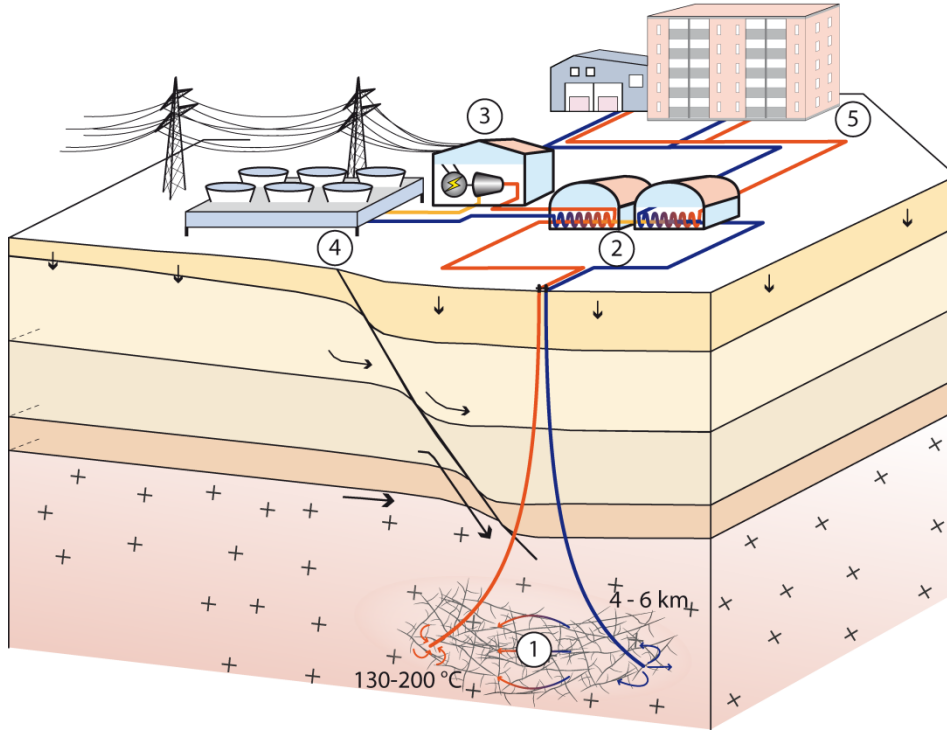
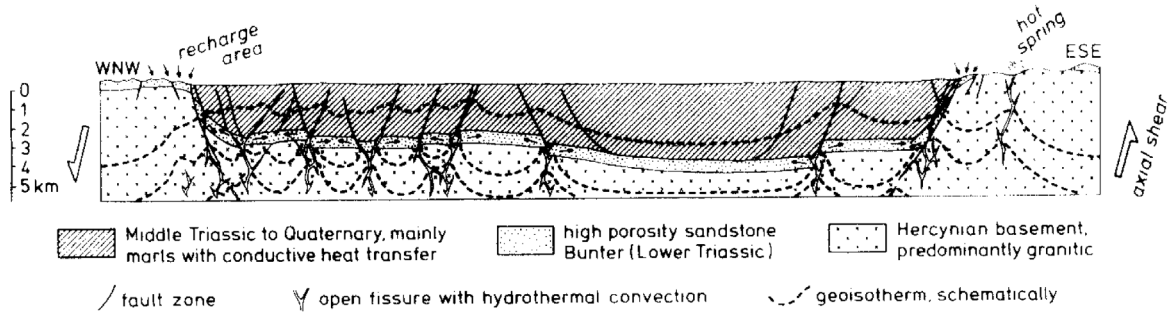


Figure 1-3 : top) Outline of a typical Enhanced geothermal system (EGS) for heat and electricity production in a fractured crystalline rock (after CREGE, 2010, Neuchâtel, Switzerland, [www.crege.ch](http://www.crege.ch)) bottom) Photograph of the surface EGS power plant of Soultz (Soultz GEIE EMC, France, <http://www.geothermie-soultz.fr>).

On a local scale, 3D thermo-hydraulic simulation of the geothermal site of Landau showed that graben-parallel faults are capable of hosting hydrothermal convection organized into cells bringing hot water from the basement to shallower levels in a N-S direction (Bächler *et al.*, 2003).





**Figure 1-4 : Generalized cross-section through the Rhinegraben South of Karlsruhe showing hydrothermal convection in shear controlled fissures of the basement, but heat conduction in the sedimentary fill (Illies *et al.*, 1981).**

of permeability required to produce temperature anomalies in the order of up to 120°C at 1 km depth has been carried out using 2D thermo-hydraulic modeling. Best-fit between the modeled and observed temperature distribution with depth in the geothermal wells of Soultz has been obtained for a permeability in the order of  $3 \cdot 10^{-14} \text{ m}^2$  (Kohl *et al.*, 2000). 3D geological models across the major geothermal anomalies in the Upper Rhine valley at Soultz-sous-Forêts and the adjacent fields of Landau and Speyer showed that these anomalies can be related to horst structures in central URG (Schill *et al.*, 2009). Horst structures reveal two relevant features. On the one hand they are characterized by boundary faults such as the Soultz and Kutzenhausen fault zones, which have revealed enhanced productivity, and on the other hand the basement, which reveals typically an enhanced radiogenic heat production and thus, contributes to the increase in heat flow. Jeannette & Edel (2005) suggest that the lithological nature of the basement, composed of Variscan granites and granodiorites intrusions (referred as crystalline ridges) is the main cause of the localization of geothermal anomalies in the URG.

In order to approach the understanding of formation and localization of naturally favorable conditions for geothermal systems in graben structures, i.e. the localization of naturally enhanced hydraulic conductivity zones, in a first step, we have analyzed the large scale relation between the geological and thermal setting of the URG. Based on the observations at graben-wide scale, the localization of possibly permeable structures has been analyzed on a smaller area corresponding in extension to the geothermal field of the Soultz site. The observations made on regional as well as on

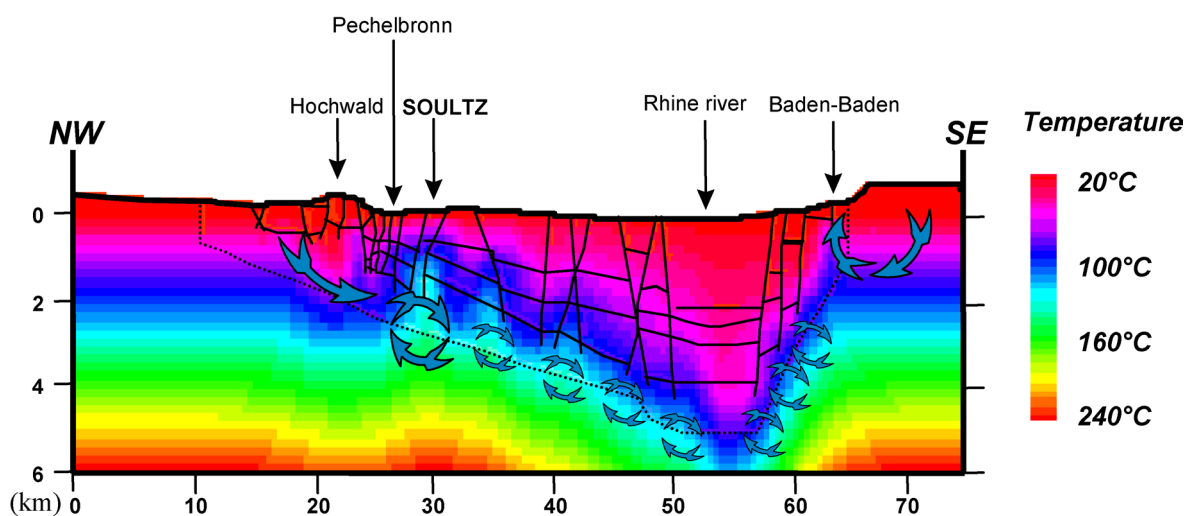


**Figure 1-5 : 2D computed temperature field across Soultz and Baden-Baden geothermal areas, modified after Sausse (1998) and Le Carlier de Veslud *et al.* (1994). Interpretation of fluid flow field (blue arrows) after Pribnow and Schellschmidt (2000).**

local level have been reproduced in a 2D mechanical numerical model of the URG opening at the latitude of Soultz, in order to understand the tectonic condition leading to a comparable distribution of thermal anomalies. In the following, we will describe shortly the geological framework of the URG. The different methodologies that have been used are presented shortly and integrated into a methodological concept, which shall provide an insight in the relation of the different studies to each other.

## 1.2 Geological framework

The Soultz area is located within the Upper Rhine Graben (URG), a preeminent structure of the European Cenozoic Rift System (ECRIS) (Ziegler, 1992). The ECRIS is an about 1100 km long system of rifts extending from the Mediterranean to the North Sea. It was activated during the Eocene in the foreland of the Pyrenees and Alps in response to the build-up of collision-related intra-plate stresses and is presently still active (Ziegler and Dezes, 2007). A number of successive rift systems align in approximately NNE-SSW direction: the Eger Graben, the Lower Rhine and Upper Rhine grabens, the Massif Central (including the Limagne graben) and Rhône Valley (including the Bresse graben) Rift Systems (Figure 1-6).

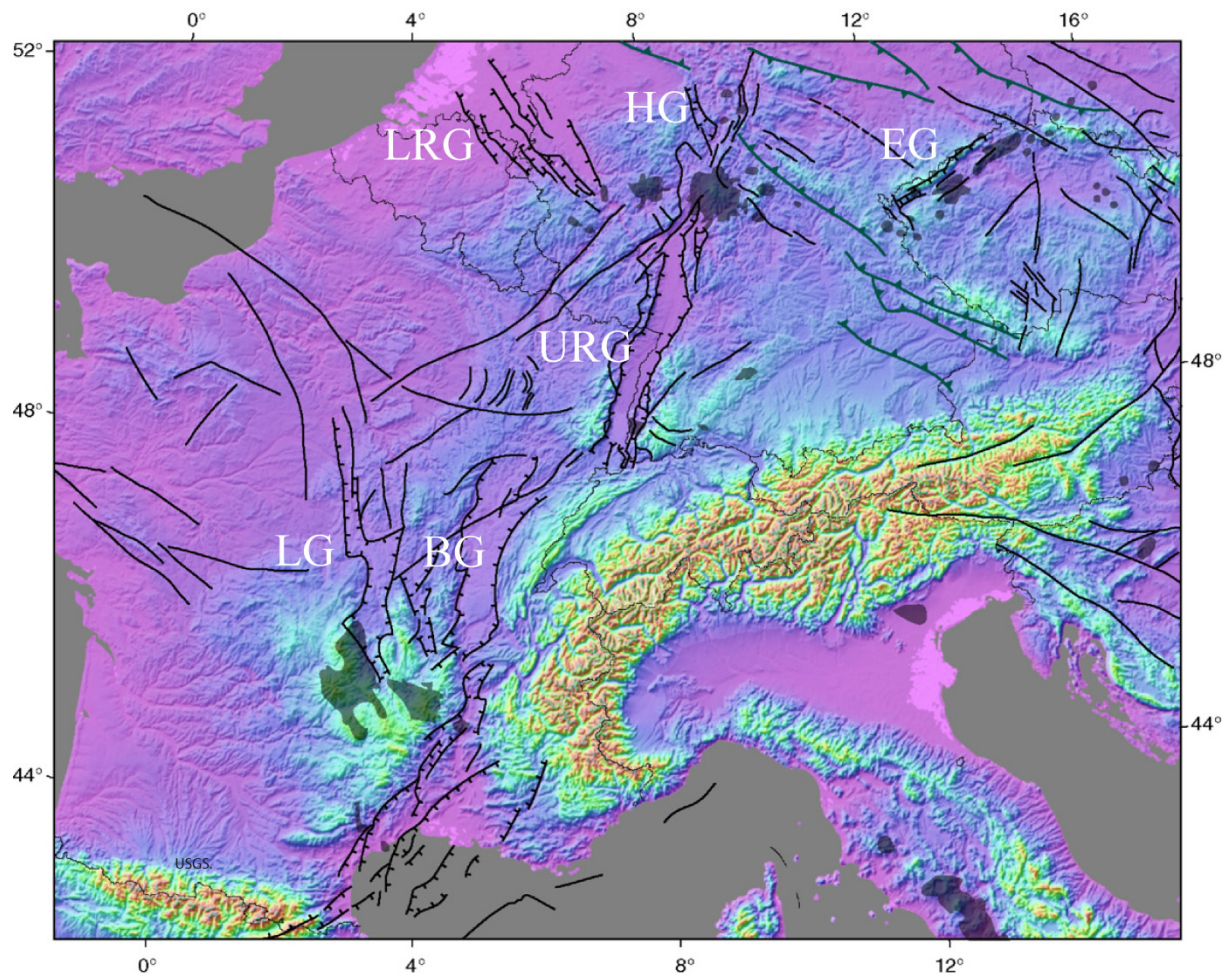


**Figure 1-6 : Emplacement of Graben Systems on the Digital Elevation Model of the European Cenozoic Rift System (ECRIS) area with superimposed ECRIS fault systems (thin lines), based on GTOPO30 with horizontal grid spacing of 30 arc sec, USGS, modified after Ziegler and Dèzes (2007). LRG: Lower Rhine Graben; HG: Hessian Graben; EG: Eger Graben; URG: Upper Rhine Graben; LG: Limagne Graben; BG: Bresse Graben.**

The general aspect of the URG can be characterized by its impressive symmetry (Illies, 1965) as depicted in Figure 1-7. From South to North, the Black Forest massif in the South is symmetrical with the Vosges massif, followed to the North by Kraichgau and Pfälzburger depression, and further to the North by Odenwald and Pfälzberger depression, and further to the North by Odenwald and Pfälzberger depression (Valley, 2007). The uplift of the Vosges and Black Forest accompanied by mantle uplift in the southern URG in Early Miocene are the cause of the overall decreasing age of rocks outcropping at the surface with increasing distance away from the E and W graben borders.

In contrast to the external symmetry, the internal part appears to be asymmetric (Figure 1-8 and Figure 1-9). The sedimentary deposition centers of the URG (as observed from the numerous

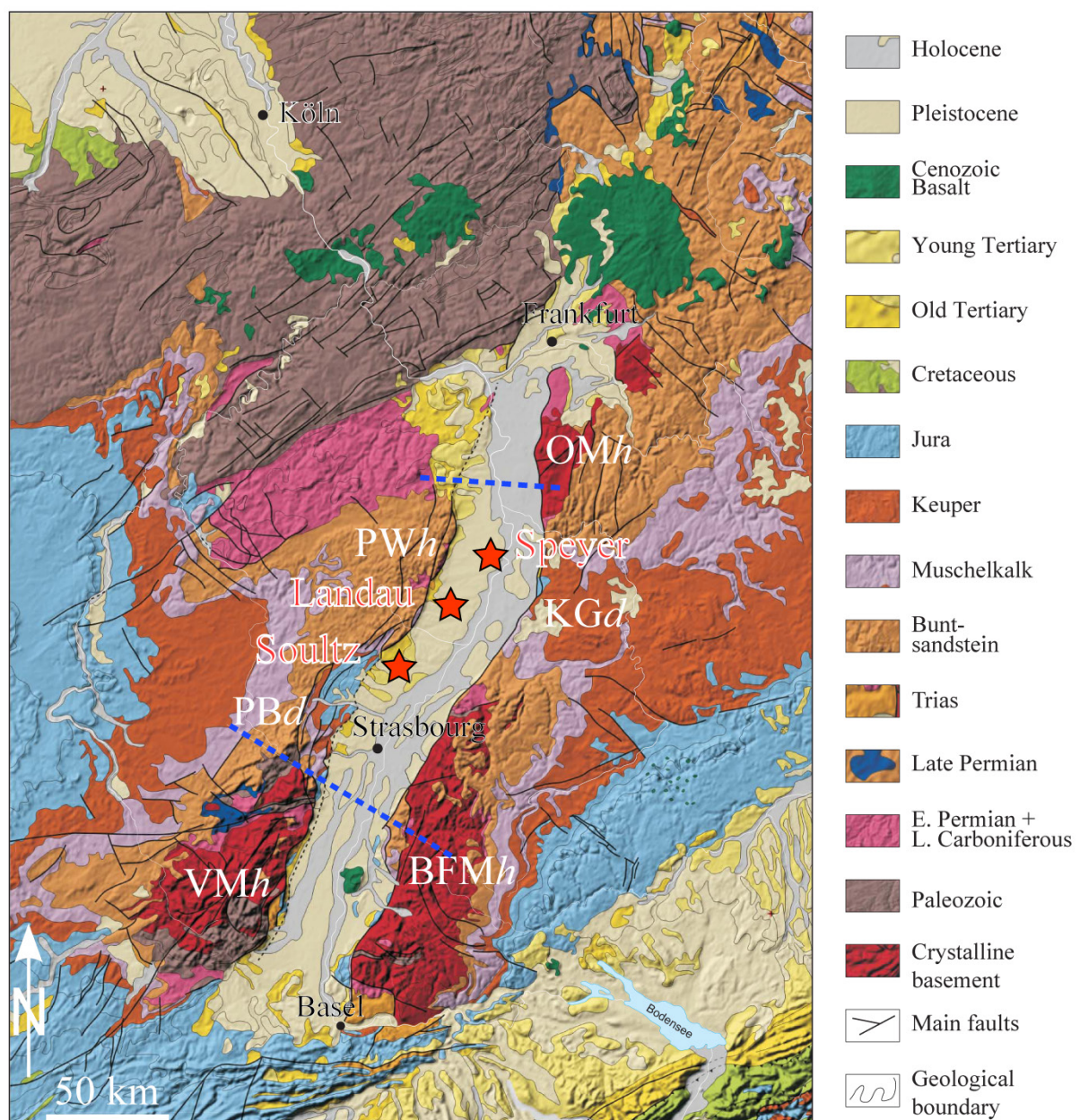
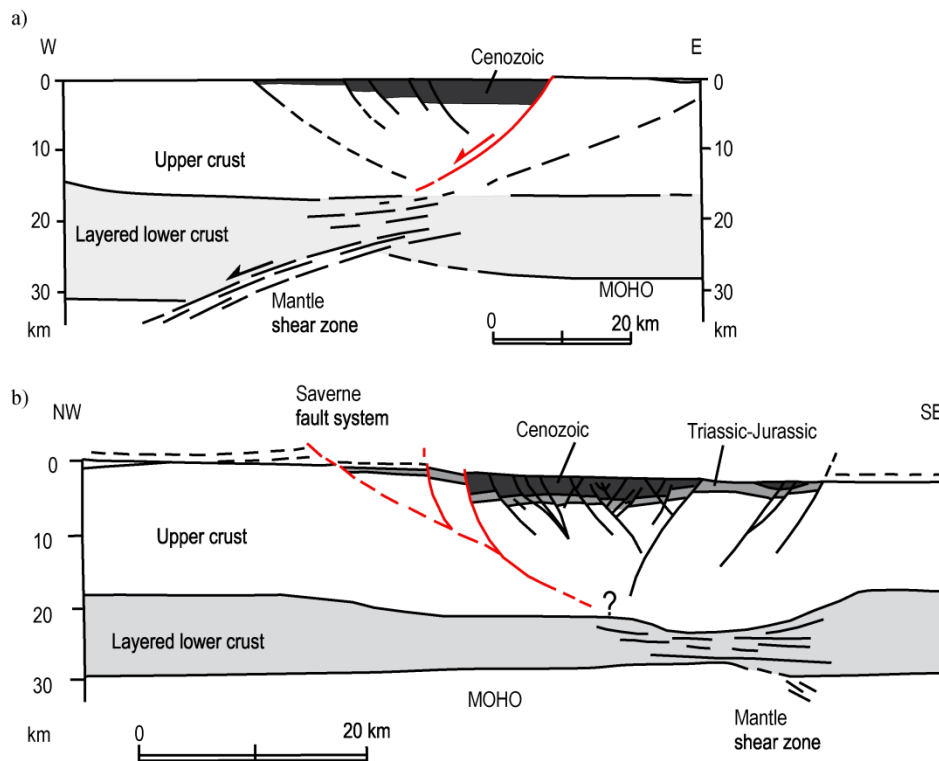


Figure 1-7 : Geological overview map of the Upper Rhine Graben area, modified after Lahner and Wellmer (2004) and Christian Röhr, 2006 (<http://www.oberrheingraben.de>). OMh: Odenwald Mountains high; PWh: Pfälzberger depression; KGd: Kraichgau depression; PBd: Pfälzburger depression; VMh: Vosges Mountains high; BFMh: Black Forest Mountains high. Location of the geothermal anomalies of the European EGS test-site Sultz, Landau and Speyer (red stars). Dashed blue lines approximately indicate location of traces of the cross-sections of Figure 1-8.

boreholes and seismic profiles acquired in the region mostly for petroleum exploration) are mostly located in the western side of the Rhine River in the southern part of the URG, but on the eastern side of the Rhine River in the northern part of the graben (Mannheim-Heidelberg trough). Deep seismic profiles were acquired to visualize the internal structure of the graben down to the mantle (Brun *et al.*, 1992). On the interpretation of seismic profiles (Figure 1-8), graben border faults appear to accommodate most of the vertical motion in an asymmetric way. In the southern part, the sediment deposition center is located on the western side of the graben (Brun *et al.*, 1991), where the vertical motion (around 3 km) was accommodated by the western border fault (Brun *et al.*, 1991; Cornu and Bertrand, 2005). In the northern part, the sediment deposition center is located on the eastern side of the graben where the vertical motion is maximal along the eastern border fault (Wenzel *et al.*, 1991).



**Figure 1-8 :** Interpreted cross-sections of the Rhine Graben from the ECORS-DEKORP seismic investigation of the crustal structure of the Upper Rhine Graben. a) northern profile. b) southern profile. Red lines denote the interpreted master fault accommodating the maximum offset. Modified after Brun *et al.* (1992) and Valley (2007). Locations of cross-sections on Figure 3.

There is a debate on-going since about 40 years on the evolution of the URG (Hinsken *et al.*, 2011 and references therein): although the most plausible and widely accepted scenario is a poly-phase Paleogene extension (Middle Eocene to Early Miocene) approximately orthogonal to the strike of the URG followed by a Neogene (Pliocene to recent) sinistral transtension (Illies and Greiner, 1978; Dèzes *et al.*, 2004), Schumacher (2002) proposes a five-stage model, while Behrmann *et al.* (2003) and Lopes Cardozo and Behrmann (2006) advance a model of continuous sinistral transtension.

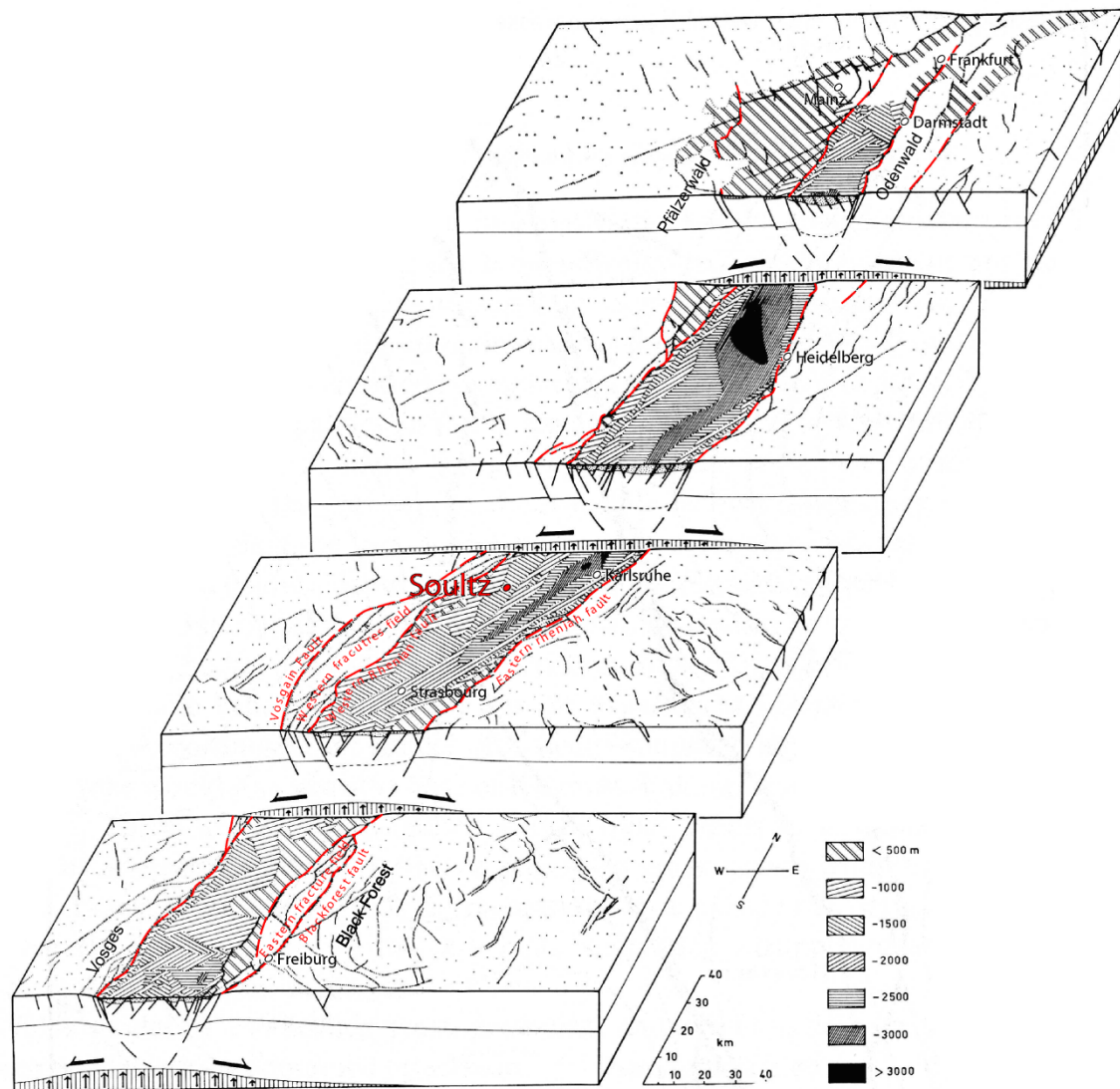


Figure 1-9: Block diagrams of the general Rhine Graben structure. Various hatching corresponds to the thickness of the Cenozoic sedimentary fill. Modified after Illies (1972) and Valley (2007). Location of the European EGS test-site Sultz (red point).

### 1.3 Methodology

Qualitative and partly quantitative analyses of the distribution of geothermal anomalies have been carried out with respect to neotectonic deformation, the lithology of the crystalline basement as well as geophysical observations such as gravity and magnetics (Chapter II). In order to understand localization of thermal anomalies in particular with respect to neotectonics and variations in basement lithology that occur typically on a graben-wide scale, different large-scale data sets have been selected according to relevant quality criteria (e.g. quality of temperature measurements), partly re-processed and combined into a comprehensive high-quality geothermal dataset of the URG. In the following, we present a list of the single data sets that have been combined:

- Subsurface temperature measurements after Pribnow and Schellschmidt (2000) and Agemar *et al.* (2012)
- Ground magnetic anomaly map: after Edel *et al.* (1982) and Papillon (1995)

Gravity maps covering the entire Graben:

-Bouguer anomalies: after Rotstein *et al.* (2006)

-Gravity vertical gradient: after Edel (2004) and Edel *et al.* (2007)

Geostatistical analyses such as cross correlation have been used to support the qualitative observations revealing correlation between temperature, magnetic and gravity fields, their interpretation in terms of basement lithology and also with neotectonic activity of the URG. The most important finding, the correlation between negative gravity anomalies and temperature maxima, has led to the conclusion that gravity can be partly linked to basement lithology, but also fracture porosity.

Thus, in a second step, the distribution of thermal anomalies on a more local level, following the extension of the geothermal field of Soultz, has been investigated, since fault zones are well-known to be related to fracture porosity and their spatial distribution can be reconstructed from a number of 2D seismic lines.

Thus, a new geometrically consistent and constrained 3D regional geological model of the faults and layers to a depth of 6 km has been elaborated using recently available seismic sections and borehole information (Baillieux *et al.*, 2011; Dezayes *et al.*, 2011- Appendix A and B). This 3D geological model is used as a basis for reinterpreting the localization of geothermal anomalies using the numerous borehole temperature measurements that have recently been gathered in the area (Chapter III). First, the temperature field is projected to the top of basement. Secondly, the structural patterns observed in the 3D geological model are compared to the temperature distribution. A geophysical reinterpretation is then carried out using the complete magnetic and gravity datasets of the area, together with the observed temperature patterns. Finally a slip and dilation tendency analysis is carried out on the fault system of the 3D geological model to understand the implication of observed stress patterns for the localization of the temperature anomalies. The major conclusion from this study leads to the hypothesis that westward oriented fault zones in horst structures provide sufficient natural hydraulic pathways to account for the major thermal anomalies in the URG.

To accomplish the aim of the research work, to understand the localization of natural permeability in graben systems, numerical mechanical modeling has been carried out (Chapter IV). The geodynamics code "Underworld" was used. It consists in a Lagrangian *particle-in-cell* finite element scheme (Moresi *et al.*, 2007) that enables the accurate tracking of stress and strain-rate history in simulations involving large-scale deformation. This platform includes a toolkit for studying the geodynamics of a viscoelastic-plastic lithosphere in 3D. It allows modeling of complex long-term geological processes such as geological creation of complex geometries such as brittle faulting, mantle upwelling in continental extension. For benchmarking these models, seismic sections through the Upper Rhine valley were selected (Brun *et al.*, 1992). The resulting models suggest asymmetry in the development of the Upper Rhine Graben and the deformation of its internal structures which corresponds to the observations and hypotheses developed in the previous chapters.

## 1.4 References

Agemar, T., Schellschmidt R. and Schulz R. (2012). Subsurface temperature distribution in Germany. *Geothermics* 44(0): 65-77.

- Aquilina, L., Pauwels H., Genter A. and Fouillac C. (1997). Water-rock interaction processes in the Triassic sandstone and the granitic basement of the Rhine Graben: Geochemical investigation of a geothermal reservoir. *Geochimica et Cosmochimica Acta* 61(20): 4281-4295.
- Bächler, D., Kohl T. and Rybach L. (2003). Impact of graben-parallel faults on hydrothermal convection - Rhine Graben case study. *Physics and Chemistry of the Earth* 28(9-11): 431-441.
- Baillieux, P., Schill E. and Dezayes C. (2011). 3D structural regional model of the EGS Soultz site (northern Upper Rhine Graben, France): insights and perspectives. *Proceedings, Thirty-Sixth Workshop on Geothermal Reservoir Engineering, Stanford University, Stanford, California, SGP-TR-191*.
- Behrmann, J. H., Hermann O., Horstmann M., Tanner D. C. and Bertrand G. (2003). Anatomy and kinematics of oblique continental rifting revealed: A three-dimensional case study of the southeast Upper Rhine graben (Germany). *AAPG Bulletin* 87(7): 1105--1121.
- Bertani, R. (2012). Geothermal power generation in the world 2005-2010 update report. *Geothermics* 41(0): 1-29.
- Brun, J. P., Gutscher M. A. and {DEKORP-ECORS teams} (1992). Deep crustal structure of the Rhine Graben from seismic reflection data: A summary. *Tectonophysics* 208(1-3): 139-147.
- Brun, J. P., Wenzel F. and {ECORS-DEKORP team} (1991). Crustal-scale structure of the southern Rhinegraben from ECORS-DEKORP seismic reflection data. *Geology* 19: 758--762.
- Cornu, T. G. M. and Bertrand G. (2005). Numerical backward and forward modelling of the southern Upper Rhine Graben (France-Germany border): new insights on tectonic evolution of intracontinental rifts. *Quaternary Science Reviews* 24(3-4): 353-361.
- Dezayes, C., Becaletto L., Oliviero G., Baillieux P., Capar L. and Schill E. (2011). 3-D visualization of a fractured geothermal field: the example of the EGS Soultz site (Northern Upper Rhine Graben, France). *PROCEEDINGS, Thirty-Sixth Workshop on Geothermal Reservoir Engineering Stanford University*
- Dèzes, P., Schmid S. M. and Ziegler P. A. (2004). Evolution of the European Cenozoic Rift System: interaction of the Alpine and Pyrenean orogens with their foreland lithosphere. *Tectonophysics* 389: 1--33.
- Edel, J. B. (2004). Structure et évolution du Fossé Rhénan, du Carbonifère à nos jours - apports de la géophysique. *Bulletin de la société d'histoire naturelle et d'ethnographie de Colmar* 65(2004): 21-50.
- Edel, J. B., Campos-Enriquez O., Goupillot M. and Kiro K. N. (1982). Levé magnétique au sol du Fossé rhénan supérieur. *Interpretation géologique. Bull. Bur. Rech.Géol. Min.* 2: 179-192.
- Edel, J. B., Schulmann K. and Rotstein Y. (2007). The Variscan tectonic inheritance of the Upper Rhine Graben: evidence of reactivations in the Lias, Late Eocene-Oligocene up to the recent. *International Journal of Earth Sciences* 96(2): 305-325.
- Genter, A. (2004). avec la collaboration de Guillou-Frottier L., Breton J.P., Denis L., Dezayes Ch., Egal E., Feybesse J.L., Goyeneche O., Nicol N., Quesnel F., Quinquis J.P., Roig J.Y., Schwartz S. *Typologie des systèmes géothermiques HDR-HFR en Europe, BRGM*: 165.
- Hinsken, S., Schmalholz S. M., Ziegler P. A. and Wetzler A. (2011). Thermo-Tectono-Stratigraphic Forward Modelling of the Upper Rhine Graben in reference to geometric balancing: Brittle crustal extension on a highly viscous mantle. *Tectonophysics* 509(1-2): 1-13.
- Hurtig, E., Gotha H. H. G.-K. A., Commission I. H. F., DDR) Z. f. r. P. d. E. A. d. W. d., Verlagsgesellschaft H. H., Potsdam K. D. and Brandenburg L. (1992). *Geothermal atlas of Europe / edited by E. Hurtig ... [et al.] ; International Association for Seismology and Physics of the Earth's Interior, International Heat Flow Commission; Central Institute for Physics of the Earth.*
- Illies, H. (1972). The Rhine graben rift system - plate tectonic and transform faulting. *Geophysical Survey* 1: 27--60.
- Illies, H. J. and Greiner G. (1979). Holocene movements and state of stress in the rhinegraben rift system. *Tectonophysics* 52(1-4): 349--359.
- Illies, J. H. (1965). Bauplan und Baugeschichte des Oberrheingrabens. Ein Beitrag zum "Upper Mantle Project". *Oberrheinische Geologische Abhandlungen* 14: 1-54.

- Illies, J. H., Baumann H. and Hoffers B. (1981). Stress Pattern and Strain Release in the Alpine Foreland. *Tectonophysics* 71(1-4): 157-172.
- Illies, J. H. and Greiner G. (1978). Rhinegraben and Alpine system. *Geological Society of America Bulletin* 89: 770-782.
- Jeannette, D. and Edel J. B. (2005). Contexte géologique du site géothermique de Soultz-Sous-Forêts. *bulletin de l'Association Philomatique d'Alsace et de Lorraine Tome 40*.
- Kohl, T., Bächler D. and Rybach L. (2000). Steps towards a comprehensive thermo-hydraulic analysis of the HDR test site Soultz-sous- Forêts. *Proc. World Geothermal Congress 2000, Kyushu-Tohoku, Japan, May-June 2000*, pp. 2671-2676.
- Lahner, L. and Wellmer F.-W. (2004). *Geowissenschaftliche Karte der Bundesrepublik Deutschland 1:2.000.000. Geologie, Bundesanstalt für Geowissenschaften und Rohstoffe; Hannover*.
- Le Carlier de Veslud, C., Royer J.-J. and Flores E. L. (1994). Convective heat transfer at the Soultz-sous-Forêts geothermal site: implications for oil potential. *EAGE vol. 12*.
- Lopes Cardozo, G. G. O. and Behrmann J. H. (2006). Kinematic analysis of the Upper Rhine Graben boundary fault system. *Journal of Structural Geology* 28(6): 1028-1039.
- Moresi, L., Quenette S., Lemiale V., Meriaux C., Appelbe B. and Muhlhaus H. B. (2007). Computational approaches to studying non-linear dynamics of the crust and mantle. *Physics of The Earth and Planetary Interiors* 163(1-4): 69-82.
- Papillon, E. (1995). *Traitements et interpretations des cartes d'anomalies magnétiques et gravimétriques du Fossé Rhénan supérieur. Dipl. Ing. Géophys. Strasbourg I, 95p*.
- Pribnow, D. and Schellschmidt R. (2000). Thermal tracking of upper crustal fluid flow in the Rhine Graben. *Geophysical Research Letters* 27(13): 1957-1960.
- Rotstein, Y., Edel J. B., Gabriel G., Boulanger D., Schaming M. and Munsch M. (2006). Insight into the structure of the Upper Rhine Graben and its basement from a new compilation of Bouguer Gravity. *Tectonophysics* 425(1-4): 55-70.
- Sausse, J. (1998). *Caractérisation et modélisation des écoulements fluides en milieu fissuré. Relation avec les altérations hydrothermales et quantification des paléocontraintes. PhD thesis, Université Henri Poincaré, Nancy 1, France [http://halshs.archivesouvertes.fr/docs/00/06/04/28/PDF/these\\_SAUSSE.pdf](http://halshs.archivesouvertes.fr/docs/00/06/04/28/PDF/these_SAUSSE.pdf)*.
- Schill, E., Kohl T., Baujard C. and Wellmann J.-F. (2009). *Geothermische Ressourcen in Rheinland-Pfalz: Bereiche Süd- und Vorderpfalz, Final report to the Ministry of Environment Rhineland-Palatine, 55p*.
- Schindler, M., Baumgärtner J., Terry G., Hauffe P., Hettkamp T., Menzel H., Penzkofer P., Teza D., Tischner T. and Wahl G. (2010). Successful Hydraulic Stimulation Techniques for Electric Power Production in the Upper Rhine Graben, Central Europe. *Proceedings World Geothermal Congress 2010 Bali, Indonesia, 25-29 April 2010*.
- Schumacher, M. E. (2002). Upper Rhine Graben: Role of preexisting structures during rift evolution. *Tectonics* 21(1).
- Valley, B. (2007). *The relation between natural fracturing and stress heterogeneities in deep-seated crystalline rocks at Soultz-sous-Forêts (France), PhD thesis, ETH-Zürich, Switzerland, <http://e-collection.ethbib.ethz.ch/view/eth:30407>, 260 p*.
- Wenzel, F., Brun J. P., Blum R., Bois C., Burg J. P., Coletta B., Durbaum H., Durst H., Fuchs K., Grohmann N., Gutscher M. A., Hubner M., Karcher T., Kessler G., Klockner M., Lucazeau F., Luschen E., Marthelot J. M., Meier L., Ravat M., Reichert C., Vernassat S. and Villemin T. (1991). A Deep Reflection Seismic Line across the Northern Rhine Graben. *Earth and Planetary Science Letters* 104(2-4): 140-150.
- Ziegler, P. A. (1992). European Cenozoic rift system. *Tectonophysics* 208(1-3): 91-111.
- Ziegler, P. A. and Dezes P. (2007). Cenozoic uplift of Variscan Massifs in the Alpine foreland: Timing and controlling mechanisms. *Global and Planetary Change* 58: 237-269.



## **Chapter II: Localization of temperature anomalies in the Upper Rhine Graben: insights from geophysics and neotectonic activity**

Paul Baillieux<sup>1</sup>, Eva Schill<sup>1</sup>, Jean-Bernard Edel<sup>2</sup>, Guillaume Mauri<sup>1</sup>

1 - Centre for Hydrogeology and Geothermics, Neuchâtel University, rue Emile Argand 11 CH-2000 Neuchâtel, Switzerland

paul.baillieux@unine.ch

2- Ecole et Observatoire des Sciences de la Terre, UMR 7516, 5 rue Descartes, 67084 Strasbourg cedex, France

### **Abstract**

Gravimetric, magnetic data and neotectonic activity patterns are used to investigate the implication of density and magnetic variations, and stress and strain patterns associated to the localization of temperature anomalies at the scale of the Upper Rhine Graben. The occurrence of compression shear and uplift regime in present day, accompanied with rather low seismicity, and emplacements of low density and fractured granitic basement (of early Carboniferous age) appear to be responsible for the localization of the major temperature anomalies.

### **2.1 Introduction**

The Upper Rhine Graben is a preeminent structure of the European Cenozoic Rift System (ECRIS) (Ziegler, 1992). The ECRIS is an about 1100 km long system of rifts extending from the Mediterranean to the North Sea. It was activated during the Eocene in the foreland of the Pyrenees and Alps in response to the build-up of collision-related intra-plate stresses and is presently still active (Ziegler and Dezes, 2007). A number of successive graben systems align in approximately ENE-WSW direction: the Eger graben, the Rhine (Lower and Upper Rhine grabens), the Massif Central (Limagne, Roanne and Forez grabens) and Rhône Valley (Bresse, Valence, Alés, Manosque and Camarque grabens) Rift Systems.

These rift systems reveal important maxima in mean surface heat flux and subsurface temperature in central Europe (Hurtig *et al.*, 1992; Genter *et al.*, 2003; Cloetingh *et al.*, 2010), where a mean surface heat flux of approximately 60 mW m<sup>-2</sup> is observed (Majorowicz and Wybraniec, 2011). While the northernmost graben systems such as the Eger, Roer Valley –Lower Rhine and Hessian grabens are characterized by a mean surface heat flux of about 70-80 mW m<sup>-2</sup> with maximum anomalies > 90 mW m<sup>-2</sup>, in the southern graben systems, the Massif Central –Rhône Valley rift systems, a mean surface heat flux of about 90-100 mW m<sup>-2</sup> is observed. Maximum mean surface heat flux of about 100-120 mW m<sup>-2</sup> with maxima of > 150 mW m<sup>-2</sup> in its central segment is observed in the Upper Rhine Graben (URG).

Maximum temperatures at depth are found in the Massif Central rift system and URG. At 5 km depth temperatures may reach 200-240 °C (Genter *et al.*, 2003). In the Rhône valley rift system, temperatures of about 160 to 200 °C are estimated at the same depth.

Local maximum values of surface heat flux and the above mentioned subsurface temperatures can even be related to shallow, in-situ oil and gas production and thus, indicate also favorable condition for geothermal utilization in central Europe away from volcanic areas (Genter *et al.*, 2003). In the URG, local high thermal gradients up to  $> 100^{\circ}\text{C km}^{-1}$  in the uppermost kilometer of the crust representing the sedimentary cover of the Variscan crystalline basement have been associated to free hydrothermal circulation at the graben scale (Schellschmidt and Clauser, 1996; Pribnow and Schellschmidt, 2000), as well as free convection along the major faults in the area of Landau (Bächler *et al.*, 2003), and at the European Enhanced Geothermal System (EGS) test-site Soultz-sous-Forêts (Kohl *et al.*, 2000).

These local phenomena emphasize that temperature is not homogeneously distributed in the URG and neither are geothermal anomalies. Different geological facts were solicited to explain the localization of geothermal anomalies on a regional level in the URG. The geothermal anomaly at Soultz, for example, has been on the one hand attributed to recent compressive shear strain occurring parallel to the central segment of the graben (Illies and Greiner, 1979), allowing hydrothermal circulation to occur along favorably oriented fracture zones in the basement and in the high porosity sandstone aquifer above it. On the other hand it has been correlated to the lithological nature of the basement and its inherited orientations (Jeannette and Edel, 2005).

The tectonic history of the Tertiary graben has a significant relevance for both interpretations, since the generally postulated poly-phase opening of this graben led to different thermo-tectonic features (Villemin and Bergerat, 1987; Schumacher, 2002; Dèzes *et al.*, 2004; Edel *et al.*, 2007; Hinsken *et al.*, 2011):

- 1) Reactivation of Variscan pre-discontinuities in normal faulting regime assumed to have occurred during Paleogene may have resulted among others in the formation of variable depth of the top of the basement and thus, in variable significance of the contribution of radiogenic heat production to the total vertical heat flux.
- 2) Reactivation of the graben fault system in main sinistral strike-slip regime assumed to have occurred during Neogene may have resulted in localization of pathways for geothermal fluid.

The lithological structure of pre-Permian basement, which may represent another source of variability in the contribution of radiogenic heat production to the total vertical heat flux, has been inferred from interpretation of crustal scale reflection seismic profiles, gravity, magnetic, outcrops and boreholes data and is provided in two basement maps covering the entire URG (Edel, 2004; Edel and Schulmann, 2009). The neo-tectonic activity of the URG can be approached by integrating the different studies: surface height changes (e.g. Zippelt and Malzer, 1987; Fuhrmann *et al.*, in press), seismicity and in situ measurement of stress field (e.g. Illies and Greiner, 1979; Plenefisch and Bonjer, 1997), thickness of Quaternary sediments (e.g. Bartz, 1974; Schumacher, 2002) and faulting styles in Quaternary sediments on seismic sections (e.g. Bertrand *et al.*, 2006; Rotstein and Schaming, 2008). The aim of the study is to understand the role of the geological inhomogeneity in the basement, and the URG tectonic history up to present with regard to the distribution of geothermal anomalies, at the URG scale. To this end, the spatial temperature distribution at depth is newly interpolated and compared to compiled basement maps as well as some of their original geophysical data and the neo-tectonic activity in the URG. In this respect the interpretation of gravity data and their correlation to the temperature distribution has been found to be a special issue.

## 2.2 Geological settings

### 2.2.1 Pre-Permian Basement in the URG

The Mid-European Variscides resulted from Late Carboniferous collision of a passive continental margin in the lower-plate position (the Rhenohercynian basin) with a continental fragment in an upper-plate position: the Saxothuringian microplate (e.g. Franke, 1989; Oncken, 1997; Oncken, 1998). Precursor of this collision is the subduction underneath the Saxothuringian zone from Late Devonian to Early Carboniferous (Engel and Franke, 1983). Remnants of an Early Carboniferous continental magmatic arc (Mid-German crystalline rise) and fore-arc (Saar basin) are observed on the former Saxothuringian upper-plate leading edge (Willner *et al.*, 1991; Flottmann and Oncken, 1992; Oncken, 1998). According to Kroner *et al.* (2007) the subdivision of the Saxo-Thuringian zone in three principal units (autochthonous domain, wrench and thrust zone, and allochthonous domain) and their heterogeneous overprint by two regional deformation events during the Variscan orogeny explains the entire geological record with a widespread occurrence of Late Devonian to Early Carboniferous high-pressure metamorphic units tectonically juxtaposed with low-grade Paleozoic successions. The Moldanubian Zone is a heterogeneous accretionary collage of various Gondwana-sourced terranes, exposed in the Massif Central, Vosges, Black Forest, and the Bohemian Massif (Banka *et al.*, 2002).

Consequently, the basement of the Upper Rhine graben has been distinguished geologically in relation with the crystalline basement in eastern Germany and the adjacent countries from North to South into Rhenohercynian, Saxothuringian, Mid-German crystalline and Moldanubian zones (Kossmat, 1927). It can be inferred that also the lithology of the pre-Permian basement of the URG is highly variable.

Several geophysical studies have been carried out to infer the lithology and structure of the URG basement hidden under Mesozoic and Tertiary sediments (Figure 2-1) using analog geological and geophysical studies in the adjacent mountain areas. On a continental scale, geophysical potential field images provide an overview of the entire Palaeozoic orogenic system of northern and central Europe (Banka *et al.*, 2002). The Trans-European suture zone is largely concealed by sedimentary basins of Permian–Cenozoic age and geological observations are largely restricted to local basement highs and deep boreholes, and the coverage of deep seismic surveys is widely spaced. The gravity and magnetic image highlight the most fundamental features of the crustal structure of this suture zone (Banka *et al.*, 2002). These includes the strong contrast between the highly magnetic crust of the East European Craton and the less magnetic Palaeozoic-accreted terranes of central Europe; the lateral continuity of terranes and their internal structure, particularly where arc-magmatic complexes are involved; and the location and geometry of the terrane boundaries (oceanic sutures and strike-slip zones) that separate them.

On a regional, graben-wide scale, a combination of gravity, magnetics, seismics, outcrops, boreholes and geological knowledge has been used to postulate a lithological map of the variscan basement (Edel, 2004 and reference therein; Edel and Schulmann, 2009). It revealed that the pre-rift structures in the crystalline basement of the URG follow as expected the continuous Vosges – Upper Rhine

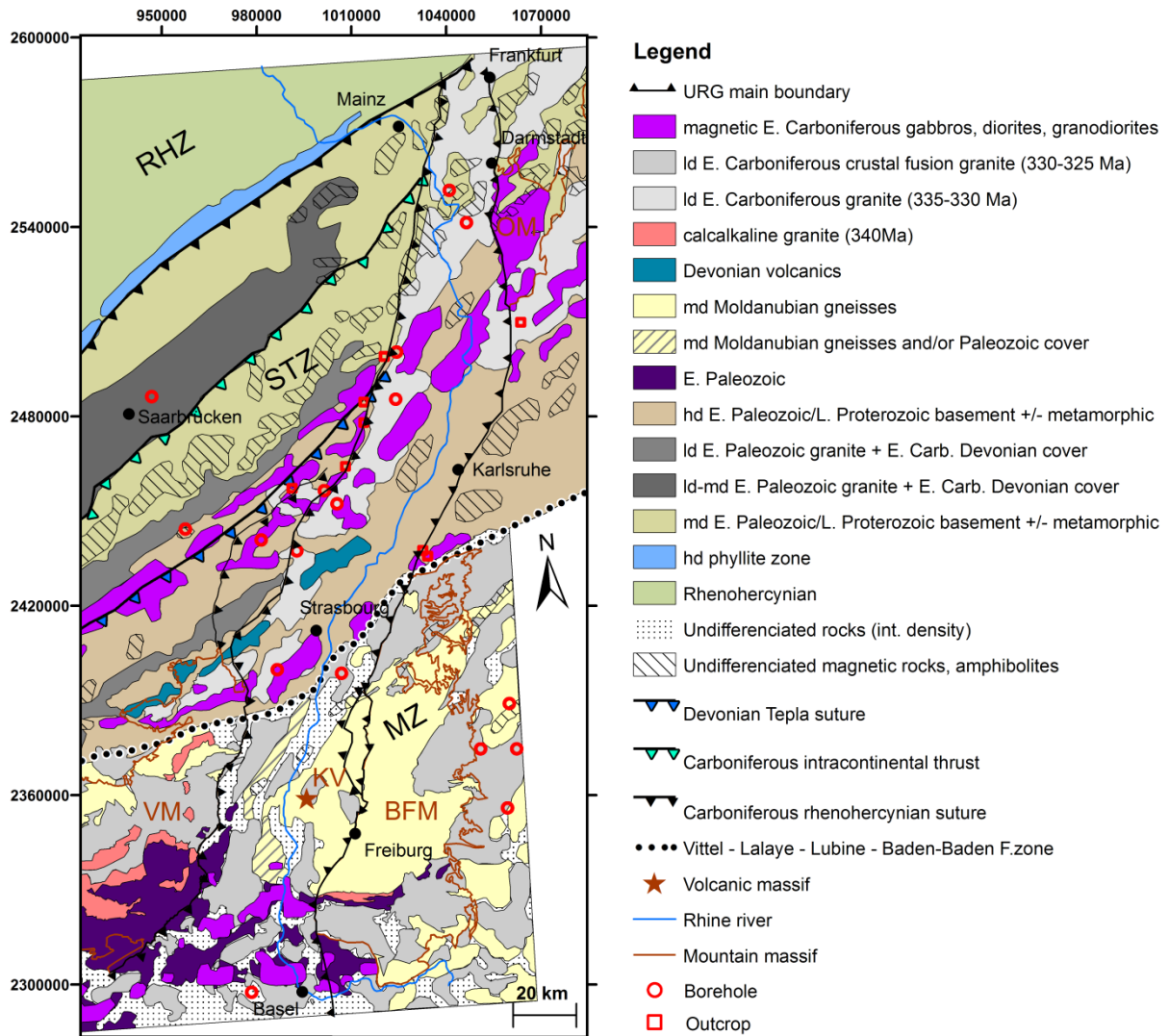


**Figure 2-1 :** Compilation of Edel (2004) and Edel and Schulmann (2009) interpretative maps showing the major units and tectonic features beneath the pre-Late Carboniferous - Permian basin. ld :low density; md: medium density; hd: high density; RHZ:Rhenohercynian Zone; STZ: Saxo-Thuringian Zone; MZ: Moldanubian Zone; VM: Vosges mountains; BFM: Blackforest mountains; OM: Odenwald mountains; KV: Kaiserstuhl Volcanic massif. Lambert II coordinates.

Graben – Black Forest massifs marked by NE-SW discontinuities developing from Devonian times on (Edel and Fluck, 1989; Edel *et al.*, 2006). From North to South, the NE-SW trending Rhenohercynian, Saxothuringian and Moldanubian zones are indicated in the basement of the URG in Figure 2-1. The geophysical approach used by Edel & Schulmann (2009) highlights the major pre-rift structures in the region as a succession of SE dipping subduction and underthrusting zones of the western Variscides. Geophysically, they are represented to a large part by positive gravity and magnetic anomalies as well as important SE dipping reflectors on the deep seismic profiles (Brun *et al.*, 1992). A NE-SW striking zone of increased magnetic intensity is observed in the northern Vosges and continuous underneath the sedimentary cover of the URG in the Saxothuringian zone. It is interpreted as a magmatic arc emplaced between 335-330 Ma. The emplacement took place along NW dipping, normal faults with a sinistral strike slip component associated with the Carboniferous subduction of the Rhenohercynian basin beneath the Saxothuringian continental plate (Edel and Weber, 1995). In the center of the Saxothuringian zone, an earlier subduction system is expected to have been active during Devonian times. It is represented by Devonian volcanics outcropping in the northern Vosges and occurring at depth between Strasbourg and Soultz. To conclude the URG basement results from

the juxtaposition of the northern Saxothuringian zone, mainly composed of Precambrian gneisses and schists crosscut by the 335-330Ma calcalkaline diorite, granodiorite and granite intrusions, and the southern Moldanubian zone dominated by high pressure metamorphism, by syenitic magmatism (340 Ma) followed by crustal origin magmatism (330-325 Ma) (Edel, 2004).

## 2.2.2 Structural development of the Upper Rhine Graben

After the Variscan orogeny, which late phase is characterized by large extensional structures causing regionally extended often NNE-SSW trending graben structures such as the Kraichgau or Schramberg troughs (Ziegler *et al.*, 2004), the eroded massif provides depositional environment throughout the Mesozoic period giving space mainly to Mesozoic platform sediments which deposited in Triassic (namely, Buntsandstein, Muschelkalk and Keuper) and Jurassic (Lias and Dogger) times. The URG originates in Paleogene times from the Alpine and Pyrenean collisions due to the build-up of far-field intraplate compressional stresses (Ziegler, 1992), and is described as a typical example of synorogenic intracontinental foreland rifting affected by Variscan crustal pre-discontinuities (cf. discussions on the topic in Schumacher, 2002; Dèzes *et al.*, 2004; Cloetingh *et al.*, 2006).

There is a debate on-going since about 40 years on the evolution of the URG (Hinsken *et al.*, 2011 and references therein): although the most plausible and widely accepted scenario is a poly-phase Paleogene extension (Middle Eocene to Early Miocene) approximately orthogonal to the strike of the URG followed by a Neogene (Pliocene to recent) sinistral transtension (Illies and Greiner, 1978; Dèzes *et al.*, 2004), Schumacher (2002) proposes a five-stage model, while Behrmann *et al.* (2003) and Lopes Cardozo and Behrmann (2006) advance a model of continuous sinistral transtension. According to Villemin (1986) and Villemin & Bergerat (1987) the tertiary tectonic history of the URG can be divided in four phases accompanied with different stress regimes from the Late Eocene rifting episodes, up to the Late Miocene, when the present stress regime was established. The URG was subjected to N–S oriented compression in the Late Eocene, E–W oriented extension in the Oligocene, and renewed NNE–SSW oriented compression in the Late Oligocene–Early Miocene (Bergerat, 1985; Villemin and Bergerat, 1987). A comprehensive summary is given recently by Edel *et al.* (2007).

The first phase (middle to late Eocene) is characterized by N–S compressive regime. During this period, Variscan Permo-carboniferous and Mesozoic crustal scale faults in the URG are reactivated (Dèzes *et al.*, 2004; Edel *et al.*, 2007). In the second phase (late Eocene to late Oligocene), major E–W extension results in maximum rifting and development of thick sedimentary sequences in the URG (DoebI, 1967; DoebI, 1970). These include two marine transgressions provoking among others the deposits of the carbon-rich Pechelbronn layers, and salt layers in the southern part of the graben. During early Miocene, a change in stress regime to a NE–SW oriented compressive phase took place associated with to a rapid counterclockwise rotation of the Alps and directional changes of the indenting Adriatic plate (e.g. Lowrie and Alvarez, 1975; Van den Berg, 1979; Montigny *et al.*, 1981; Edel *et al.*, 2001) and a general inclination of the southern part of the URG towards the North. The latter is due to the uplift of the upper mantle and the crust as suggested by the up-doming Moho to a depth of 24-25km in the southern beneath Colmar, the Kaiserstuhl volcano and the Vosges-Black Forest arch (e.g. Fuchs *et al.*, 1987). The new stress orientation causes dextral strike-slip faulting along previous structures, sedimentation in the Heidelberg basin and volcanism of the Kaiserstuhl (e.g. Ziegler and Dezes, 2007). From late Miocene up to the present, the stress regime prevailing in the URG is compressional with a NW–SE orientation such as observed over much of central Europe, resulting in a left lateral transcurrent motion (Illies and Masteller, 1977; Bergerat, 1985; Schumacher,

2002; Rotstein *et al.*, 2005), as confirmed by focal mechanism of recent earthquakes (Ahorner, 1975; Bonjer *et al.*, 1984; Bonjer, 1997; Plenefisch and Bonjer, 1997), and a simultaneous uplift of the Vosges-Black Forest arch.

### 2.2.3 Recent stress and strain distribution

Micro-tectonic studies (Bergerat, 1985; Villemin and Bergerat, 1987), in situ-stresses in boreholes (Illies and Greiner, 1979) and focal mechanisms associated with seismicity show that a NW-SE compression oblique to the graben axis due to the Alps is provoking, mostly in the upper crust, sinistral strike-slip motion on quasi N-S oriented faults (Ahorner, 1975; Plenefisch and Bonjer, 1997; Edel, 2004; Valley, 2007). Seismo-tectonic observation led Ahorner (1975) to calculate seismic slip rate of the graben to be about  $0.05 \text{ mm yr}^{-1}$ . The contribution of aseismic slip is known to occur in natural fracture systems (e.g. Evans *et al.*, 1981) and may be significant in the URG as shown in stimulation experiments of the Soultz-sous-Forest EGS test site (e.g. Cornet *et al.*, 1997). Thus, these seismic slip rates may represent a lower limit for the total slip rate. Recent preliminary geodetic measurements reveal that observed horizontal velocity components for a test region South of Strasbourg, obtained from Global Navigation Satellite Systems coordinate time series, vary around  $0.5 \text{ mm yr}^{-1}$  (Fuhrmann *et al.*, in press). These results are in general agreement with interseismic strain built-up in a sinistral strike-slip regime.

Earlier geodetical measurements showed that the central part of the graben is found to be on a  $0.5 \text{ mm yr}^{-1}$  uplift regime gradually increasing towards the West in connection with widespread subsidence along the eastern border-fault system and eastern environs with the southern and northern parts subsiding at a rate  $1 \text{ mm yr}^{-1}$  (Illies and Greiner, 1979; Zippelt and Malzer, 1987). The areas in subsidence are related to areas covered by Plio-Quaternary sediments reaching a maximum thickness of more than 1000 m (Bartz, 1974). By looking at geomorphologic observations, Illies *et al.* (1981) state that the relative height changes are mainly controlled by present-day tectonic vertical movements and that the actual rates appear about 10 times higher than the average rates throughout the Pleistocene period. Zippelt & Malzer (1987) show that seismicity in the URG can be correlated with computed height changes. In the northern part normal faulting and in the southern part strike-slip motion with secondary normal faulting are linked to subsidence. They observe that in the northern Black Forest and the adjacent Rhine Graben (central) segment, the computed height changes, as well as the observed recent seismic events, show a very low activity for the period of the last decades. Demoulin *et al.* (1998) carried out a local study of fault movements in the southern Black Forest and concluded that the faults in this region are creeping aseismically at rates varying between  $0.2 \text{ mm yr}^{-1}$  and  $1.1 \text{ mm yr}^{-1}$ . In the study by Liaghat *et al.* (1998), leveling measurements show that active deformation is happening in the southern part of the URG with upward movements at rate  $1 \text{ mm yr}^{-1}$  near Mulhouse and Selestat.

The accuracy of recent Global Navigation Satellite System (GNSS) derived vertical component is insufficient. Thus data of precise leveling networks is used to determine vertical displacement rates (Fuhrmann *et al.*, in press). The results are summarized as follows. More than 75% of the vertical in the South-eastern part of URG vary between  $-0.2 \text{ mm yr}^{-1}$  and  $+0.2 \text{ mm yr}^{-1}$ , indicating that this region behaves stable and is not in particular uplift. Higher rates of subsidence up to  $0.5 \text{ mm yr}^{-1}$  in a limited region South of Freiburg are in general agreement with active faulting.

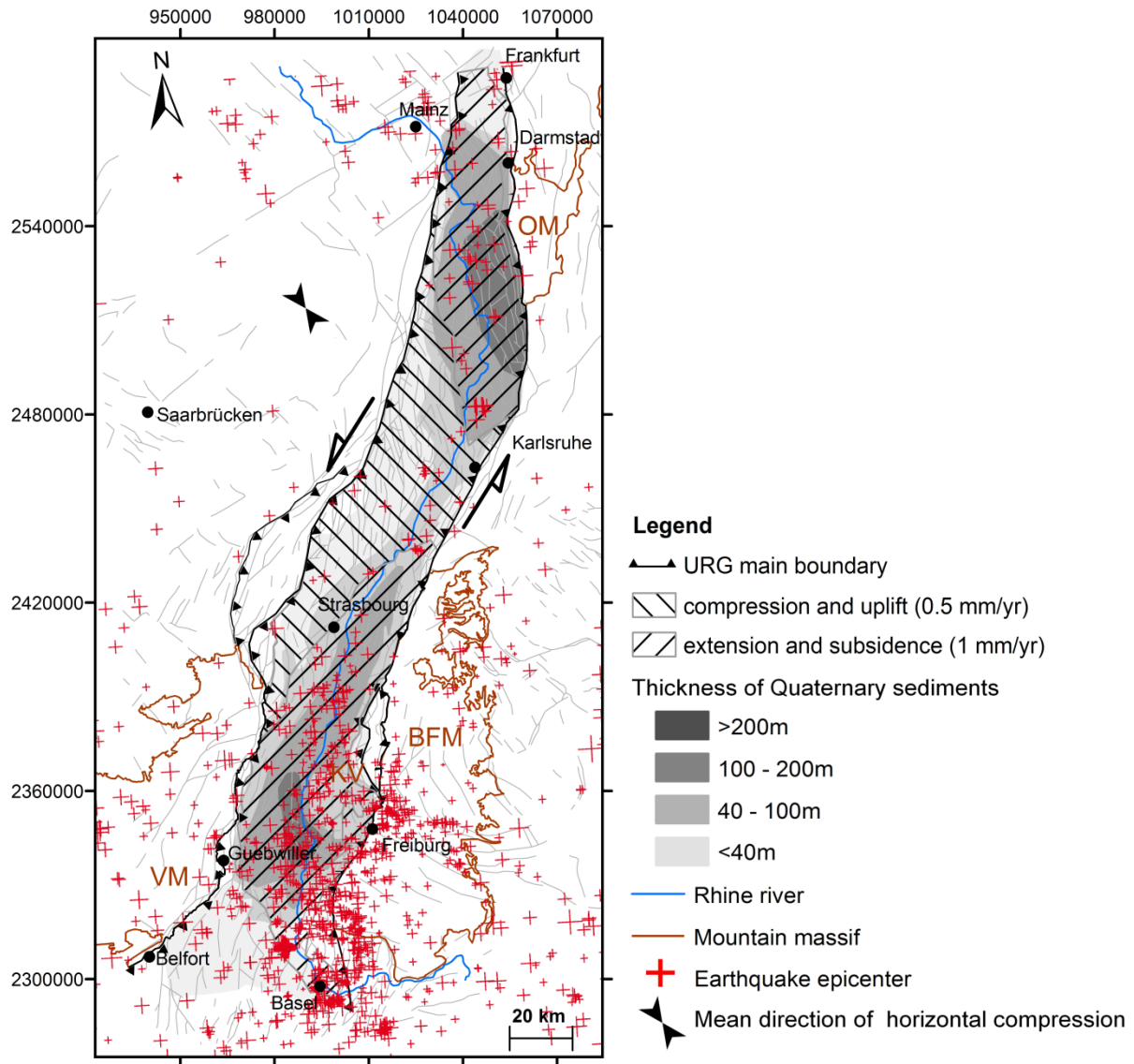


**Figure 2-2 :** Map showing the interpretation of neotectonic activity of the Upper Rhine Graben including the main direction of stress, adapted from Illies & Greiner (1979), the thickness of quaternary sediments, after Schumacher (2002), and the present day seismic activity, after Ahorner (1975), Bonjer (1997), Plenefisch & Bonjer (1997), Edel *et al.* (2006). VM: Vosges mountains; BFM: Blackforest mountains; OM: Odenwald mountains; KV: Kaiserstuhl Volcanic massif. Lambert II coordinates.

Illies and Greiner (1979) postulate that the crooked course of the Rhine Graben can explain the shear motion with compression shear motion and uplift in the central segment of the graben (with a 30-35° trend) and other parts of URG under extension shear and subsidence. The stress magnitudes determined in the Baden-Baden hot spring latitude in this central segment are higher than found in other graben segments (Illies *et al.*, 1981). Schumacher (2002) interprets this distribution of neotectonic activity as a sinistral strike-slip system with two pull-apart basins in the South and North, separated by a restraining bend in the central segment.

Recent seismic studies (Rotstein and Schaming, 2008; Rotstein and Schaming, 2011) highlighted significant transpressive patterns along the Vosges and Black Forest mountains border fault related to the Early Miocene change in the stress regime. With a shallow seismic reflector representing the Miocene-Pliocene erosional unconformity being faulted in the area of Belfort and Guebwiller, the

same study assumes that this transpression was extending at least to Late Pliocene and is possibly still active at present.

General view of the distribution of neotectonic activity adapted from Illies and Greiner (1979) and the related thickness of Quaternary sediments is shown in Figure 2-2. Modifications according to the new results from Fuhrmann *et al.* (in press) have not been taken into account, since the results N of Freiburg reveal tendency to compression and uplift. The low magnitude, however, does not indicate a significant enlargement of the compressional and uplift zone as interpreted by Illies and Greiner (1979).

## 2.3 Data processing

### 2.3.1 Temperature interpolation

The temperature distribution in the URG was known from a total of 6531 borehole temperature measurements from 1600 wells in the URG and adjacent areas (Pribnow and Schellschmidt, 2000; Agemar *et al.*, 2012). Different types of interpolation have been applied to this data set. Using temperatures from 804 boreholes, the horizontal temperature distribution was interpolated to a common depth of 800 m, representing a compromise between decreasing number of available temperature data and the attempt to reduce the influence of surface effects, such as topography and paleo-climate (Pribnow and Schellschmidt, 2000). This and other prior investigations produced a limited number of maps for certain depths using 2D-mapping algorithms like for instance a distance-weighted estimator (Schulz *et al.*, 1992; Hurter and Schellschmidt, 2003). The major disadvantage of 2D algorithms is the loss of information from shallower levels since the deep subsurface is much less explored (e.g. Agemar *et al.*, 2012). Kriging is a suitable regression method for 3D interpolation of temperature data since it allows apart from temperature prognosis in different regions and depths also the determination of probabilities of expected results (Deutsch and Journel, 1998). A statistical analysis of the temperature data and 3D multi-Gaussian kriging revealed a preferential orientation of the thermal anomalies in SSW-NNE direction (Münch *et al.*, 2005). The quality of the respective variograms is not provided. Agemar *et al.* (2012), however, provide details on their multi-Gaussian kriging. In contrast to the variogram of Northern Germany, both the Molasse basin and the URG reveal only limited fit with the Gaussian function. Following statistic criteria, the spatial relationship between the neighbour data is subordinated.

The quality of temperature measurements have been divided in three categories (Agemar *et al.*, 2012). The highest quality measurements in the URG come from undisturbed logs, drill stem tests or subsurface mining and tunnels measurements (category A). Intermediate (category B) and lowest quality (category C) measurements come from disturbed logs or from bottom hole temperature (BHT) measurements, which are disturbed by the drilling operations. Depending on the quality of the values and informations about the boreholes different correction methods have been applied. Despite the corrections, the results still have errors of up to  $\pm 8$  to 10 K, depending on the depth range (Agemar *et al.*, 2012 and references therein). For example, at a depth of 2000m, measurements from category B and C tend to underestimate the formation temperature by around 4-6 K in this database. The distribution of quality in the URG area can be seen in Figure 2-3. Around 20% of the measurements (i.e. 1280 temperature measurements) are from category B and C, and their spatial distribution is rather homogeneous in regard to the ones from category A.



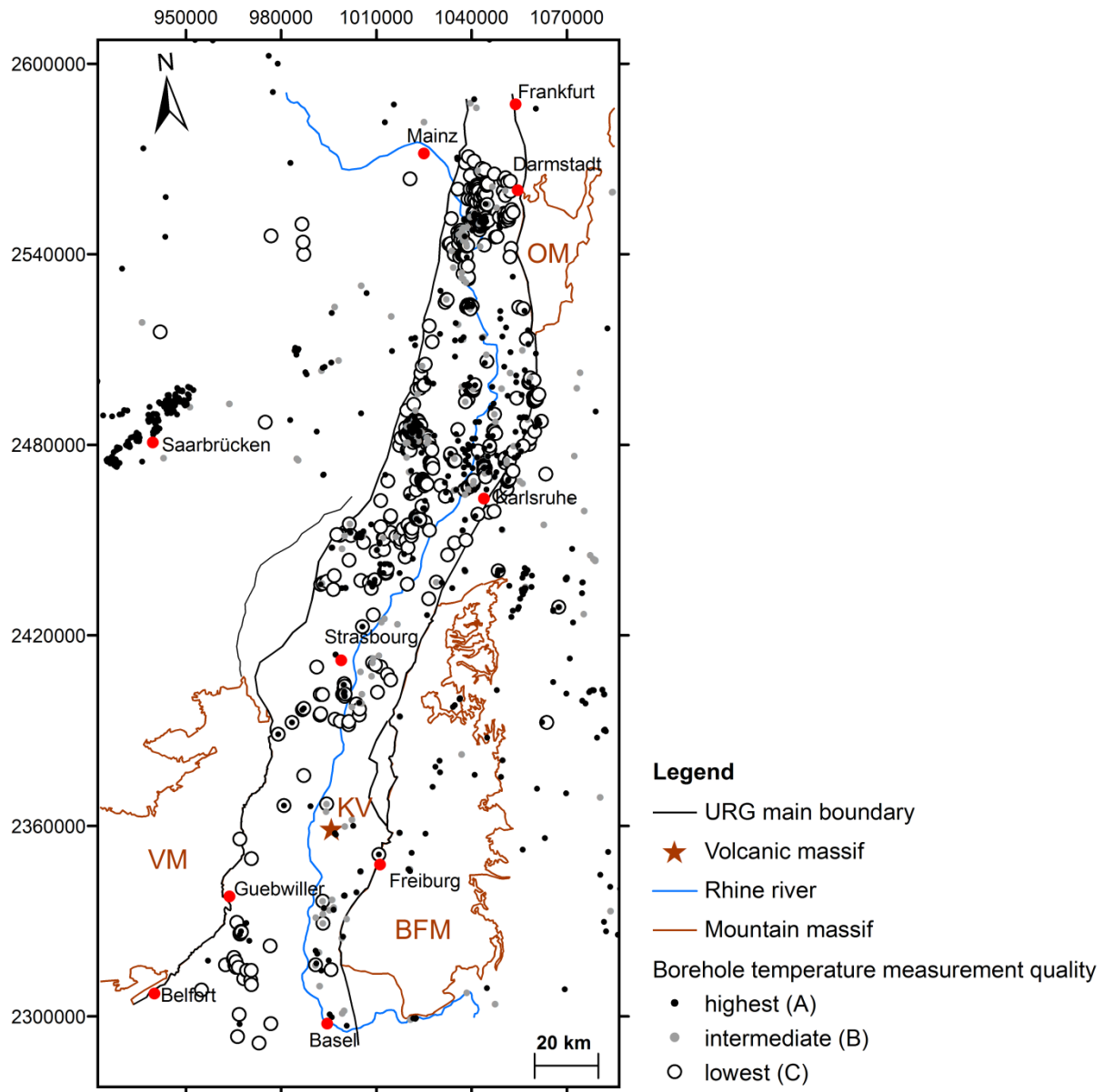


Figure 2-3 : Distribution and quality of borehole temperature measurements in the URG area. Categories of quality among the measurements come from the study by Agemar *et al.* (2012).

With the above considerations in mind, a new 3D interpolation of the entire scattered 3D temperature dataset has been carried out using a Delaunay triangulation followed by a natural neighbor interpolation on a grid with 2500 m sampling size in the X (Easting) and Y (Northing) directions and 250 m in the Z (depth) direction. The high density of boreholes, the ‘corridor’ form of the URG, and the choice of keeping exact the temperature values to known locations were in favor of this kind of interpolation.

The results of this volumetric interpolation are shown in Figure 2-4 for a true vertical depth (TVD) of 2000 m using a tri-linear interpolation, for comparison with geophysical data used for basement maps interpretation, and with neotectonic activity. At this depth, a number of 93 wells out of 121 are located inside the URG. The wells reveal still acceptable coverage and rather homogenous distribution in the central and northern part of the URG. It is obvious that in the southern part of the graben the number of wells decreases to about 15 per 5000 km<sup>2</sup>. While positive temperature anomalies, for example, of Landau and Soultz are confirmed by a number of wells of >5 at the depth

of 2000 m, others to the North (Neustadt) and South (Strasbourg) are the result of 3D interpolation from wells reaching depths < 2000 m. Measurements at shallow depth in the latter areas reveal geothermal gradients between  $56\text{ }^{\circ}\text{C km}^{-1}$  and  $120\text{ }^{\circ}\text{C km}^{-1}$  (Figure 2-5) and thus, confirm the occurrence of temperature anomalies at depth. In the following, we present a compilation of different geophysical results in relation with this interpolated temperature distribution at 2000 m TVD.

### 2.3.2 Compilation of geophysical data

#### ***Magnetics***

Total magnetic anomalies are typically compiled on national level. In the German URG, the magnetic anomaly map, with a grid spacing of 100 m, consistently images the entire anomaly pattern in Germany at an altitude of 1000 m a.s.l. related to the DGRF 1980, epoch 1980.0 (Gabriel *et al.*, 2011). This map is based on 50 shipborne, airborne and ground surveys, which were conducted between 1960 and 1990 and complemented by 17 new surveys after 1990. Data are stored in the national database FIS Geophysik ([www.fis-geophysik.de](http://www.fis-geophysik.de), LIAG Hannover). The French Magnetic Anomaly Map (BRGM, 1980) completes the western part of the URG. Since the maps image the superposition of magnetic source anomalies from different depths and therefore combines long- and short-wavelength spectra within one data set, interpretation of these data provide indication on major crustal structures. In the region of the URG, the graben itself appears in a large band of dominantly positive anomalies of up to 100 nT, extending over from southern Sachsen-Anhalt to southern Baden-Württemberg. Within the graben a dominant negative anomaly is observed in the area of the Saxothurigian zone (northern part of the URG). In the present study higher resolution is required in order to detect anomalies of higher frequency representing lithological or petrophysical changes in the upper crust at depths of about < 10 km.

Therefore, the magnetic grid presented in this study is based on ground magnetic measurements campaign that were designed for detailed geophysical investigations using signal processing such as reduction to pole, vertical gradient and downward elevation (Edel *et al.*, 1982; Papillon, 1995). The original density of measurements is about 1 station per  $1.4\text{ km}^2$ . The used dataset is limited to the central part of the graben, which includes the geothermal anomaly of Soultz and a geothermal high around Strasbourg area.

The magnetic anomaly reduced to the pole (Edel *et al.*, 1982; Papillon, 1995) is compared to the temperature distribution at 2000 m TVD (Figure 2-6) to visualize the importance of magnetic susceptibility changes in the distribution of temperature. These two data are then interpolated on a same reference grid every 2500 meters in the X and Y direction, and plotted on a graph. This graph is represented in: mean value and standard deviation of temperature values at 2000 m TVD for each 10 nT magnetic anomaly intervals.

#### ***Gravity***

The Bouguer anomaly grid with reference density  $2.67\text{ g cm}^{-3}$  presented in this study is based on the high-density compilation of Rotstein *et al.* (2006). This map shows a series of gravity highs and lows, in general elongated in the NE-SW direction. The correlation of gravity data with density measurements of outcropping rocks as well as of rocks from deep boreholes has allowed attributing the gravity anomalies to basement rock types in different areas of interest (Edel and Schulmann, 2009 and references therein).

The gravity vertical gradient grid comes from the study presented by Edel *et al.* (2007). On the gravity vertical gradient map, the effects of long wavelengths due to the sedimentary infill or of the upper mantle topography are significantly reduced. The elongated NE-SW striking short wavelengths anomalies are interpreted to reflect basement structures (Edel, 2004; Edel *et al.*, 2007).

Both Bouguer anomalies and gravity vertical gradient maps are compared to the temperature distribution at 2000 m TVD to visualize the importance of gravity changes in the distribution of temperature (Figure 2-7 and Figure 2-8). The two gravity maps are then interpolated on a same reference grid every 2500 meters in the X and Y direction, and compared to temperature values on a graph for best interpretation. This graph is represented in: mean value and standard deviation of temperature values at 2000 m TVD for each 2.5 mgals interval of Bouguer anomaly or 0.5 mgal km<sup>-1</sup> interval of gravity vertical gradient.

## 2.4 Results and discussion

### 2.4.1 Temperature distribution in the URG

The temperature at 2000 m TVD ranges from about 75 to nearly 150 °C across the entire URG (Figure 2-4). In contrast to the relatively high temperatures in the North and North-West of graben, low temperatures in the order of < 100 °C are observed in the South-eastern part of the URG with temperatures < 80 °C in the area of the Kaiserstuhl volcanic massif. A number of local anomalies with temperatures above 140 °C at 2000 m TVD are aligned along the URG between Strasbourg (France) and Mainz (Germany), and in the North of Darmstadt (Germany). These are mainly concentrated on the western side of the Rhine river. Again on the western side of the river temperatures > 110 °C can be found at the southern boundary of the URG between Belfort (France) and Guebwiller (France).

The temperature distribution in the Earth's crust can be related to different processes that are summarized in the heat transport equation. It involves mainly three mechanisms: radiogenic heat production, advection, and conduction.

Fourier's law of heat conduction describes heat transport from a heat source through a solid medium due to temperature differences. Apart from present-day radiogenic heat production, the main heat source is the Earth interior, and for the upper crust it can be assimilated to a constant heat flux at the mantle-crust boundary. In the case of the URG, the mantle up-doming revealed first from gravity and seismic refraction data (Kahle and Werner, 1980) does not seem to provide additional heat to the crust. Indeed, relatively low temperatures are observed in the area of minimum crustal thickness (about 24 km) near the Kaiserstuhl volcano area (Pribnow and Schellschmidt, 2000) (Figure 2-4).

Radiogenic heat production is an issue, in particular, in the granitic basement. A comprehensive summary on radiogenic heat production in the lithosphere is given, for example, by Vilà *et al.* (2010). Detailed measurements in the deep wells of Soultz-sous-Forêts reveal a general decrease of radiogenic heat production with increasing depth from about 1500 to 5000 m TVD across different basement lithology. A zone of altered granite ranging from 1400 to 1550 m TVD has been determined e.g. from magnetic susceptibility and mineralogical investigation (Genter, 1990; Rummel and König, 1991). Highest radiogenic heat productivities of about 5.5 to 6.5 μW m<sup>-3</sup> are measured on core samples from the well GPK1 in this narrow zone (Rummel *et al.*, 1988). Continuous logging of GPK2, however, reveals a much stronger variation in radiogenic heat production between 2 to 7 μW m<sup>-3</sup> (Pribnow, 2000; Grecksch *et al.*, 2003). The mean radiogenic heat production decreases to

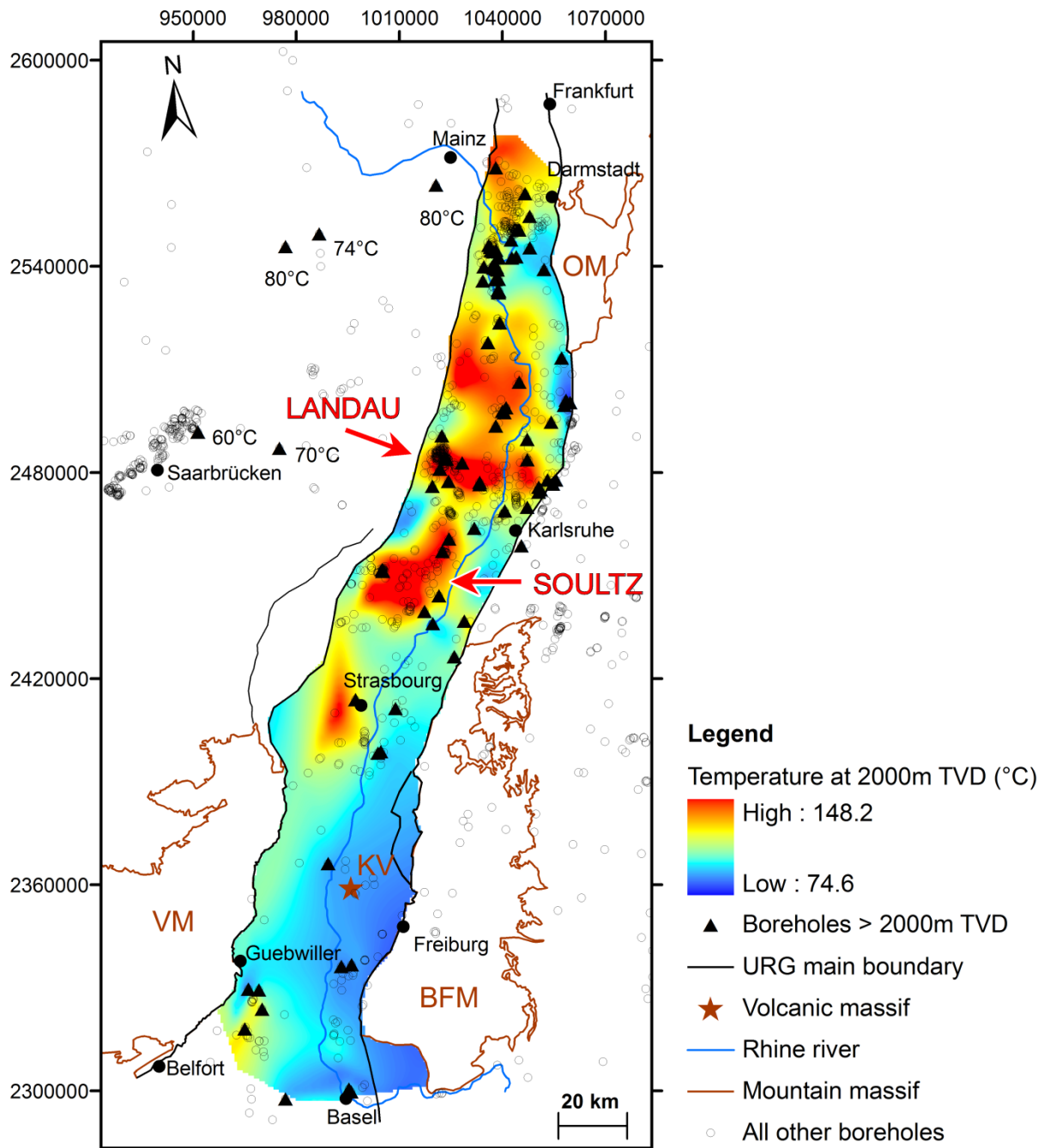


Figure 2-4 : Temperature distribution at 2000 m TVD in the Upper Rhine Graben (URG) derived from a 3D interpolation of 6531 temperature data from 1600 boreholes from the URG and adjacent areas using the dataset of Pribnow & Schellschmidt (2000) and Agemar *et al.* (2012). The location of the two main petroleum and geothermal areas at Pechelbronn/Soultz-sous-Forêts and Landau are indicated. The boreholes with a depth > 2000 m TVD are indicated by triangles. VM: Vosges mountains; BFM: Black Forest mountains; OM: Odenwald mountains; KV: Kaiserstuhl Volcanic massif. Lambert II coordinates.

about  $4 \mu\text{W m}^{-3}$  at > 2000 m TVD. Between 2000 and 3500 m TVD the mean value decreases linearly to about 3 to  $3.5 \mu\text{W m}^{-3}$  (Pribnow, 2000). From this depth downwards the mean value obtained from

logging remains rather constant (Pribnow, 2000). Extreme values of radiogenic heat production are however observed at certain depth intervals (e.g.  $> 7 \mu\text{W m}^{-3}$  between -3700 and -3800 m TVD or on one of samples at -5057 to -5060 m TVD) corresponding to the reservoir levels revealing hydrothermal alteration. Measurements at the bottom of GPK2 and 3 reveal smaller values mainly between 2 and  $3 \mu\text{W m}^{-3}$  (Grecksch *et al.*, 2003). This corresponds to the median value of  $2.43 \mu\text{W m}^{-3}$

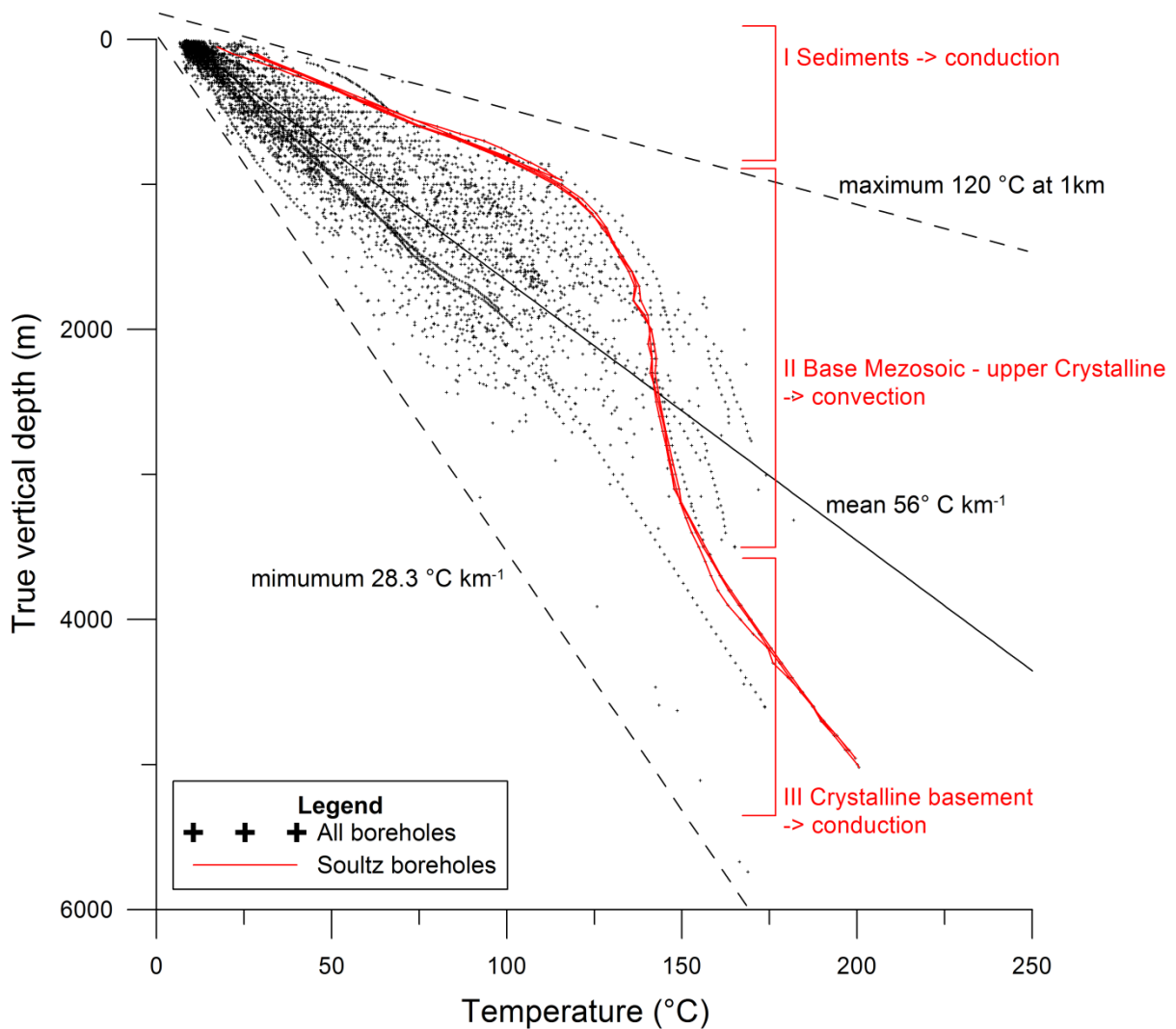


Figure 2-5 : Temperature distribution with depth in the boreholes of the URG and surroundings (after Pribnow & Schellschmidt (2000) and Agemar *et al.* (2012), with emphasis on the Soutz boreholes (red) and expected temperature regime in Soutz area (e.g. Kohl *et al.*, 2000).

<sup>3</sup> with 25<sup>th</sup> and 75<sup>th</sup> percentile value of 1.74 and 3.23  $\mu\text{W m}^{-3}$ , respectively, as suggested by Vilà *et al.* (2010). A median value of radiogenic heat production of 2  $\mu\text{W m}^{-3}$  is suggested in the same study for low grade-medium grade metamorphic rocks (such as schist) and 1.3  $\mu\text{W m}^{-3}$  for metaigneous rocks (such as gneiss). Both gneiss and schist can be found in the flanking mountains and most probably in the basement of the URG (Rotstein *et al.*, 2006; Edel and Schulmann, 2009). In addition, granites are generally more heat-conductive than layered metamorphic rocks of the basement or sediments constituting the sedimentary overburden of the URG. A contribution of lithological changes to variation in surface heat flux is illustrated, for example, in the Erzgebirge, representing a shoulder mountain range to the Eger graben (Förster and Förster, 2000). There, the localization of surface heat flow anomalies of up to 90-110  $\text{mW.m}^{-2}$  has been attributed to late Variscan granites responsible to around 40-50% of the crustal heat flow in this area (Förster and Förster, 2000). These granites are classified as high heat production (HHP) granites and reveal values of heat production between 4 to 10  $\mu\text{W m}^{-3}$ , which is similar to values that observed in Soutz boreholes. It should be mentioned here that the effect of lateral changes in radiogenic heat production is typically not taken into account in thermal modeling of the URG.

A contribution of vertical tectonic movement to the temperature distribution at depth has been reported, for example, in the Gotthard-Aar massif in the central Alps (Kohl *et al.*, 2001) where the present uplift is in the order of 0.65 to 0.75 mm yr<sup>-1</sup> (Egli *et al.*, 2007) according to recent geodetic data. Very small effect only is expected for the URG since it is linked to an extensional tectonic regime. However, a relation between horst structures and geothermal anomalies has been described in regional 3D geological and temperature models of the petroleum and geothermal areas of Soultz, Landau and Speyer (Schill *et al.*, 2009).

Advection has been discussed extensively to be a significant heat transport process in the URG. Illies & Greiner (1979) state that compressive shear strain occurring parallel to the central segment of the graben leads to the opening of the N-S oriented faults in the basement and in the overlying sandstone. They argue that this is an essential prerequisite for hydrothermal convection. In the central part of the graben, convection in these formations has been identified as a major contributor to the E-W distribution of geothermal anomalies across the URG (Schellschmidt and Clauser, 1996; Pribnow and Schellschmidt, 2000). More locally free convection has been found to occur along major N-S trending faults at Landau (Bächler *et al.*, 2003) and between the two western major faults in Soultz horst structure (Kohl *et al.*, 2000) in base Mesozoic formations (mostly Muschelkalk, Buntsandstein) and the upper part of the crystalline basement (Figure 2-5).

## 2.4.2 Links between geophysical grids and temperature

### *Links between magnetics and temperature*

Temperature anomalies in the order of about 110-115 °C at 2000 m TVD with respect to about 100 °C as background signal in the central part are characterized by magnetic anomalies in the order of about 20-40 nT (Figure 2-6).

Magnetic field reduced to the pole, and its first vertical derivative in the central URG, delineate pre-Permian basement bodies with different magnetic susceptibilities (Lauer and Taktak, 1971; Edel *et al.*, 1986; Edel and Fluck, 1989). The most common ferromagnetic minerals affecting these susceptibilities are magnetite, hematite and some iron sulphides such as pyrrhotite (Edel, 2004). Overall, magnetic data of the Upper Rhine Graben and rock susceptibility measurements from the same areas show that the magnetic bodies in the URG mostly correspond to Carboniferous gabbros, diorites and granodiorites, and their volcanic equivalents (Edel *et al.*, 2007). In the central part of the graben, magnetic structures globally coincide with the lower Triassic depth, i.e. the top of the basement (Papillon, 1995). In Soultz EPS1 borehole a large increase in magnetic susceptibility in the granite, was measured at 1550 m b.s.l. (Rummel and König, 1991). This is the depth where a standard porphyritic granite with very high pervasive alteration and abundant zones of vein alteration, along with a very high hematization of K-feldspar, was found (Hooijkaas *et al.*, 2006). In the upper part of the granite massif between 1400 and 1550m depth, the paleo-weathering effect, partly altering most of the primary iron-bearing minerals (biotite, magnetite, amphibole) into iron-hydroxide or hematite, resulted in a decrease of magnetic susceptibility 37 times (Rummel and König, 1991; Hooijkaas *et al.*, 2006). In conclusion, magnetic susceptibility changes associated with magnetic anomalies can mainly be related to lateral changes in alteration processes and lithology of basement rocks. In the area of Soultz the magnetic structure is interpreted as a granodioritic batholith with a significant radiogenic heat production.

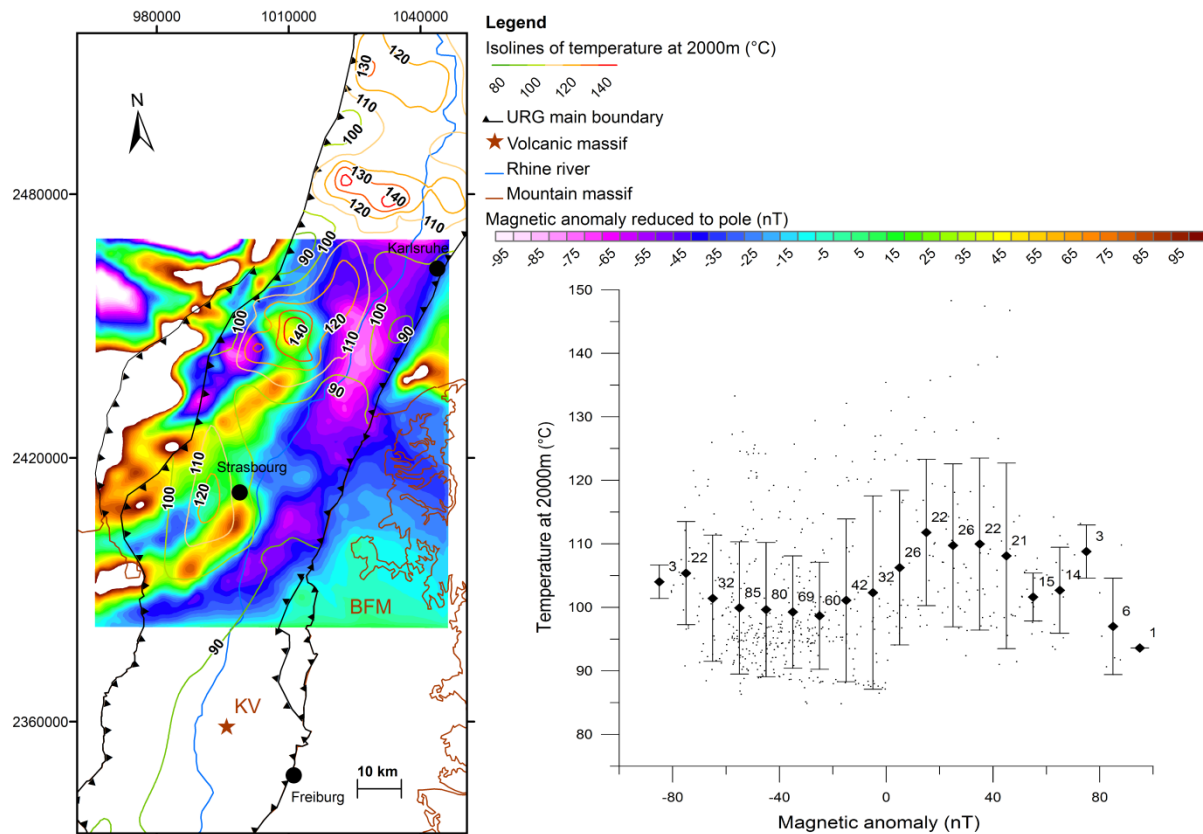


Figure 2-6 : (left) Superposition isolines of temperature at 2000 m TVD after Pribnow and Schellschmidt (2000) and Agemar *et al.* (2012), and magnetic anomaly reduced to pole map after Edel *et al.* (1982) and Papillon (1995); VM: Vosges mountains; BFM: Black Forest mountains; OM: Odenwald mountains; KV: Kaiserstuhl Volcanic massif. Lambert II coordinates. (right) Graph representing the mean value and standard deviation of temperature values at 2000 m TVD corresponding to the magnetic anomaly (10 nT interval). Label number indicates the number of information that has been used to calculate the mean value and standard deviation.

We thus interpret the additional 10-15 °C anomaly at 2000 m TVD as a result of lithological changes in basement rocks in the range 20-40 nT in the URG.

### Links between gravity and temperature

As shown in Figure 2-7, temperature above 100-110°C, mostly located in the central part of the graben, superpose with areas of low values (from -50 to -35 mgals) of Bouguer anomaly. This is not verified in the North of the graben between Mainz and Darmstadt, where temperature above 100-110°C superpose with areas of values around -20 mgals in the Bouguer anomaly. Most of the areas below 90°C superpose with Bouguer Anomalies values above -20 mgals. This relatively low temperature values are mainly observed in the South of the graben around the Kaiserstuhl volcanic massif.

The correlation trend between low values of Bouguer Anomalies and temperature at depth is confirmed in the graph in Figure 2-7: it can be found that Bouguer anomalies above -30 mgals correspond to temperature values 10 to 20°C (temperature range 85-90°C) lower than temperatures corresponding to Bouguer anomaly values below -30 mgals (temperature range 110-115°C), with the exception of Bouguer anomaly between -45 and -50 mgals, representing a small area that can be found in the eastern border close to the Odenwald mountains.

A strong correlation between temperature and gravity vertical gradient is observed. As depicted in Figure 2-8, temperature anomalies above 100-110 °C localize on negative values of gravity vertical

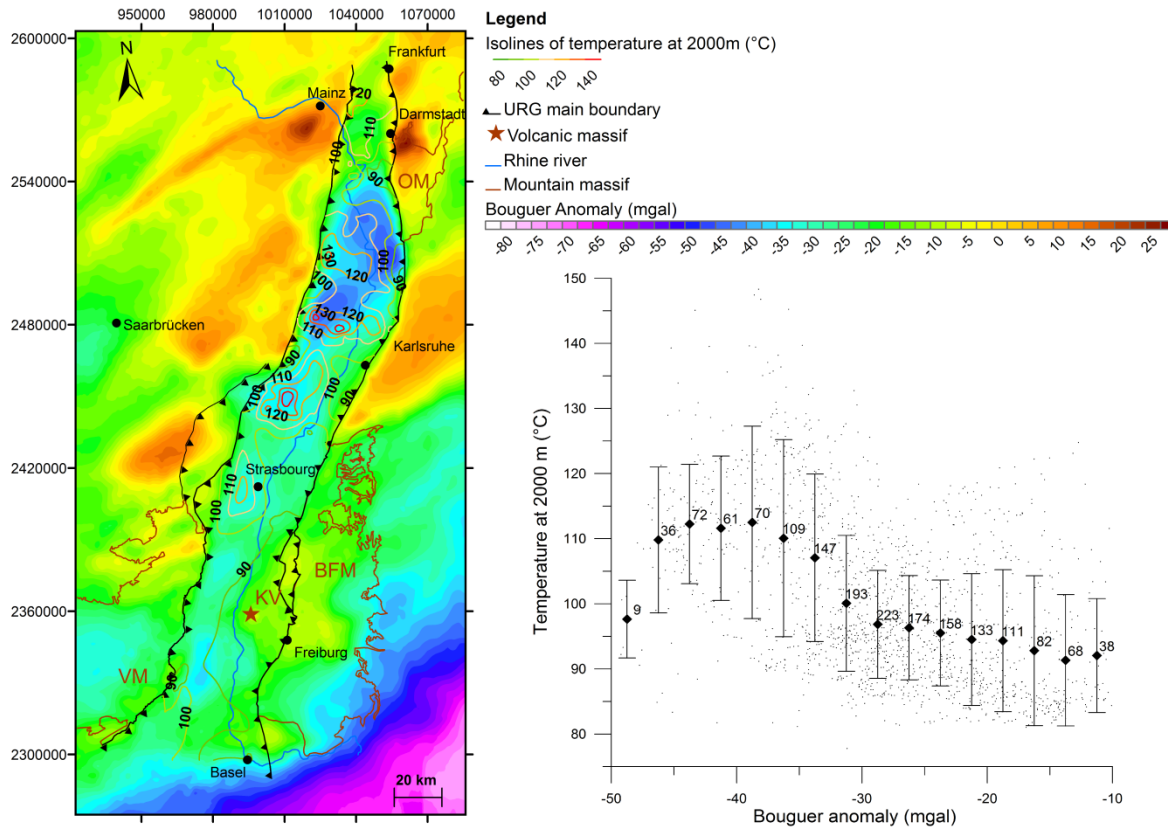


**Figure 2-7 :** (left) Superposition isolines of temperature at 2000 m TVD after Pribnow and Schellschmidt (2000) and Agemar *et al.* (2012), and Bouguer Anomaly map after Rotstein *et al.* (2006); VM: Vosges mountains; BFM: Black Forest mountains; OM: Odenwald mountains; KV: Kaiserstuhl Volcanic massif. Lambert II coordinates. (right) Graph representing the average and standard deviation of temperature values at 2000 m TVD corresponding to the Bouguer Anomaly (2.5 mgals interval). Label number indicates the number of information that has been used to calculate the mean value and standard deviation.

gradient, in the central and northern part of the graben. Temperature values in the range 85 to 90 °C are observed for positive values of gravity vertical gradient.

In the Upper Rhine Graben, gravity measurements have been interpreted in terms of subsurface density variations due to lithological heterogeneities. These were determined from outcrops in the flanking mountains (the Vosges and Black Forest) and in deep boreholes throughout the graben. Densities from the URG and its shoulders were determined and discussed by several authors, e.g. Campos-Enriquez *et al.* (1992) and Edel & Weber (1995), with the general classification from low density to high density: granites, gneisses, Devono-Dinatian volcano-sedimentary rocks, granodiorites, Paleozoic schists, gabbros and diorites (Edel and Weber, 1995; Papillon, 1995). Low vertical gradient anomalies in the gravity maps have been interpreted in granitic crystalline ridges (Edel, 2004).

In the central and northern part of the graben the negative values of gravity vertical gradient have been interpreted in crystalline ridges made of E. Carboniferous granites (335-330 Ma). In the southern part, negative gravity vertical gradient are interpreted in E. Carboniferous crustal fusion granites (330-325 Ma). Thus, temperature anomalies above 100-110°C at 2000 m TVD in the central and northern part of the graben are likely be related to the E. Carboniferous granites (335-330 Ma). However, although numerous studies have been carried out for geophysical and geological consistent interpretations of the graben floor (e.g. Edel and Schulmann, 2009), the possible porosity



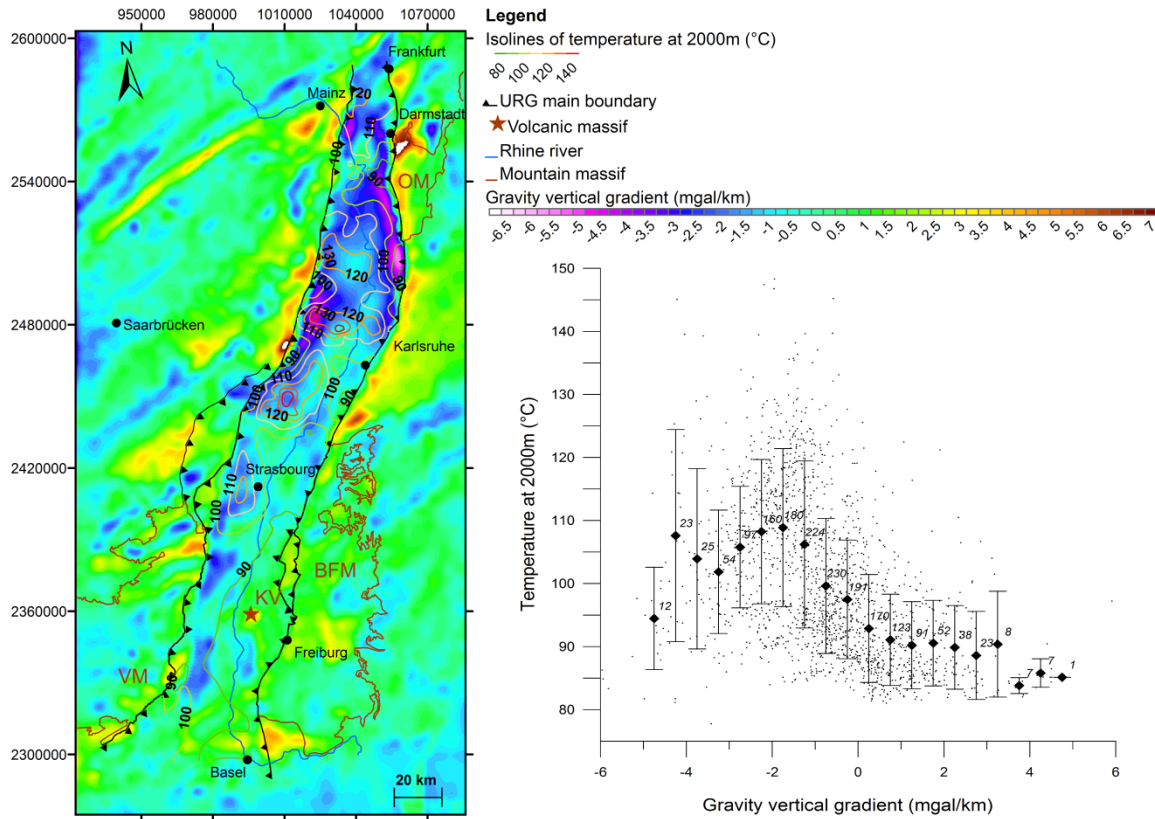


**Figure 2-8 :** (left) Superposition isolines of temperature at 2000 m TVD after Pribnow and Schellschmidt (2000) and Agemar *et al.* (2012), and Gravity vertical gradient map after Edel *et al.* (2007); VM: Vosges mountains; BFM: Black Forest mountains; OM: Odenwald mountains; KV: Kaiserstuhl Volcanic massif. Lambert II coordinates. (right) Graph representing the average and standard deviation of temperature values at 2000 m TVD corresponding to the Gravity vertical gradient (0.5 mgal/km interval). Label number indicates the number of information that has been used to calculate the mean value and standard deviation.

effect has not been taken into account for the interpretation. A density reduction of about  $250 \text{ kg.m}^{-3}$  has been reported in the granitic basement below the Soultz site on the 3D inversion of existing gravity data in combination with a previous 3D geological model (Schill *et al.*, 2010). This density anomaly is interpreted in terms of a fluid-filled porosity of approximately 15% with a brine density of  $1000 \text{ kg m}^{-3}$ . This interpretation is based on density measurements in the geothermal wells revealing a characteristic density of  $2630 \text{ kg m}^{-3}$  (Genter, 1990; Rummel and König, 1991) with local minima of down to  $2460 \text{ kg m}^{-3}$  in the hydrothermally altered zones with a high clay content and a porosity of up to 20% (Genter, 1990). Some measurements on rock samples from the deeper levels resulted in densities as low as  $2430 \text{ kg.m}^{-3}$  in GPK3 borehole (Grecksch *et al.*, 2003). In addition, the Soultz granite exhibits permeability values significantly higher than its contemporary granite of Carnmenellis which has not been affected by rifting (Stober and Bucher, 2007).

Thus, we conclude that density changes associated with gravity can either be linked to basement rocks lithology, or to porosity. Both may be linked to temperature anomalies, since in the case of Soultz, the gravity low is interpreted as a granitic batholith with a significant radiogenic heat production, and porosity values of up to 20 % indicate fracture porosity allowing for hydrothermal convection (Kohl *et al.*, 2000).

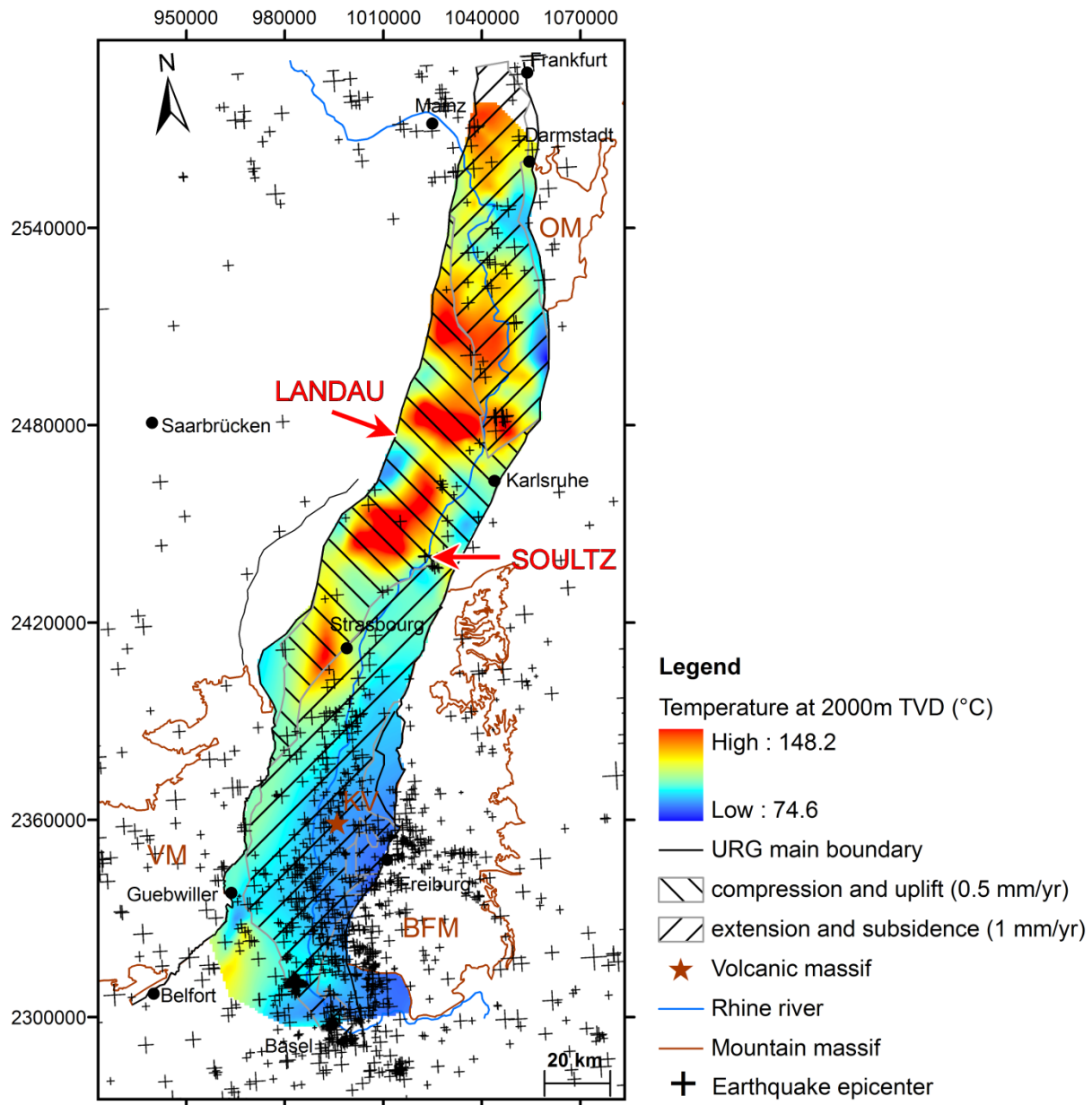


Figure 2-9 : Map representing the superposition temperature at 2000 m TVD after Pribnow and Schellschmidt (2000) and Agemar *et al.* (2012), and interpretation of neotectonic activity of the Upper Rhine Graben adapted from Illies & Greiner (1979), and the present day seismic activity, after Ahorner (1975), Bonjer (1997), Plenefisch & Bonjer (1997), Edel *et al.* (2006). VM: Vosges mountains; BFM: Blackforest mountains; OM: Odenwald mountains; KV: Kaiserstuhl Volcanic massif. Lambert II coordinates.

We thus interpret the additional 10-20 °C anomaly at 2000 m TVD as a result of lithological changes and porosity changes in the range -50 to -30 mgals on the Bouguer anomaly map and on negative values of gravity vertical gradient in the URG.

### 2.4.3 Links between recent stress and strain rate-hydrothermal convection

Areas of high temperatures such as the ones of Soutz and Landau (above 110-120°C at 2000 m TVD) are related to a zone in compressive shear and uplift in the western central part of the graben (Figure 2-9), associated with low Quaternary sedimentation (Figure 2-2) and low seismicity. In the northern part of the graben, the high temperatures are also linked, to some extent, to extension shear, normal faulting and subsidence in the northern part of the graben. To the South-West in the area between Belfort and Guebwiller, elevated temperature above 100°C can also be related to an area with low

Quaternary sedimentation and relatively lower seismicity than on the other side of the graben. This elevated temperature area is also a place where transpressive patterns are observed on seismic profiles, and this compressive regime could be related to the change in tectonic regime from the Early Miocene to up to Present (Rotstein and Schaming, 2008). Low temperatures are mostly located in the South-eastern part of the graben, between the Vosges and Black Forest, an area where extension shear, but also secondary normal faulting, subsidence and seismicity also prevails. Illies *et al.* (1981) assume that compressive shear strain parallel to the central segment of the graben controls the opening of N-S trending fissure systems in the basement, as an essential prerequisite for hydrothermal convection: this shear strain is provoking interconnected natural shear zones by the formation of an-echelon fissure, contributing to a higher permeability together with the dilatancy phenomenon (pore-volume expansion from the formation of microcracks). The same study moreover shows that the hydrostatic pressure can hold cracks open at 5km depth and relevant faults are supposedly often seismically active. Concerning the last point, only little seismic activity can be reported in the central part of the graben (Zippelt and Malzer, 1987) where the major temperature anomalies are located.

A significant amount of aseismic slip has been reported for the Le Mayet de Montagne granitic test site in central France during stimulation (Scotti and Cornet, 1994). The same behavior was recorded at Soultz (Cornet *et al.*, 1997). It is likely that the different tectonic regime occurring in this part of the graben, or the presence of fluid in the upper crust in these natural fractured zones lowers the seismicity, but further research is needed to confirm this situation. In crystalline rocks, Barton *et al.* (1995) observe that the permeability of critically stressed faults is much higher than that of faults that are not optimally oriented for reactivation or slip in the current stress field. Zoback (2007) observes that faults in strike-slip tectonic regime may be also prospective as the termination of strike-slip faults, crossing of faults may result in local extension and open fractures.

Thus we interpret the occurrence of the most important temperature anomalies (e.g.  $> 120\text{ }^{\circ}\text{C}$  at 2000 m TVD), associated to hydrothermal convection along faults reaching the basement (Schellschmidt and Clauser, 1996; Kohl *et al.*, 2000; Pribnow and Schellschmidt, 2000; Bächler *et al.*, 2003), to be mostly linked with compressive shear strain and mostly low seismicity in comparison with other parts of the URG.

## 2.5 Conclusions

In the Upper Rhine Graben, zones of high temperature can be related to the following aspects:

- 1) Occurrence of compression shear and uplift regime for the major anomalies in the central segment of the URG (Soultz, Landau) but also extension shear, normal faulting and subsidence to some extent in the northern part of the graben, and transpressive patterns in the South-western part of the URG next to Guebwiller
- 2) Relatively low natural seismicity that may be linked to aseismic slip as observed at Soultz during hydraulic stimulation
- 3) Occurrence of low density basement of E. Carboniferous granites (335-330 Ma) of the Saxothuringian unit in the central and northern part of the URG, as shown by comparison with the basement map interpreted from gravity and magnetic data. These granites offer an optimal radiogenic heat production and heat conductivity, as seen in the European EGS test-site Soultz boreholes; but also host faulting and hydrothermal circulation that may

significantly affect the gravity interpretation – this should be analyzed quantitatively on a more local scale.

## 2.6 Acknowledgements

The authors would like to thank LIAG-Hannover and EOST Strasbourg for providing input data: borehole temperatures, and geophysical data, respectively.

Albert Genter, Benoit Valley, Rüdiger Schellschmidt, Fritz Rummel and colleagues at CHYN are warmly acknowledged for their contribution in this paper.

This work is part of a PhD by Paul Baillieux financed by University of Neuchâtel.

## 2.7 References

- Agemar, T., Schellschmidt R. and Schulz R. (2012). Subsurface temperature distribution in Germany. *Geothermics* 44(0): 65-77.
- Ahorner, L. (1975). Present-day stress field and seismotectonic block movements along major fault zones in Central Europe. *Tectonophysics* 29(1-4): 233-249.
- Bächler, D., Kohl T. and Rybach L. (2003). Impact of graben-parallel faults on hydrothermal convection - Rhine Graben case study. *Physics and Chemistry of the Earth* 28(9-11): 431-441.
- Banka, D., Pharaoh T. C., Williamson J. P. and Core T. P. P. F. (2002). Potential field imaging of Palaeozoic orogenic structure in northern and central Europe. *Tectonophysics* 360(1-4): 23-45.
- Barton, C. A., Zoback M. D. and Moos D. (1995). Fluid flow along potentially active faults in crystalline rock. *Geology* 23(8): 683-686.
- Bartz, J. (1974). Die Mächtigkeit des Quartärs im Oberrheingraben. Illies JH, Fuchs K (eds) *Approaches to taphrogenesis Schweizerbart, Stuttgart*: pp 78–87.
- Behrmann, J. H., Hermann O., Horstmann M., Tanner D. C. and Bertrand G. (2003). Anatomy and kinematics of oblique continental rifting revealed: A three-dimensional case study of the southeast Upper Rhine graben (Germany). *AAPG Bulletin* 87(7): 1105--1121.
- Bergerat, F. (1985). *Déformations cassantes et champs de contraintes tertiaires dans la plateforme européenne. Paris VI. Paris, Université Pierre & Marie Curie, Paris VI. PhD.*
- Bertrand, G., Elsass P., Wirsing G. and Luz A. (2006). Quaternary faulting in the Upper Rhine Graben revealed by high-resolution multi-channel reflection seismic. *Comptes Rendus Geoscience* 338(8): 574-580.
- Bonjer, K. P. (1997). Seismicity pattern and style of seismic faulting at the eastern borderfault of the southern Rhine Graben. *Tectonophysics* 275(1-3): 41-69.
- Bonjer, K. P., Gelbke C., Rouland D., Mayer-Rosa D. and Massinon B. (1984). Seismicity and dynamics of the Upper Rhinegraben. *J Geophys* 55:1-12
- BRGM (1980). France Magnetic Anomaly Map (Carte Magnetique de la France) 1:1,000,000, BRGM.
- Brun, J. P., Gutscher M. A. and {DEKORP-ECORS teams} (1992). Deep crustal structure of the Rhine Graben from seismic reflection data: A summary. *Tectonophysics* 208(1-3): 139-147.
- Campos-Enriquez, J. O., Hubral P., Wenzel F., Lueschen E. and Meier L. (1992). Gravity and Magnetic Constraints on Deep and Intermediate Crustal Structure and Evolution Models for the Rhine Graben. *Tectonophysics* 206(1-2): 113-135.
- Cloetingh, S., Cornu T., Ziegler P. A. and Beekman F. (2006). Neotectonics and intraplate continental topography of the northern Alpine Foreland. *Earth-Science Reviews* 74(3-4): 127-196.
- Cloetingh, S., van Wees J. D., Ziegler P. A., Lenkey L., Beekman F., Tesauro M., Förster A., Norden B., Kaban M., Hardebol N., Bonté D., Genter A., Guillou-Frottier L., Ter Voorde M., Sokoutis D., Willingshofer E., Cornu T. and Worum G. (2010). Lithosphere tectonics and thermo-

- mechanical properties: An integrated modelling approach for Enhanced Geothermal Systems exploration in Europe. *Earth-Science Reviews* 102(3-4): 159-206.
- Cornet, F. H., Helm J., Poitrenaud H. and Etchecopar A. (1997). Seismic and Aseismic Slips Induced by Large-scale Fluid Injections. *Pure and Applied Geophysics* 150(3): 563-583.
- Demoulin, A., Launoy T. and Zippelt K. (1998). Recent crustal movements in the southern Black Forest (western Germany). *Geologische Rundschau* 87(1): 43-52.
- Deutsch, C. V. and Journel A. G. (1998). *GSLIB - Geostatistical Software Library and User's Guide*. 2. Edition 1998. Oxford University Press, Oxford.
- Dèzes, P., Schmid S. M. and Ziegler P. A. (2004). Evolution of the European Cenozoic Rift System: interaction of the Alpine and Pyrenean orogens with their foreland lithosphere. *Tectonophysics* 389: 1--33.
- Doehl, F. (1967). The tertiary and pleistocene sediments of the Northern and Central part of the upper Rhinegraben. In: Rothé JP, Sauer K (eds) *The Rhinegraben progress report*. *Mém Serv Carte Géol Als Lorr* 26:48–54
- Doehl, F. (1970). Die tertiären und quartären Sedimente des südlichen Rheingrabens. In: Illies JH, Mueller St (eds) *Graben problems*. E Schweizerbart'sche Verlagsbuchhandlung, Stuttgart, pp 56–66
- Edel, J.-B., Dubois D., Marchant R., Hernandez J. and Cosca M. (2001). La rotation miocene inferieur du bloc corso-sarde; nouvelles contraintes paleomagnetiques sur la fin du mouvement. *Bulletin de la Société Géologique de France* 172(3): 275-283.
- Edel, J. B. (2004). Structure et évolution du Fossé Rhénan, du Carbonifère à nos jours - apports de la géophysique. *Bulletin de la société d'histoire naturelle et d'ethnographie de Colmar* 65(2004): 21-50.
- Edel, J. B., Campos-Enriquez O., Goupillot M. and Kiro K. N. (1982). Levé magnetique au sol du Fossé rhénan supérieur. *Interpretation géologique*. *Bull. Bur. Rech.Géol. Min.* 2: 179-192.
- Edel, J. B. and Fluck P. (1989). The Upper Rhenish Shield Basement (Vosges, Upper Rhinegraben and Schwarzwald) - Main Structural Features Deduced from Magnetic, Gravimetric and Geological Data. *Tectonophysics* 169(4): 303-316.
- Edel, J. B., Montigny R., Royer J. Y., Thuizat R. and Trolard F. (1986). Paleomagnetic investigations and K-AR dating on the variscan plutonic massif of the champ du feu and its volcanic-sedimentary environment, northern vosges, France. *Tectonophysics* 122(1-2): 165-185.
- Edel, J. B. and Schulmann K. (2009). Geophysical constraints and model of the "Saxothuringian and Rhenohercynian subductions - magmatic arc system" in NE France and SW Germany. *Bulletin de la Société Géologique de France* 180(6): 545-558.
- Edel, J. B., Schulmann K. and Rotstein Y. (2006). The Variscan tectonic inheritance of the Upper Rhine Graben: evidence of reactivations in the Lias, Late Eocene-Oligocene up to the recent. *International Journal of Earth Sciences* 96(2): 305-325.
- Edel, J. B., Schulmann K. and Rotstein Y. (2007). The Variscan tectonic inheritance of the Upper Rhine Graben: evidence of reactivations in the Lias, Late Eocene-Oligocene up to the recent. *International Journal of Earth Sciences* 96(2): 305-325.
- Edel, J. B. and Weber K. (1995). Cadomian terranes, wrench faulting and thrusting in central Europe Variscides : Geophysical and geological evidences. *Geologische Rundschau* 84: 412--432.
- Egli, R., Geiger A., Wiget A. and Kahle H.-G. (2007). A modified least squares collocation method for the determination of crustal deformation: first results in the Swiss Alps. *Geophysical Journal International* 168(1): 1-12.
- Engel, W. and Franke W. (1983). Flysch Sedimentation: Its relationship to Tectonism in the European Variscides. In: MARTIN, H. & EDER, F.W. [Editors]: *Intracontinental Fold Belts. Case Studies in the Variscan Belt of Europe and the Damara Belt in Namibia*. 267-287. Berlin, Heidelberg, New York, Tokyo (Springer).
- Evans, K. F., Burford R. O. and King G. C. P. (1981). Propagating Episodic Creep and the Aseismic Slip Behavior of the Calaveras Fault North of Hollister, California. *Journal of Geophysical Research* 86(Nb5): 3721-3735.

- Flottmann, T. and Oncken O. (1992). Constraints on the Evolution of the Mid German Crystalline Rise - a Study of Outcrops West of the River Rhine. *Geologische Rundschau* 81(2): 515-543.
- Förster, A. and Förster H.-J. (2000). Crustal composition and mantle heat flow: Implications from surface heat flow and radiogenic heat production in the Variscan Erzgebirge (Germany). *Journal of Geophysical Research* 105(B12): 27.
- Franke, W. (1989). Variscan plate tectonics in Central Europe--current ideas and open questions. *Tectonophysics* 169(4): 221-228.
- Fuchs, K., Bonjer K. P., Gajewski D., Lüschen E., Prodehl C., Sandmeier K. J., Wenzel F. and Wilhelm H. (1987). Crustal evolution of the Rhinegraben area. 1. Exploring the lower crust in the Rhinegraben rift by unified geophysical experiments. *Tectonophysics* 141(1-3): 261-275.
- Fuhrmann, T., Heck B., Knöpfler A., Masson F., Mayer M., Ulrich P., Westerhaus M. and Zippelt K. (in press). Recent surface displacements in the Upper Rhine Graben - Preliminary results from geodetic networks. *Tectonophysics* (0).
- Gabriel, G., Vogel D., Scheibe R., Lindner H., Pucher R., Wonik T. and Krawczyk C. M. (2011). Anomalies of the Earth's total magnetic field in Germany - the first complete homogenous data set reveals new opportunities for multiscale geoscientific studies. *Geophysical Journal International* 184(3): 1113-1118.
- Genter, A. (1990). Géothermie roches chaudes sèches: le granite de Soultz-sous-Forêts. (Bas-Rhin, France), Fracturation naturelle, altérations hydrothermales et interaction eau-roche, Université d'Orléans. **PhD**: 201.
- Genter, A., Guillou-Frottier L., Feybesse J.-L., Nicol N., Dezayes C. and Schwartz S. (2003). Typology of potential Hot Fractured Rock resources in Europe. *Geothermics* 32(4-6): 701-710.
- Grecksch, G., Ortiz A. and Schellschmidt R. (2003). Thermophysical Study of GPK2 and GPK3 Granite Samples. HDR Project Soultz - Report.
- Hinsken, S., Schmalholz S. M., Ziegler P. A. and Wetzel A. (2011). Thermo-Tectono-Stratigraphic Forward Modelling of the Upper Rhine Graben in reference to geometric balancing: Brittle crustal extension on a highly viscous mantle. *Tectonophysics* 509(1-2): 1-13.
- Hooijkaas, G. R., Genter A. and Dezayes C. (2006). Deep-seated geology of the granite intrusions at the Soultz EGS site based on data from 5 km-deep boreholes. *Geothermics* 35(5-6): 484-506.
- Hurter, S. and Schellschmidt R. (2003). Atlas of geothermal resources in Europe. *Geothermics* 32(4-6): 779-787.
- Hurtig, E., Gotha H. H. G.-K. A., Commission I. H. F., DDR Z. f. r. P. d. E. A. d. W. d., Verlagsgesellschaft H. H., Potsdam K. D. and Brandenburg L. (1992). Geothermal atlas of Europe / edited by E. Hurtig ... [et al.] ; International Association for Seismology and Physics of the Earth's Interior, International Heat Flow Commission; Central Institute for Physics of the Earth.
- Illies, H. J. and Greiner G. (1979). Holocene movements and state of stress in the rhinegraben rift system. *Tectonophysics* 52(1-4): 349-359.
- Illies, J. and Masteller E. C. (1977). Possible Explanation of Emergence Patterns of Baetis-Vernus-Curtis (Ins-Ephemeroptera) on Breitenbach-Schlitz Studies on Productivity, Nr 22. *Internationale Revue Der Gesamten Hydrobiologie* 62(2): 315-321.
- Illies, J. H., Baumann H. and Hoffers B. (1981). Stress Pattern and Strain Release in the Alpine Foreland. *Tectonophysics* 71(1-4): 157-172.
- Illies, J. H. and Greiner G. (1978). Rhinegraben and Alpine system. *Geological Society of America Bulletin* 89: 770-782.
- Jeannette, D. and Edel J. B. (2005). Contexte géologique du site géothermique de Soultz-Sous-Forêts. bulletin de l'Association Philomatique d'Alsace et de Lorraine Tome 40.
- Kahle, H. G. and Werner D. (1980). A Geophysical-Study of the Rhinegraben .2. Gravity-Anomalies and Geothermal Implications. *Geophysical Journal of the Royal Astronomical Society* 62(3): 631-647.
- Kohl, T., Bächler D. and Rybach L. (2000). Steps towards a comprehensive thermo-hydraulic analysis of the HDR test site Soultz-sous- Forêts. Proc. World Geothermal Congress 2000, Kyushu-Tohoku, Japan, May-June 2000, pp. 2671-2676.

- Kohl, T., Signorelli S. and Rybach L. (2001). Three-dimensional (3-D) thermal investigation below high Alpine topography. *Physics of The Earth and Planetary Interiors* 126(3-4): 195-210.
- Kossmat, F. (1927). Gliederung des varistischen Gebirgsbaues. *Abhandlungen des Sächsischen Geologischen Landesamtes Bd. 1. S.: 1–39.*
- Kroner, U., Hahn T., Romer R. L. and Linnemann U. (2007). The Variscan orogeny in the Saxo-Thuringian zone-Heterogenous overprint of Cadomian/Paleozoic Peri-Gondwana crust. *Geological Society of America Special Papers* 423: 153-172.
- Lauer, J. P. and Taktak A. G. (1971). Propriétés magnétiques des roches au voisinage du contact métamorphique des schistes de Steige et des granites d'Andlau et du Hohwald (Vosges cristallines du Nord). *C.R. Acad. Sci., Paris* 272, 924-927.
- Liaghat, C., Villemin T. and Jouanne F. (1998). Déformation verticale actuelle dans la partie sud du fossé d'Alsace (France). *Comptes Rendus de l'Académie des Sciences - Series IIA - Earth and Planetary Science* 327(1): 55-60.
- Lopes Cardozo, G. G. O. and Behrmann J. H. (2006). Kinematic analysis of the Upper Rhine Graben boundary fault system. *Journal of Structural Geology* 28(6): 1028-1039.
- Lowrie, W. and Alvarez W. (1975). Paleomagnetic Evidence for Rotation of the Italian Peninsula. *J. Geophys. Res.* 80(11): 1579-1592.
- Majorowicz, J. and Wybraniec S. (2011). New terrestrial heat flow map of Europe after regional paleoclimatic correction application. *International Journal of Earth Sciences* 100(4): 881-887.
- Montigny, R., Edel J. B. and Thuizat R. (1981). Oligo-Miocene rotation of Sardinia: KAr ages and paleomagnetic data of Tertiary volcanics. *Earth and Planetary Science Letters* 54(2): 261-271.
- Münch, W., Sistenich H., Bücker C. and Blanke T. (2005). Möglichkeiten der geothermischen Stromerzeugung im Oberrheingraben. *VGB PowerTech* 10/2005.
- Oncken, O. (1997). Transformation of a magmatic arc and an orogenic root during oblique collision and its consequences for the evolution of the European Variscides (Mid-German Crystalline Rise). *Geologische Rundschau* 86(1): 2-20.
- Oncken, O. (1998). Evidence for precollisional subduction erosion in ancient collisional belts: The case of the Mid-European Variscides. *Geology* 26(12): 1075-1078.
- Papillon, E. (1995). Traitements et interpretations des cartes d'anomalies magnétiques et gravimétriques du Fossé Rhénan supérieur. *Dipl. Ing. Géophys. Strasbourg I*, 95p.
- Plenefisch, T. and Bonjer K. P. (1997). The stress field in the Rhine Graben area inferred from earthquake focal mechanisms and estimation of frictional parameters. *Tectonophysics* 275(1-3): 71-97.
- Pribnow, D. and Schellschmidt R. (2000). Thermal tracking of upper crustal fluid flow in the Rhine Graben. *Geophysical Research Letters* 27(13): 1957-1960.
- Pribnow, D. F. C. (2000). The deep thermal regime in Soultz and implications for fluid flow. *GGA Report, GGA Institut Hannover*, 7 pp
- Rotstein, Y., Behrmann J. H., Lutz M., Wirsing G. and Luz A. (2005). Tectonic implications of transpression and transtension: Upper Rhine Graben. *Tectonics* 24(6).
- Rotstein, Y., Edel J. B., Gabriel G., Boulanger D., Schaming M. and Munsch M. (2006). Insight into the structure of the Upper Rhine Graben and its basement from a new compilation of Bouguer Gravity. *Tectonophysics* 425(1-4): 55-70.
- Rotstein, Y. and Schaming M. (2008). Tectonic implications of faulting styles along a rift margin: The boundary between the Rhine Graben and the Vosges Mountains. *Tectonics* 27(2): -.
- Rotstein, Y. and Schaming M. (2011). The Upper Rhine Graben (URG) revisited: Miocene transtension and transpression account for the observed first-order structures. *Tectonics* 30.
- Rummel, F., Haack U. and Gohn E. (1988). Uranium, thorium and potassium content and derived heat production rate for the granite cores in GPK1. *RUB Yellow Reports* 6: 9.
- Rummel, F. and König E. (1991). Density, ultrasonic velocities and magnetic susceptibility measurements on the core material from borehole EPS1 at Soultz-sous-Forêts. *Yellow report* 8 (1991).

- Schellschmidt, R. and Clauser C. (1996). The thermal regime of the Upper Rhine graben and the anomaly of Soultz. *Z. Angew. Geol.* 42(1): 40-44.
- Schill, E., Geiermann J. and Kümritz J. (2010). 2-D Magnetotellurics and gravity at the geothermal site at Soultz-sous-Forêts. Proceedings World Geothermal Congress 2010 Bali, Indonesia, 25-29 April 2010.
- Schill, E., Kohl T., Baujard C. and Wellmann J.-F. (2009). Geothermische Ressourcen in Rheinland-Pfalz: Bereiche Süd- und Vorderpfalz, Final report to the Ministry of Environment Rhineland-Palatine, 55p.
- Schulz, R., Haenel R. and Kockel F. (1992). Federal Republic of Germany – West federal states. In: Hurtig, E., Cermak, V., Haenel, R., Zui, V. (Eds.), *Geothermal Atlas of Europe*. Gotha, Germany, pp. 34–37.
- Schumacher, M. E. (2002). Upper Rhine Graben: Role of preexisting structures during rift evolution. *Tectonics* 21(1).
- Scotti, O. and Cornet F. H. (1994). In Situ Evidence for fluid-induced aseismic slip events along fault zones. *International Journal of Rock Mechanics and Mining Science & Geomechanics Abstracts* 31(4): 347-358.
- Stober, I. and Bucher K. (2007). Hydraulic properties of the crystalline basement. *Hydrogeology Journal* 15(2): 213-224.
- Valley, B. (2007). The relation between natural fracturing and stress heterogeneities in deep-seated crystalline rocks at Soultz-sous-Forêts (France), PhD thesis, ETH-Zürich, Switzerland, <http://e-collection.ethbib.ethz.ch/view/eth:30407>, 260 p.
- Van den Berg, J. (1979). Paleomagnetism and the changing configurations of the western Mediterranean area in the Mesozoic and Early Cenozoic eras. *Geol Ultraectina* 20:178
- Vilà , M., Fernández M. and Jiménez-Munt I. (2010). Radiogenic heat production variability of some common lithological groups and its significance to lithospheric thermal modeling. *Tectonophysics* 490(3-4): 152-164.
- Villemin, T. (1986). Tectonique en extension, fracturation et subsidence : Le Fossé Rhénan et le bassin de Sarre-Nahe. Paris VI PhD: 270.
- Villemin, T. and Bergerat F. (1987). L'évolution structurale du fossé rhénan au cours du Cénozoïque : un bilan de la déformation et des effets thermiques de l'extension. *Bulletin de la Société Géologique de France* 3(2): 245--255.
- Willner, A. P., Massonne H. J. and Krohe A. (1991). Tectonothermal Evolution of a Part of a Variscan Magmatic Arc - the Odenwald in the Mid-German Crystalline Rise. *Geologische Rundschau* 80(2): 369-389.
- Ziegler, P. A. (1992). European Cenozoic rift system. *Tectonophysics* 208(1-3): 91-111.
- Ziegler, P. A. and Dezes P. (2007). Cenozoic uplift of Variscan Massifs in the Alpine foreland: Timing and controlling mechanisms. *Global and Planetary Change* 58: 237-269.
- Ziegler, P. A., Schumacher M. E., Dèzes P., Van Wees J.-D. and Cloetingh S. (2004). Post-Variscan evolution of the lithosphere in the Rhine Graben area: constraints from subsidence modelling. *Geological Society, London, Special Publications* 223(1): 289-317.
- Zippelt, K. and Malzer H. (1987). Results of New Geodetic Investigations in Southwestern-Germany. *Journal of Geodynamics* 8(2-4): 179-191.
- Zoback, M. D. (2007). *Reservoir Geomechanics*. Cambridge University Press: 448 pp.



# Chapter III: Insights on the localization of temperature anomalies in Soutz area from gravity, magnetics and slip and dilation tendency analysis

Paul Baillieux<sup>1</sup>, Eva Schill<sup>1</sup>, Yassine Abdelfettah<sup>1</sup> and Chrystel Dezayes<sup>2</sup>

1 - Centre for Hydrogeology and Geothermics, Neuchâtel University, rue Emile Argand 11 CH-2000 Neuchâtel, Switzerland

paul.baillieux@unine.ch

2- BRGM, Geothermal Department, 3, avenue C.-Guillemin, BP 36009, 45060 Orléans cedex 2, France

## Abstract

The recently developed new 3D geological model of Soutz area is used as a basis for understanding the localization of temperature anomalies at a regional scale. Gravimetric, magnetic, slip and dilation tendency analyses are used to investigate the implication of structural patterns of the 3D geological model, density and magnetic variations, and stress patterns associated to hydrothermal circulation along the faults. A mean temperature anomaly of 40°C at top basement is found to be linked to a light and magnetic granodioritic pluton offering a rather high radiogenic heat production. Three temperature anomalies above 60°C at top basement show similar patterns: they are located along N-S directed fault with a West dipping signature in the western side of horst structures.

## 3.1 Introduction

The European Cenozoic Rifts System (ECRIS) hosts some of the major geothermal anomalies in Europe away from active volcanic areas. The Upper Rhine Graben (URG) forms the central segment of the ECRIS, in South-West Germany and North-East France. In the URG, the European Enhanced Geothermal System (EGS) test-site located at Soutz-sous-Forêts (France) was chosen for its important surface heat flow anomaly  $> 150 \text{ mW m}^{-2}$ , which has mainly been attributed to free hydrothermal convection occurring along the fractured zones and major faults as a result of thermo-hydraulic simulation along 2D sections perpendicular to the graben in this latitude (e.g. Schellschmidt and Clauser, 1996; Kohl *et al.*, 2000; Pribnow and Schellschmidt, 2000; Cloetingh *et al.*, 2010).

In order to understand the origin of localization of the necessary permeability for free convection we first provide a summary on the discussion of the possible onset of temperature anomalies.

Illies & Greiner (1979) states that convective heat transport occurs along N-S striking fractures zones in the basement and in the high porosity sandstone (Buntsandstein) aquifer above it, because these fractures zones are favorably oriented in the present day stress conditions to be reactivated, to host slip movements and undergo dilation at depth under the influence of the hydraulic load.

In the area of Landau located 40 km in the North of Soutz, again in the URG, Bächler *et al.* (2003) show in a 3D thermo-hydraulic simulation that graben-parallel faults are capable of hosting

hydrothermal convection organized into cells bringing hot water from the basement to shallower levels.

3D geological models performed for the areas Bad Bergzabern (including the Soultz site), Landau, and Speyer have shown that the major thermal anomalies in the Rhine valley are related to horst structures in the western part of the central URG in these areas (Schill *et al.*, 2009). An observed electrical conductivity anomaly at top of basement in the western part of the Soultz horst has also been attributed to hydrothermal fluids as a result of magnetotelluric investigation (Geiermann and Schill, 2010). Thus it has been concluded not all faults are capable of hosting this free hydrothermal convection.

Geochemical analyses carried out on the geothermal fluids of Soultz (Aquilina *et al.*, 1997; Sanjuan *et al.*, 2010) show that the reservoir fluids were previously in equilibrium with a sedimentary environment of high salinity at a temperature of 250°C (geothermometers). The only place where marine transgressions are observed at depth is on the eastern side of the graben, where its depth is up to 5000m. Thus, hydrothermal convection is the main mechanism bringing the fluids to the western side of the graben.

Fluid inclusions analyses carried out at different levels in Soultz boreholes (Dubois *et al.*, 1996; Dubois *et al.*, 2000; Cathelineau and Boiron, 2010) suggest two patterns for fluids paleocirculation, 1) a downward penetration of colder sedimentary brines most probably flowing through the top basement and Triassic layers, and 2) an upward flow rooted at more than 5km of hot low salinity fluids of meteoric origin probably coming from the graben shoulder (the Vosges mountains) to the West.

Jeannette & Edel (2005) suggest that the lithological nature of the basement, composed of Variscan granites and granodiorites intrusions (referred as crystalline ridges) with inherited NNE-SSW orientations, such as the ones found in Soultz boreholes, provide a considerable contribution to the localization of geothermal anomalies. These crystalline ridges are interpreted from gravity and magnetic measurements (Edel and Fluck, 1989; Edel, 2004; Rotstein *et al.*, 2006; Edel and Schulmann, 2009).

This interpretation is consistent with situation in other grabens of the ECRIS such as the Eger graben. Here, the localization of surface heat flow anomalies of up to 90-110 mW.m<sup>-2</sup> has been attributed to late Variscan granites responsible to around 40-50% of the crustal heat flow in this area (Förster and Förster, 2000). These granites are classified as high heat production (HHP) granites and reveal values of heat production between 4 to 10 μW m<sup>-3</sup>, which is similar to what has been observed in Soultz boreholes (2-7 μW m<sup>-3</sup>) (Pribnow *et al.*, 1999; Grecksch *et al.*, 2003).

In the literature, it is often argued that apart from fractured and hydrothermal zones as well as the horst structure of Soultz, favorable conditions are accentuated by a mantle up-doming to around 24km in the South of the URG (e.g. Jeannette and Edel, 2005 (Jeannette and Edel, 2005)). No correlation, however, can be found to support this concept (Pribnow and Schellschmidt, 2000). In contrast, relatively low temperatures are observed in area of minimum crustal thickness (about 24 km) near the Kaiserstuhl volcanic massif, as shown by gravity and seismic refraction data (e.g. Kahle and Werner, 1980; Brun *et al.*, 1992; Pribnow and Schellschmidt, 2000).

These interpretations can be joined together and summarized in an a-priori concept for the localization of geothermal anomalies in the Upper Rhine Graben. In chronological order: 1) Presence of NNE-SSW directed crystalline ridges made of granites and granodiorites prior to the graben opening (Jeannette and Edel, 2005; Edel and Schulmann, 2009) offering high radiogenic heat production (Pribnow *et al.*, 1999; Grecksch *et al.*, 2003); 2) Faulting during the graben opening with main NNE-SSW orientations (Jeannette and Edel, 2005; Edel *et al.*, 2007) and creation of horst structures such as in Soultz; 3) Reopening of the NNE-SSW fracture system with the N160°E directed maximum horizontal stress (Illies and Greiner, 1979) and 4) Hydrothermal circulation occurring along the hydraulically conductive major faults crossing the basement and a main East-West oriented flow in the connected Triassic aquifers above it (Aquilina *et al.*, 1997; Kohl *et al.*, 2000; Pribnow and Schellschmidt, 2000; Cathelineau and Boiron, 2010; Sanjuan *et al.*, 2010).

These different observations or hypotheses are not contradictory, but a quantification of their implication for the localization of the geothermal anomalies needs to be discussed. In earlier approaches this has been achieved by thermo-hydraulic modeling. Our approach here is a data-based approach in order to semi-quantify or quantify the relevant parameters.

To this end, a complete new 3D geological model of the Soultz area was carried out recently (Baillieux *et al.*, 2011; Dezayes *et al.*, 2011- Appendix A and B). The localization of temperature anomalies is first compared to the structural patterns of the 3D geological model. A geophysical reprocessing and reinterpretation of gravity and magnetic data is then carried out for analyzing possible areas of fracture porosity and linked to temperature distribution. Slip and dilation tendency analysis is finally carried out on the fault system to investigate the link between observed stress patterns and postulated hydrothermal circulation along the faults.

## 3.2 Geological settings

### 3.2.1 Pre-Permian Basement inferred from Geophysics

The basement of the Rhine Graben area is related to the Variscan orogenesis. Edel & Schulmann (2009) present the major prerift structures in the region as a succession of SE dipping subduction and underthrusting zones of the western Variscides represented by gravity highs, magnetic anomalies and important SE dipping reflectors on the deep seismics profiles acquired in the region (Brun *et al.*, 1992).

From North to South, the NE-SW trending Rhenohercynian, the Saxothuringian and the Moldanubian terranes respectively join together in suture zones (Figure 3-1). An intense magnetic zone striking NE-SW is located in the northern Vosges and in the Saxothuringian zone which is interpreted as representative of the magmatic arc emplaced in the time-range 335-330Ma, along NW dipping and sinistral normal faults associated with the Carboniferous subduction of the Rhenohercynian basin beneath the Saxothuringian continental plate (Edel and Weber, 1995). The Soultz site is located on top of this magnetic zone (Figure 3-1 inlet). In the center of the Saxothuringian zone, a previous subduction system is expected to have been present during Devonian times. It is represented by Devonian volcanics outcropping in the northern Vosges. The Upper Rhine Graben results from the juxtaposition during Visean times of the northern Saxothuringian zone, mainly made of Precambrian gneisses and schists crossed by the 335-330Ma calcalkaline plutonism composed of diorites, granodiorites and granites, and the southern Moldanubian zone dominated by high pressure

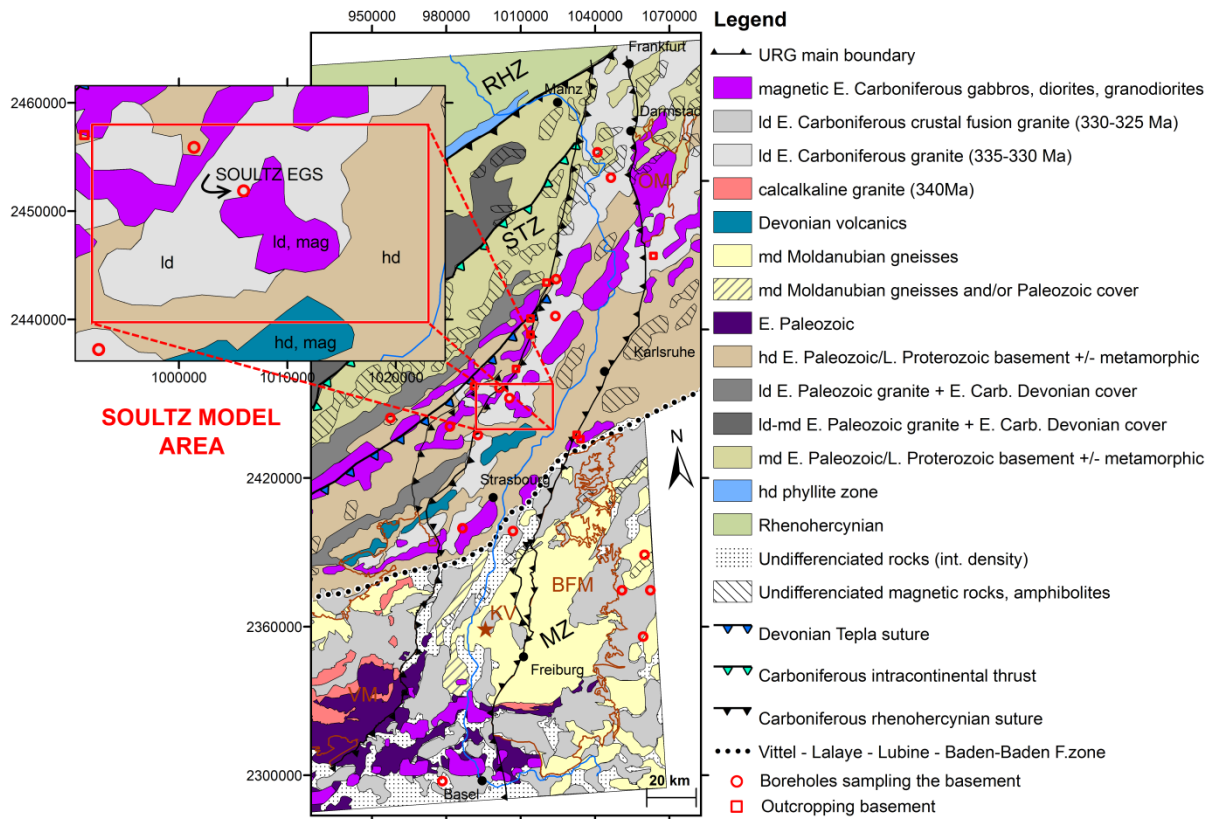


**Figure 3-1 : Compilation of Edel (2004) and Edel and Schulmann (2009) interpretative maps showing the major units and tectonic features beneath the pre-Late Carboniferous - Permian basin. Id :low density; md: medium density; hd: high density; mag: high magnetic susceptibility; RHZ:Rhenohercynian Zone; STZ: Saxo-Thuringian Zone; MZ: Moldanubian Zone; VM: Vosges mountains; BFM: Blackforest mountains; OM: Odenwald mountains; KV: Kaiserstuhl Volcanic massif. Lambert II coordinates.**

metamorphism, by syenitic magmatism (340 Ma) followed by crustal origin magmatism (330-325 Ma)(Edel, 2004).

By late Paleozoic, the whole Vosges – Upper Rhine Graben – Black Forest area forms a continuous massif marked by NE-SW discontinuities developing from Carboniferous times (Edel and Fluck, 1989; Edel *et al.*, 2007).

### 3.2.2 Structural development of the Upper Rhine Graben

After the Variscan orogeny, which late phase is characterized by large extensional structures causing regionally extended often NNE-SSW trending graben structures such as the Kraichgau or Schramberg troughs (Ziegler *et al.*, 2004), the eroded massif provides depositional environment throughout the Mesozoic period giving space mainly to Mesozoic platform sediments which deposited in Triassic (namely, Buntsandstein, Muschelkalk and Keuper) and Jurassic (Lias and Dogger) times. The URG originates in Paleogene times from the Alpine and Pyrenean collisions due to the build-up of far-field intraplate compressional stresses (Ziegler, 1992), and is described as a typical example of synorogenic intracontinental foreland rifting affected by Variscan crustal pre-discontinuities (cf. discussions on the topic in Schumacher, 2002; Dèzes *et al.*, 2004; Cloetingh *et al.*, 2006).

There is an on-going debate since about 40 years on the evolution of the URG (Hinsken *et al.*, 2011 and references therein). Overall, a most plausible scenario is a polyphase Paleogene (Middle Eocene to Early Miocene) more or less orthogonal extension followed by a Neogene (Pliocene to recent)

sinistral transtension. According to Villemin (1986) and Villemin & Bergerat (1987) the tertiary tectonic history of the URG can be divided in four phases. The first phase is characterized by a N–S compressive regime taking place in middle to late Eocene. It reactivated Variscan Permo-carboniferous and Mesozoic crustal scale faults in the URG (Dèzes *et al.*, 2004; Edel *et al.*, 2007). The second phase is the opening of the graben following an overall E–W extension. The ‘rifting’ takes place from the end of the Eocene to that of the Oligocene, including two marine transgressions provoking the deposits of the carbon-rich Pechelbronn layers, and salt layers in the southern part. In early Miocene, the change to a NE–SW oriented compressive phase due to a rapid rotation of the Alps towards the West and a general dip of the southern side towards the North (due to the uplift of the upper mantle and the crust as suggested by the updoming Moho to a depth of 24-25km in the southern beneath Colmar, the Kaiserstuhl volcano and the Vosges-Black Forest arch) takes place on Rhine Graben shoulders and surrounding, inducing dextral strike-slip faulting along previous structures, sedimentation in the northern Mannheim-Heidelberg trough and volcanism of the Kaiserstuhl (Edel, 2004; Edel *et al.*, 2007). From late Miocene up to the present, the stress regime prevailing in the Rhine Graben is the NW–SE compression seen over much of western Europe (Figure 3-2), inducing sinistral strike-slip faulting along previous faults (Ahorner, 1975; Illies and Greiner, 1979; Edel *et al.*, 2007) until nowadays, simultaneously with the uplift of the Vosges-Black Forest arch and sedimentation of Quaternary.

The neotectonic activity of the URG (Figure 3-2), with its dominantly N-S trending faults, fits within the last rifting phase characterized by Plio-Quaternary sedimentation, a consistently NW-SE directed maximum horizontal stress mainly determined from in situ measurements (Illies and Greiner, 1979) and microtectonic analysis (Villemin and Bergerat, 1987) and a main sinistral strike-slip regime as evidenced by focal plane mechanisms of upper crustal earthquakes (e.g. Illies and Greiner, 1979; Villemin and Bergerat, 1987; Dezayes *et al.*, 1995; Plenefisch and Bonjer, 1997; Cloetingh *et al.*, 2006).

### 3.2.3 3D structural model of the Soultz area

A 3D structural model of about 600 km<sup>2</sup> of the central URG, around the EGS site Soultz covering its geothermal anomaly (Figure 3-3) has been carried out (Baillieux *et al.*, 2011; Dezayes *et al.*, 2011-Appendix A and B). The collection and reprocessing of seismic profiles in the framework of different geological resource exploitation projects permitted to extend the previous and more local geological models of the Soultz area (e.g. Renard and Courrioux, 1994; Castera *et al.*, 2008).

A high density of normal faults can be observed on the seismic sections. Most of the major normal faults cross-cut the entire Cenozoic sedimentary filling of the graben as well as the Mesozoic pre-rift sediments. Numerous occurrences of strike-slip features, which form negative flower structures are present as well (Beccaletto *et al.*, 2010). Those are the most recent structures and may be related to the current stress-field.

A network of 26 faults could be constructed in a 31x18.5x6 km model of the sedimentary cover and the top basement representing the faults as surfaces (Figure 3-3). The orientation of the major faults is NNE-SSW, like the master fault to the West. These faults are normal faults with large extensions, and they affect all the geological formations from the Tertiary series to the basement. Inside the different blocks, minor faults were also built. These secondary faults trend NNW-SSE to N-S with a predominant West dipping signature (Baillieux *et al.*, 2011- Appendix A). All faults can be related to

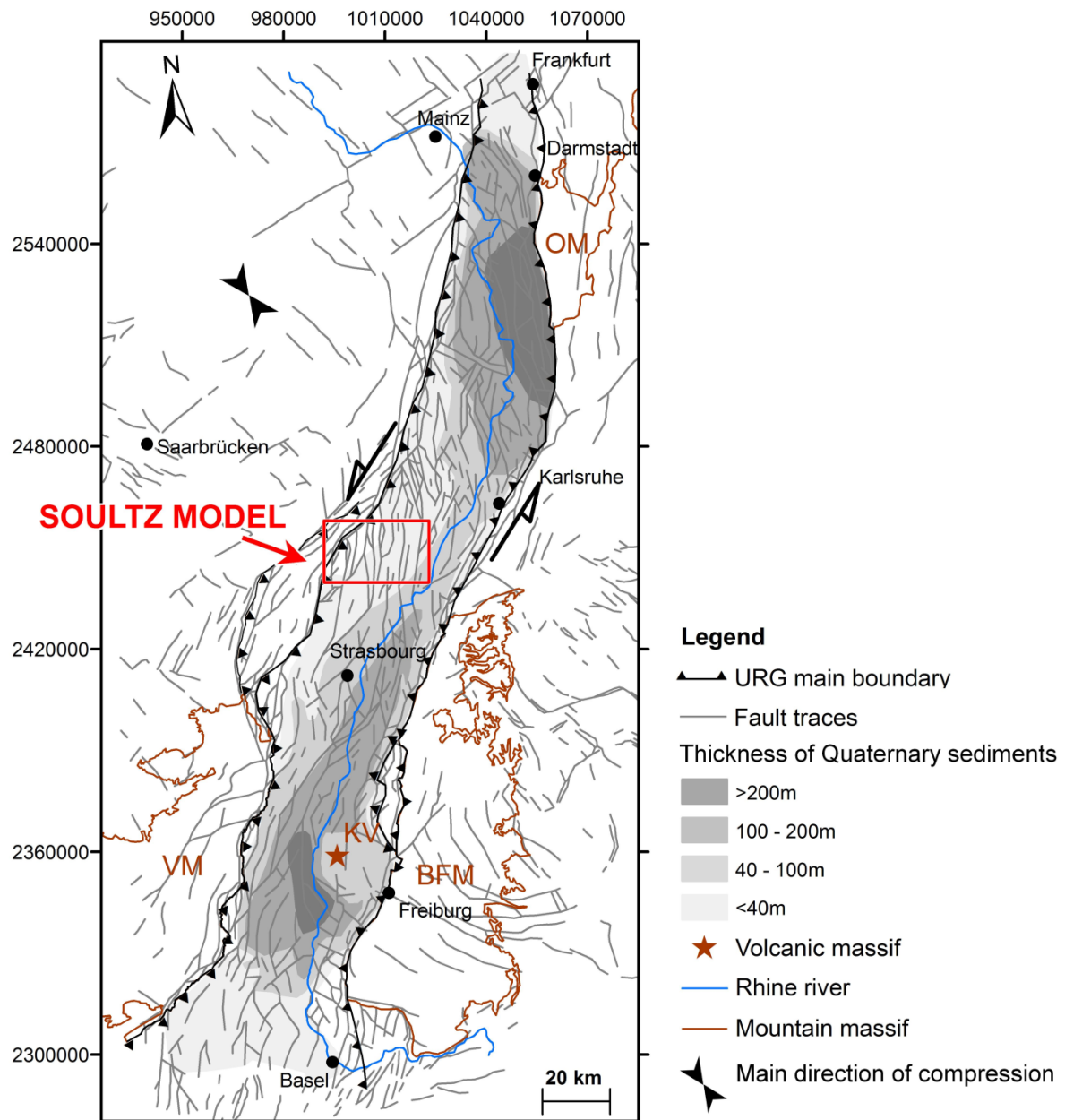
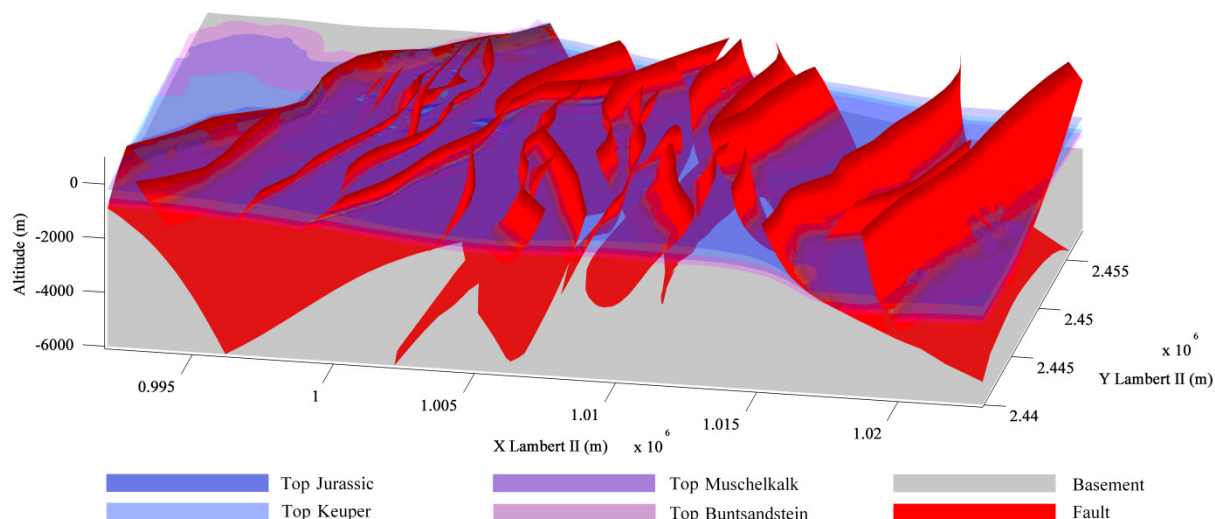


Figure 3-2 : Interpretation of neotectonic activity in the upper Rhine Graben after Illies and Greiner (1979). Superposition of fault traces (Illies and Greiner, 1979), thickness of Quaternary sediments -after Bartz (1974) and Schumacher (2002). The mean direction of stress is adapted from Illies and Greiner (1979; 2002). VM: Vosges mountains; BFM: Blackforest mountains; OM: Odenwald mountains; KV: Kaiserstuhl Volcanic massif. Lambert II coordinates.

the main phases of graben opening, characterized by a N-S compression and an E-W extension which took place from the end of the Oligocene to that of the Eocene, according to Villemin and Bergerat (1987). In the modeled area, the basement is affected by most of the faults and the horst structure is revealed beneath Soutz site in 3D (Figure 3-4).

A remarkable correlation between the secondary faults orientation in the 3D model and the reservoir fractures orientation in the deep granitic basement of Soutz EGS observed from borehole imaging, vertical seismic profiling (VSP) and microseismicity (Dezayes *et al.*, 2010; Sausse *et al.*, 2010) has been revealed (Baillieux *et al.*, 2011- Appendix A): these fractures again follow a NNW-SSE to N-S strike and have predominant West dipping signature. This suggests coupling of deformation between the sedimentary overburden and the basement at Soutz. Additionally, most these fractures are



**Figure 3-3 : visualization of the geological model of the Soultz area (31x18.5x6 km). The upper tertiary sedimentary filling was intentionally left transparent for best visualization. Location of the model area on Figure 3-1 and Figure 3-2.**

water-bearing prior to stimulation and form the main flow channeling after stimulation and during circulation (Dezayes *et al.*, 2010 and references therein). The orientation of these fractures are consistent with the present day stress field with  $\sigma_H$  N169°E  $\pm$  14° (Klee and Rummel, 1993; Valley and Evans, 2007; Dezayes *et al.*, 2010).

### 3.3 Data processing

#### 3.3.1 Temperature data

The numerous borehole temperature measurements have recently been gathered in a database covering the entire graben (Pribnow and Schellschmidt, 2000; Agemar *et al.*, 2012). The entire scattered 3-D temperature dataset (around 1600 boreholes in the URG and surrounding areas) is first interpolated using a Delaunay triangulation followed by a natural neighbor interpolation on a grid with 250m sampling size in the X (Easting) and Y (Northing) directions and 100m in the Z (depth) direction. This volumetric data is sliced at different depths using a trilinear interpolation and represented at top basement. Furthermore the minimum geothermal gradient is selected and subtracted from the absolute temperature values in order to highlight local effects.

The quality of temperature measurements have been divided in three categories (Agemar *et al.*, 2012). The highest quality measurements in the URG come from undisturbed logs, drill stem tests or subsurface mining and tunnels measurements (category A). Intermediate (category B) and lowest quality (category C) measurements come from disturbed logs or from bottom hole temperature (BHT) measurements, which are disturbed by the drilling operations. Depending on the quality of the values and informations about the boreholes different correction methods have been applied. Despite the corrections, the results still have errors of up to  $\pm 8$  to 10 K, depending on the depth range (Agemar *et al.*, 2012 and references therein). For example, at a depth of 2000m, measurements from category B and C tend to underestimate the formation temperature by around 4-6 K in this database. The distribution of quality in the area of the 3D geological model can be seen in Figure 3-8. In this area, around 16% of the measurements (i.e. around 120 temperature measurements) are from category B and C, and their spatial distribution is rather homogeneous in regard to the ones from category A.

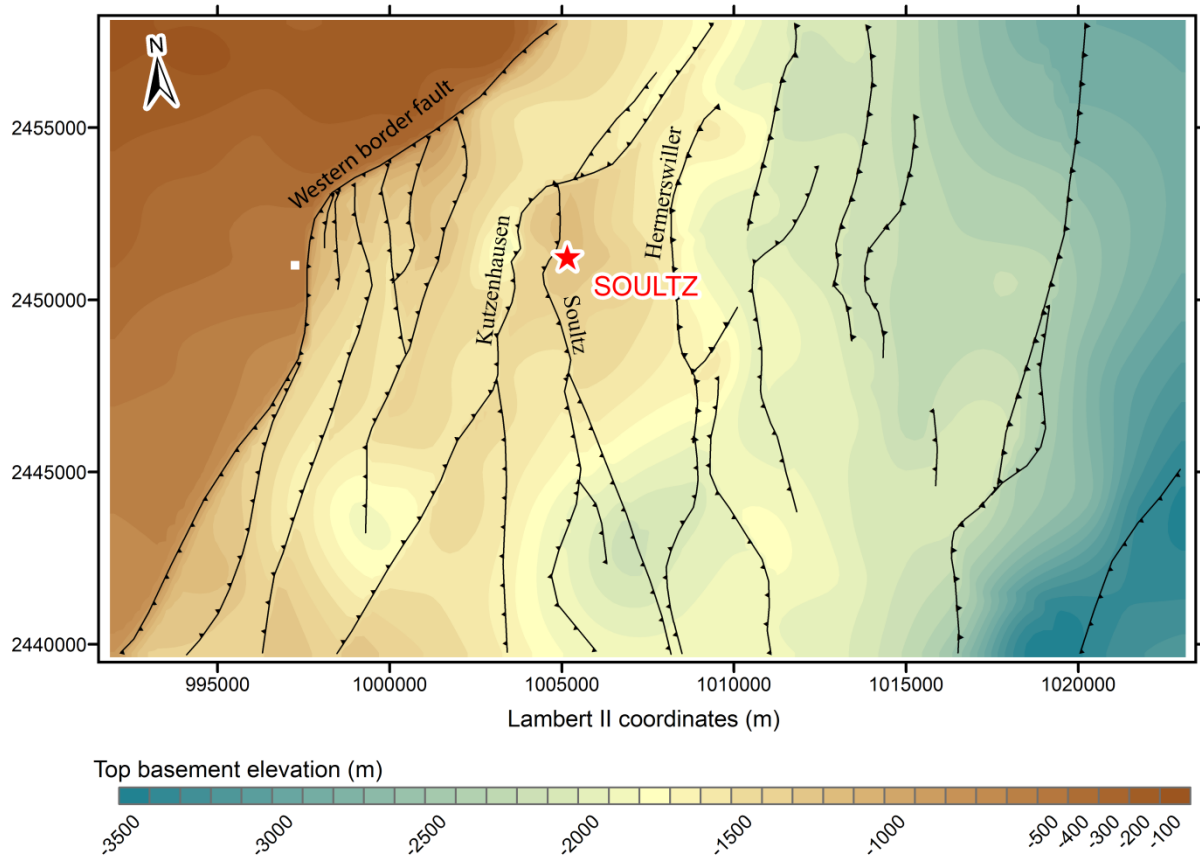


Figure 3-4 : Top basement elevation, fault traces and dip directions (black lines) at top basement in the area of the 3D geological model. Red star indicates the location of the European EGS test-site Soutz.

### 3.3.2 Geophysical data

#### *Magnetics*

The magnetic data presented in this study comes from a ground magnetic measurements campaign that was designed for detailed geophysical investigations using signal processing such as reduction to pole, vertical gradient and downward elevation (Edel *et al.*, 1982; Papillon, 1995). In this case the density of datapoints needed to be high. In the area of the 3D geological model, there are 837 ground magnetic measurements.

The magnetic anomaly is reduced to the pole and compared to the surface fault system of the 3D geological model and then compared with the contours of temperature anomaly at top basement.

#### *Gravity*

In our study a special effort is made to differentiate lateral variations of density due to lithological changes from porosity due to hydrothermal alteration and/or fracturing, which could be linked to positive temperature anomalies (upward flow) or to negative temperature anomalies (downward flow), and negative gravity anomalies.

To this end, Bouguer anomalies are first compared with the gravity forward modeling in the area of the 3D geological model. Secondly, different high pass filter wavelengths are applied on a larger area in order to remove the large scale and/or deep structures which have a regional gravimetric signature. Six filters of different wavelength have been used (20, 30, 50, 80, 100, 120, 150km). Finally, residuals and Bouguer anomalies are compared with the contours of temperature anomaly at top basement.



**Table 3-1 : Chosen densities for the gravity forward modeling of the 3D geological model**

Serie	Constituting rocks	Density (kg m <sup>-3</sup> )
Tertiary	Limestone/Marls/Sandstone	2350
Jurassic	Jurassic Limestone/Marls	2550
Keuper	Marls/Dolomite/Limestone/Sandstone	2700
Muschelkalk	Marls/Dolomite/Sandstone/Limestone	2700
Buntsandstein	Sandstone/Conglomerate	2500
Basement	Porphyric monzogranite/Fine-grained two-mica granite	2600

The gravity forward modeling is carried to quantify the gravity response of the 3D model using the code developed by Abdelfettah and Schill (2011). The densities (Table 1) were chosen by comparing measurements in Soultz boreholes (Genter, 1990; Rummel and König, 1991; Grecksch *et al.*, 2003) with determined average regional densities (Campos-Enriquez *et al.*, 1992; Edel and Weber, 1995; Papillon, 1995; Rotstein *et al.*, 2006).

A code using Butterworth filter (Butterworth, 1930) was developed to be applied on the complete Bouguer anomaly to eliminate the regional trends (Abdelfettah and Schill, 2012). This filter is characterized and controlled mainly by two parameters: (1) cut-off frequency or wavelength and (2) the filter order. The advantage of the Butterworth filter is that we can easily use different wavelength to 1) delineate and characterize different negative anomalies at depth, and 2) to choose an adequate residual anomaly which provides a comparable gravity response with the conceptual model. Depth and size of the origin of the anomalies are indicated among others by the wavelength of the filter. With increasing wavelength, it is possible to visualize increasing larger or deeper structures until approaching the Bouguer anomaly. Moreover, the filter order parameter can be also changed to delineate very small variations, for instance, in the case of low density contrasts. With increasing filter order the horizontal density contrast is emphasized.

To avoid physical inconsistency, superposed gravity campaigns are removed from the existing database from Rotstein *et al.* (2006) before being presented in this study. A total of 1011 datapoints in the area of Soultz are thus selected.

### 3.3.3 Slip and dilation tendencies analysis

#### ***Theory and equations***

Slip and dilation tendency analysis is a technique that permits rapid and easy visual assessment of stress states and related potential fault activity (Morris *et al.*, 1996; Ferrill *et al.*, 1999; Moeck *et al.*, 2009). Slip is likely to occur on a surface if resolved shear stress (the component of shear stress that is resolved in the direction of slip),  $\tau$ , equals or exceeds the frictional sliding resistance,  $\mu_s$ , which is proportional to normal stress  $\sigma_n$ .

Slip tendency ( $T_s$ ) of a surface is defined as the ratio of resolved shear stress to resolved effective normal stress ( $\sigma_n$  minus pore fluid pressure  $P_f$ ) on that surface:

$$(1) T_s = \tau / \sigma_{neff} \geq \mu_s$$

The dilation tendency is the propensity for a fault or fracture to dilate. The dilation of faults and fractures is largely controlled by the resolved normal stress which is a function of the lithostatic and tectonic stresses, and fluid pressure. The magnitude of normal stress can be computed for surfaces

of all orientation within a known or suspected stress field. This normal stress can be normalized by comparison with the differential stress to give the dilation tendency,  $T_d$ , for a surface, defined by:

$$(2) T_d = \frac{\sigma_1 - \sigma_{neff}}{\sigma_1 - \sigma_3}$$

In practice, and especially when considering the fluid transmissivity properties of a fault or fracture, a combination of slip and dilation tendency may be more useful. The slip and dilation tendency is defined as the sum of the slip tendency and dilation tendency:

$$(3) T_{s+d} = \frac{\sigma_1 - \sigma_n}{\sigma_1 - \sigma_3} + \tau / \sigma_{neff}$$

Slip, dilation, or sum of slip and dilation tendency stereoplots are obtained by solving Eqs.(1), (2) or (3) for all planes in 3D space.

### ***Stress distribution at Soultz***

The stress distribution at Soultz has been characterized in the 3 deep boreholes between depths 1.5-5.0 km, by observations of breakouts and drilling-induced tension fractures (DITFs) combined with the analysis of pressure data from stimulation tests (Valley and Evans, 2007 and references therein).

The orientation of the maximum horizontal stress,  $\sigma_{H_{max}}$ , is found to be N169°E±14°. The amplitude of the vertical stress,  $\sigma_v$ , representing the vertical load, is:

$$\sigma_v = -1.30 + 25.50 z \quad [\text{MPa}]$$

Where  $z$  represents the depth in km. The magnitude of the minimum horizontal stress,  $\sigma_{H_{min}}$ , is:

$$\sigma_{H_{min}} = -1.78 + 14.06 z \quad [\text{MPa}]$$

The maximum horizontal stress,  $\sigma_{H_{max}}$ , ranges between:

$$0.90 \sigma_v \leq \sigma_{H_{max}} \leq 1.05 \sigma_v$$

Thus,

$$-1.17 + 22.95 z \leq \sigma_{H_{max}} \leq -1.37 + 26.78 z$$

The fact that  $\sigma_{H_{max}}$  is nearly equal to  $\sigma_v$  implies that both the normal and strike-slip faulting stress regimes can coexist at Soultz. In the following it is assumed that  $\sigma_1 = \sigma_v$ ,  $\sigma_2 = \sigma_{H_{max}} = 0.975 \sigma_v$  and  $\sigma_3 = \sigma_{H_{min}}$ . At Soultz the hydraulic pressure can be considered as hydrostatic, because water occurs down to 5 km depth.

First, the sum slip and dilation tendency is represented in 3D on the fault system. For an optimal comparison with the temperature anomalies and thus an interpretation of the possible occurrence of hydrothermal circulation along the faults, the slip, dilation and sum slip and dilation tendencies on the fault system are plotted at the basement top.

## 3.4 Results and Discussion

### 3.4.1 Temperature distribution at top basement

The temperature field, covered by 112 boreholes in the Soultz area, shows a variability of temperature with a minimum gradient of  $39.2^{\circ}\text{C km}^{-1}$  and a maximum temperature of  $110\text{-}120^{\circ}\text{C}$  at 1 km (Figure 3-5) under Soultz site. The temperature measurements in boreholes offer a rather good coverage of the temperature field at top basement (Figure 3-6). For these reasons, the temperature anomalies patterns are evaluated at top basement by subtracting the lowest observed temperature gradient of  $39.2^{\circ}\text{C per km}$  from the data.

The temperature field at top basement is sufficiently well covered by temperature data in the boreholes (Figure 3-6 and Figure 3-7) to reveal interesting features:

Firstly, a minimum temperature anomaly of  $40^{\circ}\text{C}$  can be expected at top basement in the center of the model area. This average temperature anomaly can be related to the presence of a crystalline ridge made of granites and granodiorites (Figure 3-1) as expected from gravity and magnetic interpretation (Edel and Fluck, 1989; Jeannette and Edel, 2005; Rotstein et al., 2006; Edel et al., 2007; Edel and Schulmann, 2009). The high radiogenic heat production observed in Soultz boreholes (Pribnow *et al.*, 1999; Grecksch *et al.*, 2003) is also in favor of this interpretation.

Secondly, three temperature anomalies above  $60^{\circ}\text{C}$  occur in the center of the model area, and they are to be related to hydrothermal convection bringing heat to shallower level (e.g. Kohl *et al.*, 2000; Pribnow and Schellschmidt, 2000; Bächler *et al.*, 2003). One of them is the anomaly of Soultz ( $> 80^{\circ}\text{C}$ ), and it is covered by numerous boreholes (previously used for oil production). It is on the northern tip of the horst structure bounded by the Kutzenhausen, Soultz and Hermerswiller faults. Soultz anomaly seems centered on the Soultz fault in the North western side of the horst. The second temperature anomaly is the anomaly of Rittershoffen ( $> 80^{\circ}\text{C}$ ). It is located 6-7 km away from Soultz to the East, on the western side again of another horst structure, in which the western fault has a remarkably similar shape than the western fault at Soultz. This anomaly is currently being investigated for a new geothermal project, named ECOGI. About 7-8 km to the South of Soultz, the third one, Rohrlach anomaly (above  $60^{\circ}\text{C}$ ), is found between two faults dipping to the West, but it is only sampled in one borehole.

All these three anomalies are located close to N-S directed, West dipping faults, in horst structures. In Soultz reservoir most of the naturally flowing fracture zones or enhanced during stimulation have this N-S directed, West dipping signature (Dezayes *et al.*, 2010; Sausse *et al.*, 2010; Baillieux *et al.*, 2011- Appendix A).

An additional observation is the observed electrical conductivity anomaly at top of basement again in the western side of the Soultz horst also attributed to hydrothermal fluids as a result of magnetotelluric investigation (Geiermann and Schill, 2010). These observations may be related to the interpretation of Cathelineau & Boiron (2010), who record in fluid inclusions analyses a fluid paleocirculation characterized by an upward flow of hot water with a meteoric signature, and interpret this flow as deep circulation coming from the Vosges mountain basement to the West.

Another explanation is an asymmetric mechanical deformation behavior in this area. In this respect, a link can be made with a recent seismic reinterpretation of profile PHN84J crossing Soultz horst

structure (Place *et al.*, 2010). On this profile the horst eastern fault (Hermerswiller fault) appears as a detachment fault which dissipates above the basement within the top of Buntsandstein clay units. Thus the connection of this fault to the basement in the model may not be real and this may explain the absence of a temperature anomaly in this side of the horst structure.

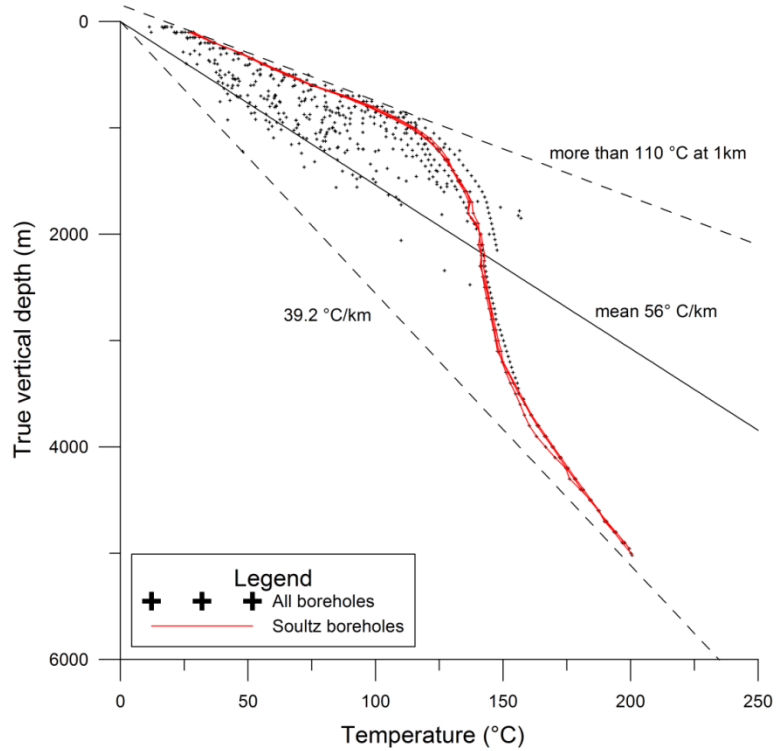


Figure 3-5 : Temperature distribution in the 112 boreholes of Soultz area. Database from Pribnow and Schellschmidt (2000) and Agemar *et al.* (2012).

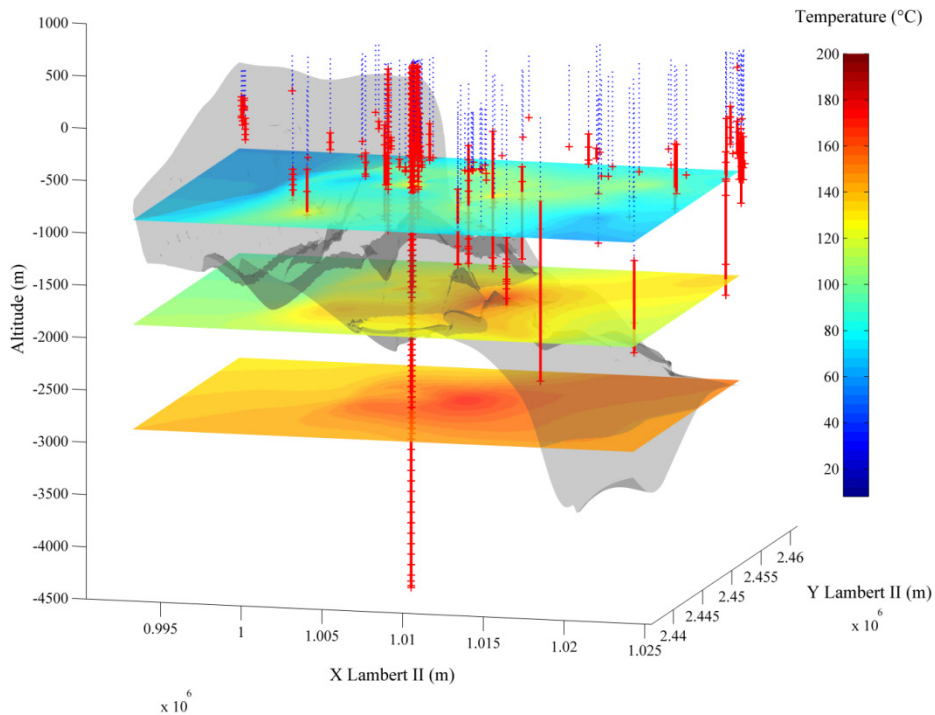
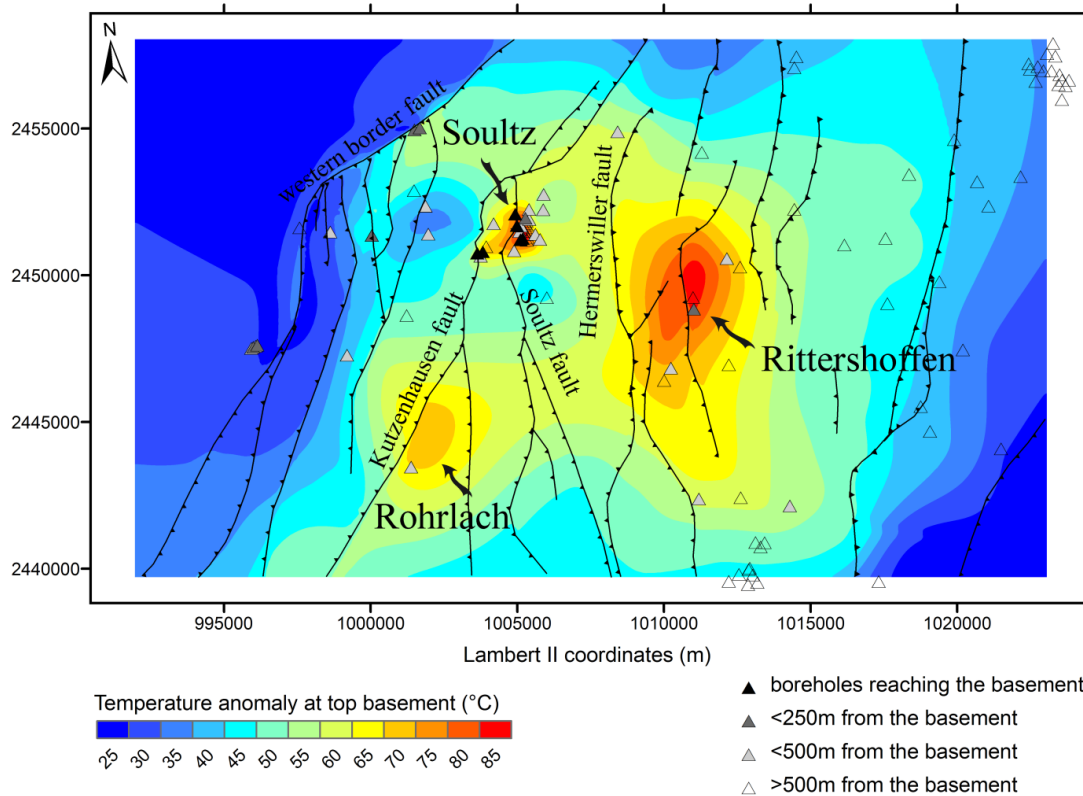
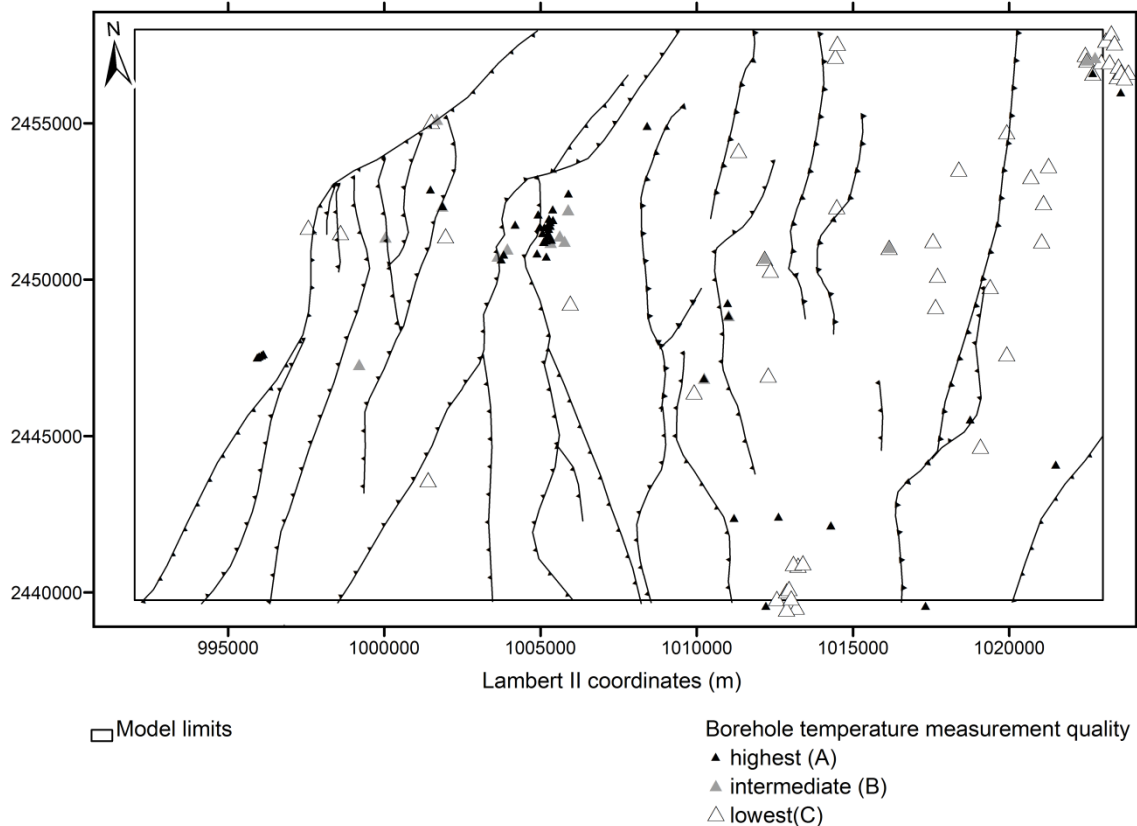


Figure 3-6 : Visualization of the temperature distribution at -1000, -2000 and -3000 m above sea-level, temperature measurements distribution along boreholes (red crosses) and 3D basement elevation (grey) within the limited area of the 3D geological model. Temperature database from Pribnow and Schellschmidt (2000) and Agemar *et al.* (2012).



**Figure 3-7 : Temperature anomaly at top basement, distribution of temperature measurements and their distance to top basement, and fault traces and dip directions (black lines) at top basement in the area of the 3D geological model. A temperature gradient of 39.2°C per km, corresponding to the lowest observed temperature gradient in the area, is subtracted from the temperature field at top basement to obtain this temperature anomaly map at top basement. Temperature database from Pribnow and Schellschmidt (2000) and Agemar et al. (2012).**



**Figure 3-8 : Distribution and quality of borehole temperature measurements in the area of the 3D geological model. Categories of quality among the measurements come from the study by Agemar et al. (2012).**

### 3.4.2 Geophysics

#### ***Magnetics***

In the central part of the model, it can be observed that the fault system follows a 15 km-large positive magnetic structure (Figure 3-9). This is in favor of the interpretation of a lateral variation of the pre-Permian basement in the area, which induced the localization of the observed normal faulting during the graben opening. This magnetic anomaly has been interpreted in a plutonic basement made diorites and granodiorites of a magmatic arc emplaced in the time-range 335-330Ma (Figure 3-1).

No clear link can be made between the magnetic anomalies and the temperature. The Soultz temperature anomaly is located on the western side of the positive magnetic anomaly (Figure 3-9), where the contrasting basement rock environment may have induced a localization of faulting during the graben opening. There, the Kutzenhausen and Soultz faults are shown to host hydrothermal convection (Kohl *et al.*, 2000). The other two temperature anomalies are either located on top or outside the magnetic anomaly.

#### ***Gravity***

The measured Bouguer anomaly in total ranges between -39 and -23 mgals, covering an interval of 16 mgals (Figure 3-10 top). An important negative gravity anomaly can be observed in the region of Soultz. It has previously been attributed to a low density granitic and granodioritic basement of Lower Carboniferous age (Figure 3-1), joining the observation of several types of granite and sub-facies in the geothermal wells (Genter, 1990; Hooijkaas *et al.*, 2006).

The negative gravity anomaly is not explained by the forward gravity response of the 3D geological model (Figure 3-10 bottom) for which the gravity values decreases gradually from West to East by 14 mgals. Although the light basement occupies 90% of the model, the observed trend on the forward gravity response reflects an overestimated gravimetric effect of the sediments, because lower values are observed on the eastern side of the model where sediment thickness is the largest. In addition, the 3D model does not include the density variations associated with fracturing and only one basement type is modeled.

The 20km residuals (Figure 3-11 top) most probably reflect the shallowest observable trends in gravity. This results in residuals variations being often surrounded by the fault system that mostly affect the first kilometers of the upper crust. Additionally, four negative gravity anomalies are observed in areas which are not highlighted by the forward gravity response of the 3D model, and they could be related to surface geology.

As shown by the 80 km residuals (Figure 3-11 bottom) the most southern negative gravity anomaly is dominated by a large negative anomaly at depth, and its effect is outwardly reduced. The 80km residuals are a trade-off between surface gravity anomalies and the longer wavelengths observed in the Bouguer anomalies. Mainly, three negative gravity anomalies are observed:

The most western one could be related to a large structure extending over 10-15km in the East-West direction. By comparison with the Bouguer anomaly map, this structure seems to have a East dipping signature.

The central negative gravity anomaly is observed in both 20km residuals and Bouguer anomaly map, with a westward migration at depth. It may be related to a West dipping structure. It may also be related to the observed central magnetic anomaly.

The most northern negative anomaly increases size at depth. Apart from the central anomaly which may be linked to a magnetic structure, no link can be made with magnetic data, surface geology or gravity response of the 3D model. These zones reflect a low density contrast with the surrounding environment, which can either be explained by fracturing or variation in lithology at depth.

On the 20 km residuals map, temperature anomalies are either distributed on positive or negative gravity anomalies, which make the comparison difficult (Figure 3-12 top).

On the 80km residuals map, Soultz and Rohrlach temperature anomalies are located at the frontier between two contrasting gravity anomalies and closely located to the large-size low gravity anomaly to the West (Figure 3-12 bottom). By comparison between the 20, 50 and 80 km residuals, this low gravity anomaly seems to migrate in a westward direction at depth. This could be interpreted in temperature anomalies being located along faults with contrasting density environments, and linked to hydrothermal circulation occurring in a probably fractured and low density environment to the West, in a basement which had not been expected from the 3D model. In the center of the model, Rittershoffen temperature anomaly is linked to a negative gravity anomaly which can also be linked to the magnetic structure; this makes the interpretation more difficult in terms of fracturing. On the 20, 50 and 80 km residuals, this low gravity anomaly migrates in eastward direction towards the center of the model at depth.

The evaluation of residual anomalies leads to the conclusion that major gravity anomalies dip eastwards when linked to the western boundary fault system and dip westwards when linked to temperature anomalies. This supports the hypothesis that westward dipping faults are main up-flow structures that account for the thermal anomalies.

On the Bouguer anomaly map, all temperature anomalies are located in negative gravity anomalies, and a minimum of 40°C temperature anomaly centered on this negative anomaly can be observed in the model area (Figure 3-13). The observation of high radiogenic heat production granites observed in Soultz boreholes (Pribnow *et al.*, 1999; Grecksch *et al.*, 2003) may explain this temperature anomaly. It can also be noted that in the southern or in the eastern part of the model, which has been interpreted in a high density basement of Early Paleozoic or Late Proterozoic age (Figure 3-1) or Paleozoic schist (Rotstein *et al.*, 2006), positive gravity anomalies is provoking a decrease of the temperature anomalies.

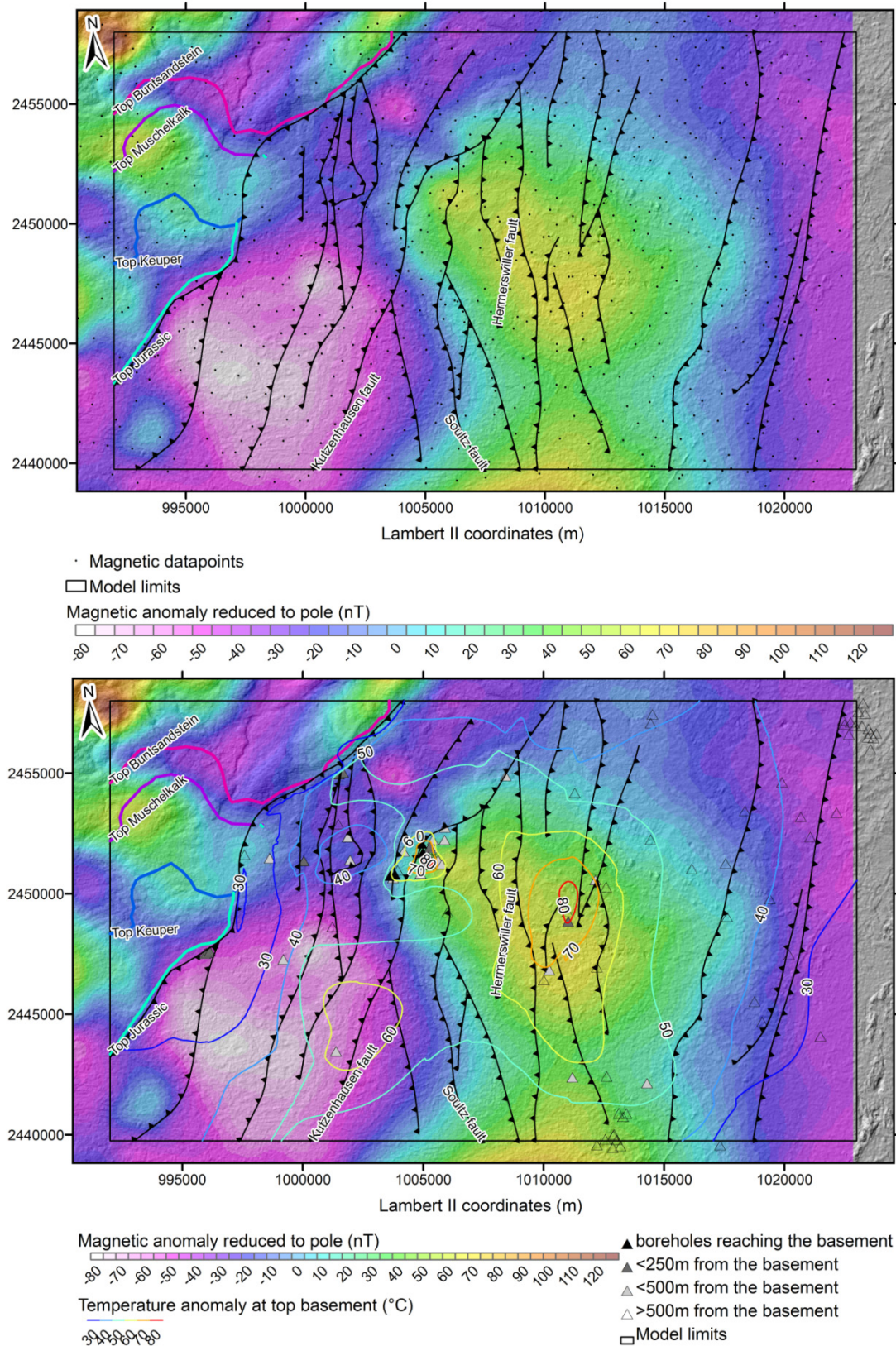


Figure 3-9: (top) Magnetic anomaly reduced to pole, surface features from the 3D model (fault system, horizons) (bottom) Magnetic anomaly reduced to pole, surface features from the 3D model (fault system, horizons) and contours of temperature anomaly at top basement



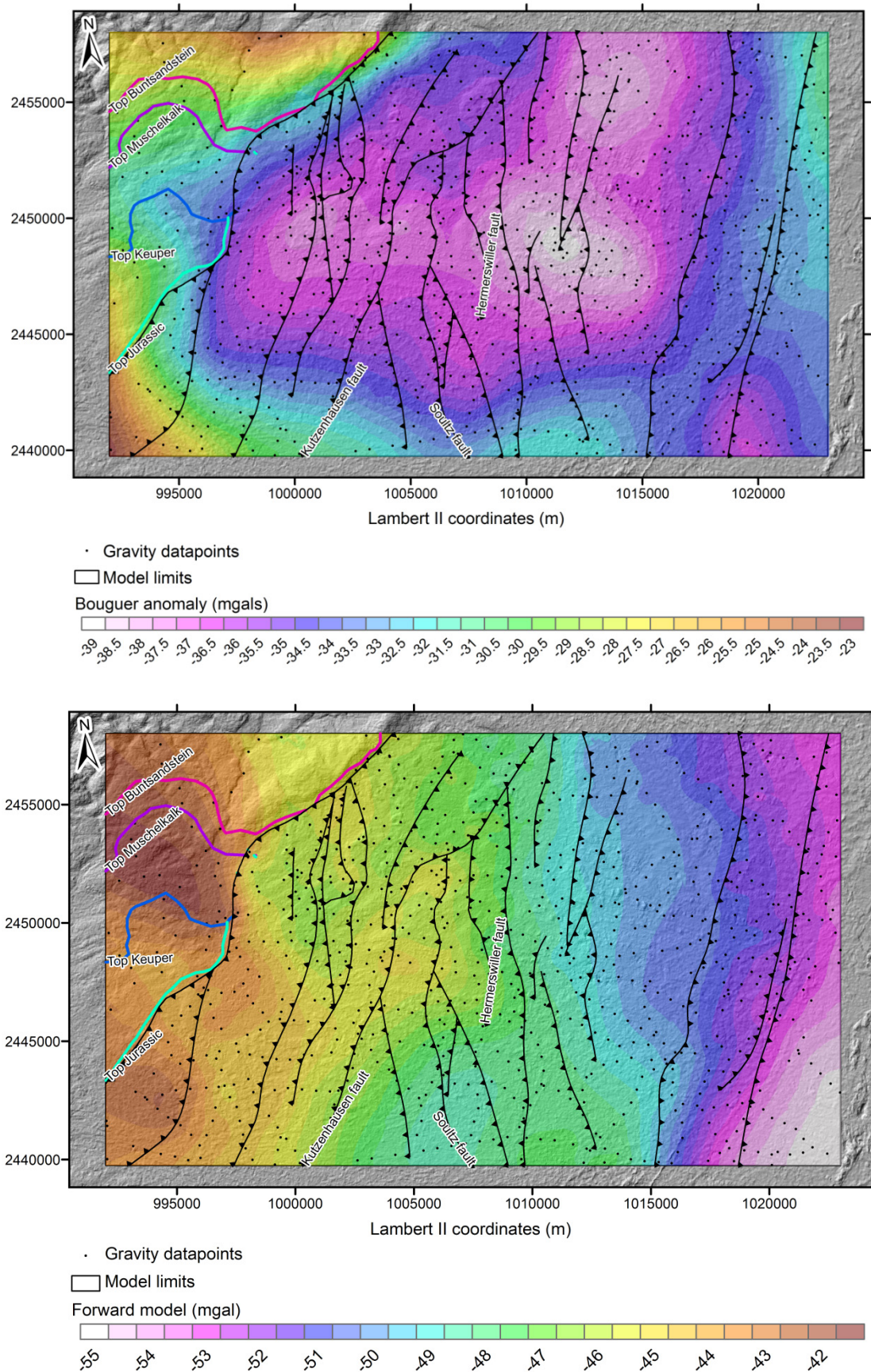


Figure 3-10 : (top) Bouguer anomaly with reference density  $2670 \text{ kg m}^{-3}$ , surface features from the 3D model (fault system, horizons). (bottom) Gravity forward response of the model with reference density  $2670 \text{ kg m}^{-3}$ , and surface features from the 3D model (fault system, horizons).

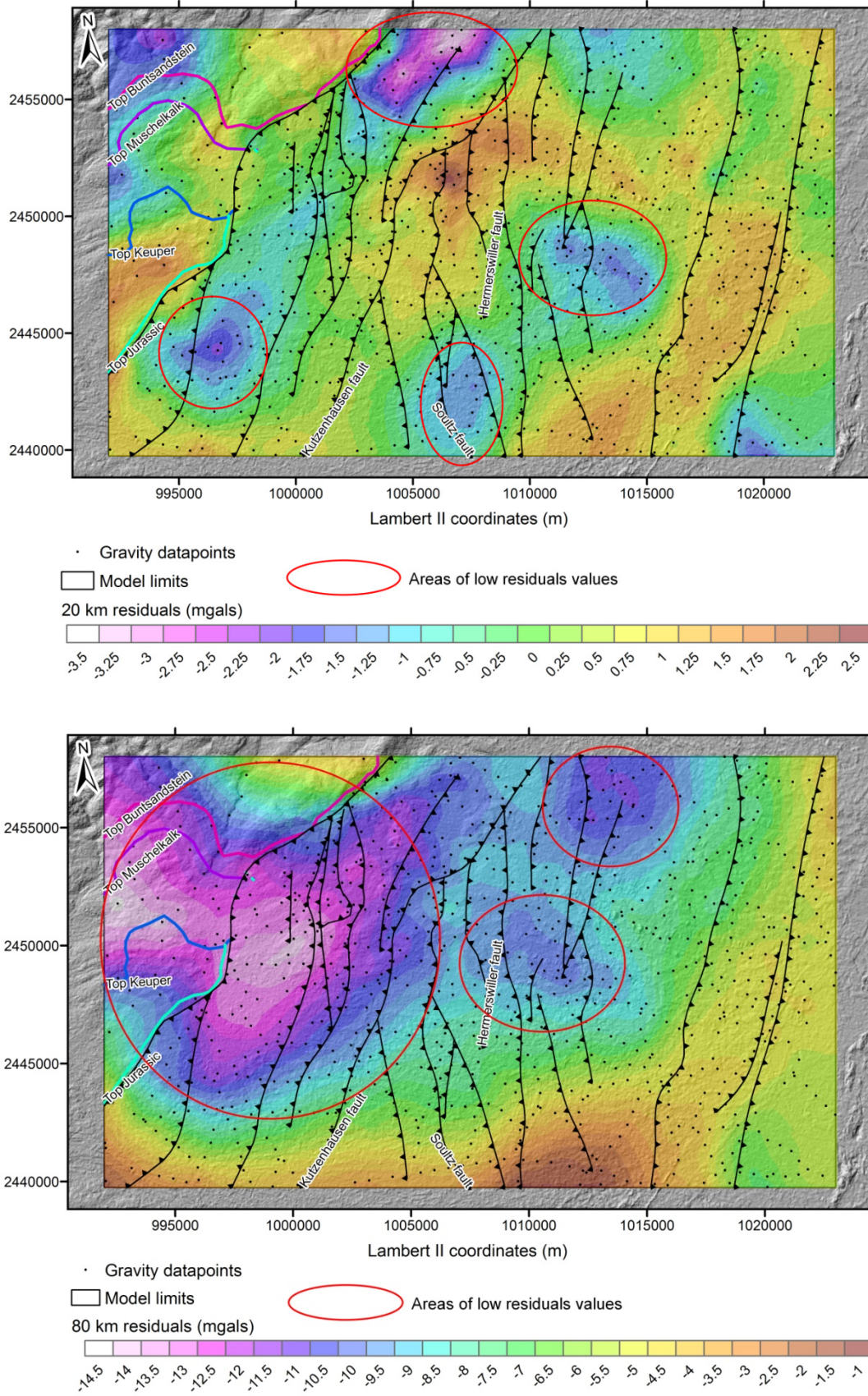


Figure 3-11 : (top) Gravity residuals after 20 km Butterworth filter, and surface features from the 3D model (fault system, horizons). Red circles refer to zones of low gravity residuals described in the text. (bottom) Gravity residuals after 80 km Butterworth filter, and surface features from the 3D model (fault system, horizons). Red circles refer to zones of low gravity residuals described in the text.

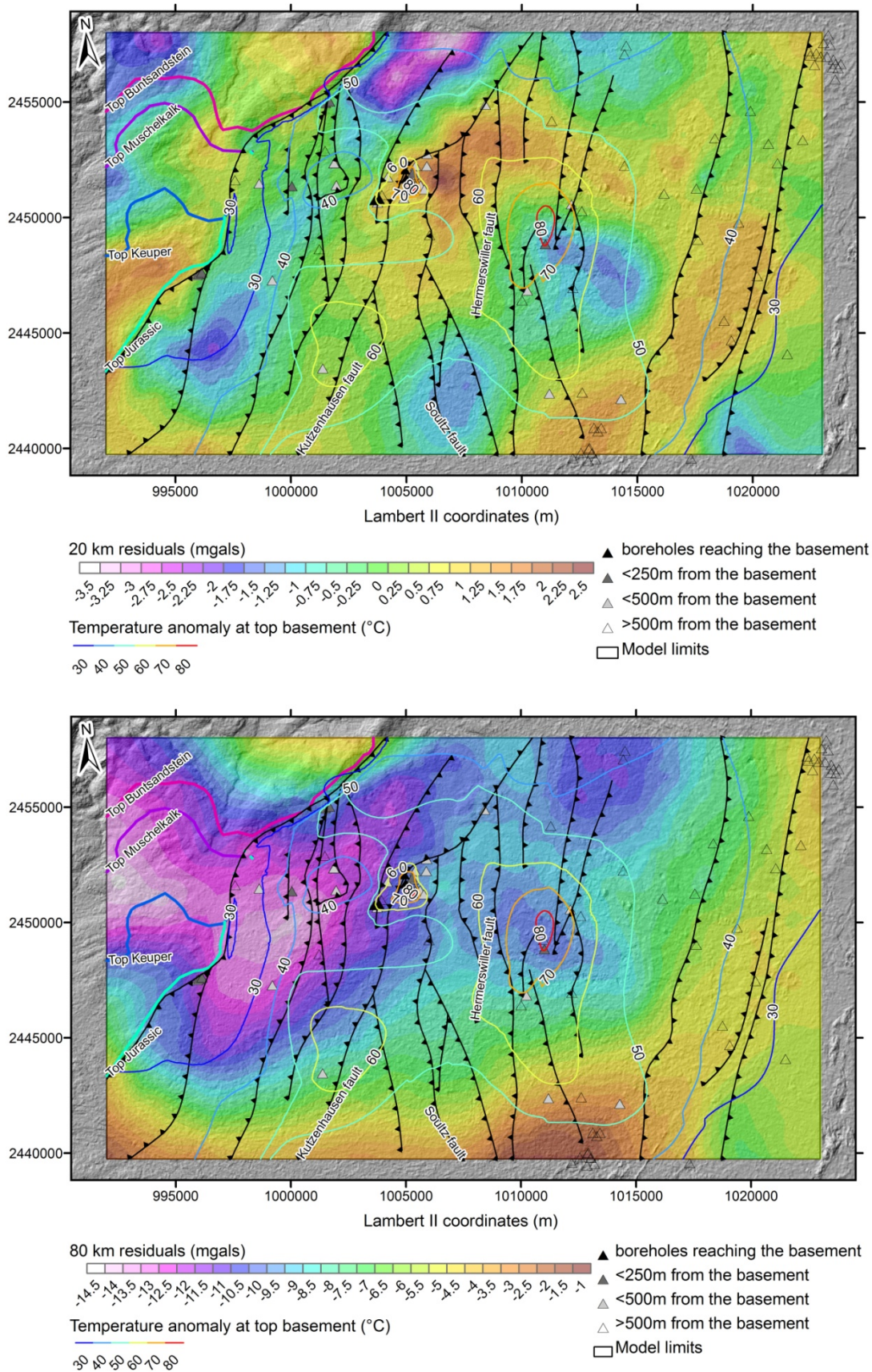
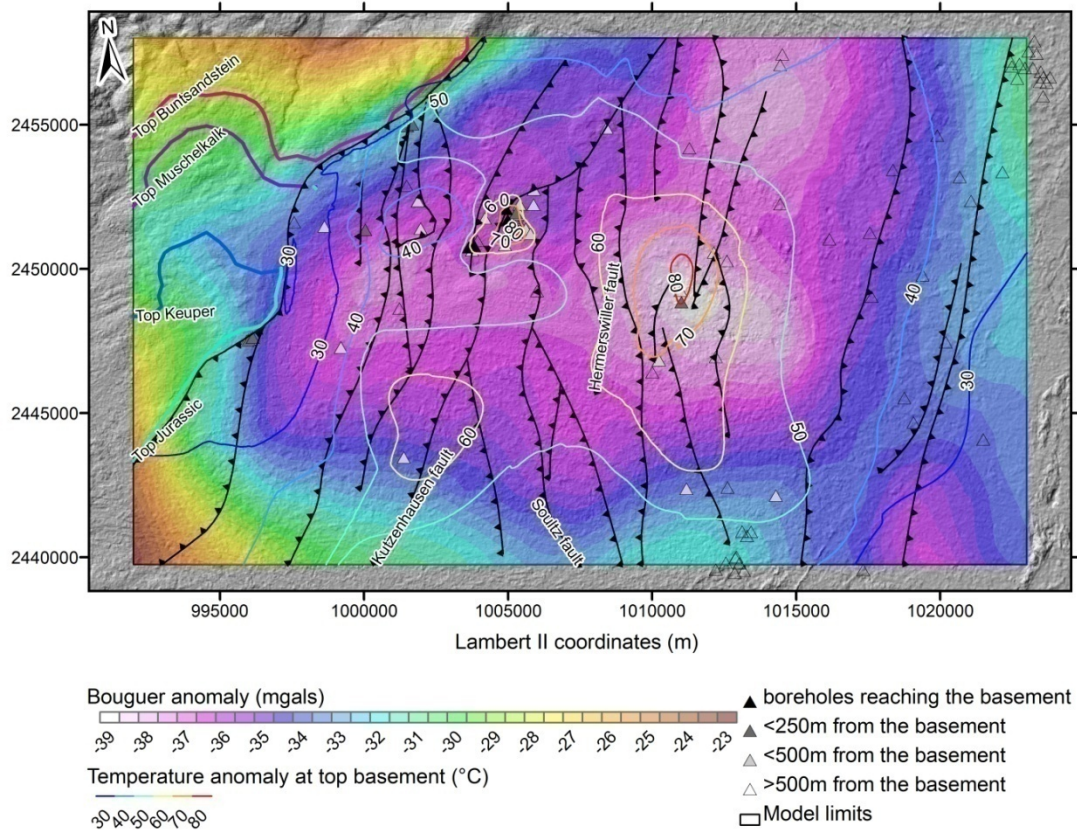


Figure 3-12 : (top) Gravity residuals after 20 km Butterworth filter, surface features from the 3D model (fault system, horizons) and contours of temperature anomaly at top basement. (bottom) Gravity residuals after 80 km Butterworth filter, surface features from the 3D model (fault system, horizons) and contours of temperature anomaly at top basement.



**Figure 3-13 : Bouguer anomaly with reference density  $2670 \text{ kg m}^{-3}$ , surface features from the 3D model (fault system, horizons) and contours of temperature anomaly at top basement**

### 3.4.3 Slip and dilation tendencies analyses

In the center of the model, most of the faults are favorably oriented in the present day stress conditions to be reactivated and host slip movements at depth under the hydraulic load (Figure 3-14). However, the maximum slip tendency,  $T_{smax}$  is quite low (0.33), so the faults do not seem to be close to “critical stress” conditions. This interpretation coincides with the comparably low natural seismicity in the area of Soultz and the surrounding thermal anomalies. Nevertheless, NNW – SSE striking faults have the highest slip or dilation tendencies (Figure 3-15). This is in agreement with the input stress distribution at Soultz obtained from breakouts and drilling-induced tension fractures combined with the analysis of pressure data from stimulation tests (Valley and Evans, 2007 and references therein).

The three temperature anomalies above  $60^\circ\text{C}$  are located along N-S trending faults having medium slip or dilation tendency (Figure 3-15). Other faults with high slip or dilation tendency do not seem to be associated with hydrothermal circulation.

Illies *et al.* (1981) show that, considering Barenblatt’s (1962) theory on equilibrium cracks in an elastic medium, a crack is likely to stay open at depth of 4-5 km under hydrostatic pressure, and can sustain a shearing stress of 10 MPa and even more without reaching the yield value of the surrounding rocks. Yield values on Soultz granites have been estimated to be 100-130 MPa (Valley and Evans, 2007) while  $SH_{max}$  is estimated to be  $113.58 < SH_{max} < 132.51$  MPa on the basis of borehole breakouts analyses (Valley and Evans, 2007).

Illies & Greiner (1979) states that convective heat transport occurs along N-S striking fractures zones in the basement and in the high porosity sandstone (Buntsandstein) aquifer above it, because these fractures zones are favorably oriented in the present day stress conditions to be reactivated, to host slip movements and undergo dilation at depth under the influence of the hydraulic load.

In crystalline rocks, Barton *et al.* (1995) observe that the permeability of critically stressed faults is much higher than that of faults that are not optimally oriented for reactivation or slip in the current stress field. Zoback (2007) observes that faults in strike-slip tectonic regime may be also prospective as the termination of strike-slip faults, crossing of faults may result in local extension and open fractures.

Our results suggest that slip and dilation tendency alone are not sufficient to explain the hydrothermal anomalies in the Soultz area, and additional factors need to be sought. As discussed earlier, a possible explanation for hydrothermal circulation is the asymmetric deformation patterns which creates opening of the West dipping faults (in horst structures), and these may be also linked to the Vosges mountain basement to the West. Other possible factors could explain this distribution: for instance, recently active faults may be more permeable than other faults. It is also possible that the faults with the highest slip and dilation tendencies have been very active in promoting hydrothermal circulation and have thus been sealed by mineralization. Additionally another explanation is that local pore fluid pressure anomalies are pushing the stress state closer to critical under the major temperature anomalies.

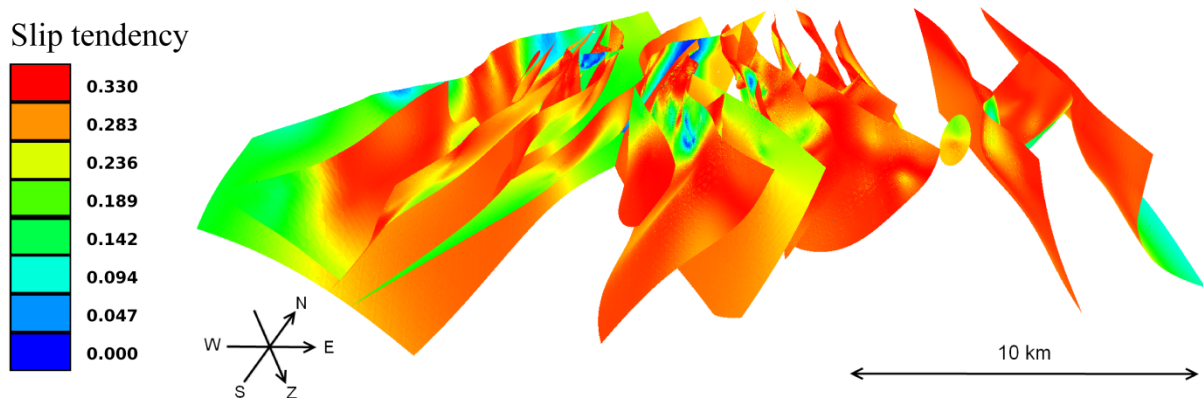
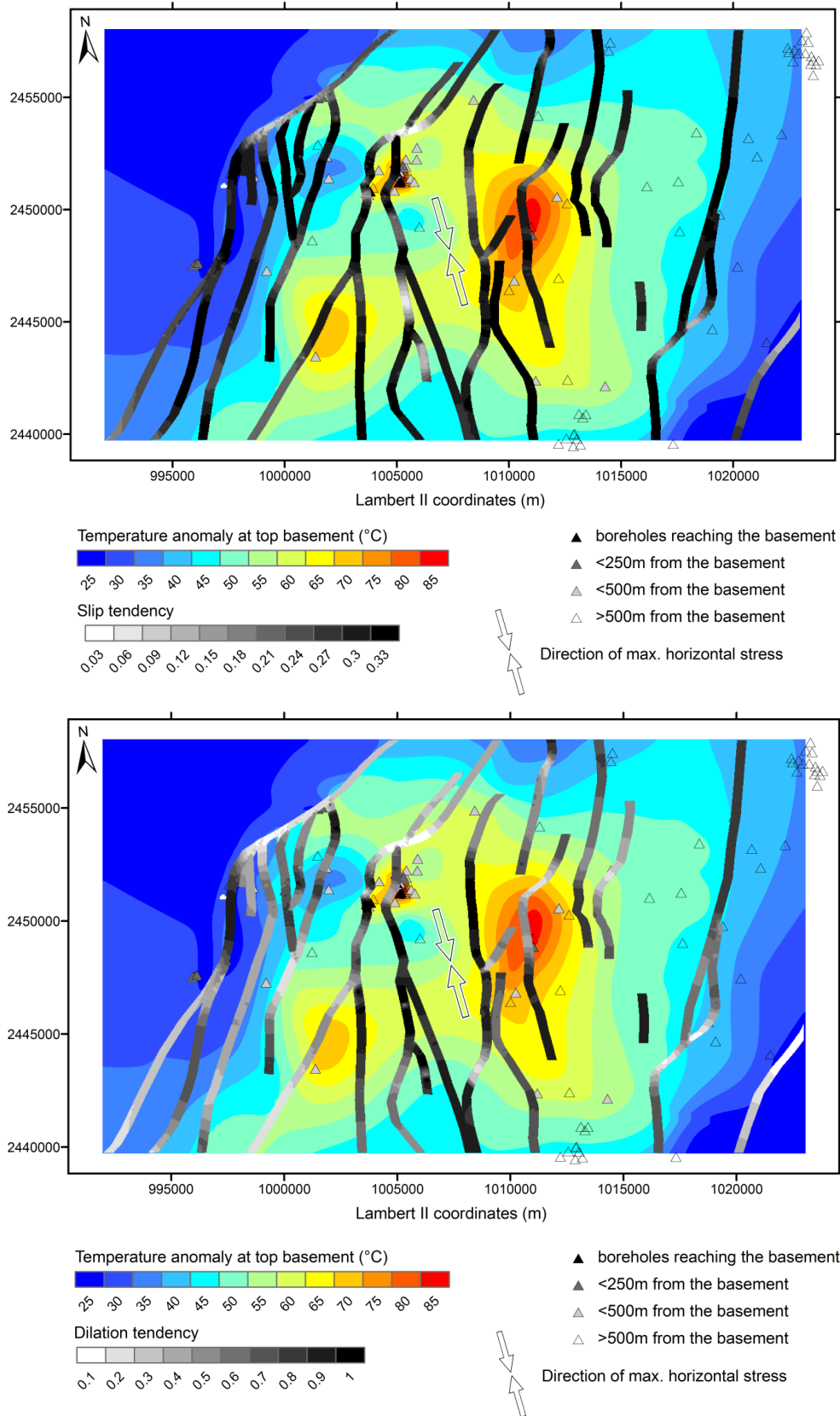


Figure 3-14 : Slip tendency on the fault system of the 3D geological model.



**Figure 3-15 : (top) Slip tendency on the fault system at top basement and temperature anomaly at top basement in the area of the 3D geological model. Direction of maximum horizontal stress at depth is taken from boreholes analysis at Soultz (Valley and Evans, 2007). (bottom) Dilation tendency on the fault system at top basement and temperature anomaly at top basement in the area of the 3D geological model. Direction of maximum horizontal stress at depth is taken from boreholes analysis at Soultz (Valley and Evans, 2007).**

### 3.5 Conclusions

The temperature anomalies in the area of Soultz may be attributed to different sources. First, the presence of a light and magnetic granodioritic pluton in the larger magmatic arc emplaced in the time-range 335-330Ma as postulated by Edel and Fluck (1989), Edel (2004), Jeannette and Edel (2005), Rotstein *et al.* (2006) and Edel and Schulmann (2009) on the basis of gravity and magnetic modeling (Figure 3-1), with an additionally high radiogenic heat production as observed in Soultz (Pribnow *et al.*, 1999; Grecksch *et al.*, 2003), appears to be responsible for 40°C additional temperature at top basement.

Three temperature anomalies above 60°C are to be related to hydrothermal convection bringing heat to shallower level (e.g. Kohl *et al.*, 2000; Pribnow and Schellschmidt, 2000; Bächler *et al.*, 2003).

Most of the faults in the model have low to moderate slip tendency at top basement despite they are trending NNE-SSW to N-S which is the direction of the current stress field observed at depth in Soultz boreholes (Valley and Evans, 2007). The 3 temperature anomalies above 60°C are located along N-S trending faults with medium slip or dilation tendency. Other faults having medium slip tendency but high dilation tendency do not seem to be associated with hydrothermal circulation.

Slip and dilation tendency alone thus are not sufficient to explain the hydrothermal anomalies in the Soultz area, and additional factors need to be sought.

The 3 temperature anomalies above 60°C are located close to N-S directed, West dipping faults, in horst structures. In Soultz reservoir most of the naturally flowing fracture zones or enhanced during stimulation have this N-S directed, West dipping signature (Dezayes *et al.*, 2010; Sausse *et al.*, 2010; Baillieux *et al.*, 2011- Appendix A). An additional observation is the electrical conductivity anomaly at top of basement again in the western part of the Soultz horst also attributed to hydrothermal fluids as a result of magnetotelluric investigation (Geiermann and Schill, 2010). These observations may be related to the interpretation of Cathelineau & Boiron (2010), who record in fluid inclusions analyses a fluid paleocirculation characterized by an upward flow of hot water with a meteoric signature, and interpret this flow as deep circulation coming from the Vosges mountain basement to the West. The gravity processing results also reinforces this interpretation, since the evaluation of residual anomalies leads to the conclusion that major gravity anomalies dip eastwards when linked to the western boundary fault system and dip westwards when linked to temperature anomalies.

Another explanation is an asymmetric mechanical deformation behavior in this area. In this respect, a link can be made with a recent seismic reinterpretation of profile PHN84J crossing Soultz horst structure (Place *et al.*, 2010). On this profile the horst eastern fault (Hermerswiller fault) appears as a detachment fault which dissipates above the basement within the top of Buntsandstein clay units. Thus the connection of this fault to the basement in the model may not be real and this may explain the absence of a temperature anomaly in this side of the horst structure.

The occurrence and connection of horst structure linked to these West dipping faults to the basement should be investigated more in details along the seismic profiles, with mechanical or geodynamic modeling, and with additional geophysical data such as magnetotelluric.

### 3.6 Acknowledgements

The authors would like to thank LIAG-Hannover, BRGM and GEIE Soultz, and EOST Strasbourg for providing input data: borehole temperatures, seismic profiles and borehole geology for the creation of the 3D geological model, and geophysical data, respectively.

Laurent Beccaletto, Philippe Calcagno, J.-B. Edel, Albert Genter, Alan Morris, Benoit Valley, Rüdiger Schellschmidt, Fritz Rummel and colleagues at CHYN are warmly acknowledged for their contribution in this paper.

This work is part of a PhD by Paul Baillieux financed by University of Neuchâtel.

### 3.7 References

- Abdelfettah, Y. and Schill E. (2011). Accurate gravity data correction and 3D gravity forward modeling. 9th Swiss Geoscience Meeting, Zurich 2011.
- Abdelfettah, Y. and Schill E. (2012). Delineation of geothermally relevant Paleozoic graben structures in the crystalline basement of Switzerland using gravity Istanbul International Geophysical Conference and Oil & Gas Exhibition, Istanbul, Turkey, 17-19 September 2012. .
- Agemar, T., Schellschmidt R. and Schulz R. (2012). Subsurface temperature distribution in Germany. *Geothermics* 44(0): 65-77.
- Ahorner, L. (1975). Present-day stress field and seismotectonic block movements along major fault zones in Central Europe. *Tectonophysics* 29(1-4): 233-249.
- Aquilina, L., Pauwels H., Genter A. and Fouillac C. (1997). Water-rock interaction processes in the Triassic sandstone and the granitic basement of the Rhine Graben: Geochemical investigation of a geothermal reservoir. *Geochimica et Cosmochimica Acta* 61(20): 4281-4295.
- Bächler, D., Kohl T. and Rybach L. (2003). Impact of graben-parallel faults on hydrothermal convection - Rhine Graben case study. *Physics and Chemistry of the Earth* 28(9-11): 431-441.
- Baillieux, P., Schill E. and Dezayes C. (2011). 3D structural regional model of the EGS Soultz site (northern Upper Rhine Graben, France): insights and perspectives. *Proceedings, Thirty-Sixth Workshop on Geothermal Reservoir Engineering, Stanford University, Stanford, California, SGP-TR-191.*
- Barenblatt, G. I. (1962). The mathematical theory of equilibrium cracks in brittle fracture. *Adv. Appl. Mech.*, 7: 55--129.
- Barton, C. A., Zoback M. D. and Moos D. (1995). Fluid flow along potentially active faults in crystalline rock. *Geology* 23(8): 683-686.
- Bartz, J. (1974). Die Mächtigkeit des Quartärs im Oberrheingraben. Illies JH, Fuchs K (eds) *Approaches to taphrogenesis Schweizerbart, Stuttgart*: pp 78–87.
- Beccaletto, L., Capar L., Cruz-Mermy D., Oliviero G., Elsass P., Perrin A., Rupf I., Nitsch E. and Tesch J. (2010). The GeORG project: seismic interpretation, structural pattern and 3-D modelling of the Upper Rhine Graben – first scientific results. . Technical workshop. *Geopotential of the Upper Rhine Graben (GeORG)*. (November 18th 2010, Freiburg (Germany)).
- Brun, J. P., Gutscher M. A. and {DEKORP-ECORS teams} (1992). Deep crustal structure of the Rhine Graben from seismic reflection data: A summary. *Tectonophysics* 208(1-3): 139-147.
- Butterworth, S. (1930). On the theory of filter amplifiers. *Wireless Engineering* 1: 536-541.
- Campos-Enriquez, J. O., Hubral P., Wenzel F., Lueschen E. and Meier L. (1992). Gravity and Magnetic Constraints on Deep and Intermediate Crustal Structure and Evolution Models for the Rhine Graben. *Tectonophysics* 206(1-2): 113-135.



- Castera, J., Dezayes C. and Calcagno P. (2008). Large-scale 3D geological model around the Soultz site. Proceedings of the EHDRA scientific conference 24-25 September 2008, Soultz-sous-forêts, France.
- Cathelineau, M. and Boiron M. C. (2010). Downward penetration and mixing of sedimentary brines and dilute hot waters at 5 km depth in the granite basement at Soultz-sous-Forets (Rhine graben, France). *Comptes Rendus Geoscience* 342(7-8): 560-565.
- Cloetingh, S., Cornu T., Ziegler P. A. and Beekman F. (2006). Neotectonics and intraplate continental topography of the northern Alpine Foreland. *Earth-Science Reviews* 74(3-4): 127-196.
- Cloetingh, S., van Wees J. D., Ziegler P. A., Lenkey L., Beekman F., Tesauro M., Förster A., Norden B., Kaban M., Hardebol N., Bonté D., Genter A., Guillou-Frottier L., Ter Voorde M., Sokoutis D., Willingshofer E., Cornu T. and Worum G. (2010). Lithosphere tectonics and thermo-mechanical properties: An integrated modelling approach for Enhanced Geothermal Systems exploration in Europe. *Earth-Science Reviews* 102(3-4): 159-206.
- Dezayes, C., Becaletto L., Oliviero G., Baillieux P., Capar L. and Schill E. (2011). 3-D visualization of a fractured geothermal field: the example of the EGS Soultz site (Northern Upper Rhine Graben, France). PROCEEDINGS, Thirty-Sixth Workshop on Geothermal Reservoir Engineering Stanford University
- Dezayes, C., Genter A. and Valley B. (2010). Structure of the low permeable naturally fractured geothermal reservoir at Soultz. *Comptes Rendus Geoscience* 342(7-8): 517-530.
- Dezayes, C., Villemin T., Genter A., Traineau H. and Angelier J. (1995). Analysis of fractures in borehole of the Hot Dry Rock project at Soultz-sous-Forêts (Rhine graben, France). *Scientific Drilling* 5: 31-41.
- Dèzes, P., Schmid S. M. and Ziegler P. A. (2004). Evolution of the European Cenozoic Rift System: interaction of the Alpine and Pyrenean orogens with their foreland lithosphere. *Tectonophysics* 389: 1--33.
- Dubois, M., Ledesert B., Potdevin J. L. and Vancon S. (2000). Determination of the formation conditions of carbonates in an alteration zone of the Soultz-sous-Forets granite (Rhine Graben): the fluid inclusion record. *Comptes Rendus De L Academie Des Sciences Serie Ii Fascicule a-Sciences De La Terre Et Des Planetes* 331(4): 303-309.
- Dubois, M., Ougougdal M. A., Meere P., Royer J. J., Boiron M. C. and Cathelineau M. (1996). Temperature of paleo- to modern self-sealing within a continental rift basin: The fluid inclusion data (Soultz-sous-Forets, Rhine graben, France). *Bericht der Deutschen Mineralogischen Gesellschaft* 8(5): 1065-1080.
- Edel, J. B. (2004). Structure et évolution du Fossé Rhénan, du Carbonifère à nos jours - apports de la géophysique. *Bulletin de la société d'histoire naturelle et d'ethnographie de Colmar* 65(2004): 21-50.
- Edel, J. B., Campos-Enriquez O., Goupillot M. and Kiro K. N. (1982). Levé magnétique au sol du Fossé rhénan supérieur. *Interpretation géologique. Bull. Bur. Rech.Géol. Min.* 2: 179-192.
- Edel, J. B. and Fluck P. (1989). The Upper Rhenish Shield Basement (Vosges, Upper Rhinegraben and Schwarzwald) - Main Structural Features Deduced from Magnetic, Gravimetric and Geological Data. *Tectonophysics* 169(4): 303-316.
- Edel, J. B. and Schulmann K. (2009). Geophysical constraints and model of the "Saxothuringian and Rhenohercynian subductions - magmatic arc system" in NE France and SW Germany. *Bulletin de la Société Géologique de France* 180(6): 545-558.
- Edel, J. B., Schulmann K. and Rotstein Y. (2007). The Variscan tectonic inheritance of the Upper Rhine Graben: evidence of reactivations in the Lias, Late Eocene-Oligocene up to the recent. *International Journal of Earth Sciences* 96(2): 305-325.
- Edel, J. B. and Weber K. (1995). Cadomian terranes, wrench faulting and thrusting in central Europe Variscides : Geophysical and geological evidences. *Geologische Rundschau* 84: 412--432.
- Ferrill, D. A., Winterle J., Wittmeyer G., Sims D., Colton S., Armstrong A. and Morris A. (1999). Stressed Rock Strains Groundwater at Yucca Mountain, Nevada. *GSA Today* 9(5): 1-8.

- Förster, A. and Förster H.-J. (2000). Crustal composition and mantle heat flow: Implications from surface heat flow and radiogenic heat production in the Variscan Erzgebirge (Germany). *Journal of Geophysical Research* 105(B12): 27.
- Geiermann, J. and Schill E. (2010). 2-D Magnetotellurics at the geothermal site at Soultz-sous-Forêts: Resistivity distribution to about 3000 m depth. *Comptes Rendus Geoscience* 342(7-8): 587-599.
- Genter, A. (1990). Géothermie roches chaudes sèches: le granite de Soultz-sous-Forêts. (Bas-Rhin, France), Fracturation naturelle, altérations hydrothermales et interaction eau-roche, Université d'Orléans. **PhD**: 201.
- Grecksch, G., Ortiz A. and Schellschmidt R. (2003). Thermophysical Study of GPK2 and GPK3 Granite Samples. HDR Project Soultz - Report.
- Hinsken, S., Schmalholz S. M., Ziegler P. A. and Wetzell A. (2011). Thermo-Tectono-Stratigraphic Forward Modelling of the Upper Rhine Graben in reference to geometric balancing: Brittle crustal extension on a highly viscous mantle. *Tectonophysics* 509(1-2): 1-13.
- Hooijkaas, G. R., Genter A. and Dezayes C. (2006). Deep-seated geology of the granite intrusions at the Soultz EGS site based on data from 5 km-deep boreholes. *Geothermics* 35(5-6): 484-506.
- Illies, H. J. and Greiner G. (1979). Holocene movements and state of stress in the rhinegraben rift system. *Tectonophysics* 52(1-4): 349--359.
- Illies, J. H., Baumann H. and Hoffers B. (1981). Stress Pattern and Strain Release in the Alpine Foreland. *Tectonophysics* 71(1-4): 157-172.
- Jeannette, D. and Edel J. B. (2005). Contexte géologique du site géothermique de Soultz-Sous-Forêts. bulletin de l'Association Philomatique d'Alsace et de Lorraine Tome 40.
- Kahle, H. G. and Werner D. (1980). A Geophysical-Study of the Rhinegraben .2. Gravity-Anomalies and Geothermal Implications. *Geophysical Journal of the Royal Astronomical Society* 62(3): 631-647.
- Klee, G. and Rummel F. (1993). Hydrofrac stress data for the European HDR research project test site Soultz-sous-Forêts. *International Journal of Rock Mechanics, Mining Science and Geomechanics Abstracts* 30: 973-976.
- Kohl, T., Bächler D. and Rybach L. (2000). Steps towards a comprehensive thermo-hydraulic analysis of the HDR test site Soultz-sous-Forêts. *Proc. World Geothermal Congress 2000, Kyushu-Tohoku, Japan, May-June 2000*, pp. 2671-2676.
- Moeck, I., Kwiatek G. and Zimmermann G. n. (2009). Slip tendency analysis, fault reactivation potential and induced seismicity in a deep geothermal reservoir. *Journal of Structural Geology* 31(10): 1174-1182.
- Morris, A., Ferrill D. A. and Henderson D. B. (1996). Slip-tendency analysis and fault reactivation. *Geology* 24(3): 275-278.
- Papillon, E. (1995). Traitements et interpretations des cartes d'anomalies magnétiques et gravimétriques du Fossé Rhénan supérieur. Dipl. Ing. Géophys. Strasbourg I, 95p.
- Place, J., Diraison M., Naville C., Géraud Y., Schaming M. and Dezayes C. (2010). Decoupling of deformation in the Upper Rhine Graben sediments. Seismic reflection and diffraction on 3-component Vertical Seismic Profiling (Soultz-sous-Forêts area). *C. R. Geoscience* 342(2010): 575-586.
- Plenefisch, T. and Bonjer K. P. (1997). The stress field in the Rhine Graben area inferred from earthquake focal mechanisms and estimation of frictional parameters. *Tectonophysics* 275(1-3): 71-97.
- Pribnow, D. and Schellschmidt R. (2000). Thermal tracking of upper crustal fluid flow in the Rhine Graben. *Geophysical Research Letters* 27(13): 1957-1960.
- Pribnow, D. F. C., Fesche W. and Friedrich H. (1999). Heat Production and Temperature to 5 km Depth at the HDR Site in Soultz-sous-Forêts. GGA report
- Renard, P. and Courrioux G. (1994). Three-dimensional geometric modeling of a faulted domain: The Soultz Horst example (Alsace, France). *Computers & Geosciences* 20(9): 1379-1390.

- Rotstein, Y., Edel J. B., Gabriel G., Boulanger D., Schaming M. and Munsch M. (2006). Insight into the structure of the Upper Rhine Graben and its basement from a new compilation of Bouguer Gravity. *Tectonophysics* 425(1-4): 55-70.
- Rummel, F. and König E. (1991). Density, ultrasonic velocities and magnetic susceptibility measurements on the core material from borehole EPS1 at Soultz-sous-Forêts. Yellow report 8 (1991).
- Sanjuan, B., Millot R., Dezayes C. and Brach M. (2010). Main characteristics of the deep geothermal brine (5 km) at Soultz-sous-Forêts (France) determined using geochemical and tracer test data. *Comptes Rendus Geoscience* 342(7-8): 546-559.
- Sausse, J., Dezayes C., Dorbath L., Genter A. and Place J. (2010). 3D model of fracture zones at Soultz-sous-Forêts based on geological data, image logs, induced microseismicity and vertical seismic profiles. *Comptes Rendus Geoscience* 342(7-8): 531-545.
- Schellschmidt, R. and Clauser C. (1996). The thermal regime of the Upper Rhine graben and the anomaly of Soultz. *Z. Angew. Geol.* 42(1): 40-44.
- Schill, E., Kohl T., Baujard C. and Wellmann J.-F. (2009). Geothermische Ressourcen in Rheinland-Pfalz: Bereiche Süd- und Vorderpfalz, Final report to the Ministry of Environment Rhineland-Palatine, 55p.
- Schumacher, M. E. (2002). Upper Rhine Graben: Role of preexisting structures during rift evolution. *Tectonics* 21(1).
- Valley, B. and Evans K. F. (2007). Stress state at Soultz-sous-Forêts to 5 km depth from wellbore failure and hydraulic observations. 32nd workshop on geothermal reservoir engineering.
- Villemin, T. (1986). Tectonique en extension, fracturation et subsidence : Le Fossé Rhénan et le bassin de Sarre-Nahe. Paris VI PhD: 270.
- Villemin, T. and Bergerat F. (1987). L'évolution structurale du fossé rhénan au cours du Cénozoïque : un bilan de la déformation et des effets thermiques de l'extension. *Bulletin de la Société Géologique de France* 3(2): 245--255.
- Ziegler, P. A. (1992). European Cenozoic rift system. *Tectonophysics* 208(1-3): 91-111.
- Ziegler, P. A., Schumacher M. E., Dèzes P., Van Wees J.-D. and Cloetingh S. (2004). Post-Variscan evolution of the lithosphere in the Rhine Graben area: constraints from subsidence modelling. Geological Society, London, Special Publications 223(1): 289-317.
- Zoback, M. D. (2007). Reservoir Geomechanics. Cambridge University Press: 448 pp.



# Chapter IV - Investigation of natural permeability in extensional tectonic settings: insights from a 2D geodynamic modeling of the Upper Rhine Graben opening

P. Baillieux<sup>1</sup>, E. Schill<sup>1</sup>, L. Moresi<sup>2</sup>

1 - Centre for Hydrogeology and Geothermics, Neuchâtel University, rue Emile Argand 11 CH-2000 Neuchâtel, Switzerland

paul.baillieux@unine.ch

2 - School of Mathematical Sciences, Monash University, Wellington Rd Clayton 3800 VIC, Australia

## Abstract

2D geodynamic models are developed to investigate the creation and localization of fault zones and natural permeability in extensional tectonic settings with potential for geothermal energy. With graben-wide seismic sections and numerous studies showing its relatively simple tectonic history and the observed crustal structural patterns down to the lower crust, the Upper Rhine Graben is used as an ideal database for benchmarking these models. Although simple assumptions are used, and first order models are developed, the patterns of deformation are successfully reproduced, and localized faulting is observed throughout the creation of the graben. As a main result, numerical simulation of instability of a viscoelastic-plastic lithosphere require a lower crustal viscosity in the order of  $5 \cdot 10^{21}$  to  $10^{22}$  Pa s to match the deformation pattern of the Upper Rhine Graben.

## 4.1 Introduction

Localization of geothermal highs (Soultz, Landau, Insheim and Speyer) in the Upper Rhine Graben (URG) can be observed at two different levels. At a region scale for example, these are found in the North western part of the graben (Figure 4-1), in the part which is opposed to the major deformation accommodated by the eastern master fault (Mauthe *et al.*, 1993). At a local scale, the example of the Enhanced Geothermal System (EGS) site Soultz is found to be located in the northern part of a horst structure. Within this horst, the thermal anomaly localizes between the Soultz and Kutzenhausen faults only at its western edge (Baillieux *et al.*, 2011- Appendix A).

Recent studies highlight the link between temperature anomaly and state of fracturing: at Soultz a thermo-hydraulic simulation around the geothermal wells predicts fluid convection with permeability up to  $3 \times 10^{-14}$  m<sup>2</sup> in these strongly fractured zones (Kohl *et al.*, 2000). At Landau and Soultz, graben-parallel faults and their important permeability structures are shown to support hydrothermal convection (Bächler *et al.*, 2003).

In this study, the aim is to understand the formation and localization of fracturing in graben systems using geodynamics. To this end, graben-wide seismic sections (Brun *et al.*, 1992) (see Figure 4-2 and their location in Figure 4-1) and geological knowledge of the well-studied URG are taken as an ideal database for benchmarking geodynamic models of crustal extension at a regional level, allowing the visualization of formation of faulted zones through time.

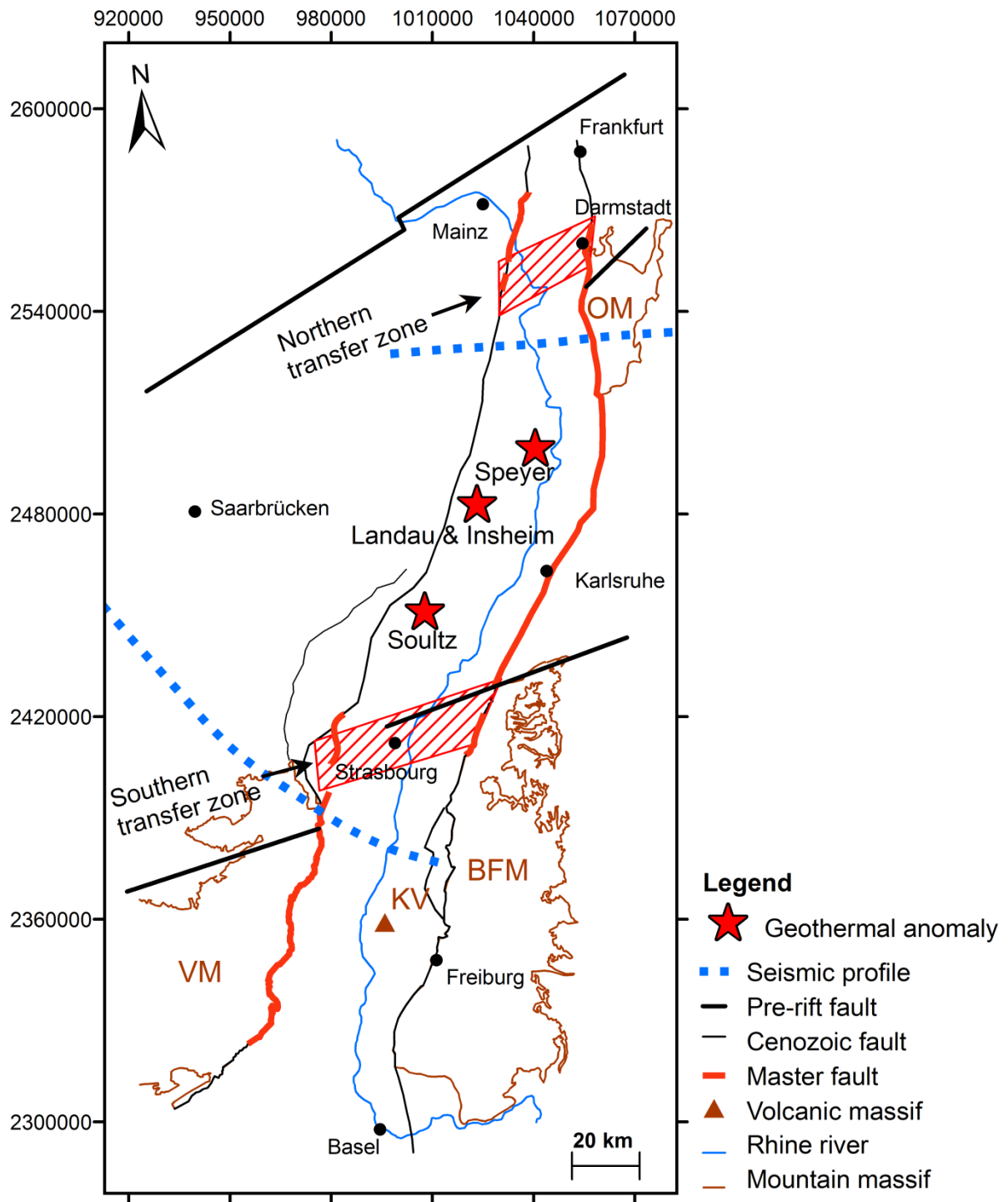
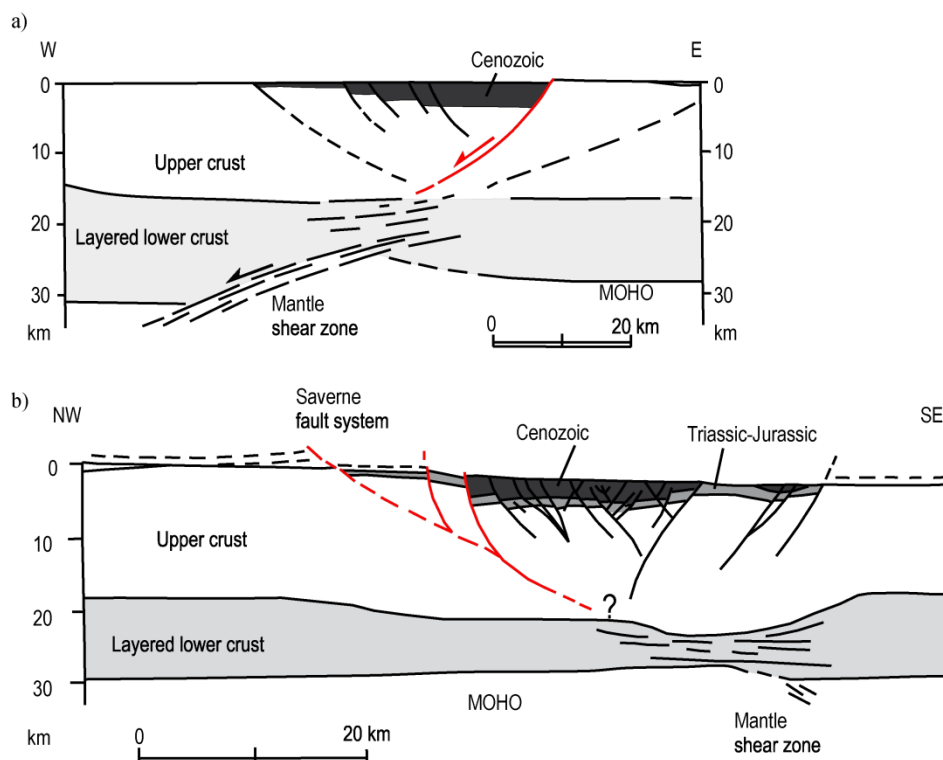


Figure 4-1 : Structural interpretation of the Upper Rhine Graben. Red lines denote the spatial distribution of the graben master faults. Blue dashed lines show the location of the ECORS-DEKORP seismic lines. Red stars show the main geothermal anomalies of the upper Rhine Graben. Modified after Derer *et al.* (2005).

Today the URG boundary faults are thought to operate in a left lateral strike slip sense under the NW–SE oriented compression (Illies and Greiner, 1979; Plenefisch and Bonjer, 1997; Lopes Cardozo and Behrmann, 2006) observed over much of western Europe.

The URG is characterized by asymmetric patterns in the distribution of deformation (Figure 4-1 and Figure 4-2):



**Figure 4-2 : Interpreted cross-sections of the Rhine Graben from the ECORS-DEKORP seismic investigation of the crustal structure of the Upper Rhine Graben. a) northern profile. b) southern profile. Red lines denote the interpreted master fault accommodating the maximum offset. Modified after Valley (2007) and Brun *et al.* (1992).**

1. In the southern part, the sediment deposition center is located on the western side of the Graben (Brun *et al.*, 1991), where the vertical motion (around 3 km) was accommodated by the western border fault (Brun *et al.*, 1991; Cornu and Bertrand, 2005).
2. In the northern part, the sediment deposition center is located on the eastern side of the graben where the vertical motion is maximum along the eastern border fault (Wenzel *et al.*, 1991).
3. The master fault is interpreted to switch side to the East in the central part of the URG (Mauthe *et al.*, 1993; Derer, 2003) (Figure 4-1).

Graben wide seismic sections reveal fault zones down to a depth of 10-15 km (Figure 4-2).

#### 4.1.1 Review of geodynamic modeling of continental extension

Recent geodynamic modeling aims at predicting observations in rifting environments such as the geometry and modes of crustal extension (e.g. Huisman and Beaumont, 2003; Huisman *et al.*, 2005; Wijns *et al.*, 2005; Buitter *et al.*, 2008), the fault and strain distribution (e.g. Lavier *et al.*, 2000; Regenauer-Lieb *et al.*, 2008) and the distribution of continental strength in general. Major interests with respect to this study are:

1. What are the effects of extension and compression, and phenomena such as structural inheritance, basin inversion, and far-field stresses on the formation and evolution of sedimentary basins in extensional, compressional, and strike-slip settings?
2. How can we define the structural styles of faulting in the shallow brittle part of the lithosphere, the brittle-ductile transition, and the shear zone in the ductile part of the lithosphere?

On a global geological point of view rifting is firstly controlled by forces controlling the movement and interaction of lithospheric plates such as boundary stresses, slab pull, ridge push, collisional resistance, frictional forces caused mainly by the influence of the convecting mantle on the base of the lithosphere (Cloetingh *et al.*, 2007). The same study argues, by looking at the best documented sedimentary basin systems in Europe (including the Upper Rhine graben), that the thermal and mechanical structure of the lithosphere is the main control on the development of sedimentary basins.

By considering direct evidence for fault strength, Scholz & Gerald (2007) conclude that stress in the lithosphere is limited by faulting and is determined, to first-order, by Byerlee's law with hydrostatic pressure (Watts and Gerald, 2007). Byerlee's law describes the stress state in the Earth's upper crust at which fracturing along a geological fault takes place by solving the Mohr-Coulomb criterion:

$$\tau = C_0 + \mu (\sigma_n - Pf)$$

In which  $\tau$  is the shear stress and  $\sigma_n$  the normal stress.  $C_0$  is the cohesion or internal strength of the material and the value  $Pf$  is the pore fluid pressure inside the rock. The fact that pore pressure is hydrostatic in the crystalline rocks of the crust is a consequence of the high permeability of the crust resulting from the presence of faults (Townend and Zoback, 2000; Scholz and Gerald, 2007).

The geometry of rifts and sedimentary basins and their mode of extension are found to be linked to the amount of strain softening (the relation which describes the decrease of strength of a rock when subject to faulting) in the brittle upper crust, the thickness of the upper crust, the viscosity and strength of the lower crust, the extension rate and other processes linked with the extension such as gravitationally driven deformation, isostasy, magmatism and necking (Buitter *et al.*, 2008 and references therein). The same study also analyze the dependence of modes of crustal extension of a brittle crust on the strength of a ductile lower crust, its effective viscosity, the extension rate, and the layer thicknesses. It is shown that an asymmetric basin is more likely to develop for a strong brittle layer which has a high amount of strain softening, a weak viscous layer (lower crust) and slow extension velocity.

## 4.2 2D crustal extension of the Upper Rhine Graben

### 4.2.1 Methods

The aim of the study is to model the crustal extension of the Upper Rhine Graben satisfying the geophysical and geological observations in Figure 4-1 and Figure 4-2 with a localization of strain at one side of the Graben, in form of concentration of fault zones.

The geodynamic platform Underworld is used. It consists in a Lagrangian *particle-in-cell* finite element scheme (Moresi *et al.*, 2007) that enables the accurate tracking of stress and strain-rate history in simulations involving large-scale deformation. This platform includes a toolkit for studying the geodynamics of a viscoelastic-plastic lithosphere in 3D. Underworld has proven to be successful in simulating plausible scenarios for the creation of rifting environments such as the *distributed faulting mode* at the North Sea or *metamorphic core complexes* of the western U.S.A. and the Aegean (Wijns *et al.*, 2005).



#### 4.2.2 Sensivity study

The effect of the initial settings on the faulting style during the extension is tested by adapting input parameters from the model of Buiter *et al.* (2008) to values recorded in the URG (Figure 4-3 and Table 4-1). The resulting models reasonably simple: constant extension rate, no isostatic compensation, no shear heating, no temperature profile, no sediment deposition, no elasticity. As such, they represent first-order but acceptable models (e.g. Huismans *et al.*, 2005; Buiter *et al.*, 2008).

A 2D two-layer model with an upper and a lower crust layer with the same uniform density is used. The upper crust deforms in a rigid-plastic manner using a Drucker-Prager frictional-plastic pressure dependent law which is an attempt to produce a smooth yield surface with otherwise similar characteristics to the Mohr–Coulomb yield surface (Moresi *et al.*, 2007). There is an air layer above the solid material to approximate a free surface and allow the formation of topography. The sidewall boundary condition is free-slip vertically, with velocity conditions applied to the left and right to drive extension. An initial 100% damaged singularity is set at the boundary between the lower and upper crust to have control on the localization of the deformation.

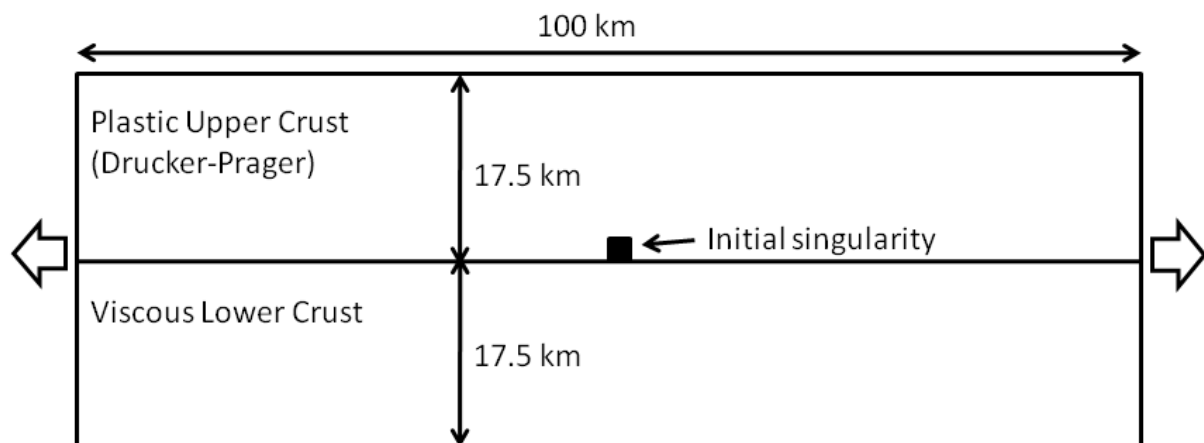


Figure 4-3 : Model setup with plastic upper crust (Drucker-Prager frictional plastic pressure dependent law) and with viscous lower crust and an initial singularity

#### 4.2.3 Variation in viscosity

For this exercise, three models were stretched to reach 10% of deformation (5km on each side). The initial 100% damaged singularity was chosen to be 2x2 km. The lower crust viscosity values are  $10^{21}$ ,  $5 \times 10^{21}$  and  $10^{22}$  Pa s are chosen in order to model the strength of an intermediately strong to a strong lower crust (Wijns *et al.*, 2005).

The results are shown in Figure 4-5, represented in the final Lagrangian particle swarm distribution and cumulative strain rate distribution after 10 km of extension. A main disadvantage of these models configuration comes from the initial singularity which leads the deformation. A single fault crossing the entire upper crust appears during the first kilometers of extension when the lower crust strength is intermediate (Figure 4-5 A) to intermediately high (Figure 4-5B). The deformation then starts to be distributed along a generation of normal and conjugate faults which forms the landscape of an asymmetric basin. When using an intermediately strong lower crust (Figure 4-5B) an extra border fault appears on the other side of the graben and a relatively equal distribution of conjugate normal faults between the two border faults. The presence of such faults are suggested in the crustal-scale seismic exploration of the Rhine Graben (Brun *et al.*, 1992) but not yet clearly observed.

Here, the effect of an initial singularity is probably too strong to see how the faults “naturally” develop. In the case where the lower crust is strong (Figure 4-5C), a symmetric basin tends to develop.

**Table 4-1 : Rheological and modeling parameters used during the presented crustal extension modeling**

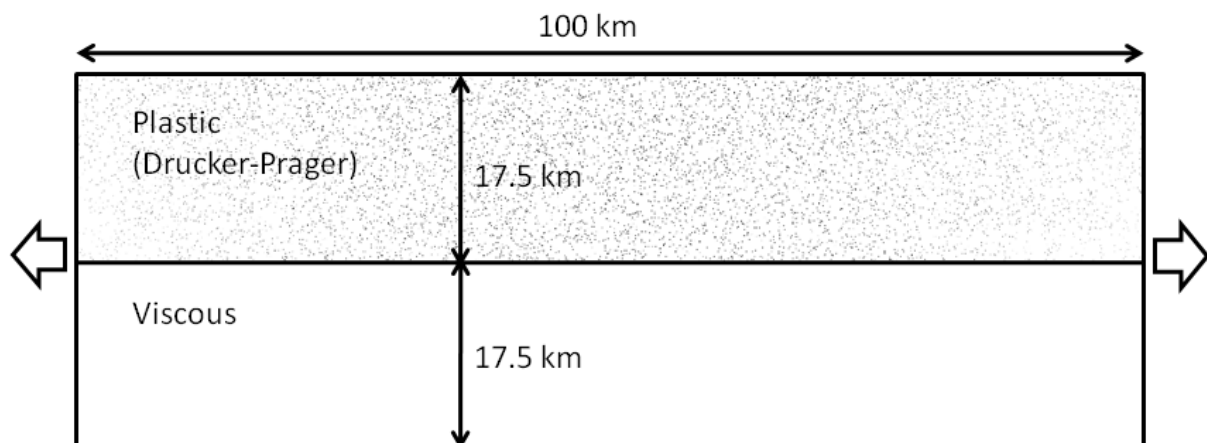
Parameter	Natural Value	Unit
<i>Thicknesses</i>		
Crust	35	km
Brittle crust	17.5	km
Viscous crust	17.5	km
Width of the model	100	km
Extension velocity (per side)	$2,19 \times 10^{-2}$ *	$\text{cm.a}^{-1}$
<i>Density</i>		
Crust	2800	$\text{kg.m}^{-3}$
Angle of internal friction	30 -> 4	°
Cohesion	20 -> 2	MPa
Strain softening range	0-1	-
Linear viscosity ( $\eta$ )	$10^{21}$ to $10^{22}$	Pa.s

\* The chosen value of extension velocity corresponds to a total amount 7km of graben extension over a 100km model during 40Ma (e.g. Villemin *et al.*, 1986; Brun *et al.*, 1992). This corresponds to a slow extension process (Hinsken *et al.*, 2011).

### ***Initial geometry***

In this part, the initial singularity was removed and replaced by a random distribution of damage within the envelope function  $\varphi = \sin^2(k1 \cdot x1)$ , where  $k1 = 1/L1$  and  $L1$  is the length of the model, allowing the damage to be kept away from the boundaries (Figure 4-4).

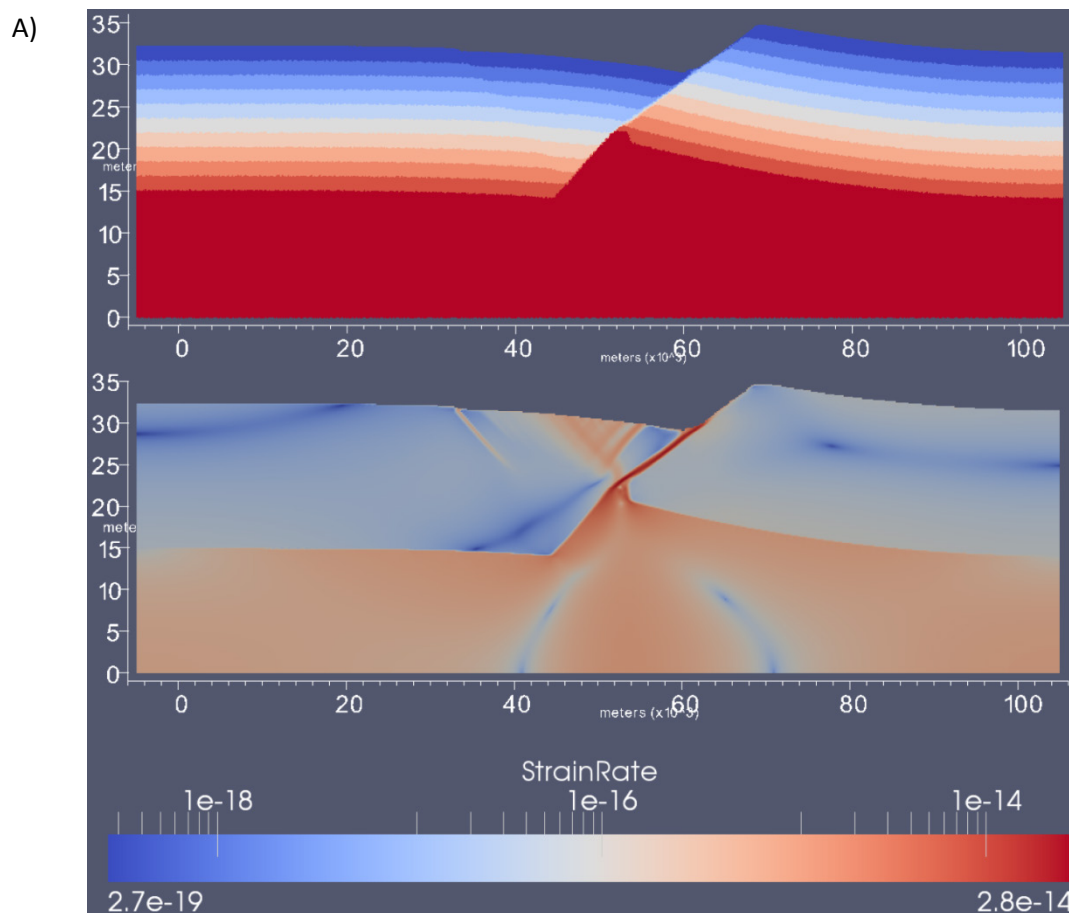
Three models were stretched to reach 15% of deformation as observed in the Upper Rhine graben (7.5 km on each side).



**Figure 4-4 : Model setup. Grey dots represent the distribution (5%) of initially damaged material.**

In the case of the low value of viscosity for the lower crust (i.e. intermediately strong lower crust), numerous faults develop in the early stages of the deformation in all model but they no longer accumulate slip after around 5% of extension and only one main fault take control over the deformation, stretching from the lower crust to the upper crust (Figure 4-6A). In the case of a stronger lower crust (i.e. viscosity values of  $5 \times 10^{21}$  and  $10^{22}$  Pa s), in the two other models, this main fault is followed by the generation of conjugate faults at the surface. One of them (after 10% of extension) eventually grows and connects to the first main fault at the border between the two crusts, forming the second border fault of the basin (Figure 4-6 B and C). Faults that are outside the basin tend to no longer accumulate slip, whereas the one that are inside the basin keep their shape and form the landscape of a graben and horst system mainly located on the side of the second border fault.

Another model with a lower crust viscosity value of  $10^{23}$  Pa s was run: the resulting model shows the formation of multiple basins as we could expect for this high value (Buiter *et al.*, 2008). This result is not comparable to what we observe in the URG.



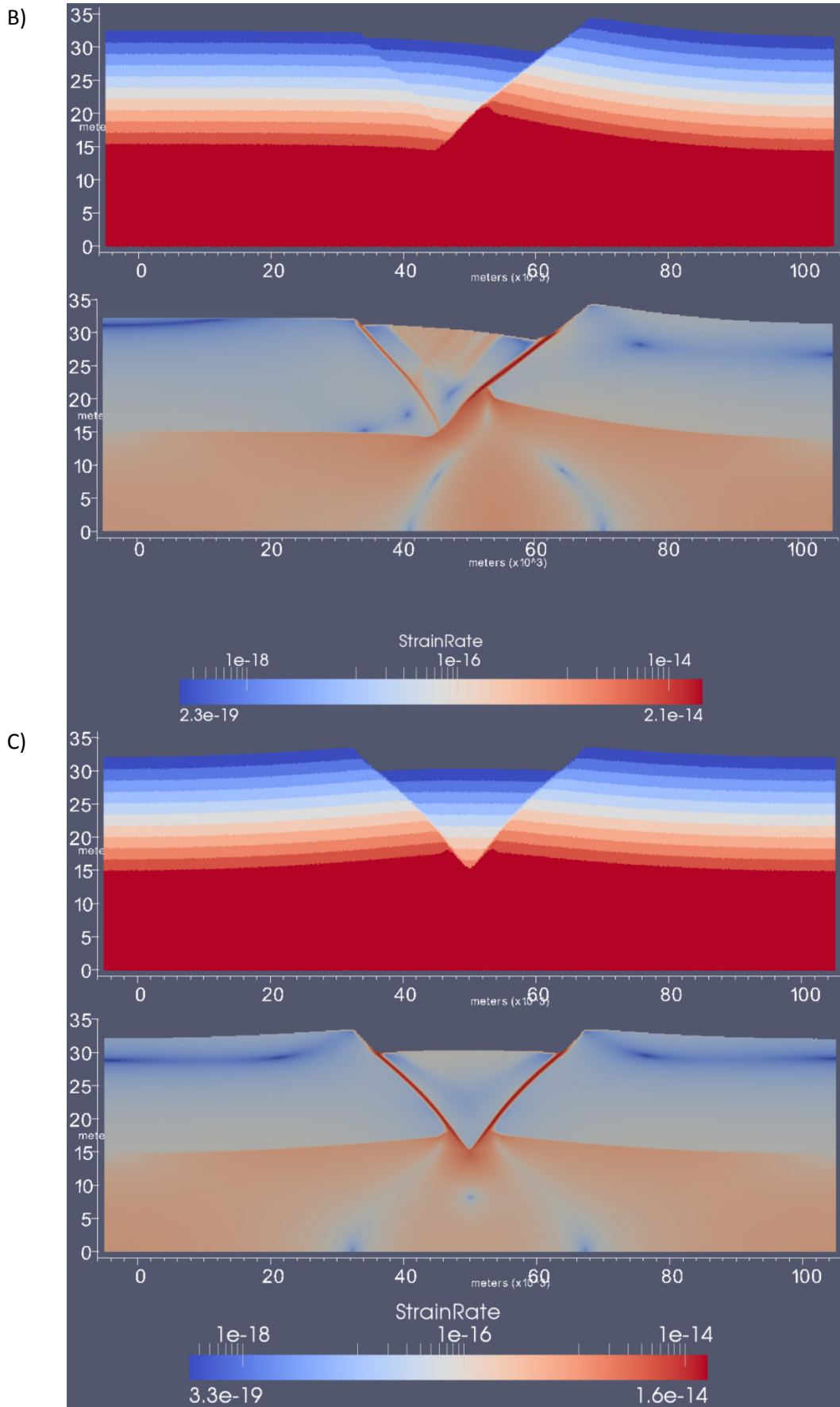
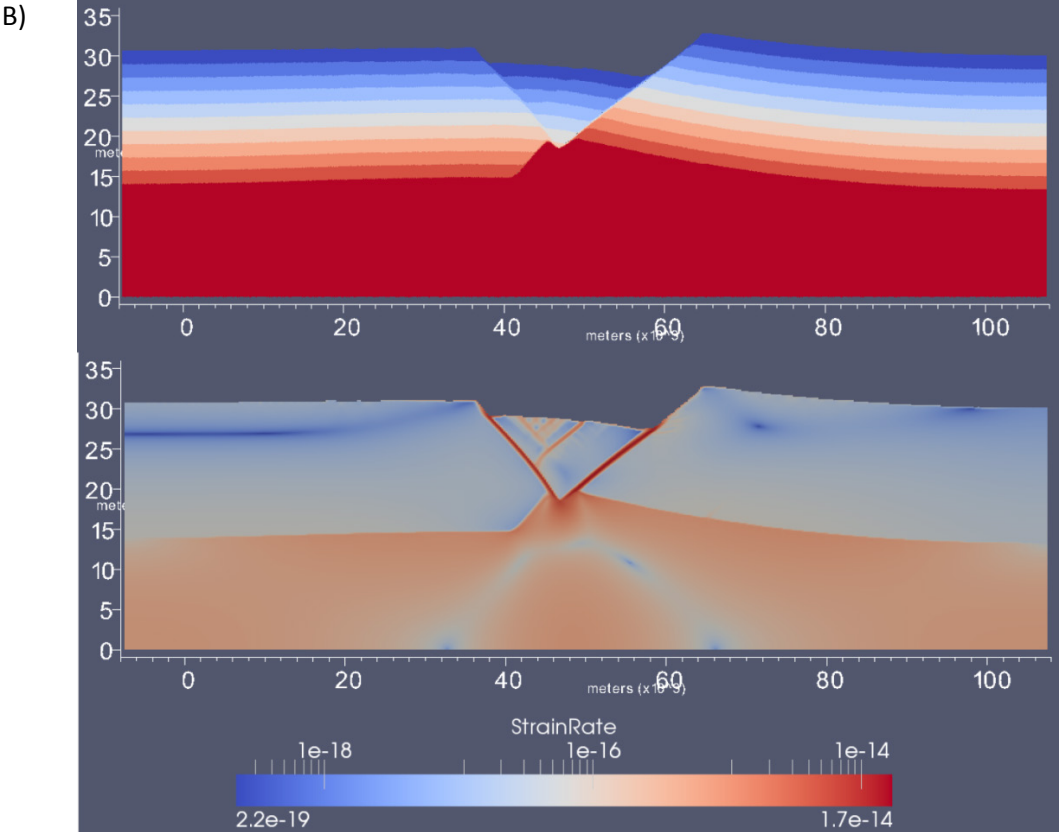
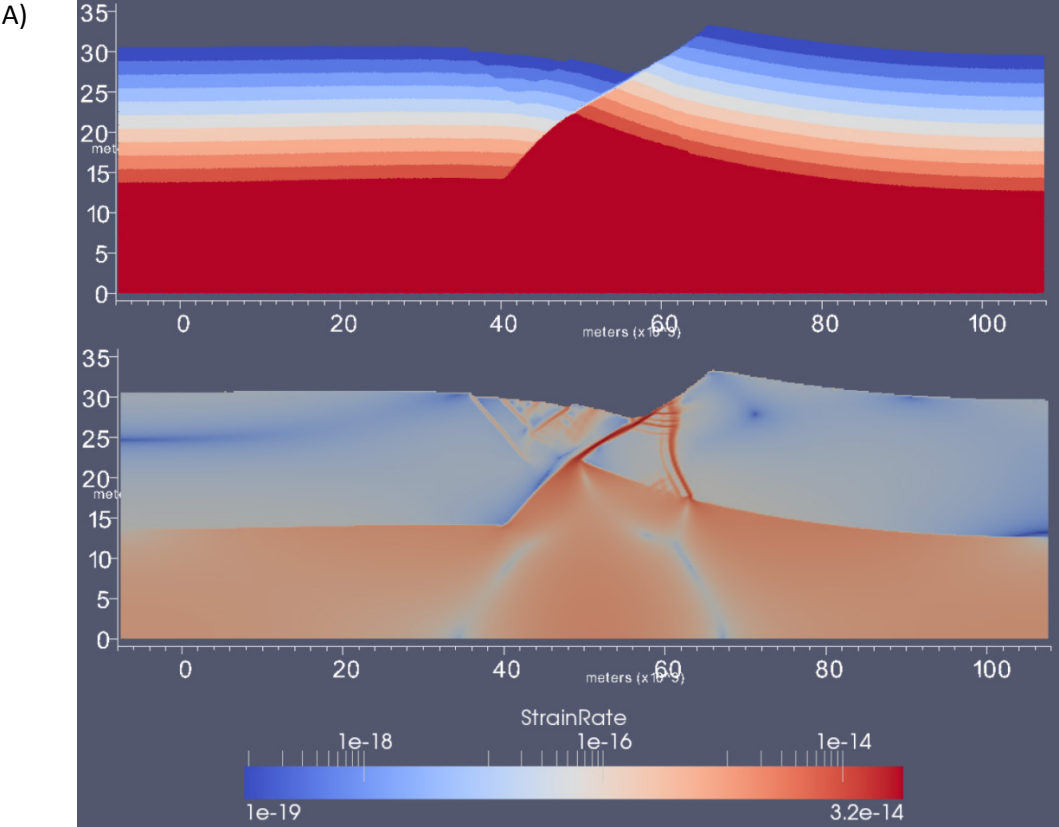


Figure 4-5 : Final Lagrangian particle swarm distribution (in km) (upper picture) and cumulative strain rate distribution ( $s^{-1}$ ) (lower picture) after 10 km of extension using a lower crust viscosity of A)  $10^{21}$  Pa s, B)  $5 \cdot 10^{21}$  Pa s, C)  $10^{22}$  Pa s.



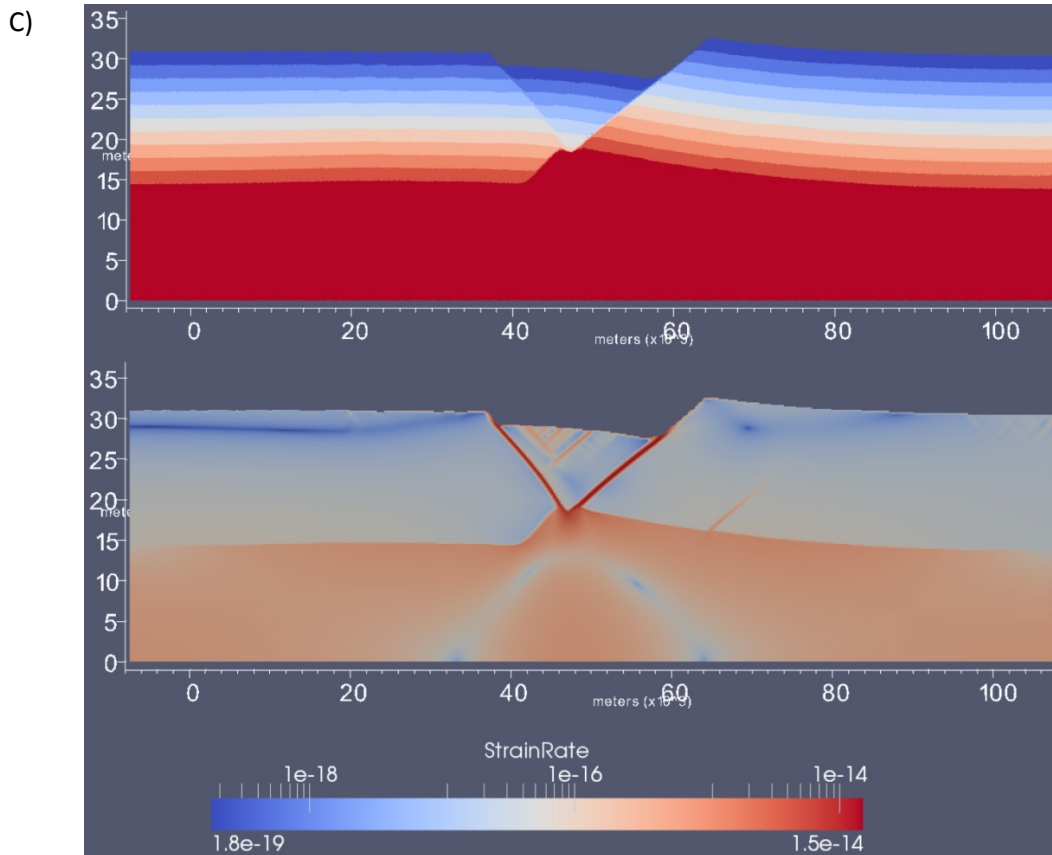


Figure 4-6 : Final Lagrangian particle swarm distribution (in km) (upper picture) and cumulative strain rate distribution ( $s^{-1}$ ) (lower picture) after 15 km of extension using a lower crust viscosity of A)  $10^{21}$  Pa s, B)  $5 \cdot 10^{21}$  Pa s, C)  $10^{22}$  Pa s.

#### 4.2.4 Comparison with independent geophysical data

The results of the geodynamic modeling find similarities with both the ECORS-DEKORP crustal-scale seismic exploration of the URG and the recent 3D geological model of the Soultz area (Baillieux *et al.*, 2011- Appendix A), located at the western side in the central part of the URG:

For an intermediately strong to a strong lower crust, the model shows that, after a phase of homogeneously distributed deformation on discrete fault zones dipping to the East and West, a preferential orientation develops into one main masterfault crossing the entire upper crust, which accommodates the deformation in this phase of the future graben formation. The presence of such a fault is suggested in the crustal-scale seismic exploration of the Rhine Graben (Brun *et al.*, 1992). The rupture cross cuts the entire 17.5 km thick plastic crust (Drucker-Prager) and offsets the upper-lower crust boundary by about 3-5 km vertically after 15 km of extension with cumulative strain rates of up to  $1.5 \cdot 10^{-14} s^{-1}$ . Strain rate in the lower crust is nearly homogeneously distributed. In the following phase the opposite boundary fault appears and accommodates deformation, along with minor fault development reactivating the initial fault zones on the same side of the graben (opposite the master fault). This second boundary fault is also observed in the seismic results and provides indication for an asymmetric distribution of fault zones within a larger tectonic unit. The larger one of these minor faults connect to the eastern boundary fault, which may open the above suggested fluid path ways. This result may be compared to the temperature distribution in the area of Soultz where faults are shown to host hydrothermal convection next to the second boundary fault of the graben.

### 4.3 Discussion and implication for geothermal exploration

Although simple assumptions and first order models are used (constant extension rate, no isostatic compensation, no shear heating, no temperature profile, no sediment deposition, no elasticity, and no inherited initial anisotropy) to model the crustal extension, first order results can be compared to geophysical data. For lower crust viscosity values of  $5 \cdot 10^{21}$  to  $10^{22}$  Pa s, patterns of deformation (asymmetric development, role of boundary faults during deformation, length and depth of deformation) observed in the Upper Rhine Graben are successfully reproduced.

These first order results have an implication for the geothermal prospection of the Cenozoic European Rift System. For example the supposed masterfaults could be potential for highly hydraulically conductive rocks. The region of horst and grabens such as the Soultz and Landau area, which show geothermal anomalies due to hydrothermal convection in faults (Figure 4-1), on the other side of the graben, appears to be a very relevant prospection zone, because of its long period of activity and permeability associated with asymmetric faulting as observed in 3D geological model of Soultz (Baillieux et al., 2011- Appendix A) and shown by the geodynamic modeling and furthermore a renewed activity of the URG from late Miocene up to Recent has been observed (Illies and Greiner, 1979; Dèzes *et al.*, 2004).

### 4.4 Conclusions

The geodynamic approach presented in this paper provides insights in the localization of permeable structures at a regional level during a graben opening, which at a first order fit the patterns of deformation and geothermal expressions observed in the Upper Rhine Graben. Further research and physical assumptions should be integrated in these physical models for even more detailed explanations.

### 4.5 Acknowledgements

We kindly thank the 'Donation Fund Bureau of Neuchâtel University' in Switzerland for supporting the research project carried out at Monash University Australia, the (geo)dynamic team of the School of Mathematical Sciences of Monash University and Dr. Gabriele Morra for their help and support during the geodynamic modeling. Benoit Valley is warmly acknowledged for providing input figures.

This work is part of a PhD by Paul Baillieux financed by University of Neuchâtel.

### 4.6 References

- Bächler, D., Kohl T. and Rybach L. (2003). Impact of graben-parallel faults on hydrothermal convection - Rhine Graben case study. *Physics and Chemistry of the Earth* 28(9-11): 431-441.
- Baillieux, P., Schill E. and Dezayes C. (2011). 3D structural regional model of the EGS Soultz site (northern Upper Rhine Graben, France): insights and perspectives. *Proceedings, Thirty-Sixth Workshop on Geothermal Reservoir Engineering, Stanford University, Stanford, California, SGP-TR-191.*

- Brun, J. P., Gutscher M. A. and {DEKORP-ECORS teams} (1992). Deep crustal structure of the Rhine Graben from seismic reflection data: A summary. *Tectonophysics* 208(1-3): 139-147.
- Brun, J. P., Wenzel F. and {ECORS-DEKORP team} (1991). Crustal-scale structure of the southern Rhinegraben from ECORS-DEKORP seismic reflection data. *Geology* 19: 758--762.
- Buiter, S. J. H., Huismans R. S. and Beaumont C. (2008). Dissipation analysis as a guide to mode selection during crustal extension and implications for the styles of sedimentary basins. *Journal of Geophysical Research-Solid Earth* 113(B6): -.
- Cloetingh, S., Ziegler P. A. and Gerald S. (2007). Tectonic Models for the Evolution of Sedimentary Basins. *Treatise on Geophysics*. Amsterdam, Elsevier: 485-611.
- Cornu, T. G. M. and Bertrand G. (2005). Numerical backward and forward modelling of the southern Upper Rhine Graben (France-Germany border): new insights on tectonic evolution of intracontinental rifts. *Quaternary Science Reviews* 24(3-4): 353-361.
- Derer, C. E. (2003). Tectono-sedimentary evolution of the northern Upper Rhine Graben (Germany), with special regard to the early syn-rift stage. Ph.D. thesis, University of Bonn, p 99 [[http://hss.ulb.uni-bonn.de:90/ulb\\_bonn/diss\\_online/math\\_nat\\_fak/2003/derer\\_christian\\_eugen](http://hss.ulb.uni-bonn.de:90/ulb_bonn/diss_online/math_nat_fak/2003/derer_christian_eugen)]].
- Derer, C. E., Schumacher M. E. and Schafer A. (2005). The northern Upper Rhine Graben: basin geometry and early syn-rift tectono-sedimentary evolution. 640-656.
- Dèzes, P., Schmid S. M. and Ziegler P. A. (2004). Evolution of the European Cenozoic Rift System: interaction of the Alpine and Pyrenean orogens with their foreland lithosphere. *Tectonophysics* 389: 1--33.
- Hinsken, S., Schmalholz S. M., Ziegler P. A. and Wetzell A. (2011). Thermo-Tectono-Stratigraphic Forward Modelling of the Upper Rhine Graben in reference to geometric balancing: Brittle crustal extension on a highly viscous mantle. *Tectonophysics* 509(1-2): 1-13.
- Huismans, R. S. and Beaumont C. (2003). Symmetric and asymmetric lithospheric extension: Relative effects of frictional-plastic and viscous strain softening. *J. Geophys. Res.* 108(B10): 2496.
- Huismans, R. S., Buiter S. J. H. and Beaumont C. (2005). Effect of plastic-viscous layering and strain softening on mode selection during lithospheric extension. *J. Geophys. Res.* 110(B2): B02406.
- Illies, H. J. and Greiner G. (1979). Holocene movements and state of stress in the rhinegraben rift system. *Tectonophysics* 52(1-4): 349--359.
- Kohl, T., Bächler D. and Rybach L. (2000). Steps towards a comprehensive thermo-hydraulic analysis of the HDR test site Soultz-sous-Forêts. Proc. World Geothermal Congress 2000, Kyushu-Tohoku, Japan, May-June 2000, pp. 2671-2676.
- Lavier, L. L., Buck W. R. and Poliakov A. N. B. (2000). Factors controlling normal fault offset in an ideal brittle layer. *Journal of Geophysical Research-Solid Earth* 105(B10): 23431-23442.
- Lopes Cardozo, G. G. O. and Behrmann J. H. (2006). Kinematic analysis of the Upper Rhine Graben boundary fault system. *Journal of Structural Geology* 28(6): 1028-1039.
- Mauthe, G., Brink H.-J. and Burri P. (1993). Kohlenwasserstoffvorkommen und -potential im deutschen Teil des Oberrheingrabens. 60.
- Moresi, L., Mühlhaus H.-B., Lemiale V. and May D. (2007). Incompressible viscous formulations for deformation and yielding of the lithosphere. Geological Society, London, Special Publications 282(1): 457-472.
- Moresi, L., Quenette S., Lemiale V., Meriaux C., Appelbe B. and Mühlhaus H. B. (2007). Computational approaches to studying non-linear dynamics of the crust and mantle. *Physics of The Earth and Planetary Interiors* 163(1-4): 69-82.
- Plenefisch, T. and Bonjer K. P. (1997). The stress field in the Rhine Graben area inferred from earthquake focal mechanisms and estimation of frictional parameters. *Tectonophysics* 275(1-3): 71-97.
- Regenauer-Lieb, K., Rosenbaum G. and Weinberg R. F. (2008). Strain localisation and weakening of the lithosphere during extension. *Tectonophysics* 458(1-4): 96-104.
- Scholz, C. H. and Gerald S. (2007). Fault Mechanics. *Treatise on Geophysics*. Amsterdam, Elsevier: 441-483.



- Townend, J. and Zoback M. D. (2000). How faulting keeps the crust strong. *Geology* 28(5): 399-402.
- Valley, B. (2007). The relation between natural fracturing and stress heterogeneities in deep-seated crystalline rocks at Soultz-sous-Forêts (France), PhD thesis, ETH-Zürich, Switzerland, <http://e-collection.ethbib.ethz.ch/view/eth:30407>, 260 p.
- Villemin, T., Alvarez F. and Angelier J. (1986). The Rhinegraben: Extension, subsidence and shoulder uplift. *Tectonophysics* 128(1-2): 47-59.
- Watts, A. B. and Gerald S. (2007). An Overview. *Treatise on Geophysics*. Amsterdam, Elsevier: 1-48.
- Wenzel, F., Brun J.-p. and group e.-d. w. (1991). A deep seismic reflection profile across the northern rhine graben.
- Wijns, C., Weinberg R., Gessner K. and Moresi L. (2005). Mode of crustal extension determined by rheological layering. *Earth and Planetary Science Letters* 236(1-2): 120-134.



## Chapter V: Discussion and conclusions

Following the research line pointed out in chapter I, the results from the regional study over the URG has revealed several qualitative and quantitative correlations between the distribution of the temperature anomalies and neotectonic processes as well as the lithology of the basement structure. Thus, it can be concluded that both, recent and inherited structures are of significance for the distribution of temperature in graben systems.

In detail it has been observed that major thermal anomalies are localizing mainly in the central to northern segment of the URG, i.e. between Strasbourg and Mainz. Apart from the E-W section between Landau and Karlsruhe, where temperature anomalies extend of the entire width of the URG, the anomalies are mainly occurring in the western part of this segment. The area to which the anomalies extend corresponds to an area in which analyses of neotectonic activity reveals a compressional shear and uplift regime. To the North, however, also extensional shearing and subsidence is observed. In general, the temperature anomalies are related also to an area of comparatively low natural seismicity. This may be linked to the neotectonic regime in the URG: the central segment is interpreted in a restraining band separating two-pull apart basins in a sinistral strike-slip regime (Illies and Greiner, 1979; Schumacher, 2002), but also to aseismic slip as observed at Soultz during hydraulic stimulation (Cornet *et al.*, 1997).

A crucial observation on graben level is the correlation between positive temperature and negative gravity anomalies. Majority of the thermal anomalies occur in areas where the crystalline basement is characterized by Early Carboniferous basaltic to granitic units of the Saxothuringian terrain, which are interpreted to be of low density, and sometimes magnetic, respectively, according to measured Bouguer and magnetic anomalies. Cross correlation of temperature and the two types of anomalies reveal in both cases a distinct bandwidth of mean gravity and magnetic intensity for high temperatures. In particular, zones of magnetic highs and gravity lows are related to additional temperature anomalies in the order 10-20°C at 2000m TVD at a graben wide scale (temperature 100-110 °C compared to a mean 90°C with minimum value of 75°C).

Thus, as a result of the two previous points, we conclude that apart from the fact that negative gravity anomalies can be attributed partly to crystalline ridges with inherited (Variscan) NE-SW orientations (Edel and Schulmann, 2009), negative gravity anomalies reflect to a significant part fracture porosity, which has been demonstrated to be a major cause of the thermal anomalies in the URG due to hydrothermal convection (Le Carlier de Veslud *et al.*, 1994; Kohl *et al.*, 2000; Pribnow and Schellschmidt, 2000; Bächler *et al.*, 2003). It should be mentioned that in the Eger Graben, another segment of the European Cenozoic Rift System, elevated heat production causes significant elevation of surface heat flow (Förster and Förster, 2000). It is well-known and confirmed also from the Soultz geothermal well that granitic basement reveals enhanced heat productivity and heat conductivity (Rummel and König, 1991; Pribnow *et al.*, 1999; Grecksch *et al.*, 2003) and thus contributes to anomalies in the temperature field. On the other hand, negative gravity anomalies can be associated to low density caused by fracture porosity (Altwegg *et al.*, in preparation). Porosity of up to 20% in the Soultz geothermal wells is known to be associated with fractures and hydrothermal circulation

(Genter, 1990) and linked to the high hydraulic conductivity inferred from circulation tests (Stober and Bucher, 2007).

The correlation between negative gravity anomalies and temperature maxima has been investigated on a more local level in the geothermal field of Soultz, where fault zones are well-known to be related to fracture porosity and their spatial distribution was reconstructed from a number of 2D seismic profiles in a 3D geological model. In this area, mean temperature anomaly with amplitude of  $> 40$  °C at top basement occurs on the low-density and magnetic granodioritic pluton, in which high radiogenic heat production was observed in particular at the top of the basement (Rummel and König, 1991; Pribnow *et al.*, 1999; Grecksch *et al.*, 2003). Additionally, the peak temperature anomaly of Soultz ( $> 60$ °C) has been with associated hydrothermal circulation occurring along N-S directed fault zones with a West dipping signature on the western side of the Soultz horst structure. This correlates with magnetotelluric data (Geiermann and Schill, 2010), fractures observations in Soultz boreholes (Dezayes *et al.*, 2010), and a possible dissipation of the Soultz horst eastern boundary fault above the basement on the recent reinterpretation of PHN84J seismic profile (Place *et al.*, 2010). In the new 3D geological model, all three major temperature anomalies  $>60$ °C at top basement are found to be linked to such oriented fault zones.

It should be mentioned here that, in contrast to graben-wide observations, the relation between gravity and temperature anomalies is not straight forward. An important negative gravity anomaly can be observed in the region of Soultz. It has previously been attributed to a low density granitic and granodioritic basement of Lower Carboniferous age, joining the observation of several types of granite and sub-facies in the geothermal wells (Genter, 1990; Hooijkaas *et al.*, 2006). First of all, the negative gravity anomaly is not explained by the forward gravity response of the 3D geological model, since the forward model does neither take into account variations in the basement composition, nor accounts for density variations due to induced by fracturing. The evaluation of residual anomalies leads to the conclusion that major gravity anomalies dip eastwards when linked to the western boundary fault system and dip westwards when linked to temperature anomalies (e.g. around the temperature anomaly of Rittershoffen). This supports the hypothesis that westward dipping faults are main up-flow structures that account for the thermal anomalies. Further indication is provided by fluid inclusion analyses, which are interpreted in terms of fluid paleocirculation patterns characterized on one hand by an upward flow of hot water with a meteoric signature (Cathelineau and Boiron, 2010), and thus interpreted as deep circulation from the fractured basement to the West. However, it must be mentioned here that on the other hand the geochemical signature of the high salinity fluid sampled in Soultz boreholes is mainly attributed to circulation in deep and hot (equilibrium temperature around 200 °C) sedimentary aquifers that can only be found in the eastern side of the graben at the same latitude (Aquilina *et al.*, 1997; Sanjuan *et al.*, 2010).

Both natural and artificial permeabilities in fractured reservoirs strongly depend on the orientation of the current stress field. In the case of the geothermal field of Soultz, we note a comparably low maximum slip tendency of about 0.33. This indicates that shear stress is far from critical condition. This interpretation coincides with the comparably low natural seismicity in the area of Soultz and the surrounding thermal anomalies. Nevertheless, NNW – SSE striking faults reveal both, highest slip and dilation tendencies. This is in agreement with the input stress distribution at Soultz obtained from breakouts and drilling-induced tension fractures combined with the analysis of pressure data from stimulation tests (Valley and Evans, 2007 and references therein). Although it can be observed that

fault zones related to the geothermal anomalies reveal intermediate values of dilation tendency, a direct link between the thermal anomalies and slip tendency is not observed. However, the permeability of the top crystalline has been proven by hydraulic testing and mud losses, revealing discrete fracture zones linked to fluid influx (Dezayes *et al.*, 2010 and references therein). Furthermore, on a low level maxima in slip tendency are observed along the western boundary fault zone as well as along the faults in the vicinity of the thermal anomalies. This may confirm the picture obtained from the residual anomalies of gravity applying different filter wavelengths. With the link between thermal anomalies and westward dipping fault zones in mind, we may alternatively postulate that locally enhanced fluid pore pressure may push the stress state closer to critical condition underneath the major temperature anomalies and thus, guarantees the transmissivity of the zones.

Summarizing the major results to this point, we have observed a link between fracture porosity reflected in the regional gravity results and the major thermal anomalies caused by convection within these fault zones. A general concentration of thermal anomalies has been observed opposite to the master fault, which at the latitude of the major thermal anomalies is located at the eastern side of the URG. On a local scale gravity reveals indication for both, infiltration of meteoric water at the western boundary fault directed towards the center of the graben and upflow of thermal water along westward oriented fault zone, by negative gravity anomalies. These westward dipping structures are typically linked to horst structures.

Geodynamic modeling reveals the mechanical condition under which deformation localizes in the above summarized form. A qualitative comparison between these elements and the localization of deformation of time reveals significant agreement. After a phase of homogeneously distributed deformation on discrete fault zones dipping to the East and West, a master fault develops on one side of the future graben. The rupture cross cuts the entire 17.5 km thick plastic crust (Drucker-Prager) and offsets the upper-lower crust boundary by about 3-5 km vertically after 15 km of extension for lower crust viscosities of  $5 \cdot 10^{21}$  to  $10^{22}$  Pa s with cumulative strain rates of up to  $1.5 \cdot 10^{-14}$  s<sup>-1</sup>. Strain rate in the lower crust is nearly homogeneously distributed. This corresponds to the observation from graben-wide seismic investigation. In a next phase the opposite graben boundary fault accommodates deformation as well along with minor fault development reactivating the initial fault zones on the same side of the graben (opposite the master fault). This result is again in good agreement with the observations from seismic sections and locally in the Soultz area, which indicate a concentration of minor fault zones on the opposite side of the master fault. The larger one of these minor faults connect to the eastern boundary fault, which may open the above suggested fluid path ways.

In conclusion,

Results from gravity and geodynamic modeling obtained in this study demonstrate:

- 1) The necessity of re-interpretation of gravity anomalies on regional scale including the possibility of negative anomalies to be related to fracture porosity
- 2) Major flow paths may be inferred using Butterworth filter techniques with different wavelengths
- 3) Additional arguments for the hypothesis of connecting infiltration along the western boundary fault with up-flow of thermal water along westward dipping faults

Re-interpolation of temperature data and geological investigation indicates that:

- 1) Temperature anomalies at the top of the crystalline basement are linked on a regional scale to a neotectonic deformation including compression and uplift as postulated in earlier studies and a low seismicity, but also to a crystalline basement characterized by Early Carboniferous basaltic to granitic units of the Saxothuringian terrane, showing evidences of important radiogenic heat production
- 2) Peak anomalies are linked to westward dipping fault zones which typically mark the western boundary of horst structures. This observation can directly be linked to the results 2) and 3) of the gravity and geodynamic analyses
- 3) Slip and dilation tendency analyses do not provide unambiguous interpretation. Slip tendency reveals a low shear stress level far from the critical value. Additional arguments such as deformation patterns and gravity lows need to be sought to explain the localization of thermal anomalies

## Outlook

In the future, suggestions of research in the domain of geophysical prospection of naturally enhanced geothermal conditions in sedimentary basins and rifts systems should involve:

-conducting magnetotelluric (MT) analyses and measurements, using recent advances in 3D inversion of these data

-acquiring and analyzing 3D seismics to better visualize directions of faults and the depth they reach, their connection, and build high resolution 3D geological models in these environments

-conducting thermo-hydraulic simulations taking into account geometrical deformation processes associated with faulting in these environments for considering natural fluid pathways, as well as including lateral variations of radiogenic heat production

-using gravity in combination with the above mentioned tools including the new considerations developed during this thesis

## References

- Altwegg, P., Schill E., Mauri G., Radogna P.-V. and Abdelfettah Y. (in preparation). Fault zone porosity determination by joint interpretation of 3D seismic and gravity data for geothermal exploration - application in the St. Gallen geothermal project.
- Aquilina, L., Pauwels H., Genter A. and Fouillac C. (1997). Water-rock interaction processes in the Triassic sandstone and the granitic basement of the Rhine Graben: Geochemical investigation of a geothermal reservoir. *Geochimica et Cosmochimica Acta* 61(20): 4281-4295.
- Bächler, D., Kohl T. and Rybach L. (2003). Impact of graben-parallel faults on hydrothermal convection - Rhine Graben case study. *Physics and Chemistry of the Earth* 28(9-11): 431-441.
- Cathelineau, M. and Boiron M. C. (2010). Downward penetration and mixing of sedimentary brines and dilute hot waters at 5 km depth in the granite basement at Soultz-sous-Forets (Rhine graben, France). *Comptes Rendus Geoscience* 342(7-8): 560-565.
- Cornet, F. H., Helm J., Poitrenaud H. and Etchecopar A. (1997). Seismic and Aseismic Slips Induced by Large-scale Fluid Injections. *Pure and Applied Geophysics* 150(3): 563-583.

- Dezayes, C., Genter A. and Valley B. (2010). Structure of the low permeable naturally fractured geothermal reservoir at Soultz. *Comptes Rendus Geoscience* 342(7-8): 517-530.
- Edel, J. B. and Schulmann K. (2009). Geophysical constraints and model of the "Saxothuringian and Rhenohercynian subductions - magmatic arc system" in NE France and SW Germany. *Bulletin de la Société Géologique de France* 180(6): 545-558.
- Förster, A. and Förster H.-J. (2000). Crustal composition and mantle heat flow: Implications from surface heat flow and radiogenic heat production in the Variscan Erzgebirge (Germany). *Journal of Geophysical Research* 105(B12): 27.
- Geiermann, J. and Schill E. (2010). 2-D Magnetotellurics at the geothermal site at Soultz-sous-Forêts: Resistivity distribution to about 3000 m depth. *Comptes Rendus Geoscience* 342(7-8): 587-599.
- Genter, A. (1990). *Géothermie roches chaudes sèches: le granite de Soultz-sous-Forêts*. (Bas-Rhin, France), Fracturation naturelle, altérations hydrothermales et interaction eau-roche, Université d'Orléans. **PhD**: 201.
- Grecksch, G., Ortiz A. and Schellschmidt R. (2003). Thermophysical Study of GPK2 and GPK3 Granite Samples. HDR Project Soultz - Report.
- Hooijkaas, G. R., Genter A. and Dezayes C. (2006). Deep-seated geology of the granite intrusions at the Soultz EGS site based on data from 5 km-deep boreholes. *Geothermics* 35(5-6): 484-506.
- Illies, H. J. and Greiner G. (1979). Holocene movements and state of stress in the rhinegraben rift system. *Tectonophysics* 52(1-4): 349-359.
- Kohl, T., Bächler D. and Rybach L. (2000). Steps towards a comprehensive thermo-hydraulic analysis of the HDR test site Soultz-sous-Forêts. *Proc. World Geothermal Congress 2000, Kyushu-Tohoku, Japan, May-June 2000*, pp. 2671-2676.
- Le Carlier de Veslud, C., Royer J.-J. and Flores E. L. (1994). Convective heat transfer at the Soultz-sous-Forêts geothermal site: implications for oil potential. *EAGE vol. 12*.
- Place, J., Diraison M., Naville C., Géraud Y., Schaming M. and Dezayes C. (2010). Decoupling of deformation in the Upper Rhine Graben sediments. Seismic reflection and diffraction on 3-component Vertical Seismic Profiling (Soultz-sous-Forêts area). *C. R. Geoscience* 342(2010): 575-586.
- Pribnow, D. and Schellschmidt R. (2000). Thermal tracking of upper crustal fluid flow in the Rhine Graben. *Geophysical Research Letters* 27(13): 1957-1960.
- Pribnow, D. F. C., Fesche W. and Friedrich H. (1999). Heat Production and Temperature to 5 km Depth at the HDR Site in Soultz-sous-Forêts. GGA report
- Rummel, F. and König E. (1991). Density, ultrasonic velocities and magnetic susceptibility measurements on the core material from borehole EPS1 at Soultz-sous-Forêts. *Yellow report 8* (1991).
- Sanjuan, B., Millot R., Dezayes C. and Brach M. (2010). Main characteristics of the deep geothermal brine (5 km) at Soultz-sous-Forêts (France) determined using geochemical and tracer test data. *Comptes Rendus Geoscience* 342(7-8): 546-559.
- Schumacher, M. E. (2002). Upper Rhine Graben: Role of preexisting structures during rift evolution. *Tectonics* 21(1).
- Stober, I. and Bucher K. (2007). Hydraulic properties of the crystalline basement. *Hydrogeology Journal* 15(2): 213-224.
- Valley, B. and Evans K. F. (2007). Stress state at Soultz-sous-Forêts to 5 km depth from wellbore failure and hydraulic observations. 32nd workshop on geothermal reservoir engineering.





## All references

- Abdelfettah, Y. and Schill E. (2011). Accurate gravity data correction and 3D gravity forward modeling. 9th Swiss Geoscience Meeting, Zurich 2011.
- Abdelfettah, Y. and Schill E. (2012). Delineation of geothermally relevant Paleozoic graben structures in the crystalline basement of Switzerland using gravity Istanbul International Geophysical Conference and Oil & Gas Exhibition, Istanbul, Turkey, 17-19 September 2012. .
- Agemar, T., Schellschmidt R. and Schulz R. (2012). Subsurface temperature distribution in Germany. *Geothermics* 44(0): 65-77.
- Ahorner, L. (1975). Present-day stress field and seismotectonic block movements along major fault zones in Central Europe. *Tectonophysics* 29(1-4): 233-249.
- Altwegg, P., Schill E., Mauri G., Radogna P.-V. and Abdelfettah Y. (in preparation). Fault zone porosity determination by joint interpretation of 3D seismic and gravity data for geothermal exploration - application in the St. Gallen geothermal project.
- Aquilina, L., Pauwels H., Genter A. and Fouillac C. (1997). Water-rock interaction processes in the Triassic sandstone and the granitic basement of the Rhine Graben: Geochemical investigation of a geothermal reservoir. *Geochimica et Cosmochimica Acta* 61(20): 4281-4295.
- Bächler, D., Kohl T. and Rybach L. (2003). Impact of graben-parallel faults on hydrothermal convection - Rhine Graben case study. *Physics and Chemistry of the Earth* 28(9-11): 431-441.
- Baillieux, P., Schill E. and Dezayes C. (2011). 3D structural regional model of the EGS Soultz site (northern Upper Rhine Graben, France): insights and perspectives. Proceedings, Thirty-Sixth Workshop on Geothermal Reservoir Engineering, Stanford University, Stanford, California, SGP-TR-191.
- Banka, D., Pharaoh T. C., Williamson J. P. and Core T. P. F. (2002). Potential field imaging of Palaeozoic orogenic structure in northern and central Europe. *Tectonophysics* 360(1-4): 23-45.
- Barenblatt, G. I. (1962). The mathematical theory of equilibrium cracks in brittle fracture. *Adv. Appl. Mech.*, 7: 55--129.
- Barton, C. A., Zoback M. D. and Moos D. (1995). Fluid flow along potentially active faults in crystalline rock. *Geology* 23(8): 683-686.
- Bartz, J. (1974). Die Mächtigkeit des Quartärs im Oberrheingraben. Illies JH, Fuchs K (eds) *Approaches to taphrogenesis Schweizerbart, Stuttgart*: pp 78–87.
- Beccalotto, L., Capar L., Cruz-Mermy D., Oliviero G., Elsass P., Perrin A., Rupf I., Nitsch E. and Tesch J. (2010). The GeORG project: seismic interpretation, structural pattern and 3-D modelling of the Upper Rhine Graben – first scientific results. . Technical workshop. Geopotential of the Upper Rhine Graben (GeORG). (Novembre 18th 2010, Freiburg (Germany)).
- Behrmann, J. H., Hermann O., Horstmann M., Tanner D. C. and Bertrand G. (2003). Anatomy and kinematics of oblique continental rifting revealed: A three-dimensional case study of the southeast Upper Rhine graben (Germany). *AAPG Bulletin* 87(7): 1105--1121.
- Bergerat, F. (1985). Déformations cassantes et champs de contraintes tertiaires dans la plateforme européenne. *Paris VI*. Paris, Université Pierre & Marie Curie, Paris VI. **PhD**.
- Bertani, R. (2012). Geothermal power generation in the world 2005-2010 update report. *Geothermics* 41(0): 1-29.
- Bertrand, G., Elsass P., Wirsing G. and Luz A. (2006). Quaternary faulting in the Upper Rhine Graben revealed by high-resolution multi-channel reflection seismic. *Comptes Rendus Geoscience* 338(8): 574-580.
- Bonjer, K. P. (1997). Seismicity pattern and style of seismic faulting at the eastern borderfault of the southern Rhine Graben. *Tectonophysics* 275(1-3): 41-69.
- Bonjer, K. P., Gelbke C., Rouland D., Mayer-Rosa D. and Massinon B. (1984). Seismicity and dynamics of the Upper Rhinegraben. *J Geophys* 55:1-12

## All references

- BRGM (1980). France Magnetic Anomaly Map (Carte Magnetique de la France) 1:1,000,000, BRGM.
- Brun, J. P., Gutscher M. A. and {DEKORP-ECORS teams} (1992). Deep crustal structure of the Rhine Graben from seismic reflection data: A summary. *Tectonophysics* 208(1-3): 139-147.
- Brun, J. P., Wenzel F. and {ECORS-DEKORP team} (1991). Crustal-scale structure of the southern Rhinegraben from ECORS-DEKORP seismic reflection data. *Geology* 19: 758--762.
- Buiter, S. J. H., Huismans R. S. and Beaumont C. (2008). Dissipation analysis as a guide to mode selection during crustal extension and implications for the styles of sedimentary basins. *Journal of Geophysical Research-Solid Earth* 113(B6): -.
- Butterworth, S. (1930). On the theory of filter amplifiers. *Wireless Engineering* 1: 536-541.
- Campos-Enriquez, J. O., Hubral P., Wenzel F., Lueschen E. and Meier L. (1992). Gravity and Magnetic Constraints on Deep and Intermediate Crustal Structure and Evolution Models for the Rhine Graben. *Tectonophysics* 206(1-2): 113-135.
- Castera, J., Dezayes C. and Calcagno P. (2008). Large-scale 3D geological model around the Soultz site. Proceedings of the EHDRA scientific conference 24-25 September 2008, Soultz-sous-forêts, France.
- Cathelineau, M. and Boiron M. C. (2010). Downward penetration and mixing of sedimentary brines and dilute hot waters at 5 km depth in the granite basement at Soultz-sous-Forets (Rhine graben, France). *Comptes Rendus Geoscience* 342(7-8): 560-565.
- Cloetingh, S., Cornu T., Ziegler P. A. and Beekman F. (2006). Neotectonics and intraplate continental topography of the northern Alpine Foreland. *Earth-Science Reviews* 74(3-4): 127-196.
- Cloetingh, S., van Wees J. D., Ziegler P. A., Lenkey L., Beekman F., Tesauro M., Förster A., Norden B., Kaban M., Hardebol N., Bonté D., Genter A., Guillou-Frottier L., Ter Voorde M., Sokoutis D., Willingshofer E., Cornu T. and Worum G. (2010). Lithosphere tectonics and thermo-mechanical properties: An integrated modelling approach for Enhanced Geothermal Systems exploration in Europe. *Earth-Science Reviews* 102(3-4): 159-206.
- Cloetingh, S., Ziegler P. A. and Gerald S. (2007). Tectonic Models for the Evolution of Sedimentary Basins. *Treatise on Geophysics*. Amsterdam, Elsevier: 485-611.
- Cornet, F. H., Helm J., Poitrenaud H. and Etchecopar A. (1997). Seismic and Aseismic Slips Induced by Large-scale Fluid Injections. *Pure and Applied Geophysics* 150(3): 563-583.
- Cornu, T. G. M. and Bertrand G. (2005). Numerical backward and forward modelling of the southern Upper Rhine Graben (France-Germany border): new insights on tectonic evolution of intracontinental rifts. *Quaternary Science Reviews* 24(3-4): 353-361.
- Demoulin, A., Launoy T. and Zippelt K. (1998). Recent crustal movements in the southern Black Forest (western Germany). *Geologische Rundschau* 87(1): 43-52.
- Derer, C. E. (2003). Tectono-sedimentary evolution of the northern Upper Rhine Graben (Germany), with special regard to the early syn-rift stage. Ph.D. thesis, University of Bonn, p 99 [[http://hss.ulb.uni-bonn.de:90/ulb\\_bonn/diss\\_online/math\\_nat\\_fak/2003/derer\\_christian\\_eugen](http://hss.ulb.uni-bonn.de:90/ulb_bonn/diss_online/math_nat_fak/2003/derer_christian_eugen)]].
- Derer, C. E., Schumacher M. E. and Schafer A. (2005). The northern Upper Rhine Graben: basin geometry and early syn-rift tectono-sedimentary evolution. 640-656.
- Deutsch, C. V. and Journel A. G. (1998). *GSLIB - Geostatistical Software Library and User's Guide*. 2. Edition 1998. Oxford University Press, Oxford.
- Dezayes, C., Becaletto L., Oliviero G., Baillieux P., Capar L. and Schill E. (2011). 3-D visualization of a fractured geothermal field: the example of the EGS Soultz site (Northern Upper Rhine Graben, France). *PROCEEDINGS, Thirty-Sixth Workshop on Geothermal Reservoir Engineering Stanford University*
- Dezayes, C., Genter A. and Valley B. (2010). Structure of the low permeable naturally fractured geothermal reservoir at Soultz. *Comptes Rendus Geoscience* 342(7-8): 517-530.
- Dezayes, C., Villemin T., Genter A., Traineau H. and Angelier J. (1995). Analysis of fractures in borehole of the Hot Dry Rock project at Soultz-sous-Forêts (Rhine graben, France). *Scientific Drilling* 5: 31-41.

- Dèzes, P., Schmid S. M. and Ziegler P. A. (2004). Evolution of the European Cenozoic Rift System: interaction of the Alpine and Pyrenean orogens with their foreland lithosphere. *Tectonophysics* 389: 1--33.
- Doebel, F. (1967). The tertiary and pleistocene sediments of the Northern and Central part of the upper Rhinegraben. In: Rothé JP, Sauer K (eds) *The Rhinegraben progress report*. Mém Serv Carte Géol Als Lorr 26:48–54
- Doebel, F. (1970). Die tertiären und quartären Sedimente des südlichen Rheingrabens. In: Illies JH, Mueller St (eds) *Graben problems*. E Schweizerbart'sche Verlagsbuchhandlung, Stuttgart, pp 56–66
- Dubois, M., Ledesert B., Potdevin J. L. and Vancon S. (2000). Determination of the formation conditions of carbonates in an alteration zone of the Soultz-sous-Forets granite (Rhine Graben): the fluid inclusion record. *Comptes Rendus De L Academie Des Sciences Serie II Fascicule a-Sciences De La Terre Et Des Planetes* 331(4): 303-309.
- Dubois, M., Ougougdal M. A., Meere P., Royer J. J., Boiron M. C. and Cathelineau M. (1996). Temperature of paleo- to modern self-sealing within a continental rift basin: The fluid inclusion data (Soultz-sous-Forets, Rhine graben, France). *Bericht der Deutschen Mineralogischen Gesellschaft* 8(5): 1065-1080.
- Edel, J.-B., Dubois D., Marchant R., Hernandez J. and Cosca M. (2001). La rotation miocene inferieur du bloc corso-sarde; nouvelles contraintes paleomagnetiques sur la fin du mouvement. *Bulletin de la Société Géologique de France* 172(3): 275-283.
- Edel, J. B. (2004). Structure et évolution du Fossé Rhénan, du Carbonifère à nos jours - apports de la géophysique. *Bulletin de la société d'histoire naturelle et d'éthnographie de Colmar* 65(2004): 21-50.
- Edel, J. B., Campos-Enriquez O., Goupillot M. and Kiro K. N. (1982). Levé magnetique au sol du Fossé rhénan supérieur. *Interpretation géologique*. Bull. Bur. Rech.Géol. Min. 2: 179-192.
- Edel, J. B. and Fluck P. (1989). The Upper Rhenish Shield Basement (Vosges, Upper Rhinegraben and Schwarzwald) - Main Structural Features Deduced from Magnetic, Gravimetric and Geological Data. *Tectonophysics* 169(4): 303-316.
- Edel, J. B., Montigny R., Royer J. Y., Thuizat R. and Trolard F. (1986). Paleomagnetic investigations and K-AR dating on the variscan plutonic massif of the champ du feu and its volcanic-sedimentary environment, northern vosges, France. *Tectonophysics* 122(1-2): 165-185.
- Edel, J. B. and Schulmann K. (2009). Geophysical constraints and model of the "Saxothuringian and Rhenohercynian subductions - magmatic arc system" in NE France and SW Germany. *Bulletin de la Société Géologique de France* 180(6): 545-558.
- Edel, J. B., Schulmann K. and Rotstein Y. (2006). The Variscan tectonic inheritance of the Upper Rhine Graben: evidence of reactivations in the Lias, Late Eocene-Oligocene up to the recent. *International Journal of Earth Sciences* 96(2): 305-325.
- Edel, J. B., Schulmann K. and Rotstein Y. (2007). The Variscan tectonic inheritance of the Upper Rhine Graben: evidence of reactivations in the Lias, Late Eocene-Oligocene up to the recent. *International Journal of Earth Sciences* 96(2): 305-325.
- Edel, J. B. and Weber K. (1995). Cadomian terranes, wrench faulting and thrusting in central Europe Variscides : Geophysical and geological evidences. *Geologische Rundschau* 84: 412--432.
- Egli, R., Geiger A., Wiget A. and Kahle H.-G. (2007). A modified least squares collocation method for the determination of crustal deformation: first results in the Swiss Alps. *Geophysical Journal International* 168(1): 1-12.
- Engel, W. and Franke W. (1983). Flysch Sedimentation: Its relationship to Tectonism in the European Variscides. In: MARTIN, H. & EDER, F.W. [Editors]: *Intracontinental Fold Belts. Case Studies in the Variscan Belt of Europe and the Damara Belt in Namibia*. 267-287. Berlin, Heidelberg, New York, Tokyo (Springer).
- Evans, K. F., Burford R. O. and King G. C. P. (1981). Propagating Episodic Creep and the Aseismic Slip Behavior of the Calaveras Fault North of Hollister, California. *Journal of Geophysical Research* 86(Nb5): 3721-3735.

## All references

- Ferrill, D. A., Winterle J., Wittmeyer G., Sims D., Colton S., Armstrong A. and Morris A. (1999). Stressed Rock Strains Groundwater at Yucca Mountain, Nevada. *GSA Today* 9(5): 1-8.
- Flottmann, T. and Oncken O. (1992). Constraints on the Evolution of the Mid German Crystalline Rise - a Study of Outcrops West of the River Rhine. *Geologische Rundschau* 81(2): 515-543.
- Förster, A. and Förster H.-J. (2000). Crustal composition and mantle heat flow: Implications from surface heat flow and radiogenic heat production in the Variscan Erzgebirge (Germany). *Journal of Geophysical Research* 105(B12): 27.
- Franke, W. (1989). Variscan plate tectonics in Central Europe--current ideas and open questions. *Tectonophysics* 169(4): 221-228.
- Fuchs, K., Bonjer K. P., Gajewski D., Lüschen E., Prodehl C., Sandmeier K. J., Wenzel F. and Wilhelm H. (1987). Crustal evolution of the Rhinegraben area. 1. Exploring the lower crust in the Rhinegraben rift by unified geophysical experiments. *Tectonophysics* 141(1-3): 261-275.
- Fuhrmann, T., Heck B., Knöpfler A., Masson F., Mayer M., Ulrich P., Westerhaus M. and Zippelt K. (in press). Recent surface displacements in the Upper Rhine Graben - Preliminary results from geodetic networks. *Tectonophysics* (0).
- Gabriel, G., Vogel D., Scheibe R., Lindner H., Pucher R., Wonik T. and Krawczyk C. M. (2011). Anomalies of the Earth's total magnetic field in Germany - the first complete homogenous data set reveals new opportunities for multiscale geoscientific studies. *Geophysical Journal International* 184(3): 1113-1118.
- Geiermann, J. and Schill E. (2010). 2-D Magnetotellurics at the geothermal site at Soultz-sous-Forêts: Resistivity distribution to about 3000 m depth. *Comptes Rendus Geoscience* 342(7-8): 587-599.
- Genter, A. (1990). Géothermie roches chaudes sèches: le granite de Soultz-sous-Forêts. (Bas-Rhin, France), Fracturation naturelle, altérations hydrothermales et interaction eau-roche, Université d'Orléans. **PhD**: 201.
- Genter, A. (2004). avec la collaboration de Guillou-Frottier L., Breton J.P., Denis L., Dezayes Ch., Egal E., Feybesse J.L., Goyeneche O., Nicol N., Quesnel F., Quinquis J.P., Roig J.Y., Schwartz S. Typologie des systèmes géothermiques HDR-HFR en Europe, BRGM: 165.
- Genter, A., Guillou-Frottier L., Feybesse J.-L., Nicol N., Dezayes C. and Schwartz S. (2003). Typology of potential Hot Fractured Rock resources in Europe. *Geothermics* 32(4-6): 701-710.
- Grecksch, G., Ortiz A. and Schellschmidt R. (2003). Thermophysical Study of GPK2 and GPK3 Granite Samples. HDR Project Soultz - Report.
- Hinsken, S., Schmalholz S. M., Ziegler P. A. and Wetzler A. (2011). Thermo-Tectono-Stratigraphic Forward Modelling of the Upper Rhine Graben in reference to geometric balancing: Brittle crustal extension on a highly viscous mantle. *Tectonophysics* 509(1-2): 1-13.
- Hooijkaas, G. R., Genter A. and Dezayes C. (2006). Deep-seated geology of the granite intrusions at the Soultz EGS site based on data from 5 km-deep boreholes. *Geothermics* 35(5-6): 484-506.
- Huismans, R. S. and Beaumont C. (2003). Symmetric and asymmetric lithospheric extension: Relative effects of frictional-plastic and viscous strain softening. *J. Geophys. Res.* 108(B10): 2496.
- Huismans, R. S., Buitter S. J. H. and Beaumont C. (2005). Effect of plastic-viscous layering and strain softening on mode selection during lithospheric extension. *J. Geophys. Res.* 110(B2): B02406.
- Hurter, S. and Schellschmidt R. (2003). Atlas of geothermal resources in Europe. *Geothermics* 32(4-6): 779-787.
- Hurtig, E., Gotha H. H. G.-K. A., Commission I. H. F., DDR) Z. f. r. P. d. E. A. d. W. d., Verlagsgesellschaft H. H., Potsdam K. D. and Brandenburg L. (1992). Geothermal atlas of Europe / edited by E. Hurtig ... [et al.] ; International Association for Seismology and Physics of the Earth's Interior, International Heat Flow Commission; Central Institute for Physics of the Earth.
- Illies, H. (1972). The Rhine graben rift system - plate tectonic and transform faulting. *Geophysical Survey* 1: 27--60.
- Illies, H. J. and Greiner G. (1979). Holocene movements and state of stress in the rhinegraben rift system. *Tectonophysics* 52(1-4): 349--359.

- Illies, J. and Masteller E. C. (1977). Possible Explanation of Emergence Patterns of Baetis-Vernus-Curtis (Ins-Ephemeroptera) on Breitenbach-Schlitz Studies on Productivity, Nr 22. *Internationale Revue Der Gesamten Hydrobiologie* 62(2): 315-321.
- Illies, J. H. (1965). Bauplan und Baugeschichte des Oberrheingrabens. Ein Beitrag zum "Upper Mantle Project". *Oberrheinische Geologische Abhandlungen* 14: 1-54.
- Illies, J. H., Baumann H. and Hoffers B. (1981). Stress Pattern and Strain Release in the Alpine Foreland. *Tectonophysics* 71(1-4): 157-172.
- Illies, J. H. and Greiner G. (1978). Rhinegraben and Alpine system. *Geological Society of America Bulletin* 89: 770-782.
- Jeannette, D. and Edel J. B. (2005). Contexte géologique du site géothermique de Soultz-Sous-Forêts. *bulletin de l'Association Philomatique d'Alsace et de Lorraine Tome* 40.
- Kahle, H. G. and Werner D. (1980). A Geophysical-Study of the Rhinegraben .2. Gravity-Anomalies and Geothermal Implications. *Geophysical Journal of the Royal Astronomical Society* 62(3): 631-647.
- Klee, G. and Rummel F. (1993). Hydrofrac stress data for the European HDR research project test site Soultz-sous-Forêts. *International Journal of Rock Mechanics, Mining Science and Geomechanics Abstracts* 30: 973-976.
- Kohl, T., Bächler D. and Rybach L. (2000). Steps towards a comprehensive thermo-hydraulic analysis of the HDR test site Soultz-sous- Forêts. *Proc. World Geothermal Congress 2000, Kyushu-Tohoku, Japan, May-June 2000*, pp. 2671-2676.
- Kohl, T., Signorelli S. and Rybach L. (2001). Three-dimensional (3-D) thermal investigation below high Alpine topography. *Physics of The Earth and Planetary Interiors* 126(3-4): 195-210.
- Kossmat, F. (1927). Gliederung des varistischen Gebirgsbaues. *Abhandlungen des Sächsischen Geologischen Landesamtes Bd. 1. S.:* 1-39.
- Kroner, U., Hahn T., Romer R. L. and Linnemann U. (2007). The Variscan orogeny in the Saxo-Thuringian zone-Heterogenous overprint of Cadomian/Paleozoic Peri-Gondwana crust. *Geological Society of America Special Papers* 423: 153-172.
- Lahner, L. and Wellmer F.-W. (2004). *Geowissenschaftliche Karte der Bundesrepublik Deutschland 1:2.000.000. Geologie, Bundesanstalt für Geowissenschaften und Rohstoffe; Hannover.*
- Lauer, J. P. and Taktak A. G. (1971). Propriétés magnétiques des roches au voisinage du contact métamorphique des schistes de Steige et des granites d'Andlau et du Hohwald (Vosges cristallines du Nord). *C.R. Acad. Sci., Paris* 272, 924-927.
- Lavier, L. L., Buck W. R. and Poliakov A. N. B. (2000). Factors controlling normal fault offset in an ideal brittle layer. *Journal of Geophysical Research-Solid Earth* 105(B10): 23431-23442.
- Le Carlier de Veslud, C., Royer J.-J. and Flores E. L. (1994). Convective heat transfer at the Soultz-sous-Forêts geothermal site: implications for oil potential. *EAGE vol. 12.*
- Liaghat, C., Villemin T. and Jouanne F. (1998). Déformation verticale actuelle dans la partie sud du fossé d'Alsace (France). *Comptes Rendus de l'Académie des Sciences - Series IIA - Earth and Planetary Science* 327(1): 55-60.
- Lopes Cardozo, G. G. O. and Behrmann J. H. (2006). Kinematic analysis of the Upper Rhine Graben boundary fault system. *Journal of Structural Geology* 28(6): 1028-1039.
- Lowrie, W. and Alvarez W. (1975). Paleomagnetic Evidence for Rotation of the Italian Peninsula. *J. Geophys. Res.* 80(11): 1579-1592.
- Majorowicz, J. and Wybraniec S. (2011). New terrestrial heat flow map of Europe after regional paleoclimatic correction application. *International Journal of Earth Sciences* 100(4): 881-887.
- Mauthe, G., Brink H.-J. and Burri P. (1993). Kohlenwasserstoffvorkommen und -potential im deutschen Teil des Oberrheingrabens. 60.
- Moeck, I., Kwiątek G. and Zimmermann G. n. (2009). Slip tendency analysis, fault reactivation potential and induced seismicity in a deep geothermal reservoir. *Journal of Structural Geology* 31(10): 1174-1182.
- Montigny, R., Edel J. B. and Thuizat R. (1981). Oligo-Miocene rotation of Sardinia: KAr ages and paleomagnetic data of Tertiary volcanics. *Earth and Planetary Science Letters* 54(2): 261-271.

## All references

- Moresi, L., Mühlhaus H.-B., Lemiale V. and May D. (2007). Incompressible viscous formulations for deformation and yielding of the lithosphere. Geological Society, London, Special Publications 282(1): 457-472.
- Moresi, L., Quenette S., Lemiale V., Meriaux C., Appelbe B. and Mühlhaus H. B. (2007). Computational approaches to studying non-linear dynamics of the crust and mantle. *Physics of The Earth and Planetary Interiors* 163(1-4): 69-82.
- Morris, A., Ferrill D. A. and Henderson D. B. (1996). Slip-tendency analysis and fault reactivation. *Geology* 24(3): 275-278.
- Münch, W., Sistenich H., Bücker C. and Blanke T. (2005). Möglichkeiten der geothermischen Stromerzeugung im Oberrheingraben. *VGB PowerTech* 10/2005.
- Oncken, O. (1997). Transformation of a magmatic arc and an orogenic root during oblique collision and its consequences for the evolution of the European Variscides (Mid-German Crystalline Rise). *Geologische Rundschau* 86(1): 2-20.
- Oncken, O. (1998). Evidence for precollisional subduction erosion in ancient collisional belts: The case of the Mid-European Variscides. *Geology* 26(12): 1075-1078.
- Papillon, E. (1995). Traitements et interprétations des cartes d'anomalies magnétiques et gravimétriques du Fossé Rhénan supérieur. Dipl. Ing. Géophys. Strasbourg I, 95p.
- Place, J., Diraison M., Naville C., Géraud Y., Schaming M. and Dezayes C. (2010). Decoupling of deformation in the Upper Rhine Graben sediments. Seismic reflection and diffraction on 3-component Vertical Seismic Profiling (Soultz-sous-Forêts area). *C. R. Geoscience* 342(2010): 575-586.
- Plenefisch, T. and Bonjer K. P. (1997). The stress field in the Rhine Graben area inferred from earthquake focal mechanisms and estimation of frictional parameters. *Tectonophysics* 275(1-3): 71-97.
- Pribnow, D. and Schellschmidt R. (2000). Thermal tracking of upper crustal fluid flow in the Rhine Graben. *Geophysical Research Letters* 27(13): 1957-1960.
- Pribnow, D. F. C. (2000). The deep thermal regime in Soultz and implications for fluid flow. GGA Report, GGA Institut Hannover, 7 pp
- Pribnow, D. F. C., Fesche W. and Friedrich H. (1999). Heat Production and Temperature to 5 km Depth at the HDR Site in Soultz-sous-Forêts. GGA report
- Regenauer-Lieb, K., Rosenbaum G. and Weinberg R. F. (2008). Strain localisation and weakening of the lithosphere during extension. *Tectonophysics* 458(1-4): 96-104.
- Renard, P. and Courrioux G. (1994). Three-dimensional geometric modeling of a faulted domain: The Soultz Horst example (Alsace, France). *Computers & Geosciences* 20(9): 1379-1390.
- Rotstein, Y., Behrmann J. H., Lutz M., Wirsing G. and Luz A. (2005). Tectonic implications of transpression and transtension: Upper Rhine Graben. *Tectonics* 24(6).
- Rotstein, Y., Edel J. B., Gabriel G., Boulanger D., Schaming M. and Munsch M. (2006). Insight into the structure of the Upper Rhine Graben and its basement from a new compilation of Bouguer Gravity. *Tectonophysics* 425(1-4): 55-70.
- Rotstein, Y. and Schaming M. (2008). Tectonic implications of faulting styles along a rift margin: The boundary between the Rhine Graben and the Vosges Mountains. *Tectonics* 27(2): -.
- Rotstein, Y. and Schaming M. (2011). The Upper Rhine Graben (URG) revisited: Miocene transtension and transpression account for the observed first-order structures. *Tectonics* 30.
- Rummel, F., Haack U. and Gohn E. (1988). Uranium, thorium and potassium content and derived heat production rate for the granite cores in GPK1. *RUB Yellow Reports* 6: 9.
- Rummel, F. and König E. (1991). Density, ultrasonic velocities and magnetic susceptibility measurements on the core material from borehole EPS1 at Soultz-sous-Forêts. *Yellow report* 8 (1991).
- Sanjuan, B., Millot R., Dezayes C. and Brach M. (2010). Main characteristics of the deep geothermal brine (5 km) at Soultz-sous-Forêts (France) determined using geochemical and tracer test data. *Comptes Rendus Geoscience* 342(7-8): 546-559.

- Sausse, J. (1998). Caractérisation et modélisation des écoulements fluides en milieu fissuré. Relation avec les altérations hydrothermales et quantification des paléocontraintes. PhD thesis, Université Henri Poincaré, Nancy 1, France [http://halshs.archivesouvertes.fr/docs/00/06/04/28/PDF/these\\_SAUSSE.pdf](http://halshs.archivesouvertes.fr/docs/00/06/04/28/PDF/these_SAUSSE.pdf).
- Sausse, J., Dezayes C., Dorbath L., Genter A. and Place J. (2010). 3D model of fracture zones at Soultz-sous-Forêts based on geological data, image logs, induced microseismicity and vertical seismic profiles. *Comptes Rendus Geoscience* 342(7-8): 531-545.
- Schellschmidt, R. and Clauser C. (1996). The thermal regime of the Upper Rhine graben and the anomaly of Soultz. *Z. Angew. Geol.* 42(1): 40-44.
- Schill, E., Geiermann J. and Kümritz J. (2010). 2-D Magnetotellurics and gravity at the geothermal site at Soultz-sous-Forêts. *Proceedings World Geothermal Congress 2010 Bali, Indonesia*, 25-29 April 2010.
- Schill, E., Kohl T., Baujard C. and Wellmann J.-F. (2009). *Geothermische Ressourcen in Rheinland-Pfalz: Bereiche Süd- und Vorderpfalz*, Final report to the Ministry of Environment Rhineland-Palatine, 55p.
- Schindler, M., Baumgärtner J., Terry G., Hauffe P., Hettkamp T., Menzel H., Penzkofer P., Teza D., Tischner T. and Wahl G. (2010). Successful Hydraulic Stimulation Techniques for Electric Power Production in the Upper Rhine Graben, Central Europe. *Proceedings World Geothermal Congress 2010 Bali, Indonesia*, 25-29 April 2010.
- Scholz, C. H. and Gerald S. (2007). *Fault Mechanics. Treatise on Geophysics*. Amsterdam, Elsevier: 441-483.
- Schulz, R., Haenel R. and Kockel F. (1992). Federal Republic of Germany – West federal states. In: Hurlig, E., Cermak, V., Haenel, R., Zui, V. (Eds.), *Geothermal Atlas of Europe*. Gotha, Germany, pp. 34–37.
- Schumacher, M. E. (2002). Upper Rhine Graben: Role of preexisting structures during rift evolution. *Tectonics* 21(1).
- Scotti, O. and Cornet F. H. (1994). In Situ Evidence for fluid-induced aseismic slip events along fault zones. *International Journal of Rock Mechanics and Mining Science & Geomechanics Abstracts* 31(4): 347-358.
- Stober, I. and Bucher K. (2007). Hydraulic properties of the crystalline basement. *Hydrogeology Journal* 15(2): 213-224.
- Townend, J. and Zoback M. D. (2000). How faulting keeps the crust strong. *Geology* 28(5): 399-402.
- Valley, B. (2007). The relation between natural fracturing and stress heterogeneities in deep-seated crystalline rocks at Soultz-sous-Forêts (France), PhD thesis, ETH-Zürich, Switzerland, <http://e-collection.ethbib.ethz.ch/view/eth:30407>, 260 p.
- Valley, B. and Evans K. F. (2007). Stress state at Soultz-sous-Forêts to 5 km depth from wellbore failure and hydraulic observations. *32nd workshop on geothermal reservoir engineering*.
- Van den Berg, J. (1979). Paleomagnetism and the changing configurations of the western Mediterranean area in the Mesozoic and Early Cenozoic eras. *Geol Ultraectina* 20:178
- Vilà , M., Fernández M. and Jiménez-Munt I. (2010). Radiogenic heat production variability of some common lithological groups and its significance to lithospheric thermal modeling. *Tectonophysics* 490(3-4): 152-164.
- Villemin, T. (1986). *Tectonique en extension, fracturation et subsidence : Le Fossé Rhénan et le bassin de Sarre-Nahe*. Paris VI PhD: 270.
- Villemin, T., Alvarez F. and Angelier J. (1986). The Rhinegraben: Extension, subsidence and shoulder uplift. *Tectonophysics* 128(1-2): 47-59.
- Villemin, T. and Bergerat F. (1987). L'évolution structurale du fossé rhénan au cours du Cénozoïque : un bilan de la déformation et des effets thermiques de l'extension. *Bulletin de la Société Géologique de France* 3(2): 245--255.
- Watts, A. B. and Gerald S. (2007). An Overview. *Treatise on Geophysics*. Amsterdam, Elsevier: 1-48.
- Wenzel, F., Brun J.-p. and group e.-d. w. (1991). A deep seismic reflection profile across the northern rhine graben.

## All references

- Wenzel, F., Brun J. P., Blum R., Bois C., Burg J. P., Coletta B., Durbaum H., Durst H., Fuchs K., Grohmann N., Gutscher M. A., Hubner M., Karcher T., Kessler G., Klockner M., Lucazeau F., Luschen E., Marthelot J. M., Meier L., Ravat M., Reichert C., Vernassat S. and Villemin T. (1991). A Deep Reflection Seismic Line across the Northern Rhine Graben. *Earth and Planetary Science Letters* 104(2-4): 140-150.
- Wijns, C., Weinberg R., Gessner K. and Moresi L. (2005). Mode of crustal extension determined by rheological layering. *Earth and Planetary Science Letters* 236(1-2): 120-134.
- Willner, A. P., Massonne H. J. and Krohe A. (1991). Tectonothermal Evolution of a Part of a Variscan Magmatic Arc - the Odenwald in the Mid-German Crystalline Rise. *Geologische Rundschau* 80(2): 369-389.
- Ziegler, P. A. (1992). European Cenozoic rift system. *Tectonophysics* 208(1-3): 91-111.
- Ziegler, P. A. and Dezes P. (2007). Cenozoic uplift of Variscan Massifs in the Alpine foreland: Timing and controlling mechanisms. *Global and Planetary Change* 58: 237-269.
- Ziegler, P. A., Schumacher M. E., Dèzes P., Van Wees J.-D. and Cloetingh S. (2004). Post-Variscan evolution of the lithosphere in the Rhine Graben area: constraints from subsidence modelling. *Geological Society, London, Special Publications* 223(1): 289-317.
- Zippelt, K. and Malzer H. (1987). Results of New Geodetic Investigations in Southwestern-Germany. *Journal of Geodynamics* 8(2-4): 179-191.
- Zoback, M. D. (2007). *Reservoir Geomechanics*. Cambridge University Press: 448 pp.



## Acknowledgements

This thesis would not have come to a successful end without the help of numerous people.

First of all, I would like to express my thanks Prof. Eva Schill for supervising my thesis and for all her support in critical moments of this thesis. I am grateful to her for letting me go in the directions of research I wanted, but also helping in shaping ideas and text in a very accurate way when it became too fuzzy!

Dr. Yassine Abdelfettah (UniNE) deserves my gratitude for his constant availability, positivism, support and his guidance.

Dr. Albert Genter (Soultz GEIE/ BRGM), Dr. Chrystel Dezayes (BRGM), Prof. Philippe Renard (UniNE), for sharing data, concepts and ideas in the area of Soultz, reviews, and fruitful scientific discussions on the topic during the whole PhD.

Prof. Jean-Bernard Edel from EOST, Rüdiger Schellschmidt from LIAG for sharing their geophysical and temperature database and knowledge, Dr. Benoit Valley (ETHZ) for constructive remarks and some very useful matlab scripts, figures, and a gigantic scientific papers database.

All the team of the Swiss Laboratory for Geothermal Energy at UniNE: Dr. Yassine Abdelfettah, Pierrick Altwegg, Nicolas Clerc, Dr. Niels Giroud, Dr. Guillaume Mauri, Dr. Romain Sonney, Dr. Luca Guglielmetti with who I had the chance to share some exceptional moments, and also Dr. François-David Vuataz, Laurent Marguet, Dr. Sandrine Portier, Stephane Cattin, and the master students I had the chance to work with: Philip Klingler, Gennaro di Tommaso, Raphaël Gangnant, Nicole Schmitt.

The great team of the Center for Hydrogeology and Geothermics (CHYN), Domagoj Babic, Alice Badin, Guillaume Bertrand, Lucien Blandenier, Andrea Borghi, Florian Breider, Gregory Deman, Pierik Falco, Damian Glenz, Martin Hendrick, Simon Jeannotat, Jahouer Kerrou, Jessica Meeks, Christian Moeck, François Negro, Fabio Oriani, Guillaume Pirot, Giona Preisig, Julien Richon, Julien Straubhaar, Lorienthe Thueler, Geoffrey Undereiner, Yuexia Wu.

All master students I had the chance to meet and share beautiful excursions (and parties): Cybèle Cholet, Cécile Vuilleumier, Damien Poffet, Lorienthe Thueler, Simona Bronzini who count as close friends from now, and all the many others of years 2009 to 2013.

All the persons I had the chance to work with at the School of Mathematical Sciences Monash University: Prof. Louis Moresi, Dr. Manuele Faccenda, Dr. Fabio Capitanio, Julian Giordani, Owen Kaluza, Wendy Sharples, Sahereh Aivazpourporgou, Jerico Revote.

Special thanks to the ones who followed my adventures through the whole process of doing this PhD: my friends from Cité Universitaire, my flatmates in Melbourne, my friends from Neuchâtel and abroad: Geoffrey & Lilou, Tarik, Fabien, Luca, Greg, Cybèle, Simona, Damien, Cécile, Lorienthe, Alexia, Hubert, François, Michele & Nico R., Valentine, Guillaume & Adeline, Mitra, Raimonda, Christophe, Laura, Guillaume P. and Guillaume M., Jesus, Harsh, Heidi & Balaji, Pradyu, Theju & Bindhu, Ashok, Oxana, the Ali-s, Miriam, Mahsa, Marlène, Marie-Anne & Alex, Icaro, Heller, Daniel, Nico P.,

Géraldine, Dipika, Alfredo & Aline, Sarah, Christa, Dashmir, Justin, Sarah, Alric, Guillaume B., Damiano, Alessandra, Clio, the Swing Ma'Neuch quintet and the Magic Jazz Combo octet!

Antoine, for your great support.

To finish, I want to dedicate this thesis to my parents Maryvonne and Jean-Pierre, and my two brothers Sylvain and Antoine: the *elastic* family!

## 3D STRUCTURAL REGIONAL MODEL OF THE EGS SOULTZ SITE (NORTHERN UPPER RHINE GRABEN, FRANCE): INSIGHTS AND PERSPECTIVES

P. Baillieux<sup>1</sup>, E. Schill<sup>1</sup>, C. Dezayes<sup>2</sup>

<sup>1</sup>Centre of Hydrogeology and Geothermics (CHYN),  
Neuchâtel University, Rue Emile Argand 11,  
CH-2000, Neuchâtel, Switzerland

<sup>2</sup>BRGM (French Geological Survey)  
3, avenue Claude Guillemin,  
BP36009, F-45060, Orléans Cedex 2, France

e-mail: paul.baillieux@unine.ch

### ABSTRACT

In a perspective of geothermal exploration in graben systems, we analyse the recently built consistent structural model of Soultz area (Dezayes *et al.*, this issue) in order to understand the links between the regional graben fault system, the tectonic history of the Upper Rhine Graben (URG) and the local reservoir features (a low permeable naturally fractured granite).

The previous geological models of the area lack constraints concerning the geometry of the structures at the regional scale. To overcome this situation, the new 3D regional geological model of the Soultz area is based on a set of 2D seismic profiles (including recently reprocessed seismic lines) as well as former structural interpretations for oil exploration in the 70-80's and numerous deep wells (Dezayes *et al.*, this issue).

A network of 26 faults could be constructed in a 30x20x6 km model of the sedimentary cover and the top basement representing the faults as surfaces. The orientation of the major and generally synthetic faults (i.e. dipping eastward) is N22.5±7.5°E, whereas a second set strikes N0±10°E (mainly dipping westward), and a third one N45±10°E. The average dip of the faults is 60°. The fault density is approximately 3.7.10<sup>-4</sup> m<sup>2</sup> of faults per cubic meter.

The resulting 3D geological model confirms the tectonic situation of the Soultz site as a horst structure and indicates a maximum vertical offset of

approximately 500m of the basement in the area of the Soultz geothermal anomaly.

A comparison between the smaller scale 3D fractured reservoir model based on borehole imaging, microseismicity and vertical seismic profiling (Sausse *et al.*, 2010) and our 3D regional structural model suggests a strong correlation between the orientation of the partly stimulated fracture zones observed at reservoir scale and the secondary set of faults observed in our regional model.

### INTRODUCTION

The geothermal anomaly of the Enhanced Geothermal Systems (EGS) European test site Soultz is strongly related to the existence of zones of relatively high hydraulic conductivity allowing heat transport by fluid circulation. Large hydraulic permeabilities favour the onset of convection and enhances the efficiency of thermal transport in the subsurface. The enhanced surface heat flux in the Upper Rhine valley has been related to the circulation of thermal water along fault zones (Illies 1965). Numerical simulation of the geothermal site of Landau have confirmed this hypothesis (Bachler *et al.*, 2003). The relatively low natural permeability in the 5 km deep reservoir at Soultz is, however, insufficient for economic exploitation. The deep reservoir has been stimulated in a series of hydraulic and chemical stimulations and transmissivity has been enhanced by a factor of up to 10 (Genter *et al.*, 2010). The microseismicity reveals a preferential stimulation of fractures with orientation parallel to

the local stress field, which is in a slight angle to the main faults observed in the regional geological context.

Geological 3D models have been designed across the major geothermal anomalies at Soultz (Renard and Courrioux 1994; Dezayes *et al.*, 2009; Schill *et al.*, 2009), Landau and Speyer (Schill *et al.*, 2009). These earlier geological models of the Soultz area are usually based on five seismic lines (Cautru J.P. (1988) in Menjot *et al.*, 1988), which are located around the reservoir area and the horst structure of Soultz. They present a good overview of the local N-S trending structures.

To enhance the picture of the geological structures and investigate the occurrence of further families of fault parallel to the stimulated fractures on regional scale, we included new datasets to the model of (Dezayes *et al.*, 2009). Firstly, the faults and layers were adapted to the new interpretations of eight recently reprocessed regional seismic lines and former isohypse interpretations (Foehn 1985) down to the Triassic sediments, allowing for a geometrically consistent structural model in the sedimentary cover down to the top of the basement at the regional scale.

### **GEOLOGICAL SETTINGS:**

The Soultz horst structure is located at the western boundary of Upper Rhine Graben (URG), which reveals strong brittle deformation in this section (Fig. 1). While the main orientation of the boundary fault in the area of Soultz is about N52° (Geiermann and Schill 2010), the Mesozoic sediments are affected by a series of subvertical normal faults with a Rhenish (N-S) strike direction in the area of the horst structure.

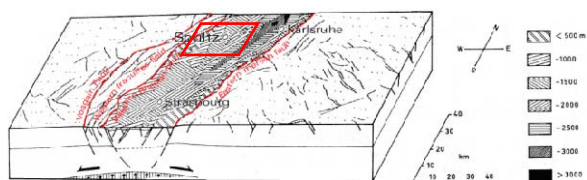


Figure 1: Bloc diagram of the Soultz area. Red rectangle is the showing the model perimeter. Various hatching corresponds to the thickness of the Cenozoic fill. Modified after (Valley 2007).

The Mesozoic platform sediments, which deposited in the Triassic (namely Buntsandstein, Muschelkalk and Keuper) and the Jurassic times (Lias and Dogger) on the peneplaned Variscan basement, rest discordantly on this Permo-Carboniferous series

which was affected by crustal discontinuities (Schumacher 2002).

A general synthesis of the Cenozoic tectonic history of the URG with a special focus on Soultz granite is described in (Valley 2007):

The Soultz granites intruded in Visean time (Early Carboniferous) (Cocherie *et al.*, 2004), during the orogenesis of the Variscan Belt in Europe, resulting from the collision of Laurasia and Gondwana (Franke 1989). During this orogenic stage, they have been affected by a main NE-SW orientation as seen in the neighboring outcrops and several geophysical studies (Edel *et al.*, 2007).

The later Cenozoic rift systems in Europe originates from the Alpine and Pyrenean collisions (Ziegler 1992). The URG can be regarded as typical example of synorogenic intracontinental foreland rifting (Schumacher 2002; Dèzes *et al.*, 2004; Cloetingh *et al.*, 2010). According to (Villemin and Bergerat 1987) and (Villemin *et al.*, 1986) the tertiary tectonic history of the URG occurred on four phases.

The first phase was characterised by a N-S compression and took place in middle to late Eocene. It reactivated Variscan Permo-carboniferous and Mesozoic crustal scale faults in the URG (Dèzes *et al.*, 2004). The second phase was an E-W extension that represents the main rifting stage of graben formation. The extension took place from the end of the Oligocene to that of the Eocene. In early Miocene, a NE-SW oriented compressive phase took place on Rhine Graben shoulders and surrounding and also in Sarre basin. From late Miocene up to the present, the stress regime prevailing in the Rhine Graben is the NW-SE compression that is seen over much of western Europe.

The geothermal reservoir of Soultz is located in a low permeable naturally fractured and hydrothermalized granite primarily related to major faults and fractures zones which, in turn, are connected to dense networks of small-scale structures (Dezayes *et al.*, 2010). The orientation of these fracture zones were estimated using imaging tools such as FMI and UBI revealing a dominant NNW-SSE direction which is different to the Rhenish orientation of large scale fault (Dezayes *et al.*, 2010).

### **NEW DATA COMPILATION:**

Our regional model is based on different recently accessible data among those, recently re-processed and re-interpreted seismic lines, information from oil and geothermal wells and geological maps (Dezayes *et al.*, this issue). These are: 69 boreholes with a mean depth of about 1km and 10 seismic profiles

acquired in the 70's and the 80's for the oil exploration and reprocessed in the framework of different project (Dezayes *et al.*, this issue) (Fig.2). We have also integrated about 15 former seismic profiles and the earlier interpretation of the fault network (Foehn 1985) to compare with our model. This fault network was described in the sedimentary cover based on a dense network of 42 seismic lines acquired in the 70-80's with a mean spacing of 1.5 km.

These data have been homogenized to be entered in a same referential. For that, we have transformed the time scale seismic profile into depth scale cross-section. The seismic horizons were converted from time to depth using velocities of the compressive seismic waves ( $V_p$ ) extracted from 7 regional boreholes (Fig.2) in which the measurements  $time=f(depth)$  were done (Fig.3).

The interval velocity of each formation 'i' can be defined as:

$$\text{Eq. 1: } V_p(i) = \frac{\Delta z(i)}{\Delta t(i)}$$

between the considered depth interval.

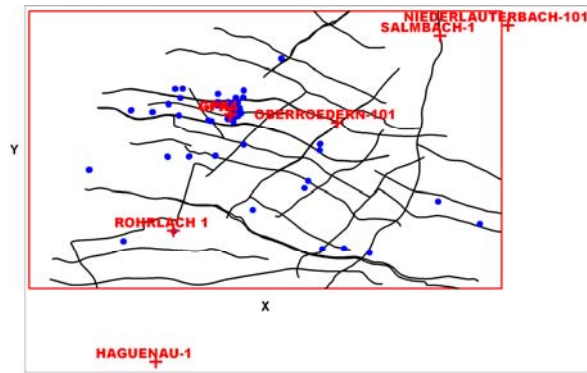


Figure 2: Model perimeter. Where black lines, blue dots and red crosses respectively show seismic lines, boreholes and the 7 boreholes where  $time=f(depth)$  measurements were done.

The information on the thickness of the major formation the area of Soultz obtained from both sources oil and geothermal wells is summarized in Table 1.

Table 1 (top right): Formations thickness observed in the 69 boreholes from oil and geothermal production

Attribute \ Formation	Formation Thickness (m)	Number of boreholes crossing the formation
Tertiary	750 ±320	69
Jurassic	148 ±76	59
Keuper	135 ±58	54
Muschelkalk	130 ±47	20
Buntsandstein	373 ±66	9

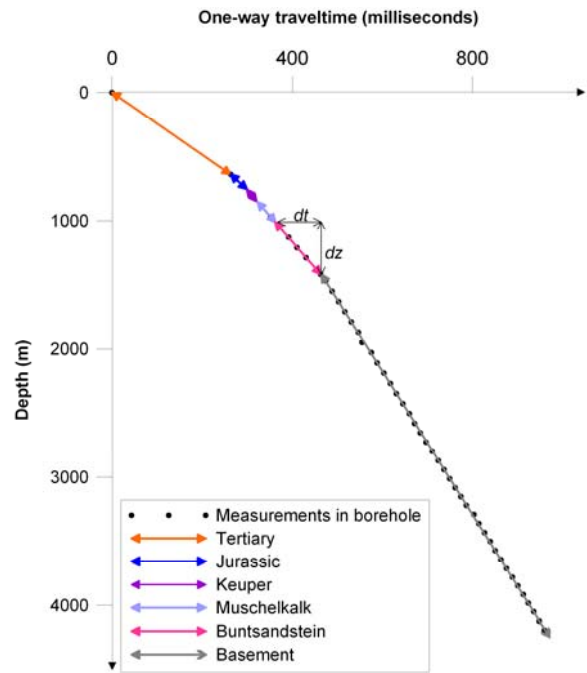


Figure 3: Representative example of the relation between one-way travel time and depth in borehole GPK4.

## METHODOLOGY

### 3D interpretation

Implicit 3D geological modeling provides a powerful tool extrapolate in particular complex fault geometries derived from 2D cross sections such as seismic profiles and borehole data to unknown parts of the model (Renard and Courrioux 1994; Castera *et al.*, 2008).

On the basis of an implicit approach geology can be modeled using the location of the geological interfaces and orientation data from structural field and 2D cross-sections. Both types of data are cokriged to interpolate a continuous 3D potential-

field function describing the geometry of the geology (Calcagno *et al.*, 2008), in which the dip of the layers represents the gradient of the field. 3DGeomodeller (BRGM, Intrepid Geophysics) was used in this study. It offers the possibility to create such geological model and generate various predicted geophysical responses or forward models from it, as well as to compare the 3D geological model against independently gathered geophysical datasets (Guillen *et al.*, 2008).

### **Faults**

The 3D interpretation consists firstly in defining the size of faults and linking them to each seismic profile to build a consistent fault network (Renard and Courrioux 1994; Castera *et al.*, 2008). The integration of the former structural maps, more dense in terms of seismic profiles and the seismic lines largely influenced our choice. We did not include smaller scale faults although they were visible on the seismic lines, because the correlation between the profiles was unclear. The faults have a defined elliptical shape and influence radius on the horizons.

### **Horizons**

The stratigraphic pile was simplified. The modeled horizons are: Tertiary, Jurassic, Keuper, Muschelkalk, Buntsandstein, and the Basement. The Triassic series (Keuper, Muschelkalk, Buntsandstein) are explicitly sub parallel, they rest on the basement series and are covered by the Tertiary series.

### **Statistics**

The calculated 3D structural model including all modeled fault zones is exported as triangulated surfaces, which contain information on strike and dip. These can be plotted in stereoplots and rose diagrams and be analyzed with classical structural approaches. The density of faults is described in  $m^2$  of faults per  $m^3$ .

## **RESULTS**

### **Velocity analysis**

We compare (Tab. 2) the interval velocities extracted from the 7 boreholes time=f(depth) measurements to different type of measurements:

- Standard values for P-wave seismic velocities ( $V_p$ ) in rocks (Kearey and Brooks 1991; Mari *et al.*, 1998)
- Ultrasonic velocities measurements on the core material from borehole EPS1 (Rummel and König 1991)

-Vertical seismic profiles analysis (VSP) (Place *et al.*, 2010)

-Sonic logs corrected by VSP in GPK1 (Beauce *et al.*, 1991)

-Tomographic studies around Soultz reservoir (Horálek *et al.*, 2008).

Even though the thicknesses and the constitutive materials of the different layers is variable in space, the values are in good agreement with  $V_p$  found in the literature (cf. Tab. 2), and are in the same range as measurements on the core material from the geothermal exploration borehole EPS1, as well as the VSP analysis and sonic logs available in well GPK1. An important variability (>15%) in the  $V_p$  of the Jurassic and Muschelkalk serie is noticeable among the different types of measurements.

### **Structural model**

The new regional 3D geological model of the Soultz area covers a volume of 31km X 18.5km X 6km including the sedimentary cover and the top of granitic basement and its structural features.

A number of 26 faults zones crossing the Mesozoic sedimentary layers and the top of the granitic basement could be constructed (Fig. 4).

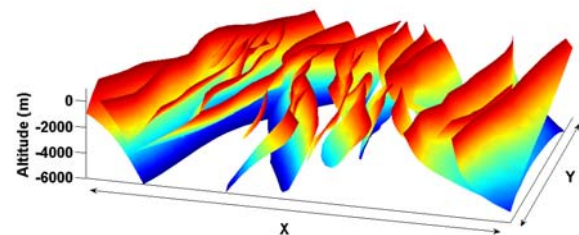


Figure 4: 3D representation of the fault planes

The 3D structural model at the regional scale shows at least three main orientations concerning the faults (Fig.5).

The orientation of the major and generally synthetic faults (i.e. dipping eastward) is  $N22.5 \pm 7.5^\circ E$ , whereas a secondary set strikes  $N0 \pm 10^\circ E$  (mainly dipping westward), and a third one  $N45 \pm 7.5^\circ E$ .

The first set represent about 30 % of the faults, the second one 33% and the third one 25%.

This fault network is only representative for the structural settings in the sedimentary cover since the resolution of faults using seismic remains mainly limited to this part.

Table 2: Comparison between interval velocities for the different formations used in the geological model and the literature

Name of the Serie	Interval velocity in this study: Vp (Km/s)	Standard deviation between boreholes (%)	Constitutive materials	Compressive wave velocities in rocks in literature: Vp (Km/s)	Ultrasonic velocities measurements on the core material from borehole EPS1(Km/s)	VSP measurements and sonic logs corrected by VSP in borehole GPK1 (Km/s)	Tomographic study around the reservoir (Km/s)
Tertiary	2.30±0.07	3.0	Limestone/Marl/Sands tone	2.0-6.0/2.0-3.0/2.0-2.5	ND	ND	≈2.28*
Jurassic	3.57±0.60	16.7	Jurassic Limestone/Marl	3.0-4.0/2.0-3.0	ND	ND	≈3.15*
Keuper	4.11±0.20	4.9	<b>Marl/dolomite</b> /limestone/sandstone	<b>2.0-3.0/2.5-6.5</b> /3.5-6.0/2.0-6.0	ND	ND	≈3.15-3.71*
Muschelkalk	4.63±0.91	19.7	<b>Marl/Dolomite</b> /Sandstone/Limestone	<b>2.0-3.0/2.5-6.5</b> /2.0-6.0/3.5-6.0	5.35 ± 0.28	3.62±0.1	3.71
Buntsandstein	4.44±0.58	13.0	Sandstone/Conglomerate	2.0-6.0/not available	4.53±0.51	4.33±0.03	4.54
Basement	5.61±0.04	0.8	Porphyric monzogranite/ Fine-grained two-mica granite	5.5-6.0	5.51±0.02	5.64 5.66 5.78	5.48 5.89

\*depth intervals chosen in the tomographic study were not chosen the same as the ones encountered in the geothermal wells, this can lead to differing values

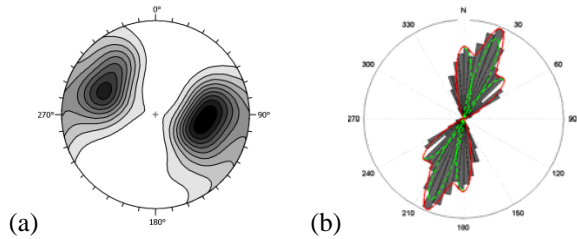


Figure 5: a) Stereographic projection of triangulated fault surfaces poles density for each triangle of the 3D model (lower hemisphere, equal area). The isolines represent 10% population intervals - b) Circular histogram of faults strike (in grey). Each set is highlighted by two symmetric green petals (Gaussian repartition). The red contour is the sum of the green petals.

The fault density is approximately  $3.7 \cdot 10^{-4} \text{ m}^2$  of faults per cubic meter.

Minor faults (not included in the model but present on the seismic profiles) are measured to be about 0.9 fault per km in the E-W direction and about 0.5 fault per km in the N-S direction and seem to follow the same trend as the one included in our model.

The resulting 3D geological model confirms the tectonic situation of the Soultz site as a horst structure and indicates a maximum vertical offset of approximately 500 meters of the basement under Soultz site (Fig. 6), in the area of the geothermal anomaly (Fig. 7).

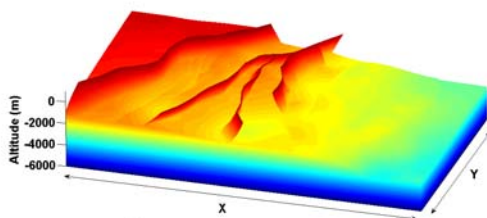


Figure 6: 3D model showing the depth of the top basement, the horst structure with its three main faults and the graben western border fault.

## DISCUSSION

The orientation of the different fault sets can be related to the tectonic history of the Upper Rhine Graben.

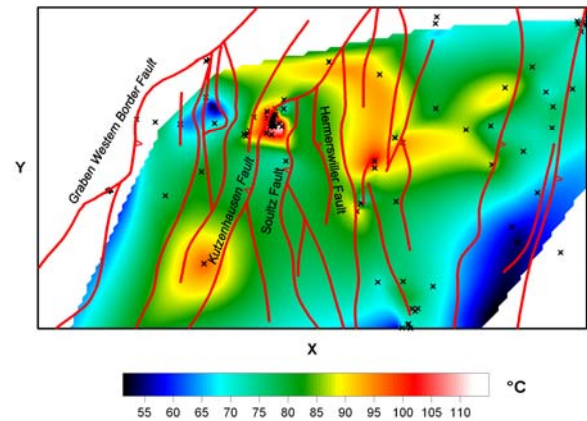


Figure 7: Superposition of the surface faults (in red) and the temperature field at 800m depth (data provided by LIAG-Hannover).

Most of the sets are probably due to the first and second main rifting phase of the Upper Rhine Graben, characterized by a N-S compression and an E-W extension which took place from the end of the Oligocene to that of the Eocene respectively (Villemain 1986) A geodynamical approach based on the present 3D model statistics could infer these interpretations.

To get insights on the possible connection of these faults to the basement we compare the 3D reservoir model of Soultz based on borehole imaging, VSP and microseismicity during stimulation, designed in (Sausse *et al.*, 2010).

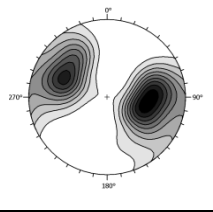
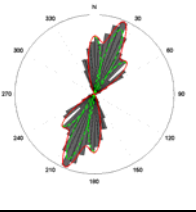
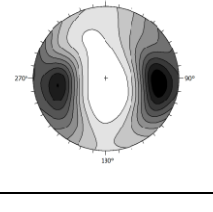
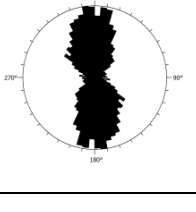
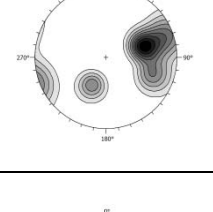
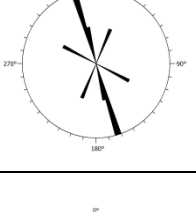
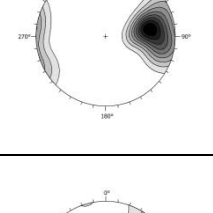
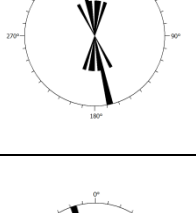
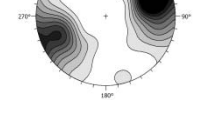
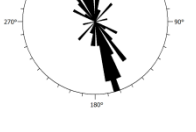
As shown in Table 3, the secondary and antithetic fault network observed in our analysis (Fig. 6) with a mean direction of  $N0 \pm 10^\circ E$  dipping at  $60 \pm 8^\circ$  dominantly to the west and the major fracture zone network in the granite reveal similar strike direction and dip direction:

- VSP: mean strike  $N165^\circ E$ , dipping at  $75^\circ$  dominantly to the west
- Microseismicity:  $N165^\circ E$ ,  $70^\circ$  to the west
- Fracture zones:  $N165^\circ E$ ,  $65^\circ$  to the west

The comparison of the fractures orientations observed in the Buntsandstein layer and the granitic basement however suggests a continuity in the deformation between the two formations (Dezayes *et al.*, 2010). The occurrence of a same family of directions of faults in the sedimentary cover and the fractures in the basement suggests similar results.

This secondary set of faults is likely to be stimulated during fracturation its orientation being parallel to the local stress field.



Data	Poles	Faults Strike
(A) 3d Model: Triangulated Surfaces		
(B) Boreholes Fractures: 4141 Data		
(C) VSP: 5 Data		
(D) Microseismicity: 7 Data		
(E) Fractures Zones: 41 Data		

In addition, the average spacing of about 500 meters between the major fracture zones highlighted in (Dezayes *et al.*, 2010) is consistent with the fault spacing in our model.

## CONCLUSIONS

The construction of the 3D structural model of Soultz region satisfies information from different sources.

The resulting fault network in the sedimentary cover was analyzed in terms of orientation, related to the tectonic history of the URG and compared with the deep granite fractures network.

Table 3 (left): a) Poles density and circular histograms of faults in the 3D model (lower hemisphere, equal area), The isolines represent 10% population intervals – b) Poles density of all fractures observed in boreholes GPK3 and GPK4 below the depth of 1450m (granitic basement) - c) Poles density of fractures observed by VSP (Sausse *et al.*, 2010) - d) Poles density of fractures observed by microseismicity (Sausse *et al.*, 2010) – e) Poles density of natural flowing fracture zones based on borehole imaging and other borehole geophysical measurements (Sausse *et al.*, 2010).

It appears that one set of secondary faults in the present model has similar strike and dip direction to the ones of the fractures observed in the deep granite reservoir of Soultz based on borehole imaging, VSP and microseismicity during stimulation, designed in (Sausse *et al.*, 2010). This suggests a continuity in the deformation between the two formations.

This secondary set of faults is likely to be stimulated during fracturation its orientation being parallel to the local stress field.

## ACKNOWLEDGEMENTS

The authors would like to thank BRGM, GEIE Soultz and LIAG-Hannover for providing data, Pierrick Altwegg, Andrea Borghi, Philippe Renard, Benoit Valley for their technical assistance, and Yassine Abdelfettah for his constant availability and his assistance in the geophysical processing.

## REFERENCES

- Bachler, D., T. Kohl and L. Rybach (2003). "Impact of graben-parallel faults on hydrothermal convection - Rhine Graben case study." *Physics and Chemistry of the Earth* **28**(9-11): 431-441.
- Beauce, A., H. Fabriol, D. Le Masne, C. Cavoit, P. Mechler and X. Kai Chen (1991). "Seismic studies on the HDR site of Soultz-Sous-Forêts (Alsace, France)." *Geotherm. Sci & Tech.* **3**(1-4): pp. 239-266.
- Calcagno, P., J. P. Chiles, G. Courrioux and A. Guillen (2008). "Geological modelling from field data and geological knowledge Part I. Modelling method coupling 3D potential-field interpolation and geological rules." *Physics of the Earth and Planetary Interiors* **171**(1-4): 147-157.

- Castera, J., C. Dezayes and P. Calcagno (2008). "Large-scale 3D geological model around the Soultz site." Proceedings of the EHDRA scientific conference 24-25 September 2008, Soultz-sous-forêts, France.
- Cautru J.P. (1988) in Menjöz, A., J. P. Cautru, A. Criaud and A. Genter (1988). "Roches sèches chaudes. Caractérisation des réservoirs fracturés:." Rapport annuel d'activités 1988n BRGM/IRG: 35-39.
- Cloetingh, S., J. D. van Wees, P. A. Ziegler, L. Lenkey, F. Beekman, M. Tesauro, A. Förster, B. Norden, M. Kaban, N. Hardebol, D. Bonté, A. Genter, L. Guillou-Frottier, M. Ter Voorde, D. Sokoutis, E. Willingshofer, T. Cornu and G. Worum (2010). "Lithosphere tectonics and thermo-mechanical properties: An integrated modelling approach for Enhanced Geothermal Systems exploration in Europe." Earth-Science Reviews **102**(3-4): 159-206.
- Cocherie, A., C. Guerrot, C. M. Fanning and A. Genter (2004). "Datation U-Pb des deux faciès du granite de Soultz (Fossé rhénan, France)." Géochimie (Géochronologie) **336**(9): 775--787.
- Dezayes, C., L. Becalotto, G. Oliviero, P. Baillieux, L. Capar and E. Schill (2011). "3-D visualization of a fractured geothermal field: the example of the EGS Soultz site (Northern Upper Rhine Graben, France)." PROCEEDINGS, Thirty-Sixth Workshop on Geothermal Reservoir Engineering Stanford University (this issue).
- Dezayes, C., J. Castera, G. Heilbronn and P. Calcagno (2009). "Regional geological model of the Soultz-sous-Forêts geothermal field (Rhine Graben, France). ." GRC transactions, Vol. 33: 175-180.
- Dezayes, C., A. Genter and B. Valley (2010). "Overview of the Fracture Network at Different Scales Within the Granite Reservoir of the EGS Soultz Site (Alsace, France)." Proceedings World Geothermal Congress 2010 Bali, Indonesia, 25-29 April 2010.
- Dezayes, C., A. Genter and B. Valley (2010). "Structure of the low permeable naturally fractured geothermal reservoir at Soultz." C. R. Geoscience **342**(2010): 517-530.
- Dèzes, P., S. M. Schmid and P. A. Ziegler (2004). "Evolution of the European Cenozoic Rift System: interaction of the Alpine and Pyrenean orogens with their foreland lithosphere." Tectonophysics **389**: 1--33.
- Edel, J. B., K. Schulmann and Y. Rotstein (2007). "The Variscan tectonic inheritance of the Upper Rhine Graben: evidence of reactivations in the Lias, Late Eocene-Oligocene up to the recent." International Journal of Earth Sciences.
- Foehn, J. P. (1985). "interprétation des campagnes sismiques 1981 et 1984, concession de Pechelbronn, permis de Haguenau. Total Exploration internal report, October 19985."
- Franke, W. (1989). "Variscan plate tectonics in Central Europe--current ideas and open questions." Tectonophysics **169**(4): 221-228.
- Geiermann, J. and E. Schill (2010). "2-D Magnetotellurics at the geothermal site at Soultz-sous-Forêts: Resistivity distribution to about 3000 m depth." Comptes Rendus Geoscience **342**(7-8): 587-599.
- Genter, A., K. Evans, N. Cuenot, D. Fritsch and B. Sanjuan (2010). "Contribution of the exploration of deep crystalline fractured reservoir of Soultz to the knowledge of enhanced geothermal systems (EGS)." Comptes Rendus Geoscience **342**(7-8): 502-516.
- Guillen, A., P. Calcagno, G. Courrioux, A. Joly and P. Ledru (2008). "Geological modelling from field data and geological knowledge Part II. Modelling validation using gravity and magnetic data inversion." Physics of the Earth and Planetary Interiors **171**(1-4): 158-169.
- Horálek, J., Z. Jechumtálová, L. Dorbath and J. Šílený (2008). "Shear vs. non-shear components in source mechanisms of microearthquakes induced in hydraulic fracturing experiment at the HDR site Soultz-Sous-Forêts (Alsace) in 2003." EHDRA scientific.
- Illies, J. H. (1965). "Bauplan und Baugeschichte des Oberrheingrabens. Ein Beitrag zum "Upper Mantle Project"." Oberrheinische Geologische Abhandlungen **14**: 1-54.
- Kearey, P. and M. Brooks (1991). "An introduction to Geophysical Exploration." 2nd ed. ix + 254 pp. Oxford: Blackwell Scientific Publications.
- Mari, J.-L., G. Arens, D. Chapellier and P. Gaudiani (1998). "Géophysique de Gisement et de Génie Civil." Institut Français du Pétrole.
- Place, J., M. Diraison, C. Naville, Y. Géraud, M. Schaming and C. Dezayes (2010). "Decoupling of deformation in the Upper Rhine Graben sediments. Seismic reflection and diffraction on 3-component Vertical Seismic Profiling (Soultz-sous-Forêts area)." C. R. Geoscience **342**(2010): 575--586.
- Renard, P. and G. Courrioux (1994). "Three-dimensional geometric modeling of a faulted

- domain: The Soultz Horst example (Alsace, France)." Computers & Geosciences **20**(9): 1379-1390.
- Rummel, F. and E. König (1991). Physical properties of Core samples, borehole EPS1, Soultz-sous-Forêts: Velocity-, Density- and magnetic susceptibility- logs, depth interval 933-2227 m. Yellow report 6. Bochum, Ruhr - Universität: 58.
- Sausse, J., C. Dezayes, L. Dorbath, A. Genter and J. Place (2010). "3D fracture zone network at Soultz based on geological data, Image logs, microseismic events and VSP results." C.R. Geoscience **342** (2010): 531-545.
- Schill, E., T. Kohl, C. Baujard and J.-F. Wellmann (2009). "Geothermische Ressourcen in Rheinland-Pfalz: Bereiche Süd- und Vorderpfalz, Final report to the Ministry of Environment Rhineland-Palatine, 55p."
- Schumacher, M., E. (2002). "Upper Rhine Graben: Role of preexisting structures during rift evolution." Tectonics **21**(1): 1006.
- Valley, B. (2007). "The relation between natural fracturing and stress heterogeneities in deep-seated crystalline rocks at Soultz-sous-Forêts (France), PhD thesis, ETH-Zürich, Switzerland, <http://e-collection.ethbib.ethz.ch/view/eth:30407>, 260 p."
- Villemin, T. (1986). Tectonique en extension, fracturation et subsidence : Le Fossé Rhénan et le bassin de Sarre-Nahe. Paris VI. Paris, Paris VI. **PhD**: 270.
- Villemin, T., F. Alvarez and J. Angelier (1986). "The Rhinegraben: Extension, subsidence and shoulder uplift." Tectonophysics **128**(1-2): 47-59.
- Villemin, T. and F. Bergerat (1987). "L'évolution structurale du fossé rhénan au cours du Cénozoïque : un bilan de la déformation et des effets thermiques de l'extension." Bulletin de la Société Géologique de France **3**(2): 245--255.
- Ziegler, P. A. (1992). "European Cenozoic rift system." Tectonophysics **208**(1-3): 91-111.

## 3-D VISUALIZATION OF A FRACTURED GEOTHERMAL FIELD: THE EXAMPLE OF THE EGS SOULTZ SITE (NORTHERN UPPER RHINE GRABEN, FRANCE)

C. Dezayes<sup>1</sup>, L. Beccaletto<sup>1</sup>, G. Oliviero<sup>1</sup>, P. Baillieux<sup>2</sup>, L. Capar<sup>1</sup>, E. Schill<sup>2</sup>

<sup>1</sup> BRGM (French Geological Survey)  
3, avenue Claude Guillemin, BP36009  
F-45060 Orléans Cedex 2.

<sup>2</sup> CHYN (Centre of Hydrogeology and Geothermics)  
Neuchâtel University, Rue Emile Argand 11  
CH-2000 Neuchâtel.

e-mail: [c.dezayes@brgm.fr](mailto:c.dezayes@brgm.fr)

### ABSTRACT

This present paper describes a 3-D geological model in the Upper Rhine Graben, around the EGS (Enhanced Geothermal System) Soultz site (France). This model is a 30x20x6 km geological model built from the surface to the crystalline basement. The goal is to visualize the complex fault network of the graben by federating the knowledge on this specific area.

The building of the 3-D geological model is based on two main kinds of data: (1) seismic profile interpretations and (2) borehole data. The seismic profiles have been acquired for oil exploration in the 70-80's, and reprocessed recently in the framework of various projects. The 2-D information is interpolated to the whole 3-D space using a geostatistical analysis.

For our model, a network of 26 fault has been built. The orientation of the major faults is NNE-SSW (i.e. Rhenish direction), with a main eastward dipping. Secondary, principally antithetic faults, trend N-S to NNW-SSE, with an average dip of 60°. This 3-D geological model could be now used as a basis for many exploration investigations and different kinds of modelling.

### INTRODUCTION

The development of renewable energy in France necessitates exploring new or poorly well-know deep geothermal reservoirs located in promising area. In this framework, the concept of EGS (Enhanced Geothermal System) developed at Soultz since twenty years must be now extended to the Upper Rhine Graben.

The EGS Soultz site is located in the northern part of the Upper Rhine Graben (France), above an important positive thermal anomaly. The area is

highly fractured due to the Cenozoic tectonic opening of the Rhine Graben. Numerous regional and local normal faults are present, most of time superimposed on previous hercynian structures. This structural network is the way for fluid circulations and probably the basis of the thermal anomaly of the area. To assemble the all the data and knowledge on this area, we built a 3-D geological model. This model allows to have a visualization of the geometry of the fault network and the deep geological formations, in order to federate people for future exploration studies (for examples gravimetric and magnetic inversions).

The building of the 3-D model is based (1) on geological investigations in the framework of the EGS Soultz project (Dezayes *et al.*, 2009), and also (2) a new exploitation of old seismic profiles acquired for oil exploration in the 70-80's. We reprocessed the profiles to improve the quality of the seismic image. This improvement was possible thanks to new algorithms, as well as in a better definition of the static and dynamic corrections. A new interpretation has been done throughout different scientific projects. The 3-D model consists in a 30x20x6 km geological model extending from the crystalline Hercynian basement to the surface, including Triassic, Jurassic and Tertiary layers.

Our study focuses on the data we used, and the building of the fault network, and presents the resulting 3-D geological visualisation of this specific area of the northern Upper Rhine Graben.

### GEOLOGICAL SETTING

The Rhine Graben is a Cenozoic graben belonging to the West European Rift System (Ziegler, 1992), which is very well-known based on numerous studies for petroleum and mining exploration (boreholes, geophysical surveys...).

It is located in the extreme NE part of France for its western part and in Germany for its eastern part (Figure 1). The graben is 30-40km large and 300km long and the Rhine river flows through it.

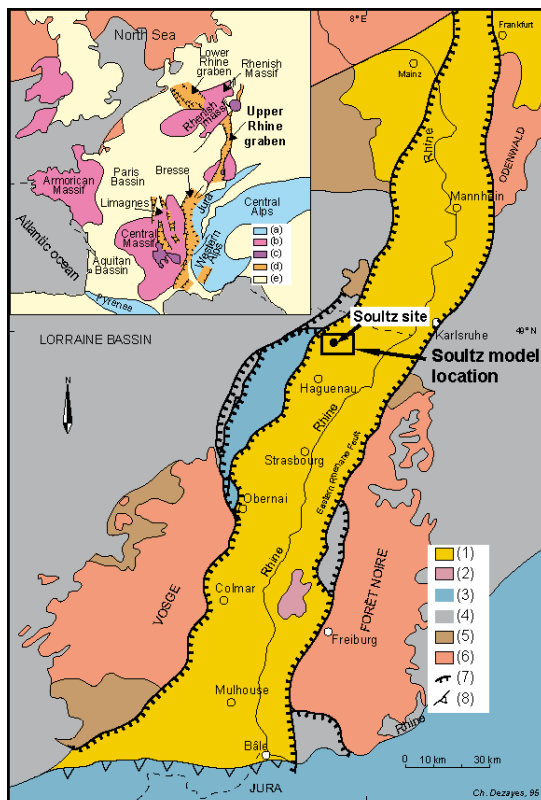


Figure 1 - Simplified geological map of western Europe and the Rhine graben with the location of the EGS Soutz site and the limits of the 3-D geological model. (a) alpin massifs, (b) hercynian massifs, (c) volcanic massifs, (d) graben filling, (e) sedimentary basin. (1) Oligocene and Miocene sedimentary filling, (2) Cenozoic volcanism, (3) Jurassic sediments (Lias and Dogger), (4) Permo-carboniferous basins, (5) Hercynian basement, (6) main border faults of the Rhine Graben, (7) thrusts.

The Rhine Graben is filled by Tertiary and Quaternary siliciclastic, lacustrine and few marine sediments with a rather discrete volcanic activity, overlaying the Jurassic and Triassic sediments together with the Paleozoic crystalline basement.

This graben is made of three segments limited by border faults oriented N15°E in the North and the South parts, and N30-35°E in the Central part (Figure 1). Two crystalline massifs surround it, namely the Vosges massif along the western side and the Black Forest along the eastern side. Fracture fields are located between these mountains and the Rhine valley. They are bands of fractured terrains, which collapse progressively giving a general stair-like framework (figure 1). In the

North, the rift valley is limited by the Hercynian fault of the Rhenish Shield, and in the South, by the Jura front and the transfer Rhine/Saône fault. The latter permits to link the Rhine Graben with other Tertiary grabens, namely the Bresse and the Limagne grabens (Bergerat & Geysand, 1980).

The opening of the Rhine graben near the late Eocene-Oligocene boundary allows to reactive the Variscan tectonic structural framework. A series of N30°E-N40°E trending discontinuous structures have been identified on gravity and magnetic maps of the Upper Rhine Graben basement, as well as in outcrops in the Vosges, Black Forest and Odenwald mountains (Edel *et al.*, 2006). These NE-SW trending discontinuities were successively reactivated during the late Eocene N-S compression and the early-middle Oligocene E-W extension (Villemin *et al.*, 1986; Schumacher, 2002) as sinistral strike-slip faults and as oblique normal fault (Edel *et al.*, 2006). Elongated depocenters appears to form in association with the reactivated Variscan wrench faults (e.g. the Rhenane border fault), particularly in the centre part of the graben.

During the Rhine graben formation, several major subsidence phases generated variable sediment thicknesses. The subsidence starts at the end of Eocene (Lutetian) and continues during Oligocene under an E-W extensional regime. From the Upper Oligocene ( Chattian), the subsidence pattern is different in the northern and the southern parts of the graben (i.e. on both sides of the Erstein limit, which is the continuation of the regional Lalaye-Lubine-Baden-Baden hercynian fault, Villemin *et al.*, 1986; Schumacher, 2002). In the southern side, the subsidence decreases and stops at the end of Oligocene ( Chattian-Aquitanian). By the end of the subsidence, the graben borders raises inducing the uplift of the Vosges and the Black Forest massif. In the northern part of the graben, the subsidence is quite regular and homogenous until the Upper Miocene. There, the subsidence rate is less important and the graben borders are less uplifted (Villemin *et al.*, 1986).

In connection with the rifting, the Moho was uplifted, implying a large-scale positive geothermal anomaly. Moreover, additional small scale geothermal anomalies are also due to fluid circulations within fracture zones (Pribnow and Schellschmidt, 2000). These local anomalies are mainly located along the Western border of the graben, where the fluid circulates from East to West (Benderitter and Elsass, 1995; Pribnow and Clauser, 2000). Inside the Rhine graben, several local geothermal anomalies occurred and are spatially distributed along a North-South: Selestat, Strasbourg, Soutz (in superimposition with the petroleum field of Pechelbronn), Landau (also a petroleum field), Wattenheim (NE Worms) and Stockstadt (SW Darmstadt). The thermal anomaly of Soutz is the most important with 130°C at

1400m depth, which correspond to the top of the granitic basement.

### **DATA USED TO BUILT THE 3-D MODEL**

The model is located in the North of the French part of the Upper Rhine Graben, including the EGS site of Soultz and its geothermal anomaly. The dimensions of the model are 30km along the E-W direction, 20km along the N-S direction, and 6km deep. As the structures are overlaid by the sediments filling the graben, two kinds of data are used to build the 3-D model: (1) seismic profile interpretations and (2) borehole data.

The seismic profiles were acquired for oil exploration in the 70-80's, following the stop of the exploitation of the Pechelbronn oil field, close to the EGS Soultz site. We reprocessed these profiles from the raw data, in the framework of various projects. This new process of the seismic data was possible thanks to new algorithms, as well as in a better definition of the static corrections and dynamic corrections. This reprocessing improves the quality of the seismic image. Compared with old-processed profile, the newly processed profiles display a better (1) continuity and horizontal-vertical resolution of the seismic horizons or groups of horizons, (2) geometric characterization of faults and fault zones (Beccaletto *et al.*, 2010).

During the first stage of the EGS Soultz project, five seismic profiles, PHN84J, PHN84K, PHN84L, PHN84R, PHN84W, close to the future EGS Soultz site, have been reinterpreted (Cautru, 1988). Numerous old petroleum boreholes have been used to interpret these profiles, then to identify the seismic horizons as geological interfaces, and convert the time scale seismic profiles into depth sections (Figure 2).

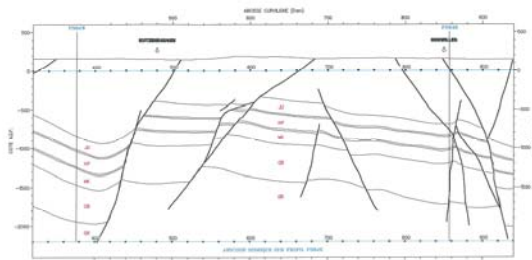


Figure 2 – Example of a geological cross-section interpreted based on seismic profiles PHN84K (Cautru, 1988).

These geological cross-sections show the detail of the structures around the EGS Soultz site. This allow us to have a good visualization of the horst structure under the EGS Soultz site, which allow to reach the granite, target of the project, at 1.4km depth. These geological cross-sections have been used to build the first 3-D geological model of Soultz (Renard & Courrioux, 1994) and the local part of our model (Dezayes *et al.*, 2009). To extend

this first model, we used a larger, regional set, of seismic sections (Figure 3). These regional sections have been built by concatenation of different single old petroleum seismic profiles acquired during the same oil exploration phase as described above. However, the raw seismic data have been homogenized, and a new process have been applied to improve the image quality. Along the entire French part of the Upper Rhine Graben, about 60 transversal seismic sections have been built with around 10 km between each other, as well as 5 longitudinal sections. The interpretation of these 1600km regional seismic profiles has been done in the framework of the European GeORG project, whose goal is to improve the knowledge of the Upper Rhine Graben for the geological resource exploitation (groundwater, geothermal energy, CO<sub>2</sub> storage.... Capar *et al.*, 2009).

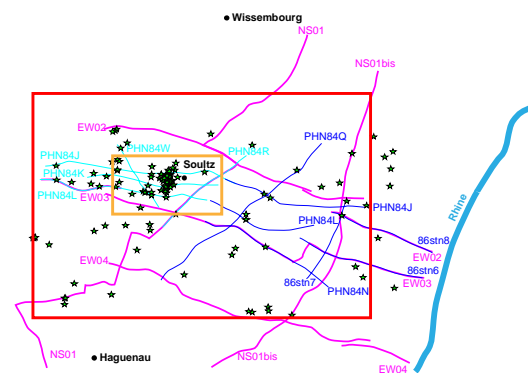


Figure 3 – Location of the data; boreholes (green stars) and seismic profiles included within the local Soultz model (orange rectangle) and the regional model (red rectangle). Light blue lines: seismic profiles interpreted in the framework of the Soultz project (Cautru, 1985), Pink lines: seismic profiles interpreted in the framework of the GeORG European project (Capar *et al.*, 2009), dark blue lines: seismic profiles interpreted in the framework of the Roquette geothermal project.

To convert the interpretation of seismic profiles from time scale to depth scale, we used velocity data related to some of the boreholes. A detailed analyse of these velocity has been presented in Baillieux *et al.* (this issue).

We observe a high density of normal fault on the seismic sections. Most of these normal faults cross-cut the entire Cenozoic sedimentary filling of the graben as well as the Mesozoic pre-rift sediments. We also observe numerous occurrences of strike-slip features, which form negative flower structures (Beccaletto *et al.*, 2010). They are the most recent structures and may be related to the early Miocene to present NW compressional stress field (Villemin *et al.*, 1986).

In addition to the data described above, we also used the interpretation of some seismic profiles located at the eastern part of the model area. These interpretations come from an exploration study for a future geothermal project, namely Roquette project, located to the east of the Soultz site. The goal of this project will be to dry starch with geothermal steam. However, the thickness of tertiary sediments is very large in this area (more than 1000m), so that it is very difficult to interpret the deepest horizons.

The data of 64 oil exploration boreholes, coming from the French Geological Survey (BRGM) database, namely BSS (Banque de données du Sous-Sol), have been integrated in to the model. Unfortunately, most of them are shallow and mainly give information on the Tertiary and Jurassic layers. The boreholes located along the seismic sections were used to constrain the position of the interfaces. These boreholes have been drilled in the past for the petroleum exploitation of the Pechelbronn field. Where there were no seismic profiles, we used essentially the geological data from the boreholes to constraints the model (Figure 4). The data of the deep boreholes of the Soultz site have been added, in the aim to model the granitic basement (Dezayes *et al.*, 2009).

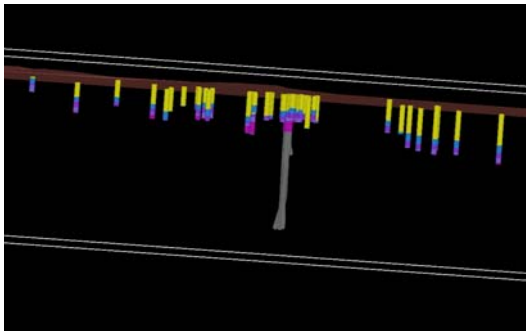


Figure 4 – Boreholes around the Soultz site. In yellow, the tertiary formations, in bleu, the Jurassic formations, in purple: the Keuper formation, in purple-blue, the Muschelkalk formation, in pink, the Buntsandstein formation, in grey, the basement. The deeper boreholes in the center represent the Soultz wells(5000m depth).

### **3-D GEOLOGICAL MODELLING**

The 3-D geological model is built on the basis of geological map, cross-sections, boreholes and a digital elevation model (DEM). To construct the 3-D volumetric bodies, we used the 3-D Geomodeller, an original software developed by the BRGM (French Geological Survey; Lajaunie *et al.*, 1997; Calcagno *et al.*, 2008) and specifically devoted to geological modelling. Using this software, lithological units are described by a pseudostratigraphic pile, intended to image the geological and structural relationships as best as possible. Compared with other existing 3-D solid

modelling approaches, a major feature of this modeller is that the 3-D description of the geological space is achieved through a potential field formulation in which geological boundaries are iso-potential surfaces, and their dips are represented by gradients of the potential. The model is built in a geo-referenced system and it takes into account:

- points, which define the location of geological interfaces or faults/fracture;
- orientations, which define the dip and polarity of geological interfaces or faults/fracture;
- a geological pile, which define the *a priori* geological knowledge about chronology and relation between the geological formations.

Our model is 30km long along the E-W direction, 20km long along the N-S direction, and 6km deep. To model the sedimentary cover, we digitized the interpretation of the seismic profiles within the cross-sections defined by the seismic profile walk-away. In this cross-section, only the location and the apparent dip of interfaces have been known, but unfortunately not the complete orientation of point data. The faults traces were digitized along each cross-section and linked from one section to the other. A fault can stop against another fault or be secant. To established associations between these tectonic structures, the 3-D Geomodeller uses a dedicated tool that links faults to faults. The same method is used to define which layers are affected by a fault. For the minor faults, we define a finished extension. Radius values limit the size and the extension of the faults within the layer and the model. Then, the software displays the fault traces on all sections. It is possible to choose which traces are the most probable when several possibilities occur. If the correlation is inconsistent, we are free to modify the interpretation, by varying the different parameters such as orientation data (dip, dip direction ...), relationship, etc.... These steps are repeated until the fault network is 3-D-consistent with the geological and tectonic context (Figure 5).

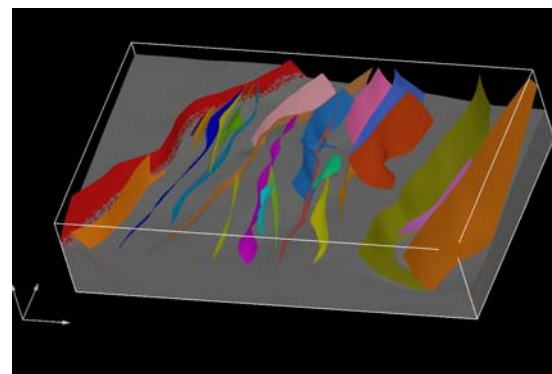


Figure 5 – 3-D representation of the fault network and the basement (in gray). In red, the rhenan border fault (dimension of the model: 30x20x6km).

We also compare our network with the former interpretation of the area done in the framework of the oil exploration (Foehn, 1985).

Resulting data for each lithological layer come from the interpretation of the interfaces on each cross-section, and the geology data based on the wells. A central step is the definition of the lithological layers of the model. The original stratigraphy has been simplified: five main layers characterize the sedimentary cover of the area (Figure 6). The different deposits of the Tertiary are grouped into one layer called Tertiary. The same unification has been done for the Jurassic deposits. The Triassic sediments are represented by the Keuper, the Muschelkalk and the Buntsandstein sediments. These formations have been grouped in the Trias serie because they have a constant thickness. The deeper serie is the basement (granite). All the layers are onlap series.

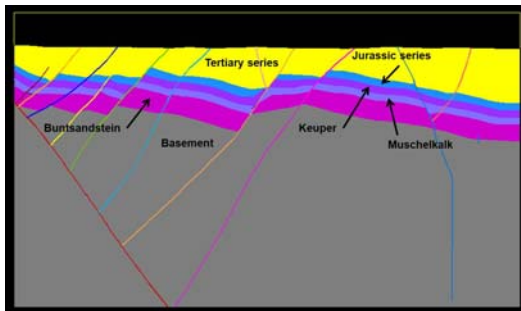


Figure 6 – Example of the cross-section interpreted based on the seismic profile PHN84J (Cautru, 1988) and the different series modeled.

Once all the data have been included, the software computes the model, by interpolating data points and orientations and taking into account the fault-to-fault and fault-to-lithological layers relationships.

### **REGIONAL MODEL DESCRIPTION**

A local 3-D geological model has been first built around the Soultz site (Figure 3) to test the feasibility of the process with only deep data (Dezayes *et al.*, 2009).

In the extended model, we built a 26 fault network. The orientation of the major faults is NNE-SSW (Figure 7). These faults are normal faults with a high eastward dip and large extensions. This kind of faults affects all the geological formations from the Tertiary series to the basement. Inside the different blocks, minor faults were also built. These secondary faults, only cutting through the sedimentary cover, are principally antithetic faults and trend N-S to NNW-SSE (Figure 7).

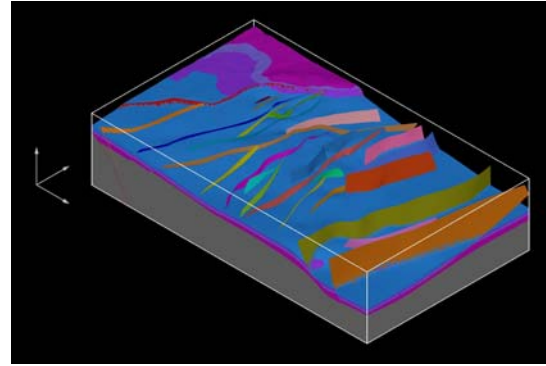


Figure 7 – 3-D representation of the regional model. In blue, the Jurassic formations, in purple: the Keuper formation, in purple-blue, the Muschelkalk formation, in pink, the Buntsandstein formation, in grey, the basement. The Tertiary series have been hidden.

A detailed analysis of this model is done in Baillieux *et al.* (this issue).

### **CONCLUSIONS**

This paper demonstrates the usefulness to build a 3-D geological model to visualize a complex regional fault network. The present model could be now used as basis for many exploration investigations and different kinds of modelling, such as geophysical inversion, thermo-hydraulically modelling ...

### **ACKNOWLEDGMENTS**

The authors are grateful to Ademe (French Agency for Environment and Energy), which has financially supported this work together with the BRGM. We also thank to ES Géothermie to give data of the Roquette projet. I would thank students, Gloria Heilbronn and Julien Castera, for their help to build the model.

### **REFERENCES**

- Baillieux P., Schill E., Dezayes C. (2011) – 3-D structural regional model of the EGS Soultz site (northern Upper Rhine Graben, France): insights and perspectives. This issue.
- Beccaletto L., Capar L., Cruz-Mermey D., Oliviero G., Elsass P., Perrin A., Rupf I., Nitsch E., Tesch J. (2010) – The GeORG project: seismic interpretation, structural pattern and 3-D modelling of the Upper Rhine Graben – first scientific results. Technical workshop Geopotential of the Upper Rhine Graben (GeORG). Novembre 18<sup>th</sup> 2010, Freiburg (Germany). <http://www.geopotenziale.org/aktuelles/workshop>.
- Benderitter Y., Elsass P. (1995) - Structural Control of Deep Fluid Circulation at the Soultz HDR Site, France: a Review, *Geothermal Science and Technology*, 4, p. 227-237.



- Bergerat, F. & Geysant, J. (1980) - La fracturation tertiaire de l'Europe du Nord : résultat de la collision Afrique-Europe. *C. R. Acad. Sci. Paris* **290**(D), p. 1521-1524.
- Calcagno P., Chilès J.P., Courrioux G., Guillen A. (2008) - *Geological modelling from field data and geological knowledge, Part I – Modelling method coupling 3-D potential-field interpolation and geological rules*. *Physics of the Earth and Planetary Interiors*, 171, p. 147-157.
- Capar L., Beccaletto L. Elsass P., Marc S., Perrin A., Oliviero G. (2009) – Apport du retraitement sismique à l'étude des bassins sédimentaires : exemple du nord du fossé rhénan. *12ième Congrès Français de Sédimentologie* 2009, Rennes; Poster.
- Cautru J.P. (1988) in Menjoz, A., Cautru, J. P., Criaud, A., and Genter, A., (1988), Roches sèches chaudes. Caractérisation des réservoirs fracturés: *Rapport annuel d'activités 1988n BRGM/IRG*, p. 35-39.
- Dezayes C., Castera J., Heilbronn G., Calcagno P. (2009) – Regional geological model of the Soultz-sous-Forêts geothermal field (Rhine Graben, France). *GRC transactions*, Vol. 33, p. 175-180.
- Edel J.-B., Schulmann K., Rotstein Y. (2006) – The Variscan tectonic inheritance of the Upper Rhine Graben: evidence of reactivations in the Lias, Late Eocene-oligocene up to the recent. *Int. J. Earth Sci. (Geol. Rundsch.)*, DOI 10.1007/s00531-006-0092-8.
- Foehn, J. P. (1985) Interprétation des campagnes sismiques 1981 et 1984, concession de Pêchebronn, permis de Haguenau. Total Exploration internal report, October 1985.
- Lajaunie C., Courrioux G. and Manuel L. (1997) - Foliation fields and 3-D cartography in geology: principles of a method based on potential interpolation, *Mathematical Geology*, 29(4):571–584.
- Pribnow D., Schelschmidt R. (2000) - Thermal tracking of upper crustal fluid flow in the Rhine Graben. *Geophysical Research Letters*, 27(13), p. 1957-1960.
- Renard, P. and G. Courrioux (1994). "Three-dimensional geometric modelling of a faulted domain: The Soultz Horst example (Alsace, France)." *Computers & Geosciences* **20**(9): 1379-1390.
- Schumacher, M. (2002) – Role of pre-existing structures during rift evolution. *Tectonics*, vol. 21, n° 1.
- Villemin T., Alvarez F., Angelier J. (1986) - The Rhinegraben: extension, subsidence and shoulder uplift. *Tectonophysics*, 128, p. 47-59.
- Ziegler P. (1992) – European Cenozoic rift system. *Tectonophysics*, 2008, p.91-111.



# Curriculum Vitae of Paul BAILLIEUX

Date of birth April 14<sup>th</sup>, 1985  
Place of birth Montpellier, France  
Nationality French



## Education

April 2009 – March 2013 Doctoral student in **Swiss laboratory for Geothermics of the Center for Hydrogeology and Geothermics** in **Neuchâtel University** under the supervision of **Prof. Eva Schill**, and **School of Mathematical Sciences, Monash University**, Melbourne, Australia, under the supervision of **Prof. Louis Moresi**.

PhD title : « Multidisciplinary approach to understand the localization of geothermal anomalies in the Upper Rhine Graben from regional to local scale »

2005- 2008 Student from **EOST** - Engineering School of Geophysics / Institute of Earth Sciences, **Louis Pasteur University**, Strasbourg, France

Multiple internships in Applied Geophysics and Research Institutes (Norway, Belgium) oriented towards environmental applications

2003 – 2005 Second year degree in Physics, Mathematics, and Chemistry – Sciences, **Montpellier II University**, Montpellier, France

2003 Baccalaureat  
France national secondary-school (*lycée*) diploma

## Practical training

Since April 2009 **Teaching assistant** in several field courses and lectures in Geothermics at the University of Neuchâtel, and participation to multiple conferences and workshops in Geothermics world-wide

February – August 2008 **Junior Geophysicist** in GBGeotechnics, Australia  
Company of geophysical investigation for geotechnical, archaeological and environmental applications